

Copyright Undertaking

This thesis is protected by copyright, with all rights reserved.

By reading and using the thesis, the reader understands and agrees to the following terms:

1. The reader will abide by the rules and legal ordinances governing copyright regarding the use of the thesis.
2. The reader will use the thesis for the purpose of research or private study only and not for distribution or further reproduction or any other purpose.
3. The reader agrees to indemnify and hold the University harmless from and against any loss, damage, cost, liability or expenses arising from copyright infringement or unauthorized usage.

If you have reasons to believe that any materials in this thesis are deemed not suitable to be distributed in this form, or a copyright owner having difficulty with the material being included in our database, please contact lbsys@polyu.edu.hk providing details. The Library will look into your claim and consider taking remedial action upon receipt of the written requests.

**WEB CRIPPLING BEHAVIOUR IN COLD-FORMED STEEL
PROFIED DECKINGS UNDER LATERAL CONCENTRATED LOADS**

Tse Wai Tak

A thesis submitted in partial fulfillment of the requirements for the
Degree of Master of Philosophy

**The Hong Kong Polytechnic University
Department of Civil and Structural Engineering**

December 2006



**Pao Yue-kong Library
PolyU • Hong Kong**

CERTIFICATE OF ORIGINALITY

I hereby declare that this thesis is my own work and that, to the best of my knowledge and belief, it reproduces no material previously published or written, nor material that has been accepted for the award of any other degree or diploma, except where due acknowledgement has been made in the text.

_____ (Signed)

Tse Wai Tak (Name of student)

Abstract

In this thesis, both extensive experimental and numerical investigations into web crippling and section failure of profiled steel deckings are carried out and reported. Cold-formed steel profiled deckings named the profiled Deck R50 consist of a unit tough width of 200mm and height of 52mm are used in this study.

For the web crippling tests, Decks R50 with different steel grades and thicknesses are tested under both internal and end loading conditions with practical range of load bearing widths. A total of 52 tests are carried out under each loading condition. From the extensive experimental investigation carried out, a mode of failure is identified among all tests, that is, the web crippling failure. For specimens tested under internal loading condition, local failure is observed at the web-trough corner directly under the point of load application. Moreover, apparent local plate buckling in the trough of the decking is observed well before the web crippling failure. While for specimens tested under end loading condition, local plate buckling in the trough of the decking is also observed well before the web crippling failure. Furthermore, local failure is observed at the web-trough corner at the inner edge of the load application length while excess web buckling is apparent near the web-flange corner at the outer edge of the load application length.

After careful execution of web crippling tests, an advanced three-dimensional finite element models with material and geometry non-linearity are established to simulate the web crippling behaviour. Different variables such as the corner radius and spring stiffness

which used to simulate the loading condition, as well as the lateral restraint for study of shear stud effect and initial geometrical imperfection are studied using the finite element models. While insignificant effect on the web crippling resistances and displacement characteristics are resulted from the variation of spring stiffness and initial geometrical imperfection, great discrepancy in the web crippling resistance is resulted due to the change of corner radius and lateral restraint. Larger corner radii use in the finite element models tend to induce a lower web crippling resistance, and vice versa. Whereas for the lateral restraint is used to study the provision of shear studs provided at different trough spacing in the deckings, the lateral restraints provided at the symmetrical axes at the trough along the longitudinal direction of the decking is for simulation of shear stud provided at every trough in the deckings, while for the case where lateral restraints released is to simulate when shear studs are provided only at every second trough. Numerical results have shown that the latter case results in a significant reduction in web crippling resistances.

Comparison on both the web crippling resistances and the deformed shapes at failure between the numerical and the test results from tests is found to be highly satisfactorily. Moreover, an extensive parametric study is performed to generate design data for web crippling resistances of re-entrant deckings with different steel grades and thicknesses under a practical range of bearing lengths. It is shown that the proposed finite element models are effective to predict the web crippling resistances of cold-formed steel deckings. Furthermore, a simple and yet effective design charts are also proposed which employs directly the numerical results obtained from the parametric study.

The second study is on section failure under co-existing moment, shear and web crippling forces. The section failure is examined experimentally using the one-point load tests. A total of 42 tests are carried out with Decks R50 of different steel grades and thicknesses. Different span lengths are also considered under four different load bearing widths. Among all tests performed, obvious combined bending and web crippling failure were observed. Moreover, local buckling at the trough is observed in all tests prior to ultimate load were reached.

For numerical investigation into section failure, advanced three-dimensional finite element models with material and geometrical non-linearity are established. Comparison on both the section failure resistances and the deformed shapes at failure between the numerical and the test results is found to be highly satisfactory. After systematic data analyses on the section failure of profiled steel deckings, design charts with improved accuracy in load prediction are developed for deckings with different steel grades and clear spans under a practical range of bearing lengths. The use of these design charts will lead to a convenient and reliable approach for design of deckings. Furthermore, the coexisting moment, shear and web crippling forces is also considered which eliminates the need of two concurrent design equations.

Publications arising from the thesis

International conference papers:

Chung K. F. and Tse W. T., 2007, An investigation into high strength cold-formed steel profiled deckings under concentrated lateral loads, Proceedings of Pacific Structural Steel Conference, 13-16 March 2007, Taupo, New Zealand, pp371-376.

Tse W. T. and Chung K. F., 2006, Web crippling failure of cold-formed steel deckings, Processings of International Colloquium on Stability and Ductility of Steel Structures, 6-8 September 2006, Lisboa, Portugal, pp721-728.

Tse W. T. and Chung K. F., 2006, Section failure due to combined moment, shear and web crippling forces in cold-formed steel deckings, Processings of International Colloquium on Stability and Ductility of Steel Structures, 6-8 September 2006, Lisboa, Portugal, pp729-736.

Acknowledgments

First and foremost, I would like to express my sincere gratitude to my supervisor Professor K F Chung for his advice, guidance and critical comments on all aspects of my research work throughout the course of my study.

Special thanks must go to Dr Faris Albermani, my supervisor for my Bachelor degree thesis, for his ongoing assistance. His patience and feedback were greatly appreciated.

I wish to thank my colleagues Dominic Yu and Esther Choy for their encouragement, helpful comments during my time as a postgraduate. In addition, I am grateful for the assistance of my colleague Aaron Wang. His opinions and assistances throughout my numerical investigation are kindly appreciated.

I would like to acknowledge my appreciation to all laboratory staffs for their aid in test setups and preparation of apparatus.

Finally, I would also like to offer my sincere thanks to my parents, David and Lisa, and to my brother Vincent for their patient and moral support. Without their encouragement, this thesis would have become a long and arduous task.

Table of contents

Abstract	i
Publications arising from the thesis	iv
Acknowledgments	v
Chapter 1 Introduction	
1.1 Cold-Formed Steel Decking in Building Construction	1
1.1.1 Web Crippling Failure	2
1.1.2 Section Failure	3
1.2 Objectives and Scope of Work	4
1.3 Methodology	5
1.4 Project Significance	7
1.5 Layout of Thesis	8
Chapter 2 Literature Review	
2.1 Introduction	15
2.2 Studies of Web Crippling Failure	15
2.2.1 Empirical Equations	15
2.2.1.1 NAS and AS4600	16
2.2.1.2 BS5950: Parts 5 and 6	18
2.2.1.3 Eurocode 3: Part 1.3	20
2.2.2 Existing Experimental-Based Researches	22
2.2.3 Existing Theoretical-Based Researches	26
2.3 Studies of Combined Effects	28
2.3.1 Empirical Equations	28
2.3.1.1 BS5950: Parts 5 and 6	29
2.3.1.2 AS4600	31
2.3.1.3 Eurocode 3: Part 1.3	32
2.3.2 Experimental and Numerical-Based Researches	33

Chapter 3 Experimental Investigation into Web Crippling Failure

3.1	Introduction	45
3.2	Experimental Investigation	45
3.2.1	Tensile Tests	46
3.2.2	Test Program of Web Crippling Tests	46
3.2.3	Instrumentation for Internal Loading Condition	48
3.2.4	Instrumentation for End Loading Condition	50
3.2.5	Failure Modes and Observations	50
3.2.6	Load-Displacement Curves	51
3.2.7	Data Analysis	52
3.3	Comparison between Test and Design Results	53
3.4	Summary	54

Chapter 4 Numerical Investigation into Web Crippling Failure

4.1	Introduction	81
4.2	Numerical Models	81
4.2.1	Material Properties	82
4.2.2	Model Geometries	82
4.2.3	Boundary and Loading Conditions	83
4.2.3.1	Vertical supports	83
4.2.3.2	Lateral restraints	84
4.2.3.3	Loading conditions	84
4.2.4	Corner Radius	85
4.2.5	Initial Geometrical Imperfection	85
4.3	Numerical Results	86
4.3.1	Comparison of Load-Displacement Curves	87
4.3.2	Deformed Shapes and Contact Areas	88
4.4	Sensitivity Study	89
4.4.1	Spring Stiffness	89
4.4.2	Corner Radius	90
4.4.3	Yield strength of Corner Regions	91

4.4.4	Magnitude of Initial Geometrical Imperfection	92
4.4.5	Mesh convergence	93
4.5	Typical Parameters for Finite Element Modeling	95
4.6	Summary	95

Chapter 5 Experimental Investigation into Section Failure

5.1	Introduction	123
5.2	Experimental Investigation	124
5.2.1	Test Program of One-Point Load Tests	124
5.2.2	Instrumentation	126
5.2.3	Test Results	127
5.3	Comparison of Design Results against Experimental Results	128
5.3.1	Combined Bending and Shear	128
5.3.2	Combined Bending and Web Crippling	129
5.3.3	Structural Efficiency of Design Rules	131
5.4	Summary	131

Chapter 6 Numerical Investigation into Section Failure

6.1	Introduction	150
6.2	Numerical Models	150
6.2.1	Material Properties	151
6.2.2	Geometry	151
6.2.3	Boundary and Loading Conditions	152
6.2.3.1	Boundary conditions	152
6.2.3.2	Loading Conditions	152
6.2.4	Initial Geometrical Imperfection	153
6.3	Numerical Results	153
6.3.1	Predicted Deformation at Failure	153
6.3.2	Predicted Load Resistances	155
6.4	Summary	155

Chapter 7	Proposed Guidance for Web Crippling Failure and Section Failure	
7.1	Introduction	165
7.2	Design Guidance for Web Crippling Resistances	166
7.3	Design Guidance for Section Failure	167
	7.3.1 Design Procedures	168
7.4	Summary	170
Chapter 8	Conclusions	
8.1	General	185
8.2	Results and Conclusions	185
	8.2.1 Web Crippling Failure	185
	8.2.2 Section Failure	187
8.3	Recommendations for Future Research	189
	References	191
	Appendix A Tensile Tests	196

List of Figures

Figure 1.1	Geometry of cold-formed steel profiled decking Deck R50	11
Figure 1.2	Multi-span cold-formed steel profiled decking	11
Figure 1.3	General view of web crippling test	12
Figure 1.4	General view of one-point load test	12
Figure 1.5	Finite element models for simulation of web crippling failure	13
Figure 1.6	Finite element models for simulation of section failure	14
Figure 2.1	Loading conditions	36
Figure 2.2	Web crippling tests with stiffened webs (Fox, S.R. and Brodland G.W. 2003)	36
Figure 2.3	Flange curling phenomenon	37
Figure 2.4	Proposed web crippling mechanism	38
Figure 2.5	Comparison of design values with finite element results (Rhodes J. and Nash D. 1998)	38
Figure 2.6	Comparison of web crippling capacity of 100 x 50 x 12.5 x 1 mm channel section (Rhodes J. and Nash D. 1998)	39
Figure 2.7	Web crippling failure modes studied by H. Hofmeyer et al (2002)	40
Figure 2.8	Interaction for combined bending and web crippling	41
Figure 2.9	Numerical results for combined bending and web crippling (A.M. Akhand et al, 2004)	41
Figure 2.10	Proposed failure mechanism by J.M. Davies et al (1997)	42
Figure 2.11	Experimental result of combined bending and shear failure by Shan M.Y., LaBoube R.A. and Yu W.W (1996)	42
Figure 2.12	Load capacities subjected to combined bending and shear failure by Shan M.Y., LaBoube R.A. and Yu W.W (1996)	43
Figure 3.1	Typical set-up of web crippling test under internal loading condition with basic instrumentation	56
Figure 3.2	General view of web crippling test under internal loading condition with basic instrumentation	57

Figure 3.3	Typical set-up of web crippling test under internal loading condition with detailed instrumentation	58
Figure 3.4	General view of web crippling test under internal loading condition with detailed instrumentation	59
Figure 3.5	Typical set-up of web crippling test under end loading condition with basic instrumentation	60
Figure 3.6	General view of web crippling test under end loading condition with basic instrumentation	61
Figure 3.7	Typical set-up of web crippling test under end loading condition with detailed instrumentation	62
Figure 3.8	General view of web crippling test under end loading condition with detailed instrumentation	63
Figure 3.9	Typical failure mode of web crippling under internal loading condition	64
Figure 3.10	Typical failure mode of web crippling under end loading condition	65
Figure 3.11	Displacements and rotations of reference points	66
Figure 3.12	Load-deflection curves of web crippling tests: G235, $N_b = 50\text{mm}$	67
Figure 3.13	Load-deflection curves of web crippling tests: G235, $N_b = 100\text{mm}$	68
Figure 3.14	Load-deflection curves of web crippling tests: G235, $N_b = 150\text{mm}$	69
Figure 3.15	Load-deflection curves of web crippling tests: G235, $N_b = 200\text{mm}$	70
Figure 3.16	Load-deflection curves of web crippling tests: G550, $N_b = 50\text{mm}$	71
Figure 3.17	Load-deflection curves of web crippling tests: G550, $N_b = 100\text{mm}$	72
Figure 3.18	Load-deflection curves of web crippling tests: G550, $N_b = 150\text{mm}$	73
Figure 3.19	Load-deflection curves of web crippling tests: G550, $N_b = 200\text{mm}$	74
Figure 3.20	Summary of normalized web crippling resistances under internal loading condition	75
Figure 3.21	Summary of normalized web crippling resistances under end loading condition	76
Figure 4.1	Different stresses adopted in finite element models	97
Figure 4.2	Idealization of finite element models	98
Figure 4.3	Boundary and loading conditions of finite element models	99
Figure 4.4	Geometry of finite element models	100

Figure 4.5	Detailed finite element models with initial geometrical imperfection	101
Figure 4.6	Load-displacement curves of Decks R50 with G235 steel	102
Figure 4.7	Load-displacement curves of Decks R50 with G550 steel	103
Figure 4.8	Deformed finite element models of G235 steel at failure – Fixed C, internal loading condition	104
Figure 4.9	Deformed finite element models of G235 steel at failure – Fixed C, end loading condition	105
Figure 4.10	Deformed finite element models of G550 steel at failure – Fixed C, internal loading condition	106
Figure 4.11	Deformed finite element models of G550 steel at failure – Fixed C, end loading condition	107
Figure 4.12	Change of contact area near the web-trough corner: internal loading condition G235, $t = 1.00\text{mm}$ and $N_b = 200\text{mm}$	108
Figure 4.13	Change of contact area near the web-trough corner: internal loading condition G550, $t = 0.75\text{mm}$ and $N_b = 50\text{mm}$	109
Figure 4.14	Change of contact area near the web-trough corner: internal loading condition G550, $t = 1.20\text{mm}$ and $N_b = 200\text{mm}$	110
Figure 4.15	Change of contact area near the web-trough corner: end loading condition G235, $t = 1.00\text{mm}$ and $N_b = 200\text{mm}$	111
Figure 4.16	Change of contact area near the web-trough corner: end loading condition G550, $t = 0.75\text{mm}$ and $N_b = 50\text{mm}$	112
Figure 4.17	Change of contact area near the web-trough corner: end loading condition G550, $t = 1.20\text{mm}$ and $N_b = 200\text{mm}$	113
Figure 4.18	Load-displacement curves of finite element models with different values of spring stiffness	114
Figure 4.19	Load-displacement curves of numerical models with different corner radii	115
Figure 4.20	Load-displacement curves of numerical models with different values of initial imperfection	116
Figure 4.21	Finite element model Ic1-Ma – Fixed C, internal loading condition	117
Figure 4.22	Finite element model Ic1-Mc – Fixed C, internal loading condition	118

Figure 5.1	Typical set-up of one-point load test	133
Figure 5.2	General view of one-point load test	133
Figure 5.3	Typical failure mode of one point load test	134
Figure 5.4	Load-deflection curves of one-point load tests: $t = 0.75\text{mm}$	135
Figure 5.5	Load-deflection curves of one-point load tests: $t = 1.00\text{mm}$	136
Figure 5.6	Load-deflection curves of one-point load tests: $t = 1.20\text{mm}$	137
Figure 5.7	Continuous structure under section failure	138
Figure 5.8	Summary of section failure resistances for G235 steel	139
Figure 5.9	Summary of section failure resistances for G550 steel	140
Figure 5.10	Model factors for section failure	141
Figure 6.1	Idealization of finite element models	157
Figure 6.2	Boundary and loading conditions of finite element models	158
Figure 6.3	Geometry of finite element models	159
Figure 6.4	Detailed finite element models with initial geometrical imperfection	160
Figure 6.5	Deformed finite element models of G550 steel at failure	161
Figure 6.6	Load-deflection curves of Decks R50 with G550 steel	162
Figure 6.7	Load-deflection curves of Decks R50 with G235 steel	163
Figure 7.1	Parametric study for web crippling failure	172
Figure 7.2	Summary of web crippling results	173
Figure 7.3	Model factors: $P_{\text{FEM}} / P_{\text{Design}}$ for profiled decking with G235 steel under web crippling failure	174
Figure 7.4	Model factors: $P_{\text{FEM}} / P_{\text{Design}}$ for profiled decking with G350 steel under web crippling failure	175
Figure 7.5	Model factors: $P_{\text{FEM}} / P_{\text{Design}}$ for profiled decking with G450 steel under web crippling failure	176
Figure 7.6	Model factors: $P_{\text{FEM}} / P_{\text{Design}}$ for profiled decking with G550 steel under web crippling failure	177
Figure 7.7	Scope of parametric study for section failure	178
Figure 7.8	Bending and shear interaction curves	179
Figure 7.9	Bending and web crippling interaction curves	180

Figure 7.10	Model factors: P_{FEM} / P_{Design} for profiled decking with G235 and G350 steel under section failure	181
Figure 7.11	Model factors: P_{FEM} / P_{Design} for profiled decking with G450 and G550 steel under section failure	182
Figure A.1	Decking profile	196
Figure A.2	Typical dimensions of coupon tensile specimen	196
Figure A.3	Typical setup of tensile test	196
Figure A.4	Stress-strain curves of specimens A1 and A2	198
Figure A.5	Series A specimens	198
Figure A.6	Stress-strain curves of specimens B1 and B2	199
Figure A.7	Series B specimens	199
Figure A.8	Stress-strain curves of specimens C1 and C2	200
Figure A.9	Series C specimens	200
Figure A.10	Stress-strain curves of specimens D1 and D2	201
Figure A.11	Series D specimens.	201
Figure A.12	Stress-strain curves of specimens E1 and E2	202
Figure A.13	Series E specimens	202

List of Tables

Table 2.1	Coefficients for the design of profiled deckings under web crippling resistances to AISI and AS4600	44
Table 2.2	Coefficients for the design of single web channel-sections under web crippling resistances to AISI and AS4600	44
Table 3.1	Measured material properties of cold-formed steel deckings	77
Table 3.2	Details of web crippling test	77
Table 3.3	Summary of equations for calculation of reference points	78
Table 3.4	Summary of measured web crippling resistances	79
Table 3.5	Summary of normalized web crippling resistances	80
Table 4.1	Summary of finite element model series	119
Table 4.2	Summary of finite element models with different corner strength enhancement, boundary and loading conditions	119
Table 4.3	Summary of finite element models with different spring stiffness	120
Table 4.4	Summary of finite element models with different corner radii	120
Table 4.5	Summary of finite element models with different values of initial imperfection	121
Table 4.6	Summary of finite element models with different numbers of elements	121
Table 4.7	Summary of parameters for finite element modeling	122
Table 5.1	Summary of test program for one-point load test	142
Table 5.2	Summary of one-point load test results for profiled decking with G550 steel	143
Table 5.3	Summary of one-point load test results for profiled decking with G235 steel	144
Table 5.4	Normalized results of one-point load tests for profiled decking with G550 steel	145
Table 5.5	Normalized results of one-point load tests for profiled decking with G235 steel	145

Table 5.6	Design against combined bending and shear for profiled decking with G550 steel	146
Table 5.7	Design against combined bending and shear for profiled decking with G235 steel	147
Table 5.8	Design against combined bending and web crippling for profiled decking with G550 steel	148
Table 5.9	Design against combined bending and web crippling for profiled decking with G235 steel	149
Table 6.1	Summary of numerical models	164
Table 6.2	Summary of load resistance under section failure	164
Table 7.1	Summary of web crippling resistances	183
Table 7.2	Summary of numerical results for section failure	184
Table A.1	Result summary of specimens A1/2 and B1/2	197
Table A.2	Result summary of specimens C1/2, D1/2 and E1/2	197
Table A.3	Summary of specimens A1 and A2	198
Table A.4	Summary of specimens B1 and B2	199
Table A.5	Summary of specimens C1 and C2	200
Table A.6	Summary of specimens D1 and D2	201
Table A.7	Summary of specimens E1 and E2	202

Chapter 1

Introduction

1.1 Cold-Formed Profiled Steel Decking in Building Construction

Cold-formed profiled steel deckings are nowadays commonly adopted in floor construction due to their fast erection as temporary formwork. Moreover, cold-formed profiled steel deckings demonstrate their benefits as being light in self-weight whilst strong in strength, and these advantages allow reduced usage of construction materials, resulting in a more economical building solution. Figure 1.1 illustrates the geometry of the profiled steel decking Deck R50 which is extensively investigated in the project. Figure 1.2 illustrates a typical multi-span cold-formed steel profiled decking under uniformly distribution loads together with various internal forces diagrams. As shown in Figure 1.2, web crippling failure and associated section failure are two common modes of failure occur in internal supports of multi-span deckings under lateral concentrated loads. It should be noted that the section failure is often critical in multi-span decking under the combination of coexisting bending, shear and web crippling forces.

1.1.1 Web Crippling Failure

In the past, web crippling tests were carried out on different profiled deckings with specific material properties and geometrical dimensions for calibration of the web crippling resistances. After data analysis, empirical formulae are developed for typical design for cold-formed profiled steel deckings under concentrated lateral loads. It should be noted that these design equations are, in general very conservative and they are only applicable to a specific range of profiled decking shapes with high structural efficiency. In general, similar tests will be required for other decking profiles if high structural efficiency is sought. Moreover, the design equation is very cumbersome and provides little understanding on the relationships between different design parameters such as thickness, steel grade and load bearing width. Hence, improvement in design efficiency with structural understanding is highly desirable by develop improved design guidance which allows comprehension on the structural behaviour of multi-span deckings during design.

As reported in the literatures, many attempts using finite element models to simulate the web crippling failure in cold-formed steel profiled deckings are shown to be unsatisfactory, in particular, in the deformation characteristics of the profiled deckings. The complexity of the numerical prediction of the deformation characteristics is partly due to the change of contact area under the entire deformation history as well as the amount of lateral restraint provided to the test specimens.

1.1.2 Section Failure

In modern cold-formed steel codes of practice such as BS5950: Part 6 and Eurocode 3: Part 1.3, many important improvements on strength predictions have been provided in their latest revisions. Some of those improvements associated with high strength steels as well as distortional buckling and its interaction with both local plate buckling and overall buckling. However, simple design formulae are still adopted in the form of a linear interaction relationship for sections and deckings under lateral loads:

Loading Case I Combined bending and shear forces; and

Loading Case II Combined bending and web crippling forces

According to current design recommendations, both Loading Cases I and II should be checked separately over internal supports of multi-span deckings during the construction stage of composite slabs using cold-formed profiled steel deckings. However, it is argued in this project that co-existing bending, shear and web crippling forces should be considered all together, and the actual loading condition over internal supports should be as follows:

Loading Case III Combined bending, shear and web crippling forces

Hence, the cold-formed profiled steel deckings over internal supports are subjected to three types of co-existing internal forces, namely, hogging bending moments, lateral shear forces and local concentrated (reaction) forces. Structural adequacy of the profiled

deckings over internal supports against section failure due to these three co-existing actions often controls the effective use of the profiled deckings. In the past, empirical design formulae are adopted in predicting the web crippling resistances of the profiled deckings, and a linear interaction relationship for each of Loading Cases I and II is generally considered to be acceptable. However, it is now possible to simulate web crippling behavior in cold-formed profiled steel decking with high accuracy through advanced finite element modeling. Thus, it is highly desirable to formulate non-linear interaction formulae for profiled deckings under co-existing bending, shear and web crippling forces, i.e. to design directly against Loading Case III.

1.2 Objectives and Scope of Work

The aims of this project are to investigate the structural behaviour of cold-formed steel profiled deckings subjected to lateral concentrated loads. The widely used re-entrant type cold-formed steel profiled deckings, referred as Deck R50, is selected for this project. The geometry of Deck R50 is shown in Figure 1.1 with detailed dimensions.

For simplicity, the two critical failure modes namely, web crippling failure and section failure are studied independently through extensive experimental and numerical investigations.

This project aims to achieve the following objectives:

- a) To study the web crippling failure and the associated section failure of cold-

formed profiled steel deckings and how these failure modes are influenced by steel grade and thickness of the profiled decking, and load bearing width and loading conditions.

- b) To establish finite element models that are capable to predict the web crippling failure and the associated section failure with accurate load resistances and deformation characteristics.
- c) To provide design guidance with improved accuracy in load prediction and enhanced understandings on the structural behaviour of cold-formed steel profiled deckings under concentrated lateral loads.

1.3 Methodology

The research project is divided into three main tasks of investigation.

Task 1: Experimental Investigation

In order to provide test data to generate effective design rules to predict web crippling resistances and ultimate load resistances under combined actions in cold-formed profiled steel deckings, Decks R50 with a wide range of steel grades and thicknesses are tested under different loading conditions. Both web crippling tests and one-point load tests on cold-formed steel profiled deckings with nominal steel grades of 235N/mm^2 and 550N/mm^2 and thicknesses of 0.75, 1.00 and 1.20mm under load bearing widths of 50, 100, 150 and 200mm. The typical setup of the web crippling test and the one-point load

test are presented in Figures 1.3 and 1.4, respectively. As a whole, over 150 tests are carried out. In addition, test results are compared against design resistances obtained from BS5950: Part 6 for validity check of the current design rules.

Task 2: Numerical Investigation

Advanced finite element modeling onto the structural behaviour of cold-formed profiled steel deckings against web crippling failure and associated section failure are carried out. As reported in the literature, among many attempts on finite element investigations into web crippling failure, only limited successful results are reported. While the web crippling resistances of cold-formed profiled steel deckings are readily attained in many of the finite element models, the predicted load deformation characteristics are found to significantly different to the measured ones from web crippling tests. In this project, both measured material properties and detailed simulation on the experimental loading and boundary conditions are carefully incorporated in the finite element models, and highly satisfactory results in both ultimate load resistances and deformation characteristics are obtained. Both the effects of corner radius and change of local contact areas are examined in details. Furthermore, additional information such as stress patterns are also obtained and analyzed to understand yielding propagation in the profiled deckings during loading. Moreover, satisfactory results are also attained in the prediction of both strength and deformation characteristics of section failure in profiled decking using non-linear material, geometrical and boundary analyses. The idealization of finite element models for simulation of the web crippling failure and section failure are shown in Figures 1.5 and 1.6, respectively.

Task 3: Design development

After systematic data analyses on the web crippling resistances and the load resistances under combined actions of cold-formed profiled steel deckings, design information with improved structural efficiency are developed with the help of finite element models. The use of these design information will lead to a convenient and reliable approach for the design of profiled deckings under concentrated lateral loads.

1.4 Project Significance

This project aims to provide detailed understandings on the structural behaviour of web crippling failure and associated section failure of cold-formed profiled steel deckings, and also the effects to the structural behaviour of profiled deckings under different steel grades and thicknesses and loading conditions. Through detailed understandings on the web crippling failure and the associated section failure of profiled steel deckings, engineers are able to apply the proposed design method to typical profiled deckings with high structural efficiency as well as to non-typical profiled deckings effectively. Moreover, by providing design guidance for cold-formed profiled steel deckings covering a wide range of cross-section geometries, steel grades and loading conditions, engineers can work efficiently with comprehension.

1.5 Layout of Thesis

This thesis comprises 8 Chapters and a brief summary of each of the chapter is presented as follows:

Chapter 1 provides an introduction to the scope and the methodology of the research project. The deficient of the design rules for web crippling failure and section failure are also addressed.

Chapter 2 presents a literature review of different approaches adopted for the study of multi-span cold-formed profiled steel deckings. Experimental, theoretical and numerical-based researches related to the web crippling failure as well as the section failure are presented. It should be noted that the review is not limited to profiled decking, and other commonly used sections are also covered. Furthermore, empirical equations adopted in current design codes are also described.

Chapter 3 presents the experimental investigation of cold-formed steel profiled deckings subjected to concentrated lateral force, i.e. the web crippling tests. Special attention is given to investigate the effects of steel grade, thickness, load bearing width and loading condition to the web crippling behaviour of the profiled decking. Moreover, the validity of the current design BS5950: Part 6 is evaluated through careful comparison against experimental results.

Chapter 4 provides an extensive numerical study on web crippling failure using finite element models. Special attention is given to the effects of different boundary and loading conditions, corner radii, corner strength enhancement and initial geometrical imperfections to the web crippling behaviour. After careful calibration of the model against the measured load deformation characteristic of the web crippling tests, the stress patterns, the yielding propagation as well as the failure mechanism are studied thoroughly. A sensitivity study on the values of various parameters is also reported.

Chapter 5 is the experimental investigations into section failure of Deck R50, which such failure mode readily occurs in multi-span profiled steel decking subjected to a uniformly distributed load. A total of 42 one-point load tests are carried out to study the structural behaviour of section failure, and to provide test data for calibration of the finite element models as well as for comparison with design values.

Chapter 6 is the numerical investigations into section failure of Deck R50. A series of advanced finite element models are established in this chapter with material and geometrical non-linearity in order to simulate the actual testing conditions in one-point load tests. Furthermore, the load resistances due to the change of steel grades, thicknesses, load bearing widths, span lengths and magnitudes of initial geometrical imperfection are studied, and detailed deformation characteristics of profiled deckings are examined.

Chapter 7 reports the extensive parametric study and proposed design charts for design of web crippling failure and section failure with accurate predictions. For the proposed design chart for web crippling failure, linear interaction relationship is adopted. While for

section failure, linear relationships between moment ratio against load bearing widths are adopted, which such design charts incorporated the effect of coexisting bending, shear and web crippling forces.

Chapter 8 presents the overall conclusions of the research project.

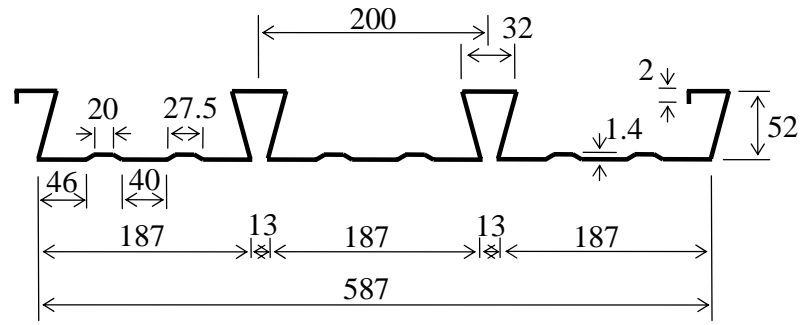


Figure 1.1: Geometry of cold-formed steel profiled decking Deck R50.

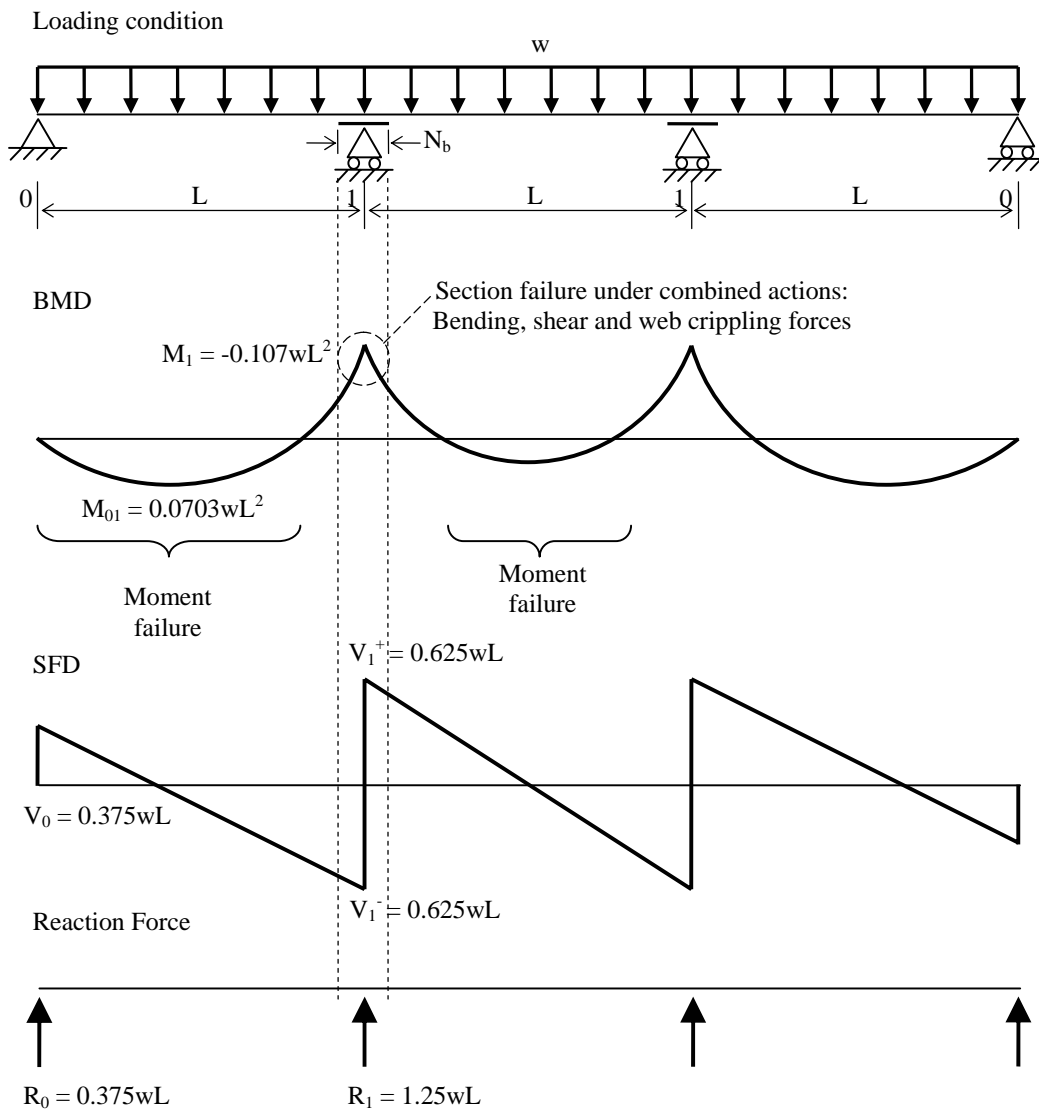


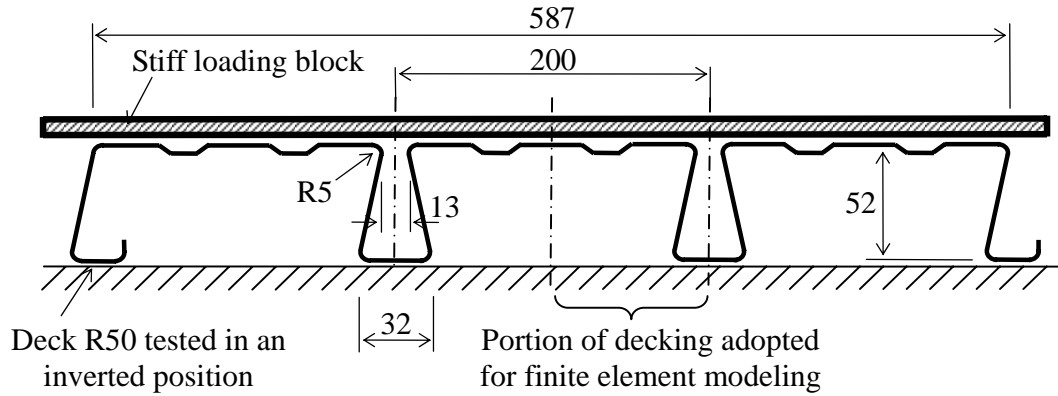
Figure 1.2: Multi-span cold-formed steel profiled decking.



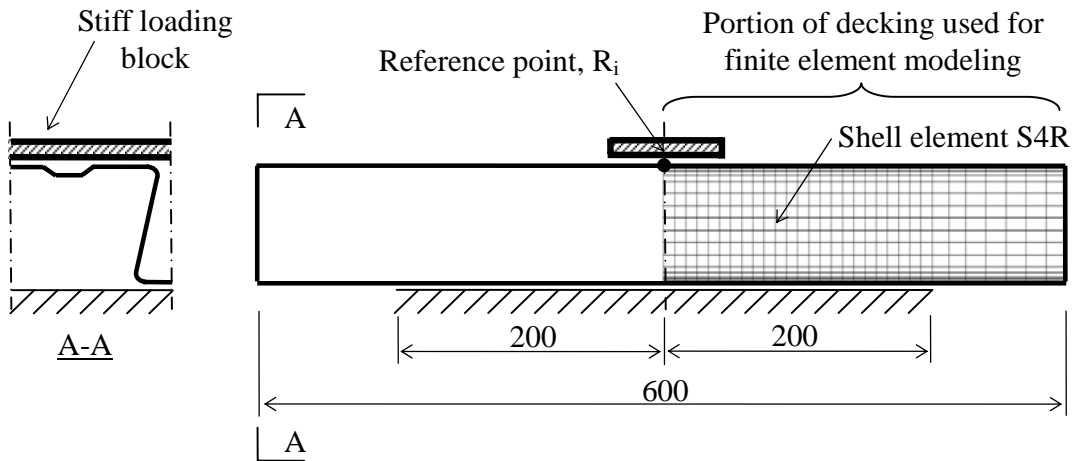
Figure 1.3: General view of web crippling test.



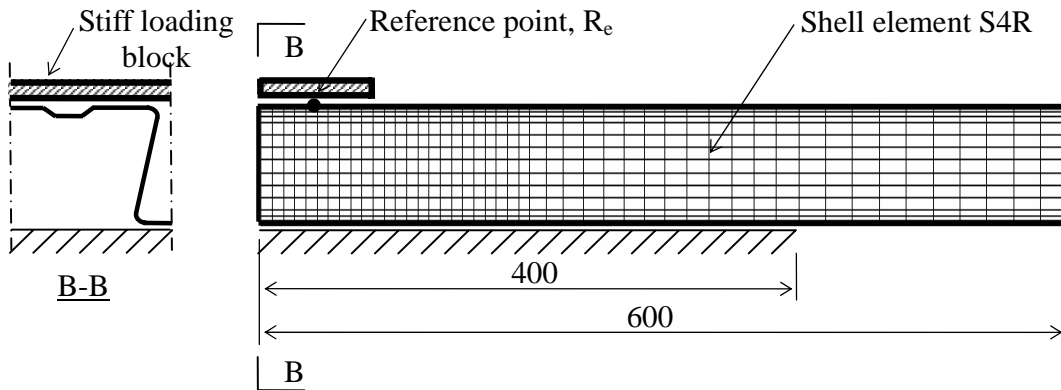
Figure 1.4: General view of one-point load test.



a) Cross sectional details of the test specimen

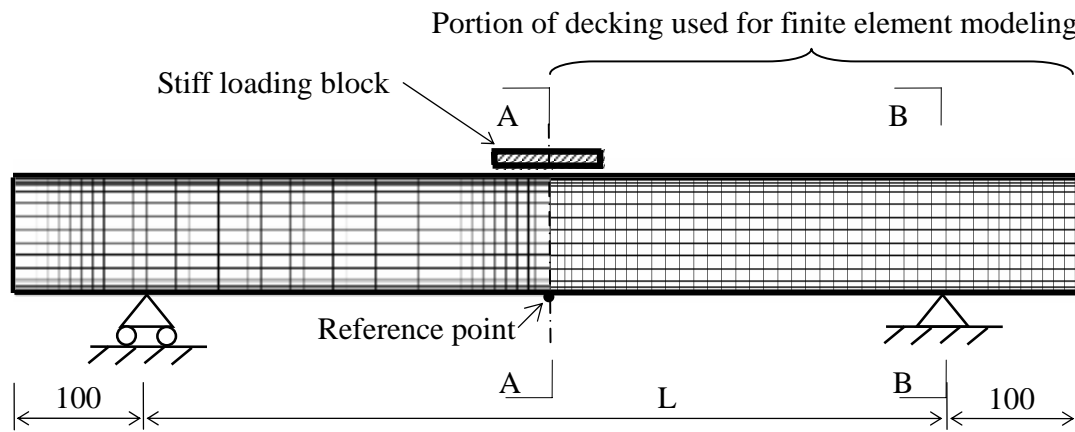


b) Finite element model under internal loading condition

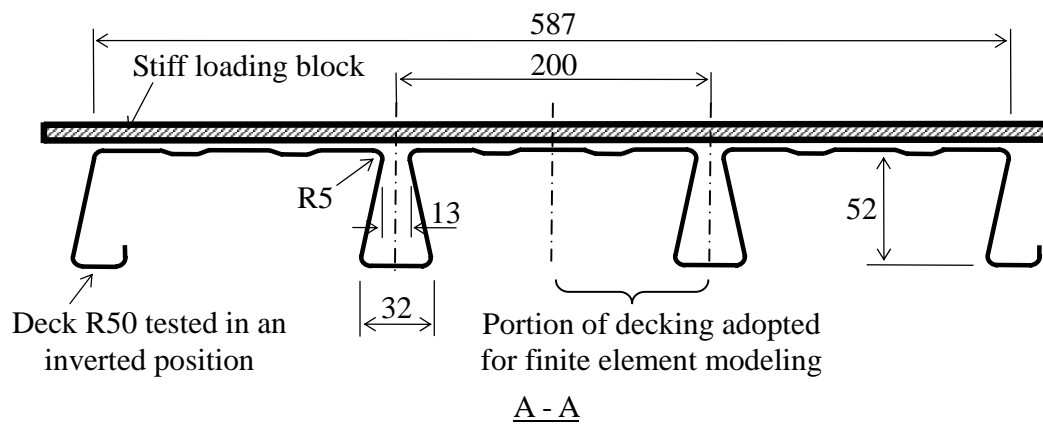


c) Finite element model under end loading condition

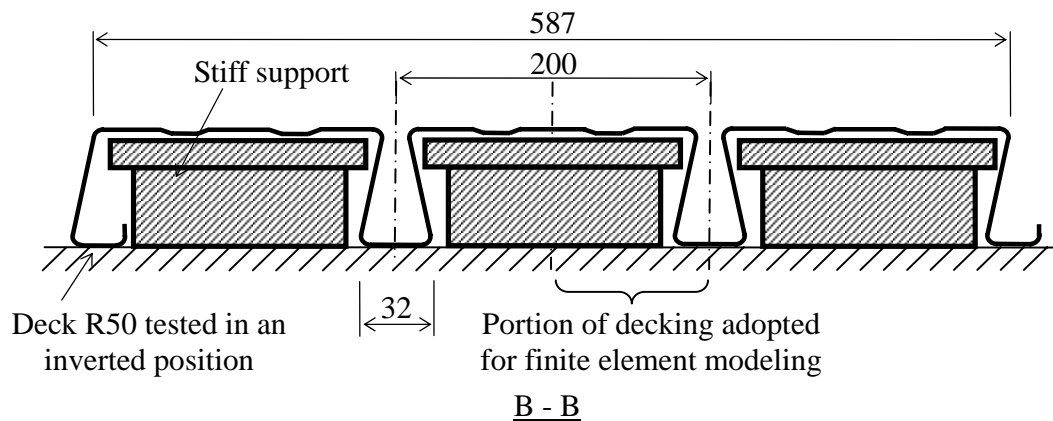
Figure 1.5: Finite element models for simulation of web crippling failure.



a) Overview of one-point load test



b) Cross sectional detail of the test specimen at the loaded position



c) Cross sectional detail of the test specimen at the support

Figure 1.6: Finite element models for simulation of section failure.

Chapter 2

Literature Review

2.1 Introduction

This chapter presents a collection of codified design methods as well as research findings regarding web crippling failure of cold-formed steel profiled decking. It should be noted that the review is not limited to cold-formed steel profiled decking, and other commonly used hot-rolled and cold-formed steel sections are also covered.

2.2 Studies of Web Crippling Failure

2.2.1 Empirical Equations

In hot-rolled steel members, the theory of web crippling is derived by considering load transfer from the region of load application to the end web fillets against web bearing failure, and also to mid-height of web against web buckling. However, the level of complexity in the web crippling of cold-formed steel sections and deckings increases dramatically because of the large corner radius to thickness ratios and the large web depth to thickness ratios. Hence, empirical formulae are commonly adopted to design against

web crippling failure for cold-formed steel sections and deckings, e.g. AISI (1996), BS5950: Part 5 (1998) and Part 6 (1995). A list of the difficulties in the theoretical derivation of the web crippling resistance of cold-formed steel sections and deckings (Yu Wei-Wen, 2000) is given as follows.

1. Non-uniform stress distribution along the load bearing width and the adjacent portions of the web leading to local yielding near the edge of the load bearing width of load application.
2. Elastic and inelastic buckling of the web.
3. Bending in the web caused by eccentric load (or reaction).
4. Initial out-of-plane imperfection of the web.
5. Different degrees of rotational restraints provided by the section flanges and interaction between the section flanges and the section web.
6. Inclined webs in the profiled decking.

2.2.1.1 NAS and AS4600

There were a number of experimental investigations into the web crippling behaviour of cold-formed steel members reported in the literature: Winter and Pian (1946), and Zetlin (1955) at Cornell University, Hetrakul and Yu (1978) at the University of Missouri Rolla. Baed on the results of these studies, web crippling design equations, as shown in Equation 2.1, was progressively developed into the present form adopted in AISI. It should be noted that the Australian Standard also adopted Equation 2.1 for design of

cold-formed steel profiled deckings and sections. As shown in Figure 2.1, a total of four different loading conditions, namely end one-flange loading (EOF), interior one-flange loading (IOF), end two-flange loading (ETF), and interior two-flange loading (ITF) were provided to cover the entire range of practical loading conditions.

$$R_b = C t_w^2 f_y \sin\theta \left(1 - C_r \sqrt{\frac{r_i}{t_w}} \right) \left(1 + C_l \sqrt{\frac{l_b}{t_w}} \right) \left(1 - C_w \sqrt{\frac{d_l}{t_w}} \right) \quad (2.1)$$

where C is the coefficient given in Tables 2.1 and 2.2 for profiled deckings and single web channel-sections, respectively;

t_w is the web thickness;

θ is the angle between the plane of the web and the plane of the bearing surface. θ shall range between 45° and 90° :

C_r is the coefficient of internal corner radius given in Tables 2.1 and 2.2 for profiled deckings and single web channel-sections, respectively;

r_i is the internal corner radius;

C_l is the coefficient of bearing length given in Tables 2.1 and 2.2 for profiled deckings and single web channel-sections, respectively;

l_b is the actual bearing length. In the case of two equal but opposite concentrated loads distributed over unequal bearing lengths, the smaller value of l_b shall be taken;

d_l is the depth of the flat portion of the web measured along the plane of the web.

2.2.1.2 BS5950: Parts 5 and 6

In BS5950: Part 6 (1995), similar design expressions for different practical loading conditions are given for end one flange (EOF) loading, interior one flange (IOF) loading, end two flange (ETF) loading and interior two flange (ITF) loading. However, a 50% reduction to the web crippling resistance is required for end loading condition, i.e. when the nearest edge of the applied load or the support reaction is located less than $1.5D_w$ from the end of the member, where D_w is the sloping distance between the intersection points of the web and the flanges. This reduction in the web crippling resistances is represented by the symbol Ω . The empirical equation from BS5950: Part 6 (1995) is given as follows.

$$P_w = 0.15 \Omega t^2 \sqrt{E p_y} \left(1 - 0.1 \sqrt{r/t}\right) \left(0.5 + \sqrt{\frac{N}{50t}}\right) \left\{2.4 + \left(\frac{\theta}{90}\right)^2\right\} \quad (2.2)$$

where r is the internal corner radius;

N is the length of the stiff bearing;

θ is the inclination of the web;

E is the modulus of elasticity;

p_y is the design strength of steel;

t is the net thickness of steel material;

$\Omega = 1.0$ if the applied load or the support reaction has its nearest edge at a distance of not less than $1.5 D_w$ from the end of the member;

$\Omega = 0.5$ if the nearest edge of the applied load or the support reaction is at a

distance of less than $1.5 D_w$ from the end of the member;

D_w is the sloping distance between the intersection points of a web and the flanges.

In comparison with the design rules for web crippling resistances for cold-formed sections, a much detailed consideration in the loading condition is included in BS5950: Part 5 (1998), i.e. the four loading conditions classified from the distance between the load and reaction force, and the distance between load and end of member, as shown in Figure 2.1. For cold-formed sections having single thickness webs with unstiffened flanges, the following equation should be used:

$$\text{For EOF condition: } P_w = t^2 k C_3 C_4 C_{12} [1350 - 1.73 (D/t)] \times [1 + 0.01 (N/t)] \quad (2.3)$$

$$\text{For IOF condition: } P_w = t^2 k C_1 C_2 C_{12} [3350 - 4.6 (D/t)] \times [1 + 0.007 (N/t)] \quad (2.4)$$

$$\text{For ETF condition: } P_w = t^2 k C_3 C_4 C_{12} [1520 - 3.57 (D/t)] \times [1 + 0.01 (N/t)] \quad (2.5)$$

$$\text{For ITF condition: } P_w = t^2 k C_1 C_2 C_{12} [4800 - 14 (D/t)] \times [1 + 0.0013 (N/t)] \quad (2.6)$$

where r is the internal corner radius;

t is the net thickness of steel material;

N is the length of the stiff bearing;

D is the overall depth of the web;

$$k = p_y / 228; \quad (2.7)$$

θ is the inclination of the web;

$$C_1 = (1.22 - 0.22k); \quad (2.8)$$

$$C_2 = (1.06 - 0.06r/t) \leq 1.0; \quad (2.9)$$

$$C_3 = (1.33 - 0.33k); \quad (2.10)$$

$$C_4 = (1.15 - 0.15r/t) \leq 1.0 \text{ but } \geq 0.5; \quad (2.11)$$

$$C_{12} = (0.7 - 0.3 (\theta/90)^2); \quad (2.12)$$

2.2.1.3 Eurocode 3: Part 1.3

Whereas for design rules in the EC3: 1.3, the following design equation is provided for profiled decking with unstiffened webs:

$$R_{w,Rd} = \alpha t^2 (f_{yb} E)^{0.5} [1 - 0.1 (r/t)^{0.5}] [0.5 + (0.02 l_a / t)^{0.5}] [2.4 + (\theta/90)^2] / \gamma_{M1} \quad (2.13)$$

where r is the internal corner radius;

l_a is the effective length of the stiff bearing;

θ is the inclination of the web;

E is the modulus of elasticity;

f_{yb} is the design strength of steel;

t is the net thickness of steel material;

$\alpha = 0.075$ for ITF and EOF conditions as shown in Figure 2.1;

$\alpha = 0.115$ for IOF conditions as shown in Figure 2.1;

$\gamma_{M1} = 1.1$

The formulation of the above equation is identical to Equation (2.2) but with different designation and with an additional safety factor γ_{M1} .

For design of web crippling resistances for cold-formed sections, similar approach is used as to the British Standard, which accommodates for the different loading condition as shown in Figure 2.1:

For end one-flange loading condition:

$$R_{w,Rd} = k_1 k_2 k_3 [9.04 - (h_w/t)/60] [1 + 0.01 (s_s/t)] t^2 f_{yb}/\gamma_{M1} \quad \text{with } s_s/t \leq 60 \quad (2.14)$$

$$R_{w,Rd} = k_1 k_2 k_3 [5.92 - (h_w/t)/132] [0.71 + 0.015 (s_s/t)] t^2 f_{yb}/\gamma_{M1} \quad \text{with } s_s/t > 60 \quad (2.15)$$

For interior one-flange loading condition:

$$R_{w,Rd} = k_3 k_4 k_5 [14.7 - (h_w/t)/49.5] [1 + 0.007 (s_s/t)] t^2 f_{yb}/\gamma_{M1} \quad \text{with } s_s/t \leq 60 \quad (2.16)$$

$$R_{w,Rd} = k_3 k_4 k_5 [14.7 - (h_w/t)/49.5] [0.75 + 0.011 (s_s/t)] t^2 f_{yb}/\gamma_{M1} \quad \text{with } s_s/t > 60 \quad (2.17)$$

For end two-flange loading condition:

$$R_{w,Rd} = k_1 k_2 k_3 [6.66 - (h_w/t)/64] [1 + 0.01 (s_s/t)] t^2 f_{yb}/\gamma_{M1} \quad (2.18)$$

For interior two-flange loading:

$$R_{w,Rd} = k_3 k_4 k_5 [21.0 - (h_w/t)/16.3] [1 + 0.0013 (s_s/t)] t^2 f_{yb}/\gamma_{M1} \quad (2.19)$$

where r is the internal corner radius;

h_w is the overall depth of the web;

s_s is the actual length of the stiff bearing;

f_{yb} is the design strength of steel;

t is the net thickness of steel material;

θ is the inclination of the web;

$$\gamma_{M1} = 1.1;$$

$$k = p_y / 228; \quad (2.20)$$

$$k_1 = (1.33 - 0.33 k); \quad (2.21)$$

$$k_2 = (1.15 - 0.15 r/t); \quad (2.22)$$

$$k_3 = 0.7 - 0.3 (\theta/90)^2; \quad (2.23)$$

$$k_4 = (1.22 - 0.22 k); \quad (2.24)$$

$$k_5 = (1.06 - 0.06 r/t); \quad (2.25)$$

2.2.2 Existing Experimental-Based Researches

Continual research have been carried out on web crippling behaviour of trapezoidal shaped panels (Wing B.A. and Schuster R.M. 1986, Studnicka J. 1991, and Avci O. and Easterling W.S. 2002) and test results are often evaluated against design equations such as AISI (1996) design equations. Similar to the study of cold-formed steel trapezoidal panel, many experimental studies on web crippling failure of cold-formed steel sections were carried out (Young B. and Hancock G.J. 2003, Holesapple M.W. and LaBoube R.A. 2003, LaBoube R.A., Yu W.W., Deshmukh S.U. and Uphoff C.A., 1999, Roberts T.M. and Newark A.C.B., 1997, Zhou F. and Young B. 2006).

While many web crippling investigations focused on the unfastened condition, Young B. and Hancock G.J. (2004) carried out tests on unlipped channels with fastened and unfastened flanges under both ETF and ITF loading conditions. For testing of one flange fastened sections, the bottom flange was bolted onto the support to provide a positional

restraint to the section flange. For testing of two flange fastened sections, bolts were provided to both the top and the bottom flanges to prevent any positional movement. Moreover, a coupled of tests on unlipped channels with unfastened flanges were also carried out. The experimental results of the web crippling resistances of unlipped channels with different flange fastening conditions were compared. In general, an increase in the web crippling resistances found to be within 1 to 7% for both flange fastened sections, when compared with one flange fastened sections. Moreover, increases in the web crippling resistances from 9 to 15% are achieved for one flange fastened sections, when compared with sections without fastened flanges. Back analyses on the test results using the design equations from Australian/New Zealand Standard and American Iron and Steel Institute Specification are also performed, and it is found that in general, these design codes provide unconservative resistances.

While many studies on web crippling behaviour of cold-formed steel sections and deckings, investigation into web crippling behaviour of stainless steel cold-formed sections was also of great interest. Korvink S.A., Van Den Berg G.J. and Van De Merwe P. (1995) carried out laboratory tests on cold-formed stainless steel lipped channels under concentrated loads. The tests cover three types of stainless steel, namely Type 304 and Type 430 stainless steel, as well as Type 3CR12 corrosion-resisting steel. For each type of specimens, the load bearing width-to-thickness ratios are found to range from 10.26 to 49.23 and with an overall height ranging from 90.0 to 317.7mm. The ASCE Specification (1990) was used to check against the test results. In summary, the average test-to-design resistance ratios are found to be 1.203, 1.072 and 1.105 for the aforementioned stainless steel types, respectively.

Similarly, Zhou F. and Young B. (2006) reported a study into cold-formed stainless steel sections. They presented an extensive experimental investigation into cold-formed stainless steel hollow sections under two loading conditions, namely, end-two-flanges and interior-two-flange loadings. Moreover, the test results of web crippling tests carried out by other researchers on cold-formed stainless steel lipped channel sections under both end-one-flange and interior-one-flange loading conditions were also adopted for back analyses using the design rules in both the North American Specification (NAS) and ASCE. In general, while unconservative web crippling resistances were evaluated from NAS under ETF loading condition, and from ASCE under both ITF and EOF loading conditions, conservative design resistances were obtained for all other cases. However, the average test-to-design ratio was found to be 5.11. Through validation of the test results of a wide range of cold-formed stainless steel sections and loading conditions, a unified equation is proposed which is considered to be applicable to cold-formed stainless steel sections with different steel grades and thicknesses under different loading conditions.

In addition to the research works of web crippling failure of channels studied by Young B. and Hancock G.J. (2004), an investigation into fastened channels subjected to high concentrated loads was also carried out by Fox. S.R. and Brodland G.W. (2003). However, a primary distinction between the works carried out by Young B. and Hancock G.J. (2004) is that screws are fastened on the webs of the channels against bearing stiffeners, as shown in Figure 2.2. Over 170 tests were conducted under end- and intermediate-two-flange loading conditions with different number of fastening screws adopted during the test. Numerical investigation was also reported, and finite element models were

established in accordance with the tests performed. Moreover, a parametric study was carried out to cover different channel thicknesses, web slenderness ratios, screw numbers and loading conditions. Based on the results from the parametric study, and together with the experimental results, an equation with accurate prediction on web crippling resistances was proposed. The proposed equation is found to be able to predict web crippling resistances with maximum discrepancies of 11% and 3% when compared with the test and the numerical results, respectively. Moreover, the proposed equation is able to predict web crippling resistances of channels with webs stiffened with different numbers of screws at various locations.

In general, numerical studies into the web crippling behaviour of cold-formed steel sections using finite element models are often carried out as a tool to provide visual stress patterns throughout the deformation ranges. This approach was performed by Sivakumaran K.S. (1989), and Xiao R.Y., Chin G.P.W. and Chung K.F. (2002) on lipped channel sections under IOF loading. However, while similar ultimate loads were obtained, discrepancy in the predicted displacement characteristic was observed due to the complicated loading and boundary conditions, such as flange curling effect and change in contact area.

Flange curling is a well known behaviour in both hot-rolled steel and cold-formed steel members. Generally, a flange with a low aspect ratio will induce large local deflection even subjected to a low applied load. Figure 2.3 (Winter, G, 1940) shows a load transfer mechanism from bending of an I section to flange curling. For I sections subjected to bending, both compressive and tensile stresses are induced at the top and the bottom

flanges respectively (Figures 2.3a and b). It is assumed that the compressive stresses and the tensile stresses are evenly distributed across the top and the bottom flanges (at the plane of the cross-section) respectively. As shown in Figure 2.3c, flange curling is resulted from the stresses at the top and the bottom flanges. Through integration along the member length, a design equation for flange curling was obtained. It should be noted that the primary factors contributive to flange curling are the width and the thickness of the flange, and the distance of the flange from the neutral axis.

2.2.3 Existing Theoretical-Based Researches

Due to the complexity of web crippling failure, theoretical formulation is too difficult for practical design, and design equations are often based on empirical formulation (Beshara B. and Schuster R.M., 2000). Young B. and Hancock G.J. (2001) have developed a refined design equation for web crippling failure based on plasticity failure mechanism. The mechanism assumes that the stresses disperse at specific angles from the regions of load application, and reach the yield strengths of the members at mid-height, as shown in Figure 2.4. Refer to Young B. and Hancock G.J. (2001) for details.

Another approach to predict the web crippling resistance of channel sections is to use the proposed equations developed by Rhodes J. and Nash D. (1998). These equations were derived from the conventional energy method as well as finite strip and finite element studies. The proposed equations enable both the web buckling and the web crushing resistances to be computed with relatively high accuracy, when compared with the finite

element results of channels with web height ranging from 50 to 200mm, and under different load bearing widths. A typical comparison of the theoretical and the numerical results presented by Rhodes J. and Nash D. (1998) is shown in Figure 2.5. It is noteworthy that significant reduction in the ultimate loads is observed in the numerical results with an impractical load bearing width close at 0mm. This reduction in the ultimate loads is resulted due to extremely high concentrated loads through the use of narrow load bearing widths. Such prediction matches closely with the proposed equation for web crushing resistance. Moreover, the phenomenon of reduction in web crippling resistances gradually vanished for load bearing widths greater than 40mm. Furthermore, the design equations in BS5950: Part 5 is evaluated by comparing the design values against the numerical results. In general, design equations tend to under-estimate the web crippling resistances, and the discrepancies increase with a decrease in the load bearing widths. For the case of 100 x 50 x 12.5 x 1mm channel sections under a load bearing width of 10mm, as shown in Figure 2.6, the design-to-numerical resistance ratio is found to be approximately 2.0. For the same section but with a load bearing width of 50mm, the design-to-numerical resistance ratio is found to be 1.25. As mentioned earlier that a high concentrated load is induced under an extremely narrow load bearing width, therefore, the large discrepancy in the design value for a load bearing width of 10mm indicates that the current design code does not take the issue into the design considerations, although narrow load bearing widths are not commonly used.

It should be noted in the literature that a yield line method on the web crippling behaviour of trapezoidal panels is reported by H. Hofmeyer et al (2002). In this semi-theoretical based approach, yield line patterns are acquired and the failure modes are classified into

three categories: rolling post-failure mode, yielding arc post-failure mode and yield eye post-failure mode. The physical failure modes together with the associated load-deflection curves are shown in Figure 2.7. Yield line pattern I indicates a symmetric yield pattern formed at the bottom flange, the corners intersecting the web and the bottom flange, and the bottom region of the web. Similar symmetric yield line pattern is also observed in yield line pattern II, but this time the yield lines propagate across the web height. In yield line pattern III, asymmetric eye pattern is found with yield lines appeared only on one side of the loaded bottom flange; this pattern may be caused by uneven load distribution.

Using the above yield line patterns together with the aid of finite element analyses, an accurate design equation was presented. However, due to the highly empirical-dependence of the equation, this equation might not be applicable to panels of different shapes, and therefore, similar design development work would be required for different sections and deckings.

2.3 Studies of Combined Effects

2.3.1 Empirical Equations

Empirical interaction formula for the design of combined bending and web crippling, and combined bending and shear are adopted in many design codes. Such an empirical formula was originated from a series of one-point load tests with specimens at various

span lengths. For one-point load tests with short span lengths, failure is primarily caused by web crippling while the effect of bending moment is considered to be small. The effect of bending moment to the web crippling resistance becomes more noticeable with increasing span length. A graphic representation of the empirical interaction formula is shown in Figure 2.8 (Bakker M.C.M., 1994). The symbols α , β and γ are the empirical parameters which vary from sections to sections.

It is shown that in the absence of a concentrated force, the moment capacity of a member can be fully achieved. Moreover, in the absence of bending moment, the web crippling resistance can also be fully achieved. If both bending moment and concentrated force are present at the same location, then interaction effect occurs, leading to significant reduction in both resistances.

2.3.1.1 BS5950: Parts 5 and 6

For design of profiled deckings subjected to combined effects, two checks are provided in BS5950: Part 6. The first check is the combined bending and shear shown in Equations 2.26 to 2.28, which the second check is the combined bending and web crippling shown in Equations 2.29 to 2.31:

$$F_v \leq P_v \quad (2.26)$$

$$M \leq M_c \quad (2.27)$$

$$\left(\frac{F_v}{P_v}\right)^2 + \left(\frac{M}{M_c}\right)^2 \leq 1 \quad (2.28)$$

$$F_w \leq P_w \quad (2.29)$$

$$M \leq M_c \quad (2.30)$$

$$\frac{F_w}{P_w} + \frac{M}{M_c} \leq 1.25 \quad (2.31)$$

where F_v is the applied shear force;

P_v is the design shear capacity;

F_w is the applied load;

P_w is the design web crippling resistance;

M is the applied moment;

M_c is the design moment capacity;

For the design of cold-formed sections, similar formulations is also found, which involves two separate checks and both checks are calculated in terms of moment and shear ratios, and moment and web crippling ratios.

For sections having single-thickness webs subjected to combined bending and shear:

$$F_v \leq P_v \quad (2.32)$$

$$M \leq M_c \quad (2.33)$$

$$\left(\frac{F_v}{P_v}\right)^2 + \left(\frac{M}{M_c}\right)^2 \leq 1 \quad (2.34)$$

For sections having single-thickness webs subjected to combined bending and web crippling:

$$F_w \leq P_w \quad (2.35)$$

$$M \leq M_c \quad (2.36)$$

$$1.2 \left(\frac{F_w}{P_w} \right) + \left(\frac{M}{M_c} \right) \leq 1.5 \quad (2.37)$$

2.3.1.2 AS4600

In accordance to the AS4600, the design provision for profiled deckings with unstiffened webs under combined bending and shear is:

$$\text{For } \frac{V^*}{\phi_v V_v} \leq 0.7 \text{ and } \frac{M^*}{\phi_b M_s} \leq 0.5: \quad \left(\frac{V^*}{\phi_v V_v} \right)^2 + \left(\frac{M^*}{\phi_b M_s} \right)^2 \leq 1 \quad (2.38)$$

$$\text{Otherwise:} \quad \left(\frac{V^*}{\phi_v V_v} \right)^2 + 0.6 \left(\frac{M^*}{\phi_b M_s} \right)^2 \leq 1.3 \quad (2.39)$$

where V^* is the shear force;

V_v is the shear capacity;

M^* is the bending moment;

M_s is the moment capacity;

ϕ_b is the capacity reduction factor for bending;

= 0.90;

ϕ_v is the capacity reduction factor for shear;

= 0.90;

The design provision for profiled deckings under combined bending and web crippling is:

$$0.82 \left(\frac{R^*}{\phi_w R_b} \right) + \left(\frac{M^*}{\phi_b M_s} \right) \leq 1.32 \quad (2.40)$$

where R^* is the concentrated force;

R_b is the web crippling capacity;

ϕ_w is the capacity reduction factor for web crippling given in Table 2.1;

It should be noted that the design rules given in Equations 2.38 and 2.39 are also applicable to cold-formed sections under combined bending and shear. However, for cold-formed sections having single unstiffened webs subjected to combined bending and web crippling, the design provision is:

$$1.07 \left(\frac{R^*}{\phi_w R_b} \right) + \left(\frac{M^*}{\phi_b M_s} \right) \leq 1.42 \quad (2.41)$$

2.3.1.3 Eurocode 3: Part 1.3

For design of cold-formed sections subjected to combined effects, two separate checks of combined bending and shear, and combined bending and web crippling are required. The interaction formulae of these checks are identical to the Equations 2.28 and 2.31.

2.3.2 Experimental and Numerical-Based Researches

An experimental investigation into combined bending and web crippling failure was preformed (Sutton F.S. & LaBoube R.A., 2003, Young B. & Hancock G.J. 2002) and the test results were compared against different specifications, In general, the occurrence of local buckling induces great difficulty in the numerical modeling of the web crippling behaviour. As a result, uniformly distributed load is no longer appropriate, and the best solution is by adopting contact or spring elements which allow a change in the loading area explicitly along the entire deformation history. Alternatively, Akhand A.M. et al (2004) chose to model the web crippling behaviour of re-entrant profiled deckings with the application of pressures only at the web-flange intersections. It should be noted that these regions are where the loading blocks are observed to remain in contact with the members throughout the tests. In addition to the test loading condition, four additional finite element models with different analytical parameters are used: linear elastic analysis, analysis with material nonlinearity only, analysis with geometrical nonlinearity only, and analysis with both material and geometric nonlinearities. The results of the models are presented in Figure 2.9 (Akhand A.M. et al, 2004).

It is shown that the finite element models with only geometric non-linearity can predict the initial stiffness accurately. Moreover, the finite element models with both material and geometric non-linearities are capable to predict ultimate loads accurately. However, the prediction of deformation is accurate only at the initial loading stage. The finite element model predicts that the failure occurs at vertical deformation of approximately 7.5mm while the test result shows that the failure only occurs at a vertical deformation of 10mm.

While the discrepancy in the vertical displacement of failure is large, the ultimate load and the initial deformation are well predicted. Hence, this analysis implies that the failure of the profiled decking is controlled by both geometrical and material properties.

In addition to the numerical study, combined bending and web crippling failure was studied analytically by Davies J.M. and Jiang C. (1997) and an improved theory for Pseudo-Plastic design was proposed. This design theory, validated against re-entrant and trapezoidal deckings, assumes the formation of plastic hinges at and near the internal supports, as shown in Figure 2.10.

Solving the failure mechanism in Figure 2.10 using virtual work, the redistribution of bending moment after the onset of yielding or the buckling of internal support is included. Although the validity of this theory was assessed, the moment-rotation relationship is essential for completion of the calculation, and therefore laboratory testing or finite element analysis is inevitable to compute this relationship.

Another approach to predict the ultimate loads of the combined failure is to adopt the analytical model presented by Hofmeyer H. et al (2001). The proposed analytical model is applicable to trapezoidal steel deckings. The analytical model enables the prediction of two failure modes, one is the yield arc mechanism under high concentrated loads while the other is the yield eye mechanism under high bending moment. The computation procedure of the model is rather complicated, and therefore it is readily used in practical design. Comparison on the predicted ultimate loads from the analytical model with those resistances obtained from Eurocode 3 (1996) is carried out and same accuracy as to the

design equations is found.

While a lot of studies were found to focus on web crippling or combined bending and web crippling failure, few researches examine the combined bending and shear failure. Shan M.Y. et al (1996). performed an experimental investigation into the combined bending and shear failure on channel sections with web openings. In the test program, three different web opening sizes, 38.1 x 101.6mm, 19.1 x 101.6mm and 19.1 x 50.8mm, were selected. Test specimens were simply supported and a concentrated load is applied on the top flanges of the specimens. Simultaneous bending failure at mid-span and diagonal shear failure across the web opening were observed, as shown in Figure 2.11. Based on the experimental results, the validity of the interaction equation in the American Iron and Steel Institute (AISI) specification was examined. The comparison is summarized graphically in Figure 2.12. The design equations is found to over-predict the actual ultimate load in almost all tests. It is noteworthy that the shear capacities and the moment capacities of the corresponding test specimens subjected to combined bending and shear failure are obtained through tests.

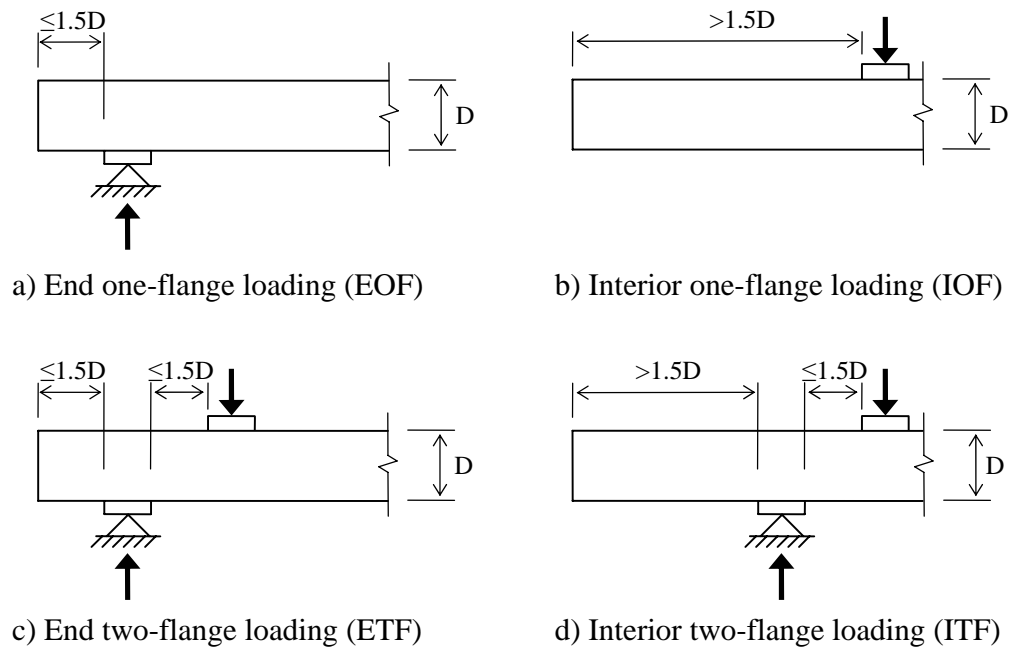


Figure 2.1: Loading conditions.

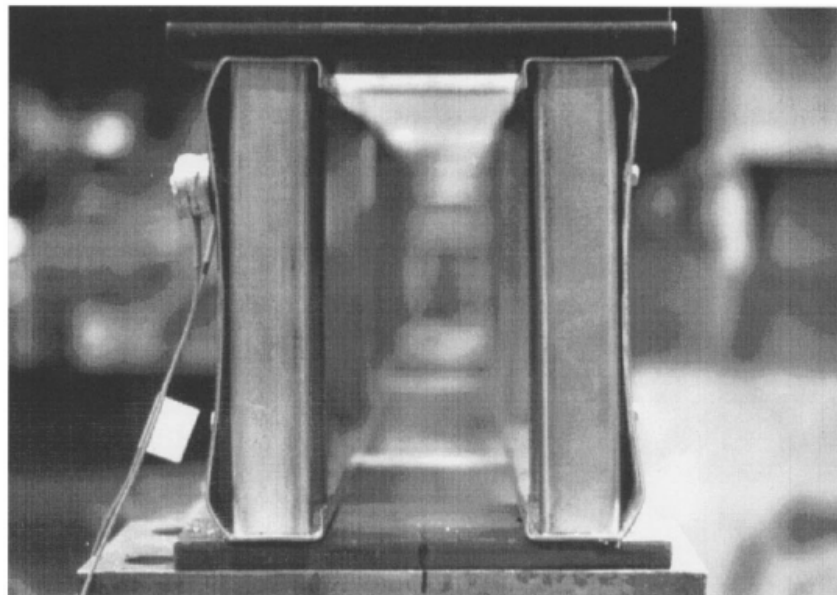


Figure 2.2: Web crippling tests with stiffened webs
(Fox, S.R. and Brodland G.W. 2003).

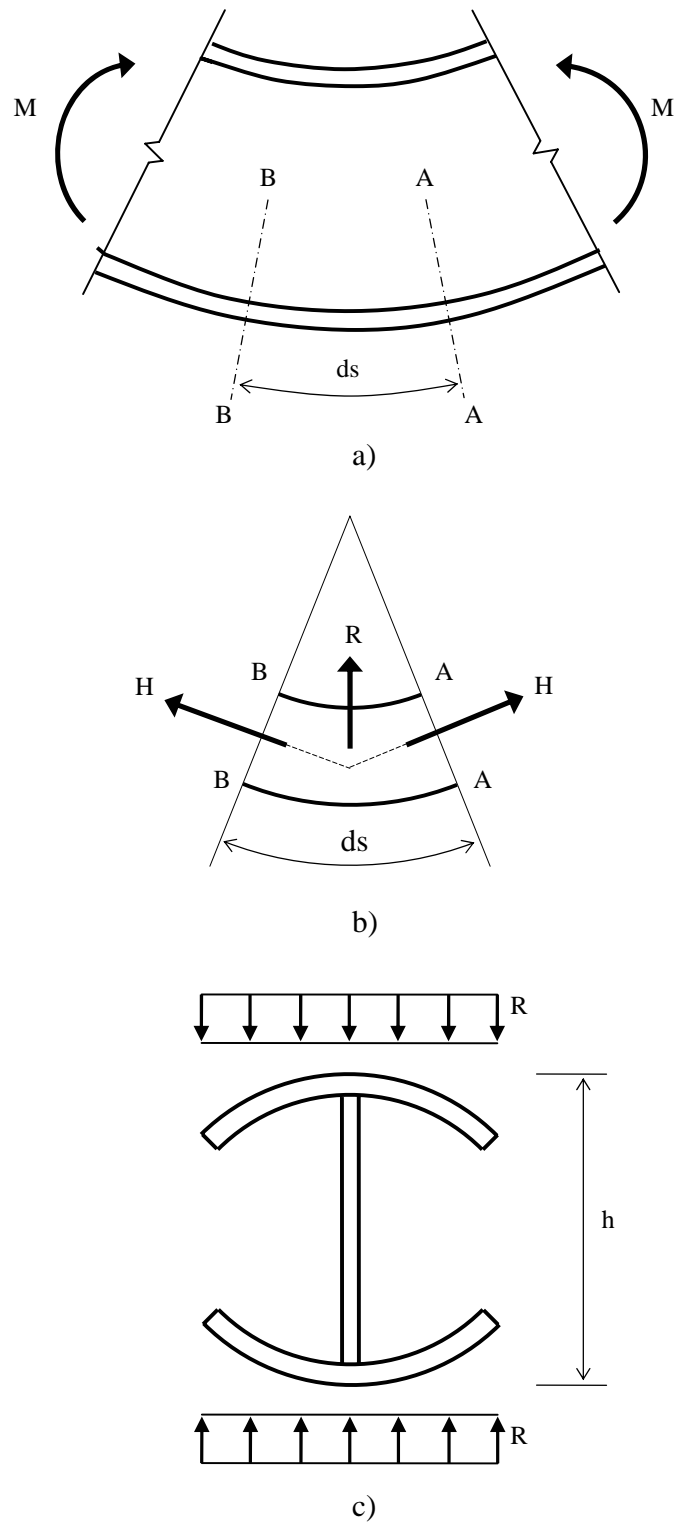


Figure 2.3: Flange curling phenomenon a) beam elemental length b) flange element length c) beam cross-section.

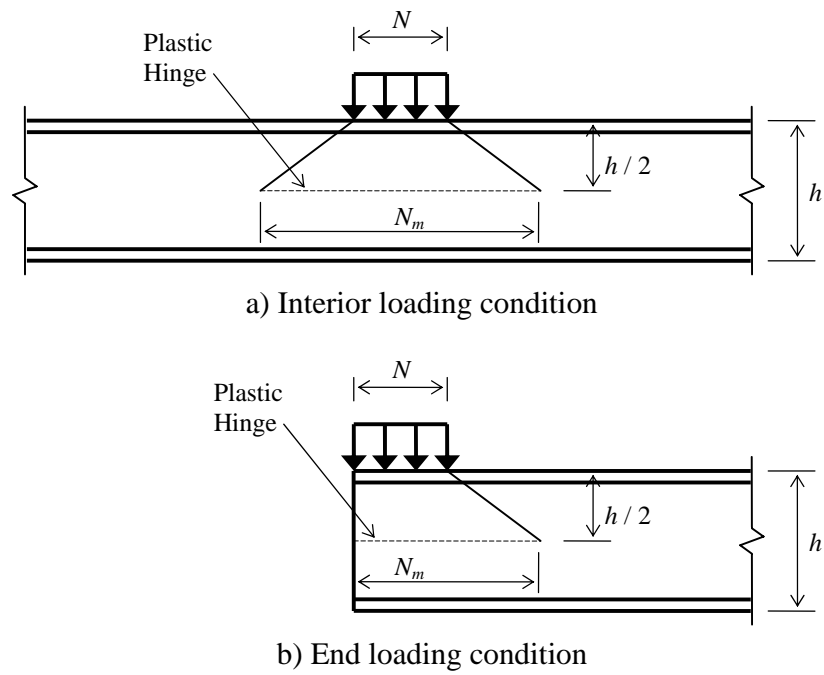


Figure 2.4: Proposed web crippling mechanism.

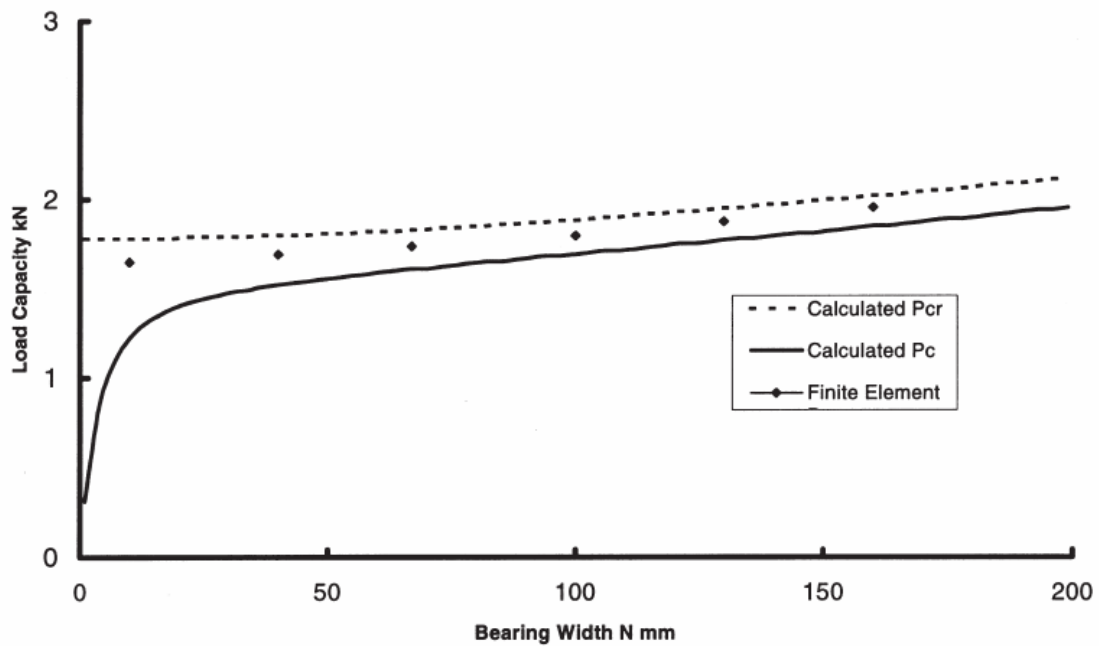


Figure 2.5: Comparison of design values with finite element results (Rhodes J. and Nash D. 1998).

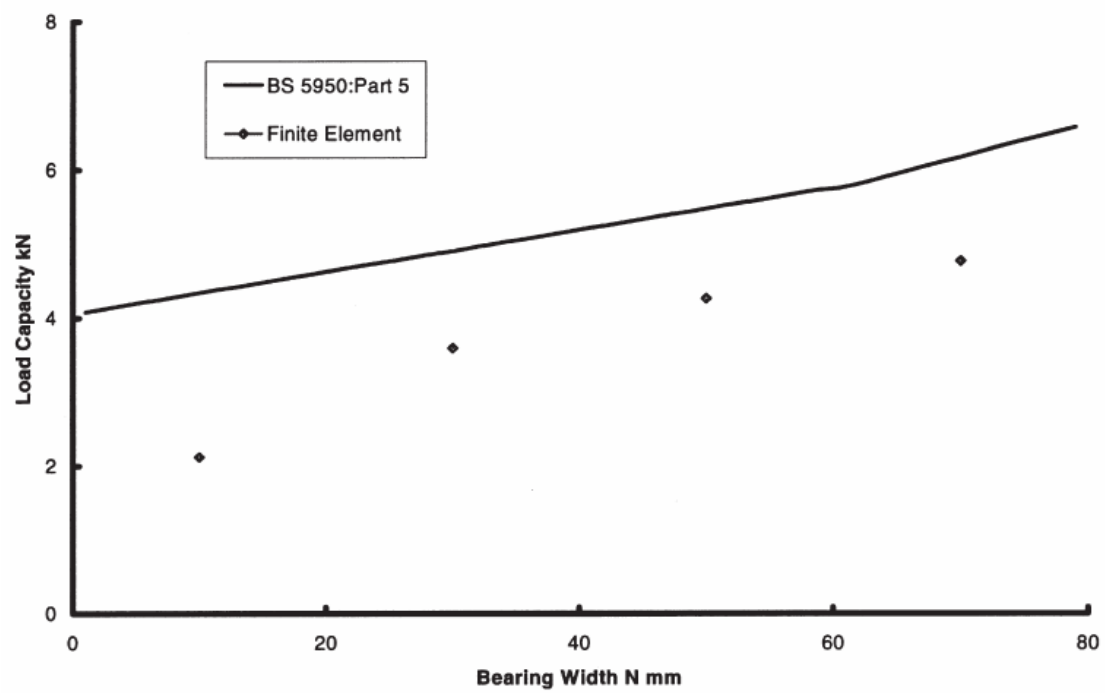


Figure 2.6: Comparison of web crippling capacity of 100 x 50 x 12.5 x 1 mm channel section (Rhodes J. and Nash D. 1998).

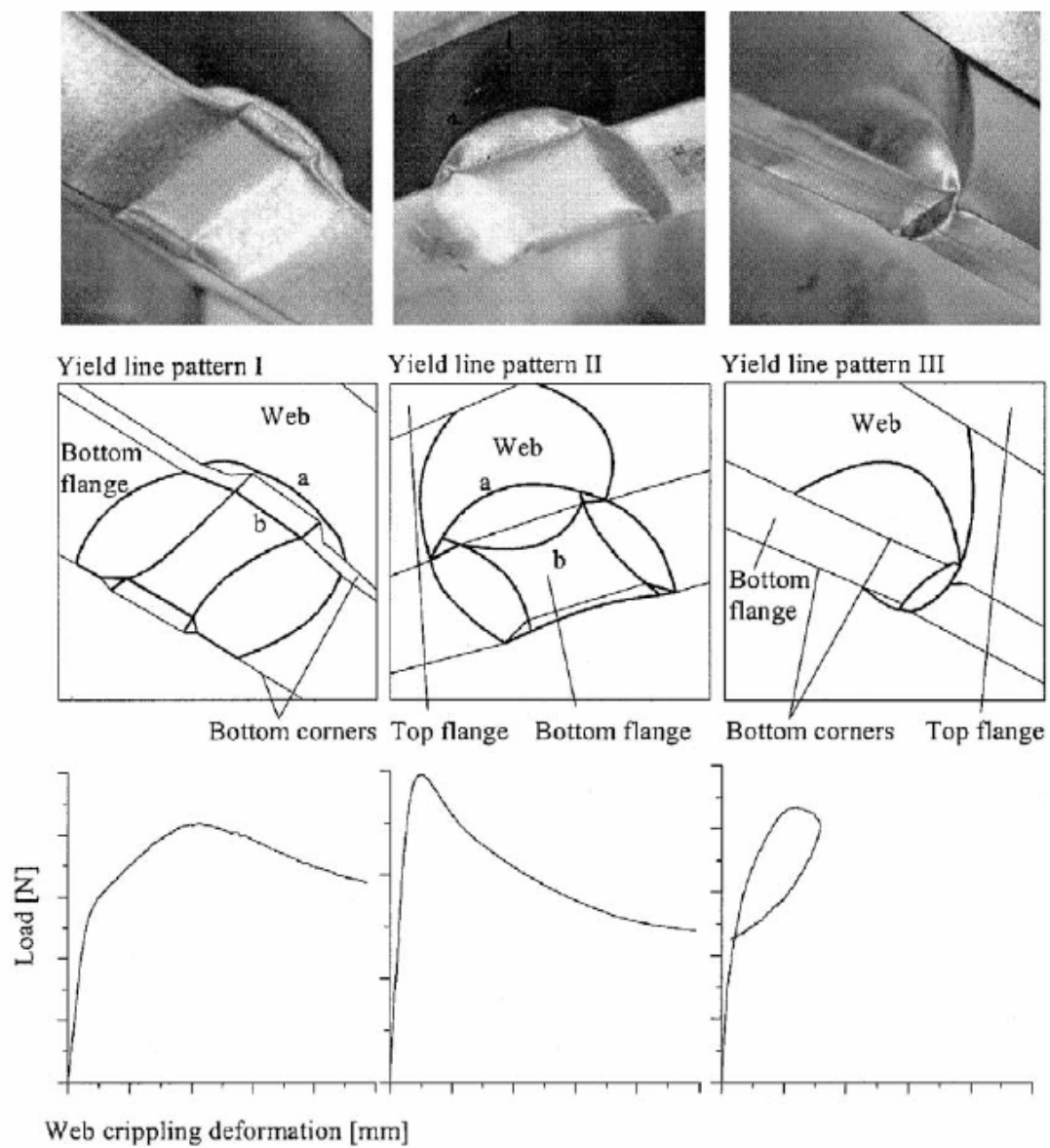


Figure 2.7: Web crippling failure modes studied by H. Hofmeyer et al (2002).

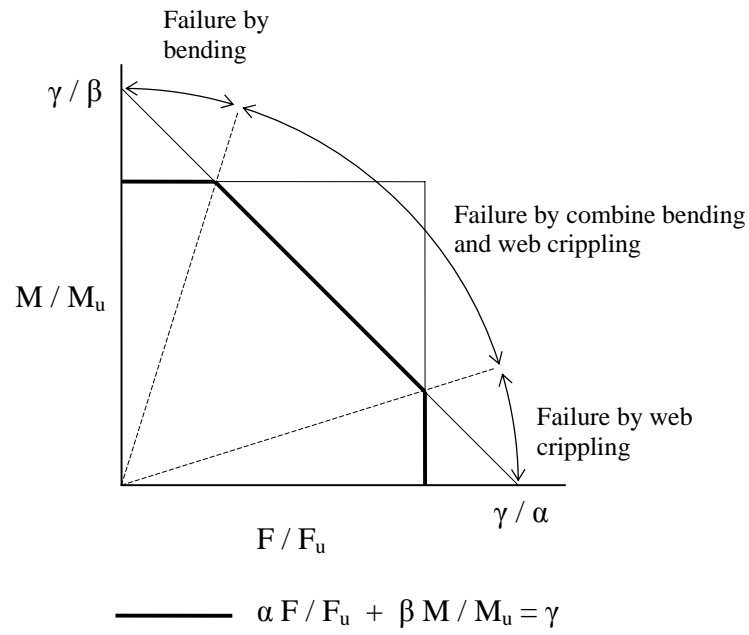


Figure 2.8: Interaction for combined bending and web crippling.

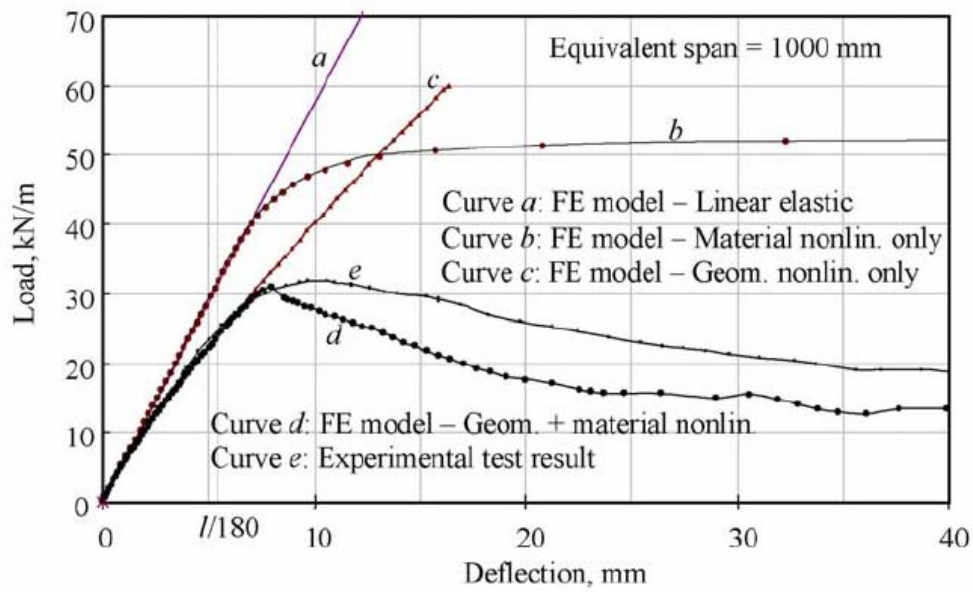


Figure 2.9: Numerical results for combined bending and web crippling (A.M. Akhand et al, 2004).

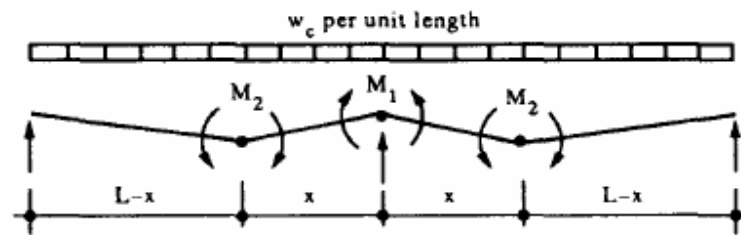


Figure 2.10: Proposed failure mechanism by J.M. Davies et al (1997).

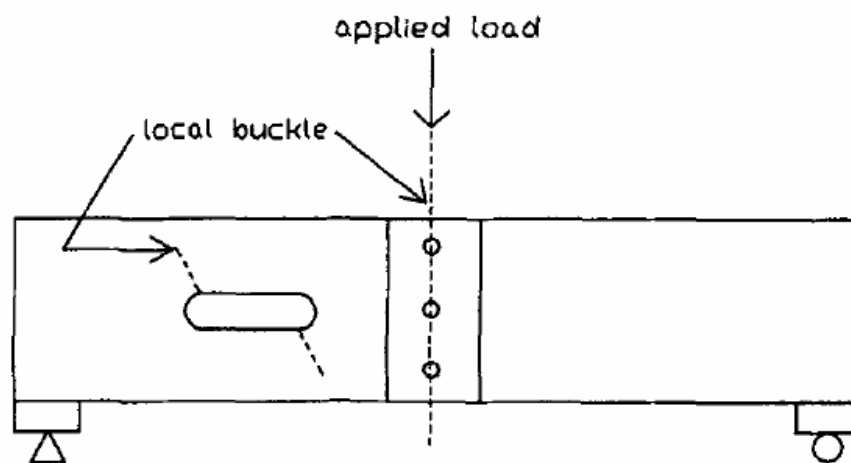


Figure 2.11: Experimental result of combined bending and shear failure by Shan M.Y., LaBoube R.A. and Yu W.W (1996).

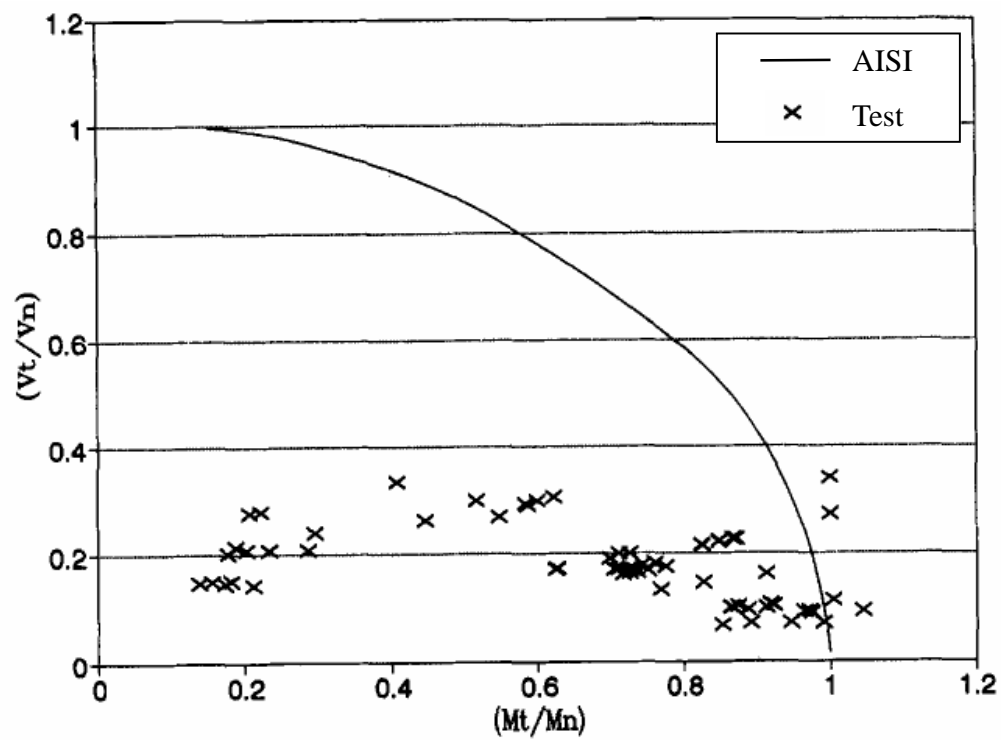


Figure 2.12: Load capacities subjected to combined bending and shear failure by Shan M.Y., LaBoube R.A. and Yu W.W (1996).

Table 2.1: Coefficients for the design of profiled deckings under web crippling resistances to AISI and AS4600.

Support conditions	Load cases		C	C_r	C_l	C_w	ϕ_w	Limits
Fastened to support	One-flange loading or reaction	End	4	0.04	0.25	0.025	0.90	$r_i/t_w \leq 20$
		Interior	8	0.10	0.17	0.004	0.85	$r_i/t_w \leq 10$
	Two-flange loading or reaction	End	9	0.12	0.14	0.040	0.85	$r_i/t_w \leq 10$
		Interior	10	0.11	0.21	0.020	0.85	
Unfastened	One-flange loading or reaction	End	3	0.04	0.29	0.028	0.60	$r_i/t_w \leq 20$
		Interior	8	0.10	0.17	0.004	0.85	
		End	6	0.16	0.15	0.050	0.90	$r_i/t_w \leq 5$
		Interior	17	0.10	0.10	0.046	0.90	

Table 2.2: Coefficients for the design of single web channel-sections under web crippling resistances to AISI and AS4600.

Support conditions		Load cases		C	C_r	C_l	C_w	ϕ_w	Limits
Fastened to support	Stiffened or partially stiffened flanges	One-flange loading or reaction	End	4	0.14	0.35	0.02	0.85	$r_i/t_w \leq 9$
			Interior	13	0.23	0.14	0.01	0.90	$r_i/t_w \leq 5$
		Two-flange loading or reaction	End	7.5	0.08	0.12	0.048	0.85	$r_i/t_w \leq 12$
			Interior	20	0.10	0.08	0.031	0.85	
Unfastened	Stiffened or partially stiffened flanges	One-flange loading or reaction	End	4	0.14	0.35	0.02	0.80	$r_i/t_w \leq 5$
			Interior	13	0.23	0.14	0.01	0.90	
		Two-flange loading or reaction	End	13	0.32	0.05	0.04	0.90	$r_i/t_w \leq 3$
			Interior	24	0.52	0.15	0.001	0.80	
	Unstiffened flanges	One-flange loading or reaction	End	4	0.40	0.60	0.03	0.85	$r_i/t_w \leq 2$
			Interior	13	0.32	0.10	0.01	0.85	$r_i/t_w \leq 1$
		Two-flange loading or reaction	End	2	0.11	0.37	0.01	0.75	$r_i/t_w \leq 1$
			Interior	13	0.47	0.25	0.04	0.80	

Chapter 3

Experimental Investigation into Web Crippling Failure

3.1 Introduction

In this chapter, an extensive experimental investigation into the web crippling failure of the cold-formed profiled steel decking R50 is carried out. Special attention is given to investigate the effects of steel grade, thickness, load bearing width and loading condition to the web crippling behaviour of the profiled decking. Moreover, the validity of the current design BS5950: Part 6 is evaluated through careful comparison against experimental results.

3.2 Experimental Investigation

An extensive experimental investigation into web crippling failure of cold-formed profiled steel decking are conducted at the Heavy Structures Laboratory of the Department of Civil and Structural Engineering. It should be noted that with the help of steel building product supplier, all the test specimens with the same steel grades and same thicknesses are cold-rolled from the same steel coils. This will improve the consistency of

the test results due to the minimized variations in both materials and manufacturing process.

3.2.1 Tensile Tests

In order to obtain the mechanical properties of the profiled deckings, a total of 10 tensile tests are carried out, two for each profiled decking of different steel grades and thicknesses.

The tensile tests are carried out according to the test procedures given in BS10001: Part 1 (2001) for the evaluation of material properties such as the yield strength and the Young's modulus. The bare metal thicknesses of the profiled decking are measured after the galvanized coatings at the surfaces of the specimens are removed using sand papers carefully in order to ensure that no metal of the coupon specimens is sanded off. A summary of the material properties are given in Table 3.1.

3.2.2 Test Program of Web Crippling Tests

As mentioned previously, the steel grade, thickness, load bearing width N_b and loading condition are the four primary parameters under investigation. Therefore, web crippling tests with a wide range of combination of the aforementioned parameters are conducted.

The cross sectional shape of the profiled decking is shown in Figure 1.1 with detailed dimensions while Tables 3.2 presents the scope of the test program. However, it should be noted that Deck R50 of grade 235 steel with a thickness of 1.20mm is not included in the test program. As shown in Table 3.2, each specimen is given a designation according to the steel grade, the thickness, the load bearing width and the loading condition. The representation of each designation is explained as follows:

$$“Lsw-n”$$

where L denotes the loading condition:

= I for internal loading condition

= E for end loading condition

s denotes the specimen type:

= a for profiled decking with a steel grade of 235 and a thickness of 0.75mm

= b for profiled decking with a steel grade of 235 and a thickness of 1.00mm

= c for profiled decking with a steel grade of 550 and a thickness of 0.75mm

= d for profiled decking with a steel grade of 550 and a thickness of 1.00mm

= e for profiled decking with a steel grade of 550 and a thickness of 1.20mm

w denotes the load bearing width:

= 1 for a loading bearing width of 50mm

= 2 for a loading bearing width of 100mm

= 3 for a loading bearing width of 150mm

= 4 for a loading bearing width of 200mm

n denotes the test number:

= 1 for test number one

= 2 for test number two

= 3 for test number three

A total of 52 web crippling tests are carried out each under internal and end loading conditions.

3.2.3 Instrumentation for Internal Loading Condition

The test setup of the web crippling tests under internal loading condition is shown in Figures 3.1 and 3.2. A test specimen with a member length of 600mm is placed onto a 400mm long support. It should be noted that lateral restraints are provided along the external webs of the profiled decking in order to prevent excessive cross-section distortion, or section spreading. Such restraint condition is achieved by fastening the external webs of the test specimens against steel angle sections using C-clamps, and the steel angle sections are also fastened securely to the support using C-clamps.

In each test, a vertical load is applied through a stiff loading block to the mid-length of the test specimen. The stiff loading block is comprises of a steel I section and a wooden

block covered with a steel plate at its bottom. The steel plate is the interface that comes to direct contact with the test specimen, and it is provided to eliminate any local deformation of the wooden block. The length of the stiff loading block is about 1000mm long which is adequate to cover the entire width of the profiled decking allowing the load to spread evenly.

Vertical displacements of the stiff loading blocks are measured using displacement transducers throughout the loading history. It should be noted that the locations of the transducers are positioned to measure the vertical displacements of the stiff loading block instead of the profiled decking in order to avoid improper measurements caused by potential local buckling. Therefore, the points where the vertical displacements are measured are located at the steel plate that comes into direct contact with the profiled decking. In order to determine possible rotations in the loading block during testing, eight displacement transducers are positioned at different locations in the trial tests of profiled decking with load bearing widths of 50 and 200mm to ensure measurement of a consistent vertical displacement of the stiff loading block. The locations of the displacement transducers are shown in Figures 3.3 and 3.4. After justifying that no rotation occurs in the stiff loading block, the eight displacement transducers are replaced with only two displacement transducers positioned at the two ends of the steel plate, as shown in Figures 3.1 and 3.2. A summary of the two instrumentations, i.e. the basic instrumentation with only 2 transducers, and the detailed instrumentation with 8 transducers, are presented in Table 3.2.

3.2.4 Instrumentation for End Loading Condition

For web crippling tests under end loading condition, the test setup is similar to that for tests under internal loading condition. A 600mm long profiled decking is positioned onto a 400mm long support. However, unlike the internal loading condition where the applied loading, the profiled decking and the support are all aligned at the mid-length, the loading is applied to one end of the profiled decking while the edge of the support is aligned with the edge of the profiled decking under end loading condition. Typical view of the test setup is shown in Figures 3.5 and 3.6.

Similar to the internal loading condition, eight displacement transducers are used to measure the vertical displacements of the profiled decking, as shown in Figures 3.7 and 3.8. It should be noted that in order to maintain a consistent test setup with the internal loading condition, the detailed instrumentation, with 8 displacement transducers are only adopted in tests involving load bearing widths of 50mm and 200mm while the other tests adopt only the basic instrumentation with 2 displacement transducers, as shown in Figures 3.5 and 3.6. A summary on the instrumentation is presented in Table 3.2.

3.2.5 Failure Modes and Observations

Among all the tests, the following two modes of failure are observed in the failed profiled decking: For specimens tested under internal loading condition, the failure mode WI is

identified as shown in Figure 3.9 where local failure is observed at the web-trough corner which is directly under the point of load application. Apparent local plate buckling in the trough of the decking is observed well before the web crippling failure.

For specimens tested under end loading condition, the failure mode WE is identified, as shown in Figure 3.10. Local failure is also observed at the web-trough corner at the inner edge of the load application length (i.e. section P-P in Figure 3.10b) while excess web buckling is apparent near the web-flange corner at the outer edge of the load application length (i.e. section Q-Q in Figure 3.10c). Local plate buckling in the trough of the decking is also observed well before the web crippling failure.

3.2.6 Load-Displacement Curves

As there are a number of transducers adopted in the web crippling tests, the vertical displacements at specific reference points are presented for easy comparison. The reference point, R_i , is adopted in profiled decking under the internal loading condition while the reference point, R_e , is adopted in profiled decking under end loading condition, as shown in Figure 3.11. In general, only the measured rotation about the x axis of the stiff loading block, θ_x , for tests under end loading condition is found to be significant while the rotations about both the y and the z axes of the stiff loading block, θ_y and θ_z , for both the internal and the end loading conditions are found to be very small. A summary

of the calculation expressions of the reference points under internal and end loading conditions are shown in Table 3.4.

Whereas for the vertical displacement, the experimental load-displacement curves of the web crippling tests are shown in Figures 3.12 to 3.29. Through observations on the test results, it is noticed that at the initial stage of the loading application, relatively large vertical displacement is measured under a small applied load, hence, the stiffness of the profiled decking is small. As the applied load increases, the slope gradually increases to a constant value and this slope is considered to be the nominal stiffness of the profiled deckings. This is caused by deficient provision of lateral restraint to the profiled decking which allows lateral movement of the profiled deckings under loads. In general, the lack of full lateral restraint will cause significant reduction to the rigidity but not the resistance of the profiled deckings. An extensive investigation into the effect of lateral restraint into the web crippling behaviour of profiled decking is carried out with advanced finite element analysis, refer to Chapter 4 for details.

3.2.7 Data Analyses

A summary of the measured web crippling resistances is shown in Table 3.4 while the normalized test results are presented in Figures 3.20 and 3.21. It should be noted that the normalized test results are calculated by linear conversion from measured thicknesses and yield strengths to normalized values, for example, from a measured thickness of 0.79mm

to a normalized thickness of 0.75mm, and from a measured yield strength of 649 N/mm² to a normalized yield strength of 550N/mm².

The self weights of the load attachments have been included in the values of the ultimate loads of the test specimens. As shown in Figures 3.20 and 3.21, the relationships between the web crippling resistances and the load bearing widths are shown to be fairly linear under both the internal and the end loading conditions. Hence, the non-linear design equation given in BS5950: Part 6 (1995) is found to be too complicated, and therefore simple design equations with linear functions are considered to be more rational. Furthermore, the web crippling resistances under both internal and end loading conditions shown to have increased with higher steel grades. However, for profiled decking within the same thickness and the same loading condition, steeper slopes are resulted in the web crippling resistance to bearing width curves with grade 550 steel than those with grade 235 steel, as shown in Figures 3.20 and 3.21. This shows that larger increase in the web crippling resistances against the load bearing width are achieved in profiled decking with grade 550 steel.

3.3 Comparison between Test and Design Results

Test results are compared with the design resistances obtained from BS5950: Part 6 (1995). According to BS5950: Part 6, the design values of the web crippling resistances P_w for Deck R50 is determined according to Equation 2.2. For ease of comparison, the

design resistances and the normalized test results are summarized in Table 3.5, Figure 3.20 and Figure 3.21.

Comparison of the design and the normalized test results shows that Equation 2.2 underestimates the web crippling resistances of all Decks R50. With the lowest and the highest test-to-design ratios of 1.11 for Test Aa4 and 2.68 for Test Bc3, respectively, this design equation clearly shows its conservatism in predicting the web crippling resistance of profiled deckings, in particular, for profiled deckings with high strength steel. Moreover, it is also evident that the web crippling resistances are reduced to 78% of their basic values when the end loading condition is adopted, as shown in Tests Ae1 and Be1. Such increment is considered to be significantly different from the design rules given in BS5950: Part 6 where only 50% of the web crippling resistances is permitted.

3.4 Summary

A systematic experimental investigation into the web crippling behavior of cold-formed profiled steel decking R50 is reported in which a total of 104 profiled decking with different steel grades, and thicknesses under different load bearing widths in both internal and end loading conditions are carried out. Lateral restraints are provided to the test specimens in order to simulate the practical loading condition. Study on the load-displacement curves reveals that while most profiled deckings are effectively restrained in the tests, there are some profiled deckings, in particular thick profiled deckings, exhibit

certain flexibility during the web crippling tests. It should be noted that when no lateral restraints are provided to the profiled decking in web crippling tests, the measured web crippling resistance tend to be the lower bound values. In the presence of effective lateral restraint, the measured web crippling resistances are significantly higher. Moreover, it is evident from the load-displacement curves that the deformation characteristics of the profiled decking are also significantly affected by the effectiveness of lateral restraints. Lastly, the suitability of the design rules given in BS5950: Part 6 has been evaluated through comparisons between the test and the design values of the web crippling resistances. In general, very conservative design values are obtained when compared with the test data, in particular, for those profiled deckings with high strength steel.

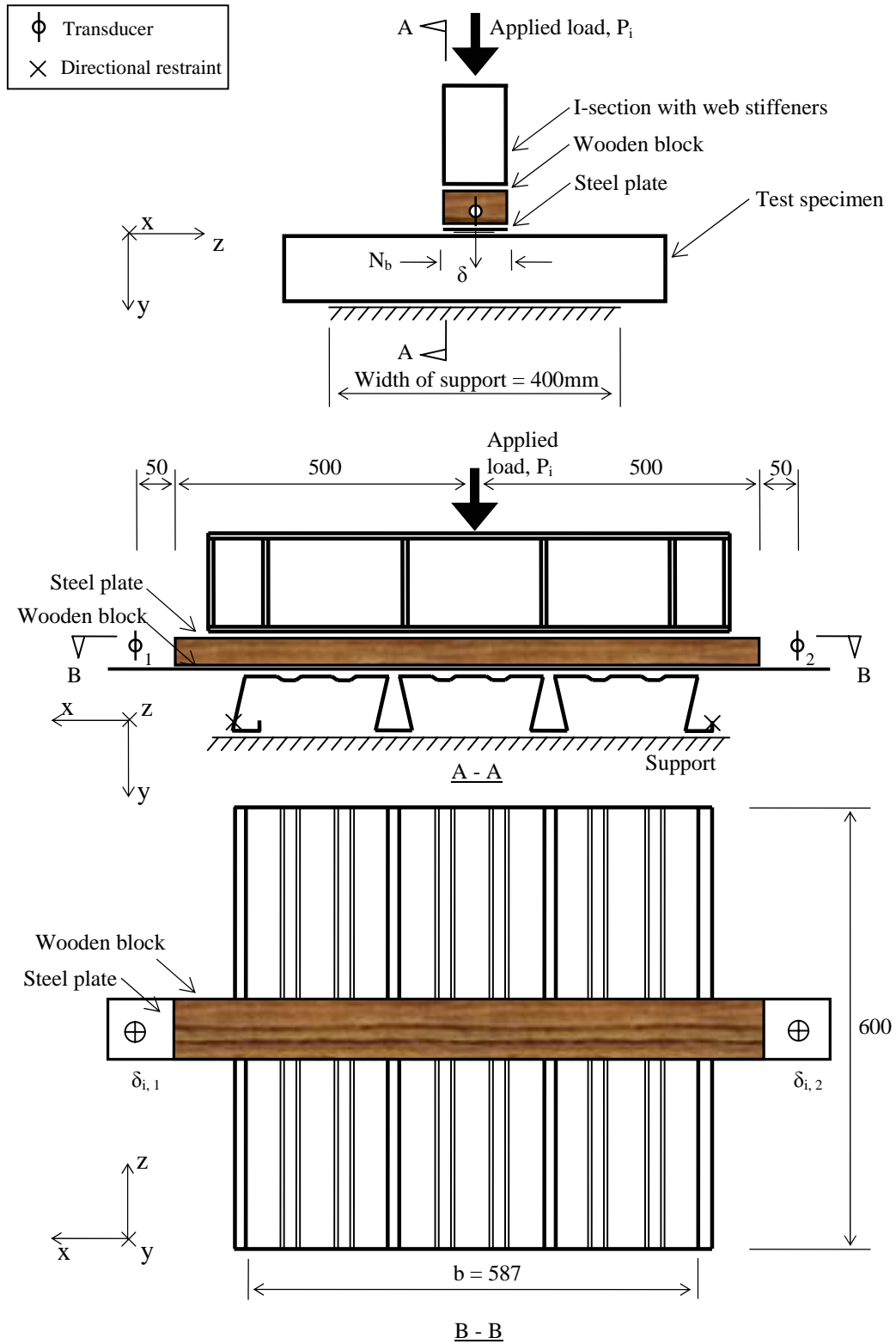


Figure 3.1: Typical set-up of web crippling test under internal loading condition with basic instrumentation.

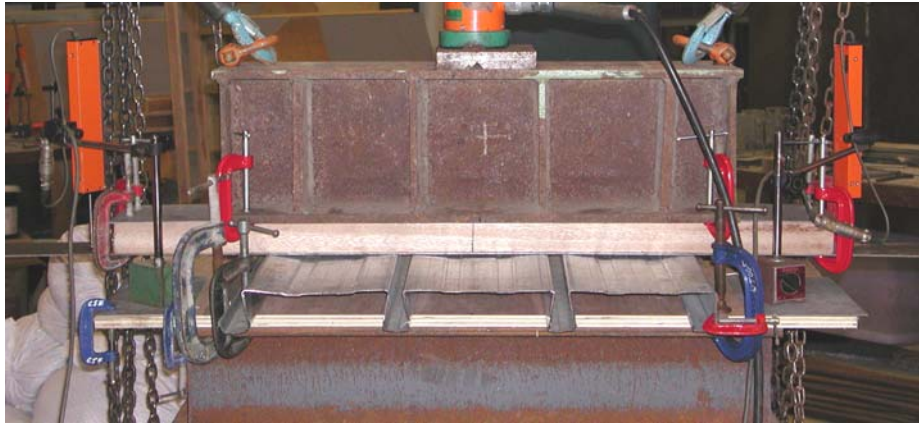


Figure 3.2: General view of web crippling test under internal loading condition with basic instrumentation.

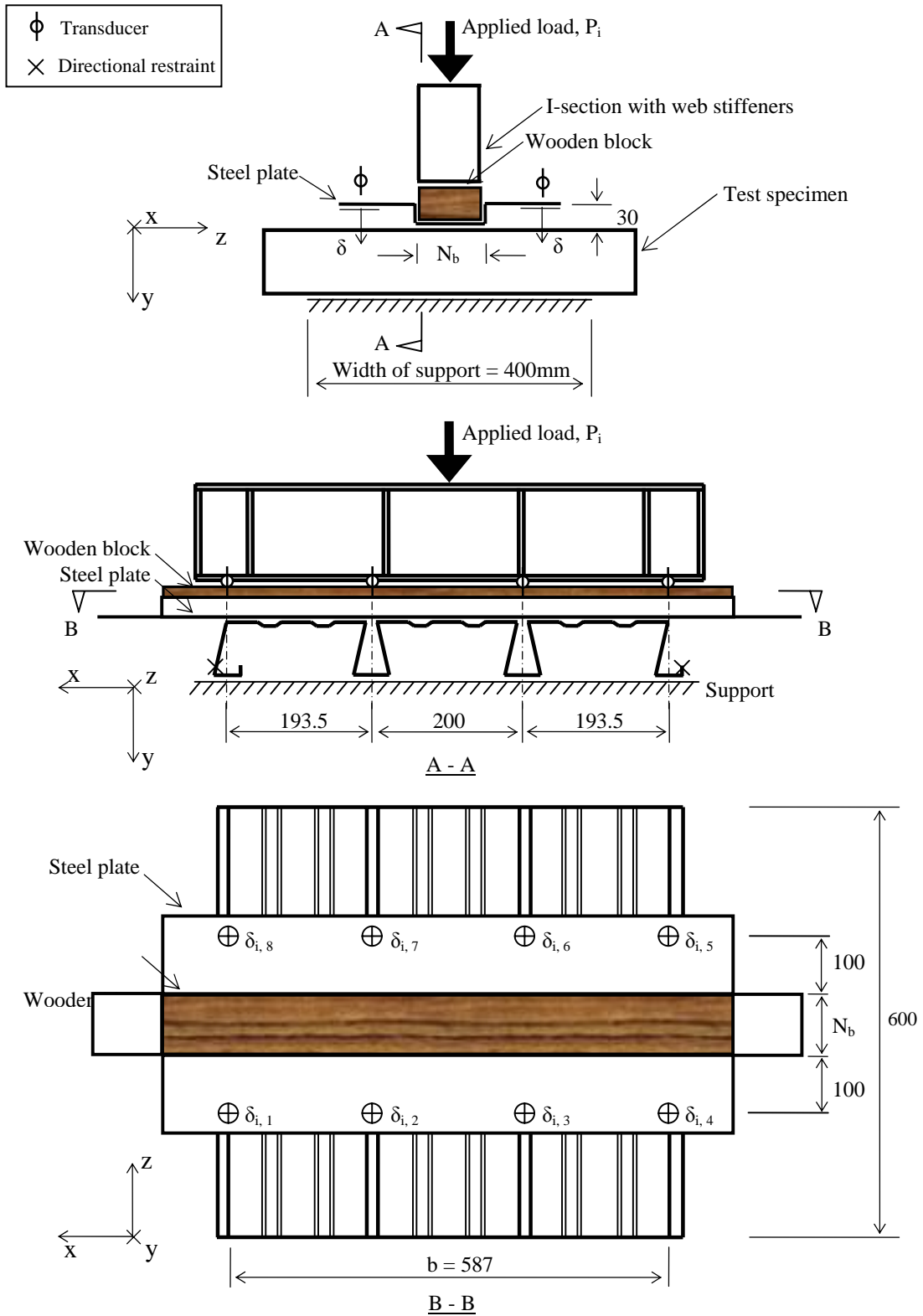


Figure 3.3: Typical set-up of web crippling test under internal loading condition with detailed instrumentation.



Figure 3.4: General view of web crippling test under internal loading condition with detailed instrumentation.

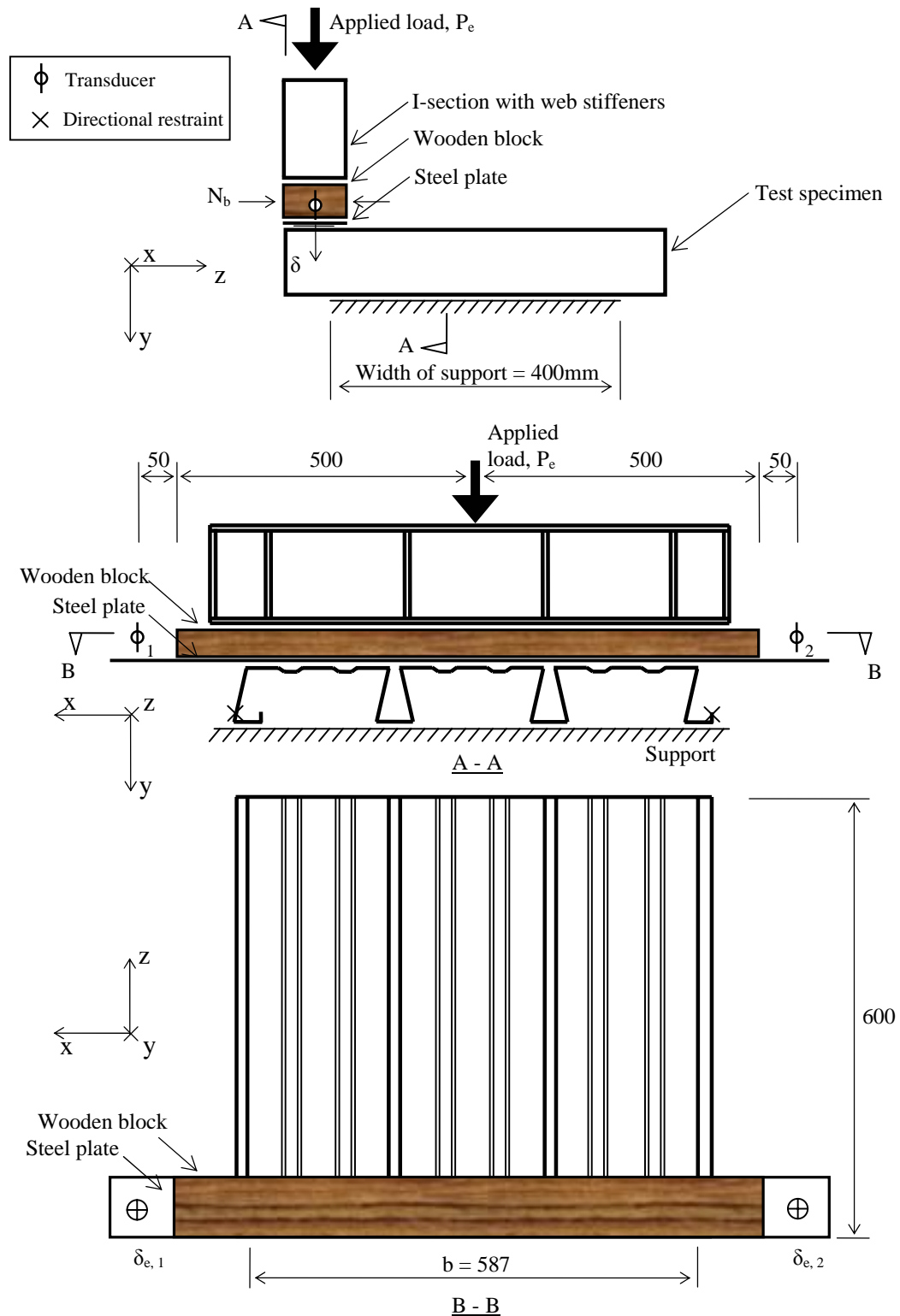


Figure 3.5: Typical set-up of web crippling test under end loading condition with basic instrumentation.



Figure 3.6: General view of web crippling test under end loading condition with basic instrumentation.

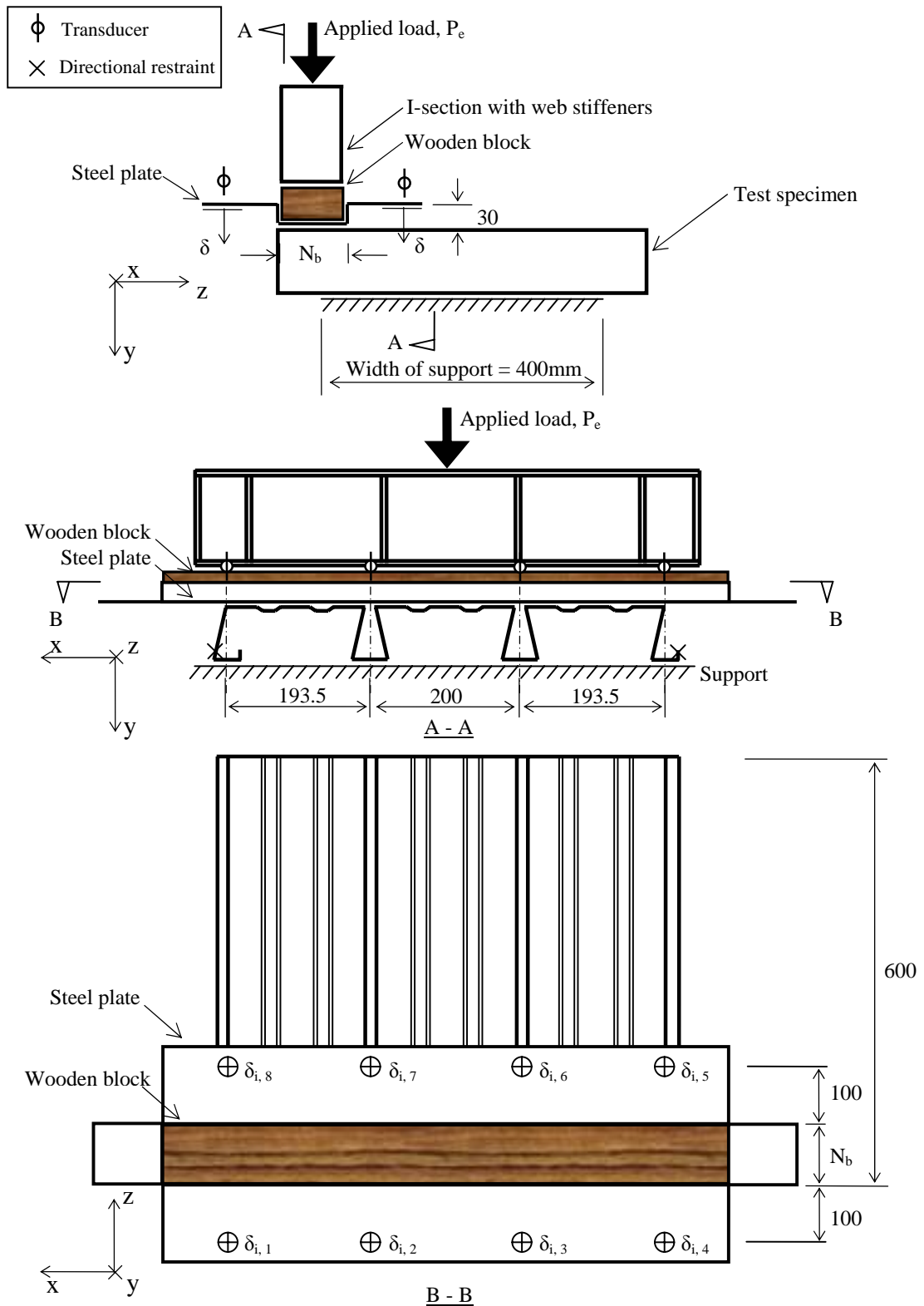


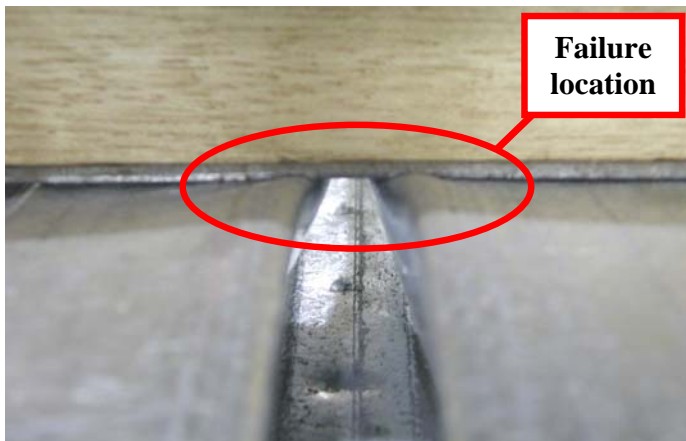
Figure 3.7: Typical set-up of web crippling test under end loading condition with detailed instrumentation.



Figure 3.8 General view of web crippling test under end loading condition with detailed instrumentation.



a) Overall view



b) Close-up

Failure mode WI:

Local failure at the
web-trough corner

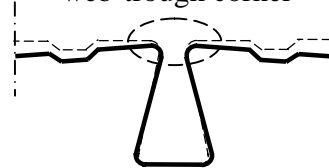


Figure 3.9: Typical failure mode of web crippling under internal loading condition.



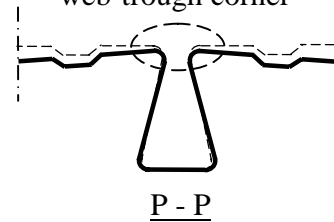
a) Overall view



b) Close-up

Failure mode WE:

Local failure at the web-trough corner



c) Large deformation at Region L.

Web buckling near the web-flange corner

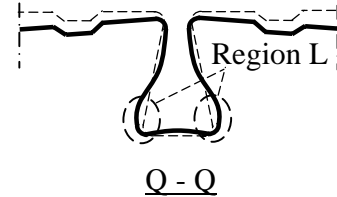


Figure 3.10: Typical failure mode of web crippling under end loading condition.

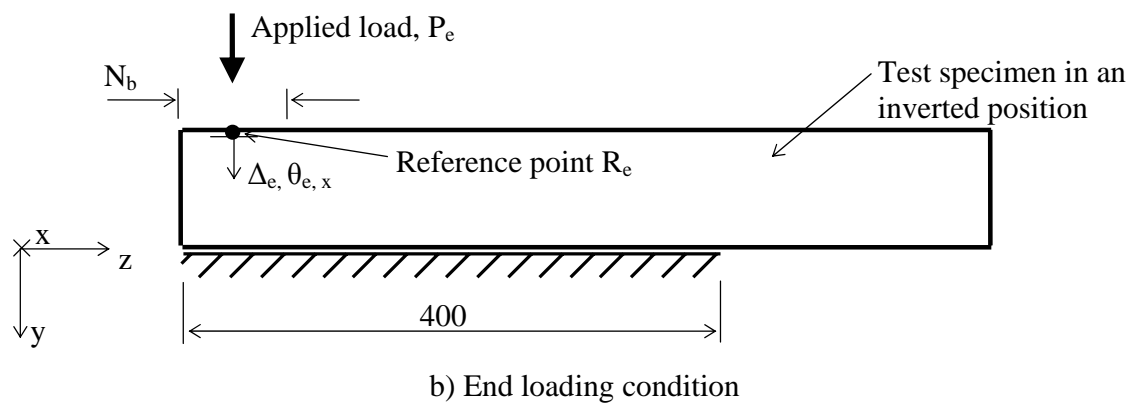
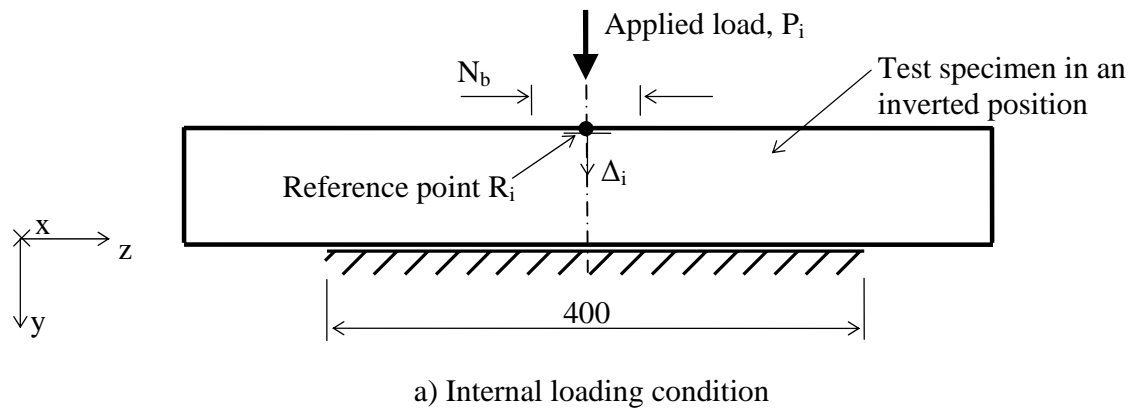
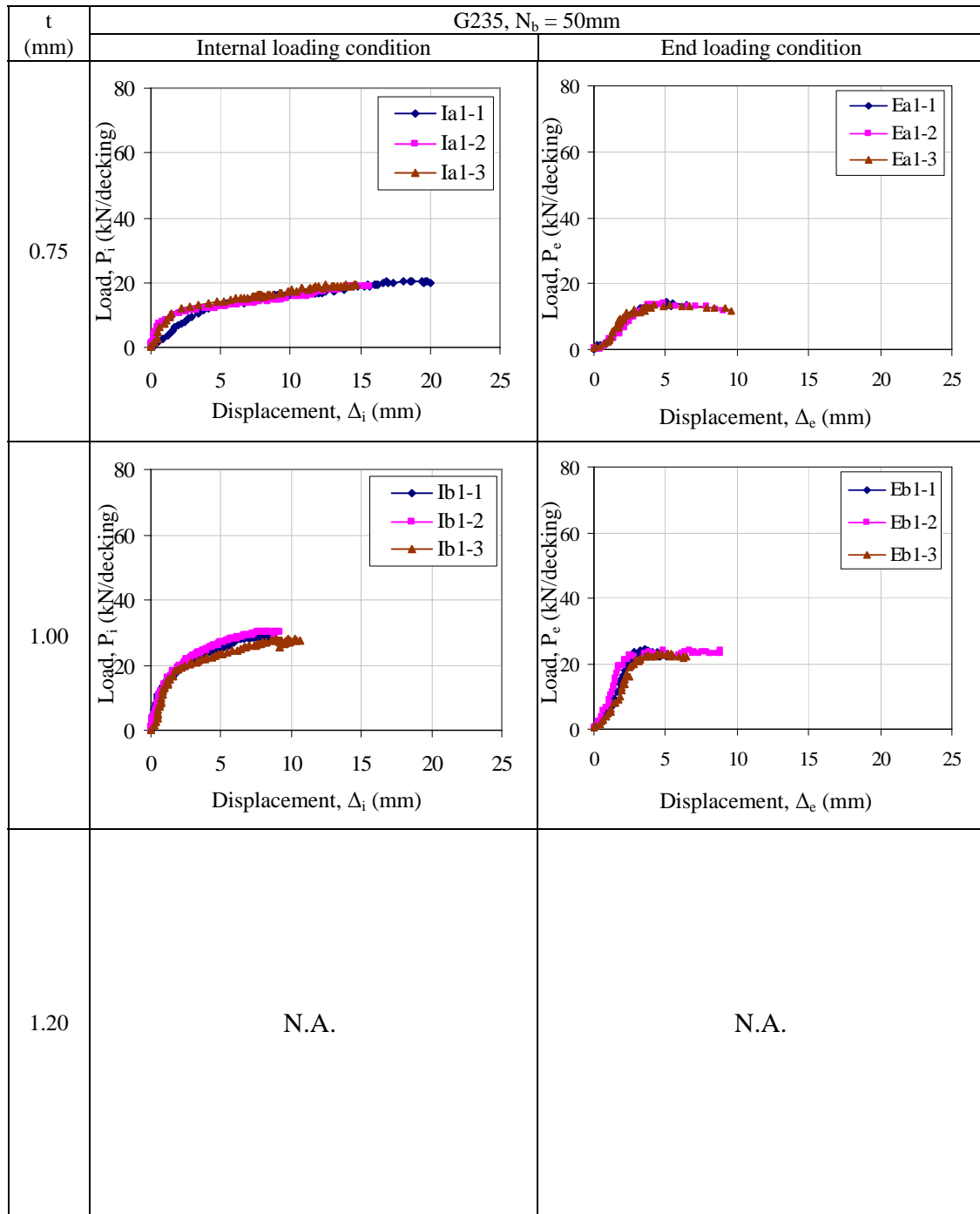
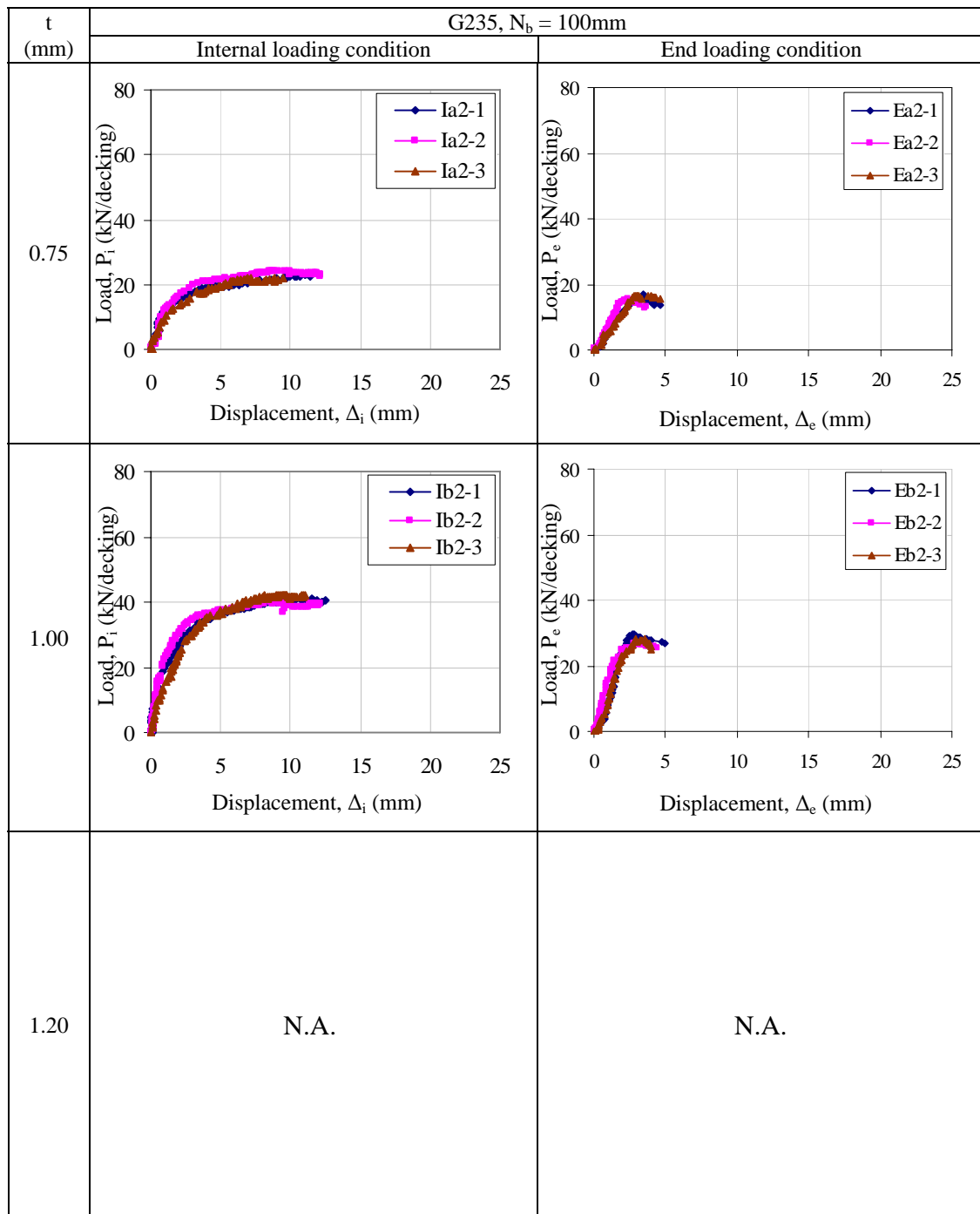
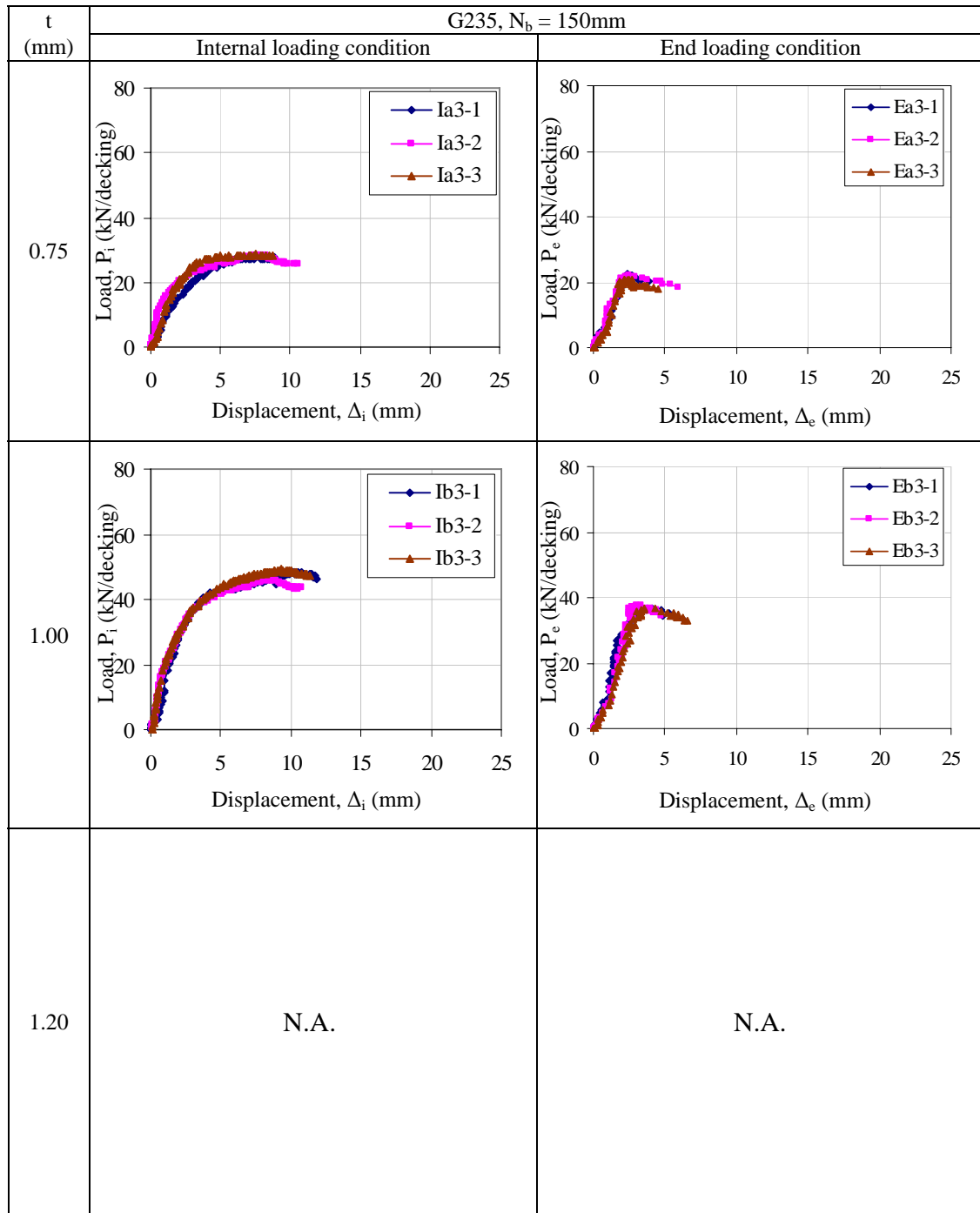
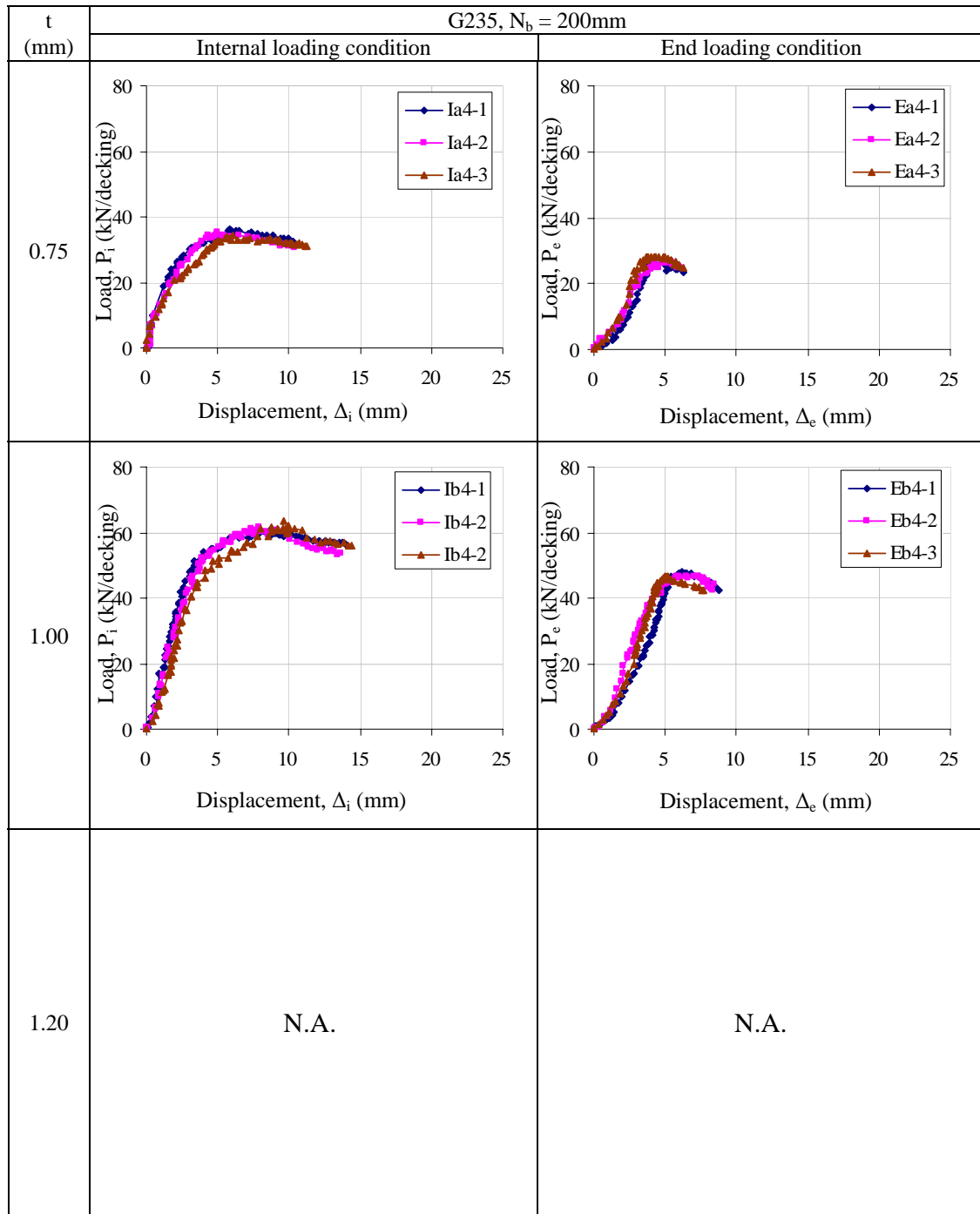


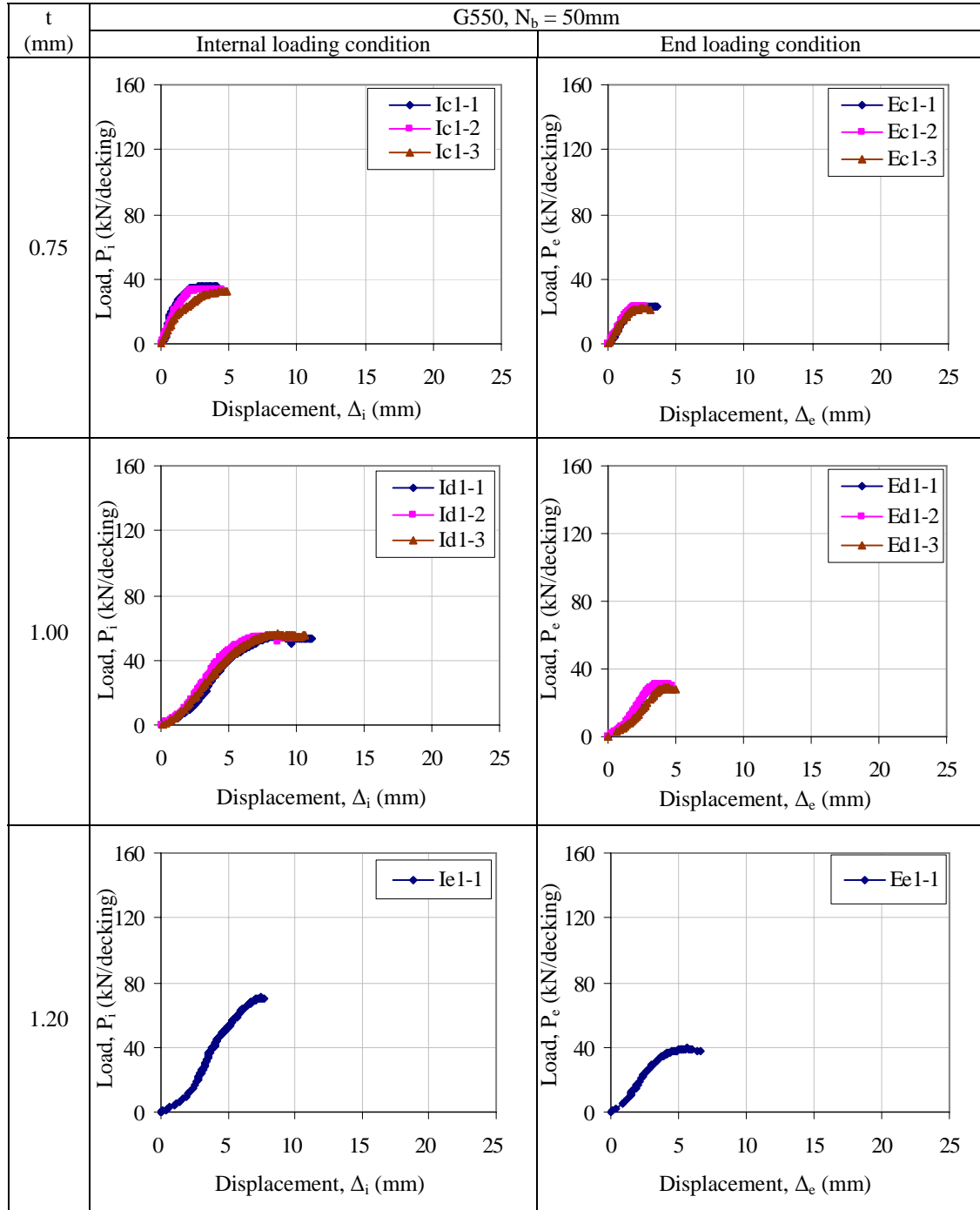
Figure 3.11: Displacements and rotations of reference points.

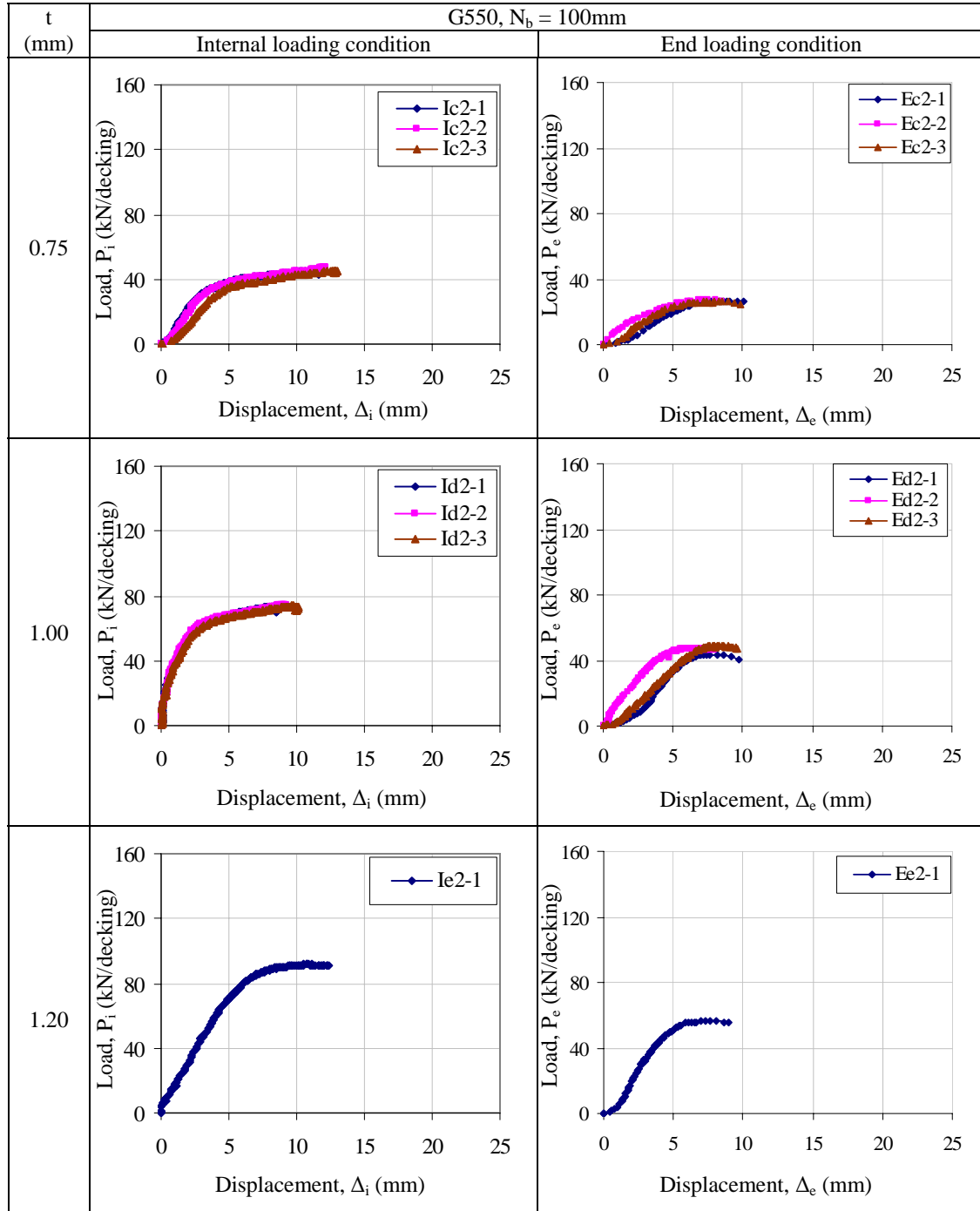
Figure 3.12: Load-deflection curves of web crippling tests: G235, $N_b = 50\text{mm}$.

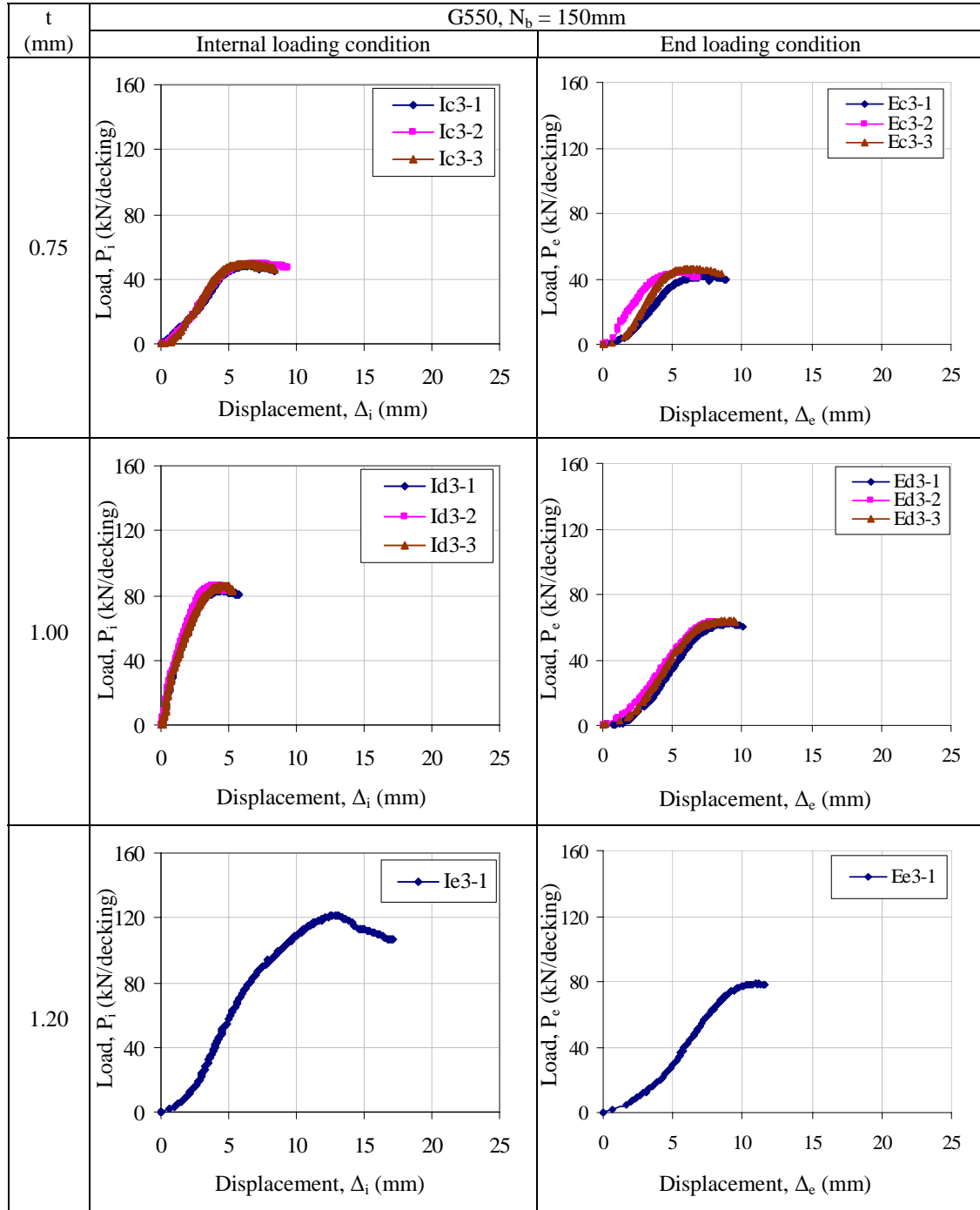
Figure 3.13: Load-deflection curves of web crippling tests: G235, $N_b = 100\text{mm}$.

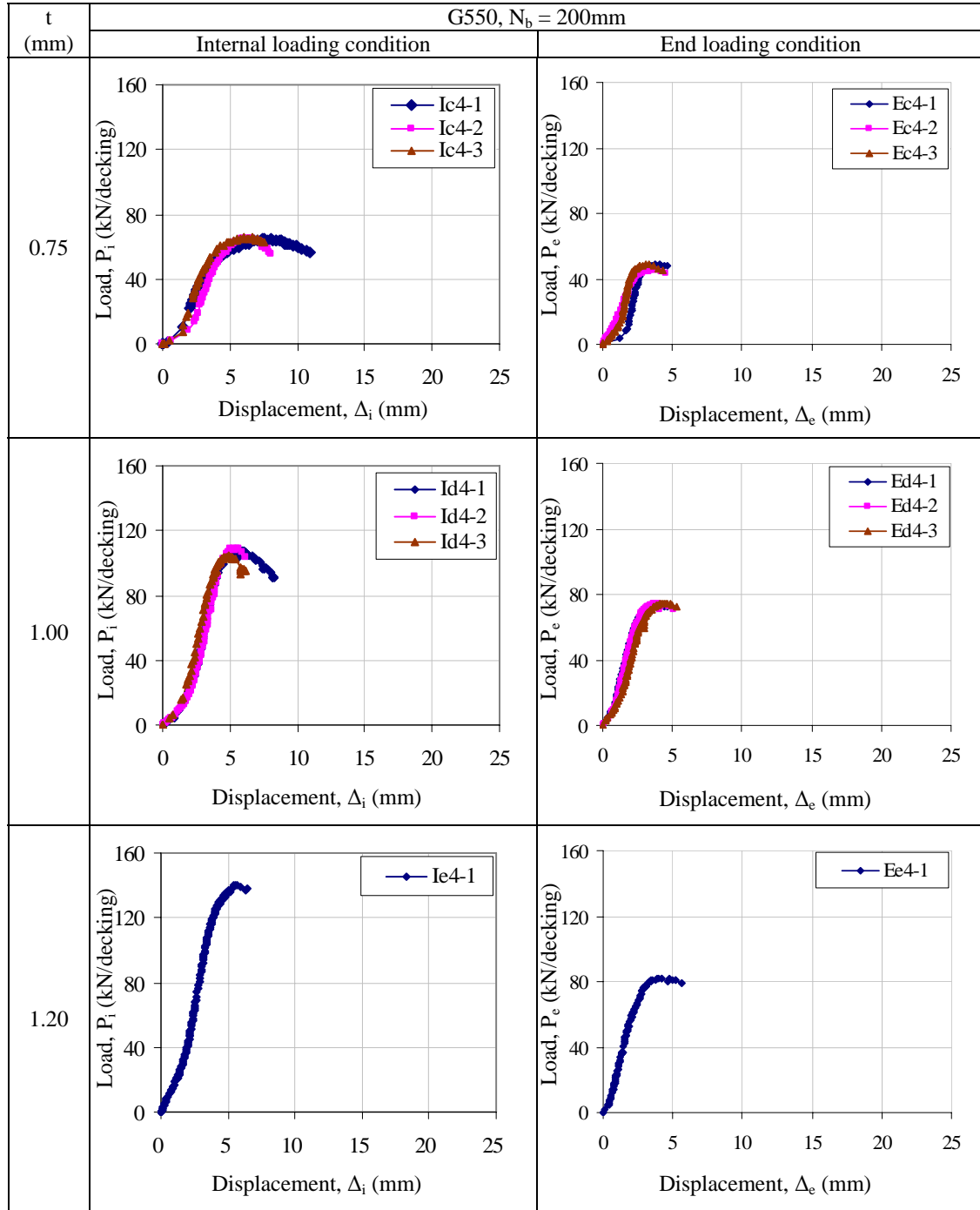
Figure 3.14: Load-deflection curves of web crippling tests: G235, $N_b = 150\text{mm}$.

Figure 3.15: Load-deflection curves of web crippling tests: G235, $N_b = 200\text{mm}$.

Figure 3.16: Load-deflection curves of web crippling tests: G550, $N_b = 50\text{mm}$.

Figure 3.17: Load-deflection curves of web crippling tests: G550, $N_b = 100\text{mm}$.

Figure 3.18: Load-deflection curves of web crippling tests: G550, $N_b = 150\text{mm}$.

Figure 3.19: Load-deflection curves of web crippling tests: G550, $N_b = 200\text{mm}$.

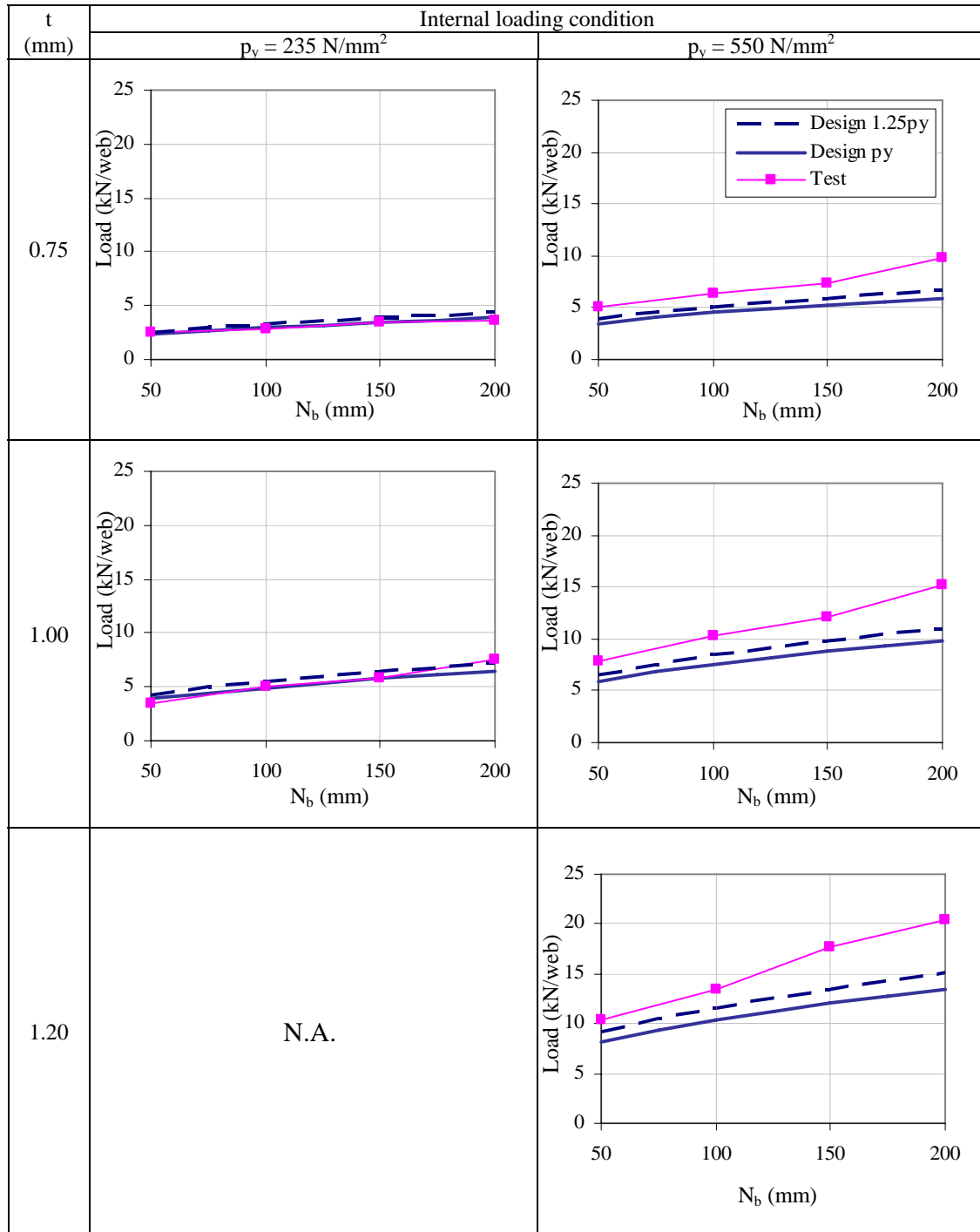


Figure 3.20: Summary of normalized web crippling resistances under internal loading condition.

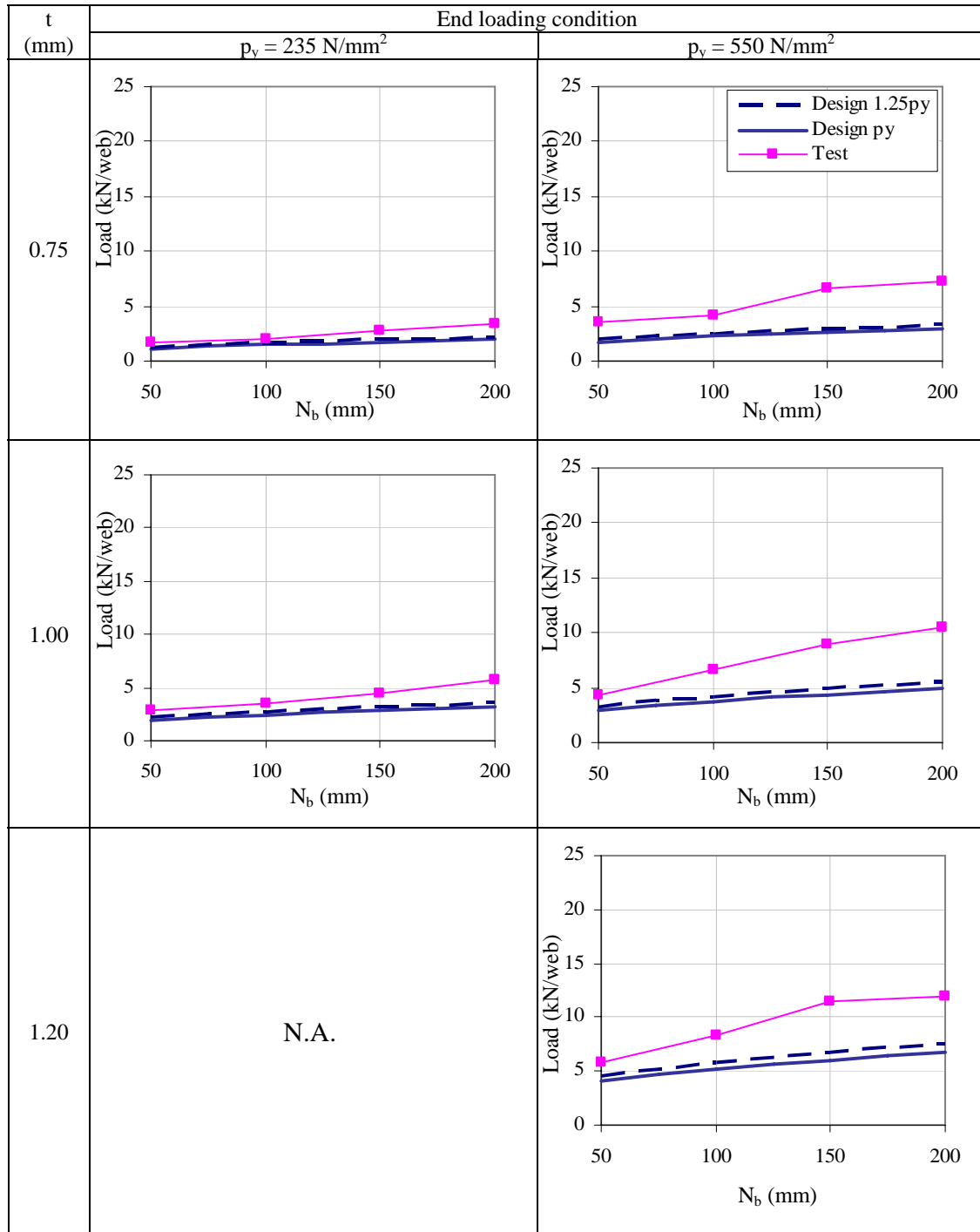


Figure 3.21: Summary of normalized web crippling resistances under end loading condition.

Table 3.1: Measured material properties of cold-formed steel deckings.

Nominal values		Measured values				Averaged values		
Steel grade	Thickness, t (mm)	Specimen	Base metal thickness, t (mm)	Young's modulus, E (kN/mm ²)	Yield strength, p_y (N/mm ²)	Base metal thickness, t (mm)	Young's modulus, E (kN/mm ²)	Yield strength, p_y (N/mm ²)
G235	0.75	A1	0.77	191	315	0.78	184	308
		A2	0.78	177	300			
	1.00	B1	0.99	184	330	0.99	188	335
		B2	0.99	192	340			
G550	0.75	C1	0.79	200	576	0.79	190	583
		C2	0.78	181	590			
	1.00	D1	1.05	206	623	1.05	197	621
		D2	1.06	189	619			
	1.20	E1	1.20	192	630	1.21	195	628
		E2	1.21	198	626			

Table 3.2: Details of web crippling test.

Load bearing width, N_b (mm)	Steel grade	Thickness, t (mm)	Internal loading condition		End loading condition	
			Name of test specimen	Type of instrumentation	Name of test specimen	Type of instrumentation
50	G235	0.75	Ia1-1/2/3	DI	Ea1-1/2/3	DI
		1.00	Ib1-1/2/3	DI	Eb1-1/2/3	DI
	G550	0.75	Ic1-1/2/3	DI	Ec1-1/2/3	DI
		1.00	Id1-1/2/3	DI	Ed1-1/2/3	DI
		1.20	Ie1-1	DI	Ee1-1	DI
100	G235	0.75	Ia2-1/2/3	BI	Ea2-1/2/3	BI
		1.00	Ib2-1/2/3	BI	Eb2-1/2/3	BI
	G550	0.75	Ic2-1/2/3	BI	Ec2-1/2/3	BI
		1.00	Id2-1/2/3	BI	Ed2-1/2/3	BI
		1.20	Ie2-1	BI	Ee2-1	BI
150	G235	0.75	Ia3-1/2/3	BI	Ea3-1/2/3	BI
		1.00	Ib3-1/2/3	BI	Eb3-1/2/3	BI
	G550	0.75	Ic3-1/2/3	BI	Ec3-1/2/3	BI
		1.00	Id3-1/2/3	BI	Ed3-1/2/3	BI
		1.20	Ie3-1	BI	Ee3-1	BI
200	G235	0.75	Ia4-1/2/3	DI	Ea4-1/2/3	DI
		1.00	Ib4-1/2/3	DI	Eb4-1/2/3	DI
	G550	0.75	Ic4-1/2/3	DI	Ec4-1/2/3	DI
		1.00	Id4-1/2/3	DI	Ed4-1/2/3	DI
		1.20	Ie4-1	DI	Ee4-1	DI
Notes: BI = basic instrumentation DI = detailed instrumentation						

Table 3.3: Summary of equations for calculation of reference points.

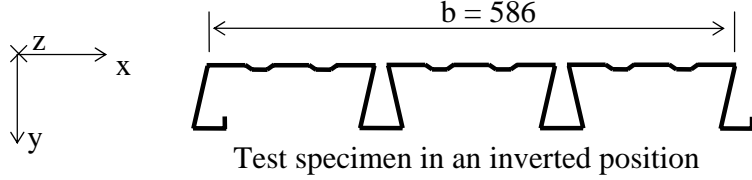
 <p>Test specimen in an inverted position</p>		
Internal loading condition		
	Basic instrumentation (BI)	Detailed instrumentation (DI)
Figure no.	Figure 3.1	Figure 3.3
Δ_i	$\Delta_i = \frac{\delta_{i,1} + \delta_{i,2}}{2}$	$\Delta_i = \frac{1}{4} \sum_{j=1}^{n=4} \delta_{i,j,average}$ where $\delta_{i,j,average} = \frac{\delta_{i,9-j} + \delta_{i,j}}{2} + h_{sp} \cos \left[\tan^{-1} \left(\frac{\delta_{i,9-j} - \delta_{i,j}}{200 + N_b} \right) \right] - h_{sp}$ h_{sp} = level of steel plate = 30 mm as shown in Figure 3.3
θ_x	N.A.	$\theta_x = \frac{1}{4} \sum_{j=1}^{n=4} \theta_{i,j,average} \approx 0$ where $\theta_{i,j,average} = \frac{\delta_{i,9-j} - \delta_{i,j}}{200 + N_b}$
θ_z	$\theta_z = \frac{\delta_{i,1} - \delta_{i,2}}{1100} \approx 0$	$\theta_z = \left[\frac{(\delta_{i,1} + \delta_{i,8})}{2} - \frac{(\delta_{i,4} + \delta_{i,5})}{2} \right] / b \approx 0$ where b = width of profiled decking = 587 mm as shown in Figure 3.3
End loading condition		
	Basic instrumentation (BI)	Detailed instrumentation (DI)
Figure no.	Figure 3.5	Figure 3.7
Δ_i	$\Delta_i = \frac{\delta_{i,1} + \delta_{i,2}}{2}$	$\Delta_i = \frac{1}{4} \sum_{j=1}^{n=4} \delta_{i,j,average}$ where $\delta_{i,j,average} = \frac{\delta_{i,9-j} + \delta_{i,j}}{2} + h_{sp} \cos \left[\tan^{-1} \left(\frac{\delta_{i,9-j} - \delta_{i,j}}{200 + N_b} \right) \right] - h_{sp}$ h_{sp} = level of steel plate = 30 mm as shown in Figure 3.7
θ_x	N.A.	$\theta_x = \frac{1}{4} \sum_{j=1}^{n=4} \theta_{i,j,average} \neq 0$ where $\theta_{i,j,average} = \frac{\delta_{i,9-j} - \delta_{i,j}}{200 + N_b}$
θ_z	$\theta_z = \frac{\delta_{i,1} - \delta_{i,2}}{1100} \approx 0$	$\theta_z = \left[\frac{(\delta_{i,1} + \delta_{i,8})}{2} - \frac{(\delta_{i,4} + \delta_{i,5})}{2} \right] / b \approx 0$ where b = width of profiled decking = 587 mm as shown in Figure 3.7

Table 3.4: Summary of measured web crippling resistances.

Load bearing width, N_b (mm)	Steel grade	Thickness, t (mm)	Internal loading condition*			End loading condition*		
			Test	Applied load (kN/web)	Averaged applied load (kN/web)	Test	Applied load (kN/web)	Averaged applied load (kN/web)
50	G235	0.75	Ia1-1	3.52	3.39	Ea1-1	2.54	2.40
			Ia1-2	3.28		Ea1-2	2.39	
			Ia1-3	3.36		Ea1-3	2.33	
		1.00	Ib1-1	4.85	4.90	Eb1-1	4.16	4.04
			Ib1-2	5.11		Eb1-2	4.00	
			Ib1-3	4.74		Eb1-3	3.97	
	G550	0.75	Ic1-1	6.01	5.72	Ec1-1	4.05	3.94
			Ic1-2	5.68		Ec1-2	4.02	
			Ic1-3	5.46		Ec1-3	3.74	
		1.00	Id1-1	9.19	9.28	Ed1-1	5.31	5.20
			Id1-2	9.20		Ed1-2	5.37	
			Id1-3	9.47		Ed1-3	4.93	
1.20	Ie1-1	11.89	11.89	Ee1-1	6.67	6.67		
100	G235	0.75	Ia2-1	3.79	3.89	Ea2-1	2.92	2.84
			Ia2-2	4.13		Ea2-2	2.70	
			Ia2-3	3.76		Ea2-3	2.89	
		1.00	Ib2-1	6.97	6.97	Eb2-1	4.96	4.79
			Ib2-2	6.78		Eb2-2	4.61	
			Ib2-3	7.15		Eb2-3	4.80	
	G550	0.75	Ic2-1	7.23	7.05	Ec2-1	4.55	4.57
			Ic2-2	7.16		Ec2-2	4.66	
			Ic2-3	6.76		Ec2-3	4.49	
		1.00	Id2-1	12.33	12.19	Ed2-1	7.37	7.89
			Id2-2	12.20		Ed2-2	8.01	
			Id2-3	12.03		Ed2-3	8.31	
1.20	Ie2-1	15.40	15.40	Ee2-1	9.54	9.54		
150	G235	0.75	Ia3-1	4.64	4.81	Ea3-1	3.87	3.74
			Ia3-2	4.80		Ea3-2	3.77	
			Ia3-3	4.99		Ea3-3	3.58	
		1.00	Ib3-1	8.19	8.09	Eb3-1	6.23	6.28
			Ib3-2	7.77		Eb3-2	6.39	
			Ib3-3	8.30		Eb3-3	6.23	
	G550	0.75	Ic3-1	8.27	8.31	Ec3-1	7.03	7.42
			Ic3-2	8.30		Ec3-2	7.36	
			Ic3-3	8.35		Ec3-3	7.86	
		1.00	Id3-1	14.01	14.28	Ed3-1	10.47	10.63
			Id3-2	14.42		Ed3-2	10.66	
			Id3-3	14.42		Ed3-3	10.76	
1.20	Ie3-1	20.33	20.33	Ee3-1	13.26	13.26		
200	G235	0.75	Ia4-1	6.16	6.00	Ea4-1	4.54	4.67
			Ia4-2	6.00		Ea4-2	4.62	
			Ia4-3	5.85		Ea4-3	4.86	
		1.00	Ib4-1	10.32	10.48	Eb4-1	8.12	7.99
			Ib4-2	10.40		Eb4-2	7.93	
			Ib4-3	10.72		Eb4-3	7.91	
	G550	0.75	Ic4-1	10.97	11.03	Ec4-1	8.23	8.04
			Ic4-2	11.03		Ec4-2	7.65	
			Ic4-3	11.10		Ec4-3	8.25	
		1.00	Id4-1	18.09	17.99	Ed4-1	12.36	12.49
			Id4-2	18.28		Ed4-2	12.54	
			Id4-3	17.61		Ed4-3	12.57	
1.20	Ie4-1	23.49	23.49	Ee4-1	13.80	13.80		
*Mode of failure: Internal loading condition WI: Web crippling failure End loading condition WE: Web crippling failure with web buckling near the web-flange corner								

Table 3.5: Summary of normalized web crippling resistances.

Design yield strength p_y (N/mm ²)	Load bearing width, N_b (mm)	Thick-ness, t (mm)	Internal loading condition			End loading condition			$P_{Test, e} / P_{Test, i}$
			Averaged normalized load, $P_{Test, i}$ (kN/web)	Design load, P_{Design} (kN/web)	$P_{Test, i} / P_{Design}$	Averaged normalized load, $P_{Test, e}$ (kN/web)	Design load, P_{Design} (kN/web)	$P_{Test, e} / P_{Design}$	
235	50	0.75	2.49	2.29	1.09	1.76	1.14	1.54	0.71
		1.00	3.52	3.86	0.91	2.91	1.93	1.51	0.83
	100	0.75	2.85	2.95	0.97	2.08	1.47	1.41	0.73
		1.00	5.01	4.93	1.02	3.45	2.46	1.40	0.69
	150	0.75	3.53	3.46	1.02	2.74	1.73	1.58	0.78
		1.00	5.82	5.74	1.01	4.52	2.87	1.57	0.78
	200	0.75	3.67	3.88	0.95	3.43	1.94	1.77	0.93
		1.00	7.54	6.43	1.17	5.75	3.22	1.79	0.76
Averaged value			-	-	1.02	-	-	1.57	0.78
550	50	0.75	5.12	3.50	1.46	3.53	1.75	2.02	0.69
		1.00	7.83	5.90	1.33	4.39	2.95	1.49	0.56
		1.20	10.33	8.21	1.26	5.79	4.10	1.41	0.56
	100	0.75	6.31	4.51	1.40	4.09	2.26	1.81	0.65
		1.00	10.28	7.53	1.37	6.66	3.77	1.77	0.65
		1.20	13.38	10.41	1.29	8.29	5.20	1.59	0.62
	150	0.75	7.43	5.29	1.40	6.65	2.64	2.52	0.89
		1.00	12.05	8.79	1.37	8.97	4.39	2.04	0.75
		1.20	17.66	12.09	1.46	11.52	6.05	1.90	0.65
	200	0.75	9.88	5.94	1.66	7.20	2.97	2.42	0.73
		1.00	15.17	9.84	1.54	10.54	4.92	2.14	0.69
		1.20	20.40	13.51	1.51	11.99	6.76	1.77	0.59
Averaged value			-	-	1.42	-	-	1.91	0.67

Chapter 4

Numerical Investigation into Web Crippling Failure

4.1 Introduction

Using the finite element package ABAQUS (2004), the web crippling behaviour of cold-formed profiled steel decking Deck R50 is examined in details. Special attention is given to the effects of different boundary and loading conditions, corner radii, corner strength enhancement and initial geometrical imperfections to the web crippling behaviour. After careful calibration of the model against the measured load deformation characteristic of the web crippling tests, the stress patterns, the yielding propagation as well as the failure mechanism are studied thoroughly. A sensitivity study on the values of various parameters is also reported.

4.2 Numerical Models

In order to study the web crippling behaviour of profiled deckings Deck R50 under both the internal and the end loading conditions, a total number of 42 finite element models are established with different steel thicknesses and load bearing widths, as summarized in

Table 4.1. In each series of the finite element models, the effects of different boundary and loading conditions, corner radii, corner strength enhancement and initial geometrical imperfections on the web crippling behavior of Deck R50 are examined. Details of the numerical studies covering these effects are summarized in Tables 4.2 to 4.5.

4.2.1 Material Properties

The non-linear stress-strain relationship obtained from coupon tests is adopted in all finite element models reported in this chapter. It should be noted that in the coupon tests, only flat portions of the decking is selected as test coupons. Hence, the enhanced strength of the steel at the round corners are calibrated using two different values, a) equal to the yield strength of the flat portion and b) 1.25 times the yield strength of the flat portions measured directly from coupon tests. Refer to Figure 4.1 for details. The value of corner yield strength is equal to 1.25 of the yield strength at the flat portion of test specimen according to the experimental results summarised in Zhao X. L. et al (2005).

4.2.2 Model Geometries

The idealization of the finite element models are presented in Figure 4.2 while the boundary and the loading conditions of the finite element models under internal and end loading conditions are shown in Figure 4.3. As shown in Figure 4.4, the finite element

models are established according to the measured dimensions of the test specimens, and shell elements S4R with six degrees of freedom at each node are adopted to model the profiled decking.

It should be noted that in all tests, the external webs are properly restrained with the use of C-clamps in order to eliminate section spreading. Hence, for simplicity, the finite element models with only half of a re-entrant unit are considered to be representative in the present study. Whereas in the longitudinal direction, only half of the decking is adopted in the model of the test specimens under internal loading condition owing to symmetry while full length models are established for test specimens under end loading condition.

4.2.3 Boundary and Loading Conditions

4.2.3.1 Vertical supports

In order to simulate the support conditions of the profiled deckings, vertical restraints are applied to the nodes at the tangent of the round corner of the profiled decking at the support, as shown in Figures 4.3 to 4.5. Vertical restraints are applied over a length of 400mm, which is the length of the support in all the tests.

4.2.3.2 Lateral restraints

As shown in some of the measured load-deflection curves, there is a significant flexibility in the test specimens under low applied loads, i.e. a vertical deflection of 1 to 4mm. In order to study the possible source of the flexibility, two different boundary conditions are adopted in the models. The first boundary condition, namely Boundary Condition Fixed C is provided in the finite element models by preventing any lateral movement along both longitudinal edges, as shown in Figure 4.3c. The second boundary condition, namely Boundary Condition Free C is provided in the finite element models by preventing any lateral movement along one of the longitudinal edges. It should be noted that Boundary Condition Fixed C is considered to give the upper bound solution while Boundary Condition Free C will give the lower bound solution.

4.2.3.3 Loading conditions

Spring elements are provided along the interface between the rigid elements, which act as the stiff loading block, and the shell elements, which act as the profiled decking. They are provided to simulate any possible change in the contact (or loaded) areas due to gross deformation of the profiled decking at the proximity of the round corners under high concentrated loads. A schematic drawing on the loading condition of the numerical models is shown in Figure 4.3. Each spring element possesses a vertical compression spring stiffness, k_v , while its tensile spring stiffness is taken to be zero. It should be noted

that a typical area of an element is 37mm^2 ($6.66\text{mm} \times 5.55\text{mm}$). In order to study the sensitivity of the value of k_v to the web crippling resistance, three values of spring stiffness, 1.0kN/mm , 10.0kN/mm and 100kN/mm , are also adopted for comparison. Refer to Section 4.4 for details.

4.2.4 Corner Radius

It is observed in the tests that the profiled deckings experience a continuous change of loading area around the corner region along the entire deformation history. Hence, the structural behaviour of the profiled deckings is significantly affected by the corner radius. Thus, three finite element models are established with different corner radii at 2.5, 5.0 and 7.5mm to study their effects onto the web crippling resistances. Refer to Section 4.4 for details. It should be noted that only Boundary Condition Fixed C is adopted in these finite element models.

4.2.5 Initial Geometrical Imperfection

In the present study, initial geometrical imperfection is incorporated into the numerical models, and the deformed mode shape at first bifurcation, i.e. the eigenmode corresponding to the lowest eigenvalue, is extracted to be the initial geometrical imperfection, which is then superimposed to the geometry of the profiled decking. The

typical eigenmodes of the profiled decking adopted for both internal and end loading conditions are shown in Figures 4.5a and 4.5b, respectively. The presence of the initial geometrical imperfections in the finite element models facilitates smooth transition over bifurcation limits and prevents numerical divergence during equilibrium iterations. As the measured magnitudes of the initial geometrical imperfection vary from specimens to specimens, the magnitude of initial geometrical imperfection requires calibration so that its effect to the web crippling resistance can be evaluated. Hence, three different magnitudes of $0.00t$, $0.25t$ and $1.00t$ are adopted in the finite element models. Refer to Section 4.4 for details.

4.3 Numerical Results

Typical detailed finite element models with initial geometrical imperfection under internal and end loading conditions are shown in Figure 4.5. A total of 42 models are established. For ease of presentation, the results of only six finite element models are presented in details, namely FEM Ib4-Ba, Eb4-Ba, Ic1-Ba, Ie4-Ba, Ec1-Ba and Ee4-Ba. The load-displacement curves of the models are presented in Figures 4.6 and 4.7. The deformed shapes of these six models under internal and end loading conditions at failure loads are presented in Figures 4.8 to 4.11 respectively together with the associated stress distribution. It should be noted that the numerical analyses are terminated once unloading in the profiled decking is detected.

4.3.1 Comparison of Load-Displacement Curves

The load-displacement curves for Decks R50 of 235 and 550 steel grades are shown in Figures 4.6 to 4.7, respectively. It is shown in Figure 4.6 that the predicted load-displacements of the models with lateral restraints for Decks R50 with G235 steel follow closely with the measured data. Similarly, for 0.75mm thick Decks R50 with G550 steel, the predicted load displacement curves of the models with lateral restraint also follow closely with the measured data.

However, for 1.2mm thick Decks R50 with G550 steel, the measured load displacement curves deviate significantly from the predicted curves obtained from the models with either laterally restraint or no restraint. Moreover, the variation in the web crippling resistances is found to be 29% difference between finite element models with and without lateral restraints, hence precaution on the lateral movement of the profiled deckings should be taken during the web crippling tests. While all test results lay between the upper and the lower bound solutions, only test Ae4 is found to be close to the lower bound solution, i.e. FEM Ie4-Bb. This measured displacement characteristic indicates that full lateral restraint is not provided in the test. Moreover, it is also found that in Test Ie4, the measured web crippling resistance is the largest among all the tests in the test program, thus the test setup on the lateral restraint is shown to be sufficient just to thin profiled decking, but not sufficient for thick profiled decking. Hence, it is shown that the effectiveness of lateral restraint also affects the deformation characteristics of the profiled decking.

4.3.2 Deformed Shapes and Contact Areas

Among the six models, only one failure mode, i.e. the web crippling failure, is identified with significant material yielding at the web-trough corners. Moreover, high stress concentration is also found near the web-flange corners as shown in Figures 4.9 to 4.11. It should be noted that the stresses plotted onto the deformed shape of the finite element models are Von Mises Stresses at the mid-thickness of the shell elements.

Figures 4.12 to 4.17 present detailed results on the contact areas between the profiled decking and the rigid element during the entire deformation history. Under internal loading conditions, the spring elements k_{i1} and k_{e1} , which are located at the intersections between the trough and the round corner, remain in contact with the rigid elements throughout the deformation history. At the ultimate loads, due to the deformed shape of the profiled decking, additional contact is made at the spring elements k_{i2} , and k_{e2} for both internal and end loading conditions. Furthermore, for profiled decking with G235 steel, additional contact is made at the spring element k_{i3} , as shown in Figures 4.12 and 4.15. This spring element does not make contact with the rigid element for profiled deckings with G550 steel due to their corresponding small deformation at failure.

Whereas for the change of contact areas under end loading condition at the outer side of the load bearing width, additional contact is made at spring element k_{e3} to k_{e4} as shown in Figures 4.15 to 4.17. It should be noted that in such cases, only one spring element makes contact rather than two at any one time.

4.4 Sensitivity Study

In order to examine the sensitivity of various parameters to the web crippling behaviour of the profiled deckings, a comprehensive study is carried out using the finite element models established in the last section. The following parameters are covered:

- Spring stiffness, k_s
- Corner radius, r
- Design yield strength of corner radius, $p_{y,c}$
- Magnitude of initial geometrical imperfection, i
- Mesh convergence

4.4.1 Spring Stiffness

The following values of the spring stiffness, k_s , are assigned to the finite element models to examine their effect to the web crippling behaviour of the profiled decking:

- 1.0 kN/mm
- 10 kN/mm
- 100 kN/mm.

The predicted load-displacement curves of the finite element models with different stiffness are plotted in Figure 4.18 while the corresponding web crippling resistances are summarized in Table 4.3. It is shown that the failure loads of the finite element models

with different spring stiffness differ slightly among themselves, i.e. with a discrepancy of less than 1%. Moreover, the corresponding load-displacement curves are found to be very close among themselves. Hence, it is demonstrated that there is negligible effect on the web crippling resistances as well as the deformation characteristics when the value of the spring stiffness varies between 1 to 100 kN/mm.

4.4.2 Corner Radius

The following values of the corner radius, r , are assigned to the finite element models to examine their effect to the web crippling behaviour of the profiled decking:

- 2.5 mm
- 5.0 mm
- 7.5 mm

The predicted load-displacement curves of the finite element models with different corner radii are plotted in Figure 4.19 while the corresponding web crippling resistances are summarized in Table 4.4. In general, it is shown that the finite element models with a corner radius of 2.5mm often give the largest web crippling resistances together with a more sudden change in the load-displacement curves after attaining their maximum resistances, when compared with those with corner radii of 5 and 7.5mm.

Moreover, among the finite element models with corner radii of 2.5, 5.0 and 7.5 mm, the ratios of the measured resistance, P_{Test} , to the predicted resistance, P_{FEM} , are shown to vary from 0.86 to 1.03, i.e. with a discrepancy of about 20%. The corresponding load-displacement curves are also found to differ significantly, although to a lesser extent. Hence, it is important to obtain the actual values of the corner radii in finite element modeling of profiled deckings. It should be noted that among all the test specimens, the measured value of the corner radius is found to be typically 5 mm, and this value is shown to give very close results to the measured web crippling resistances.

4.4.3 Yield strength of Corner Regions

The yield strengths of corner regions are relatively higher than those of the flat regions due to the effect of cold-working. The effect of strength enhancement at the corner regions to the web crippling behaviour of profiled steel decking is studied with the yield strength of the corner region $p_{y,c}$ equal to:

- the yield strength of the flat portions, p_y
- 1.25 times the yield strength of the flat portions, p_y

The results are summarized in Table 4.2. It is shown that the ratios of the web crippling resistances using finite element models with and without corner strength enhancement ranges from 1.06 to 1.17. In comparison with the tested web crippling resistances, conservative results are predicted for all finite element models without corner strength

enhancement. While for finite element models with corner strength enhancement, accurate web crippling resistances are predicted. Hence, the corner strength enhancement at the corner regions should be properly adopted in finite element modeling, and an increase of 1.25 times the yield strength of the flat portions is considered appropriate.

4.4.4 Magnitude of Initial Geometrical Imperfection

Using the RIKS method in ABAQUS [2004] for solution iterations, the numerical models with initial geometrical imperfection are analyzed, and the following values of the magnitude of initial geometrical imperfection, i , are assigned to the finite element models to examine its effect to the web crippling behaviour of the profiled decking:

- 0
- 0.25 t
- 1.0 t

where t is the thickness of the profiled decking.

The predicted load-displacement curves of the finite element models with different magnitudes of the initial geometrical imperfections are plotted in Figure 4.20 while the corresponding web crippling resistances of are summarized in Table 4.5.

It is shown that the failure loads of the finite element models under internal loading condition with different magnitudes of initial geometrical imperfection differ slightly

among themselves, i.e. with a maximum discrepancy of 2%. Moreover, the corresponding load-displacement curves are found to be very close among themselves. Hence, it is demonstrated that there is negligible effect on the web crippling resistances as well as on the deformation characteristics when the magnitude of the initial geometrical imperfection varies significantly.

However, for finite element models under end loading condition with different magnitudes of initial geometrical imperfection, the web crippling resistances are found to differ among themselves with a maximum discrepancy of 6 %. Nevertheless, the corresponding load-displacement curves are found to be fairly close among themselves. Hence, it is demonstrated that there is a significant effect on the web crippling resistances when the variation of the magnitude of the initial geometrical imperfection varies significantly. This can be explained by material discontinuity in the finite element models under end loading condition which allows additional flexibility, leading to certain reduction in the web crippling resistances.

4.4.5 Mesh Convergence

To ensure numerical mesh convergence is achieved in the finite element models with the present number of elements, finite element models with different numbers of elements are established, as summarized below:

- 20 x 18 number of elements

- 31 x 31 number of elements
- 46 x 62 number of elements

where the first and second numbers denote the number of elements in the longitudinal and transverse directions of the profiled deckings, respectively.

The deformed shapes of the finite element models with 20 x 18 and 46 x 62 numbers of elements are shown in Figures 4.21 and 4.22, respectively, while the deformed shape of the finite element with 31 x 31 number of elements is shown in Figure 4.10a. Similar deformed shapes and stress patterns are found when compared against finite element models with different numbers of elements, which significant material yielding at the web-trough corners is observed. Moreover, high stress concentration is also found near the web-flange corners.

The predicted web crippling resistances of the finite element models with different numbers of elements are summarized in Table 4.6. It is shown that the failure loads of the finite element models with 31 x 31 and 46 x 62 numbers of elements differ slightly among themselves, i.e. with a maximum discrepancy of 1%. However, greater discrepancy of 5% in prediction of web crippling resistances is found for finite element models with 20x 18 and 31x 31 numbers of elements. Hence, it is demonstrated that there is a significant effect on the web crippling resistances when the number elements is less than 31x 31, while for mesh convergence is proven to have achieved for finite element models with number of elements more than 31 x 31.

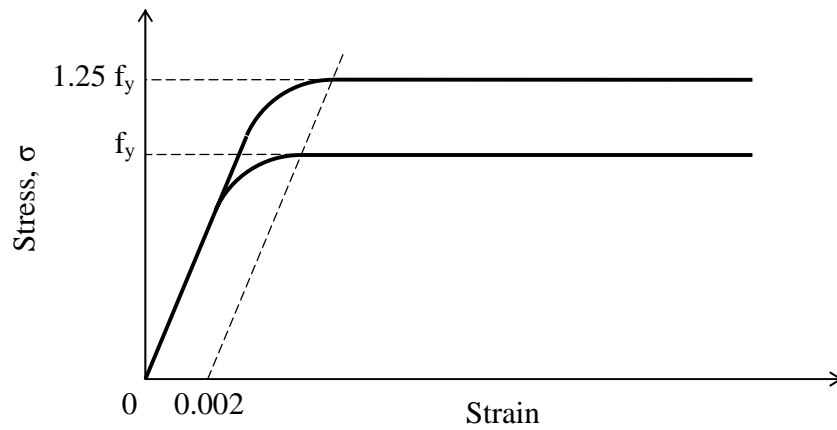
4.5 Typical Parameters for Finite Element Modeling

In order to provide a set of parameters suitable for general finite element modeling, Table 4.7 summarizes the recommended values of various parameters after careful calibration against the test results. Moreover, in general, these values may be used to provide indicative results on the web crippling behaviour of profiled decking in the absence of any measured data. It should be noted that these recommended values of the parameters are adopted in the subsequent chapters.

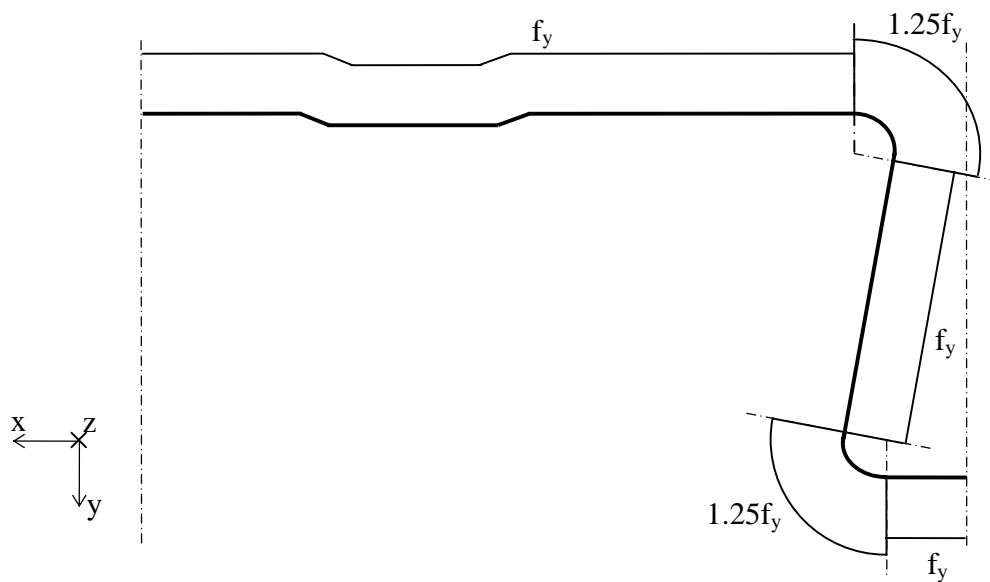
4.6 Summary

A comprehensive finite element modeling on the web crippling behaviour of profiled decking is reported in this chapter. The numerical results of the finite element models are carefully compared with test data, and it is shown that the models are capable to simulate the deformation characteristics of the cold-formed profiled steel decking R50 undergoing web crippling failure. Moreover, a comprehensive sensitivity study is also reported, and the effects of spring stiffness, corner radius, corner strength enhancement and magnitude of initial geometrical imperfection on the web crippling behaviour are studied thoroughly. It is found that the corner radius is very important to the accurate prediction of the web crippling resistances of the profiled decking while the value of spring stiffness is not. The magnitude of initial geometrical imperfection is important to those finite element models under end loading condition, but not so to those under internal loading condition.

The findings of this chapter will be adopted in the subsequent analyses, in particular, in those finite element models of section failure under combined actions.

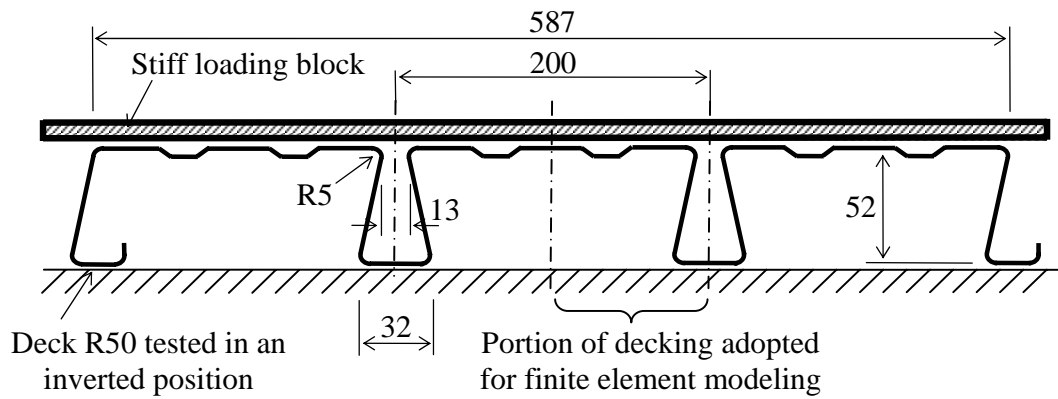


a) Stress strain curves adopted in finite element models

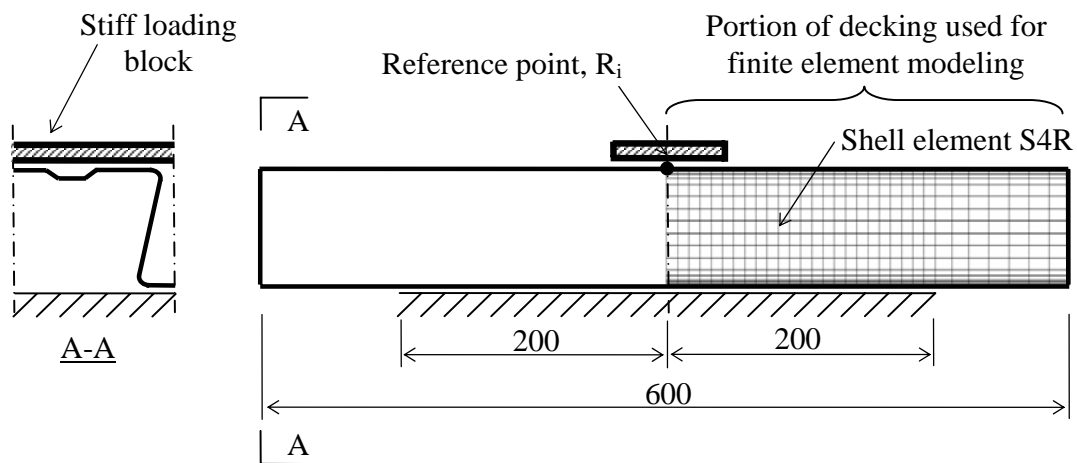


b) Stresses adopted in flat and corner portion of the section

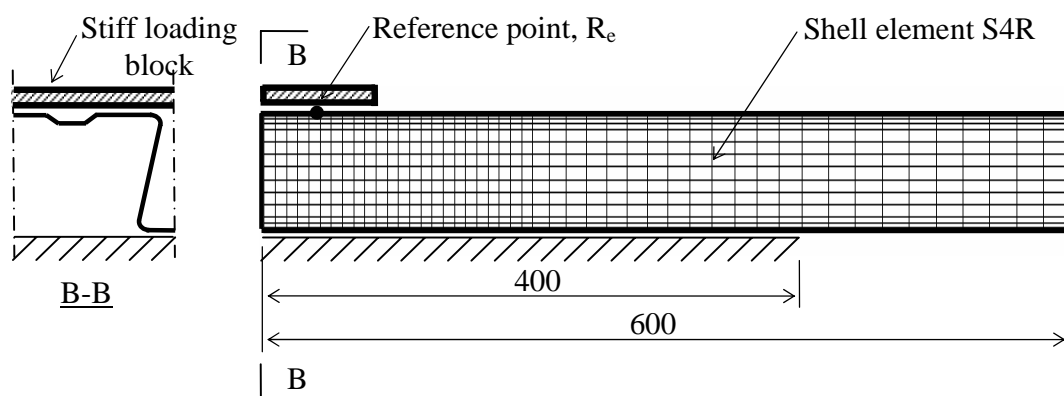
Figure 4.1: Different stresses adopted in finite element models.



a) Cross sectional details of the test specimen



b) Finite element model under internal loading condition



c) Finite element model under end loading condition

Figure 4.2: Idealization of finite element models.

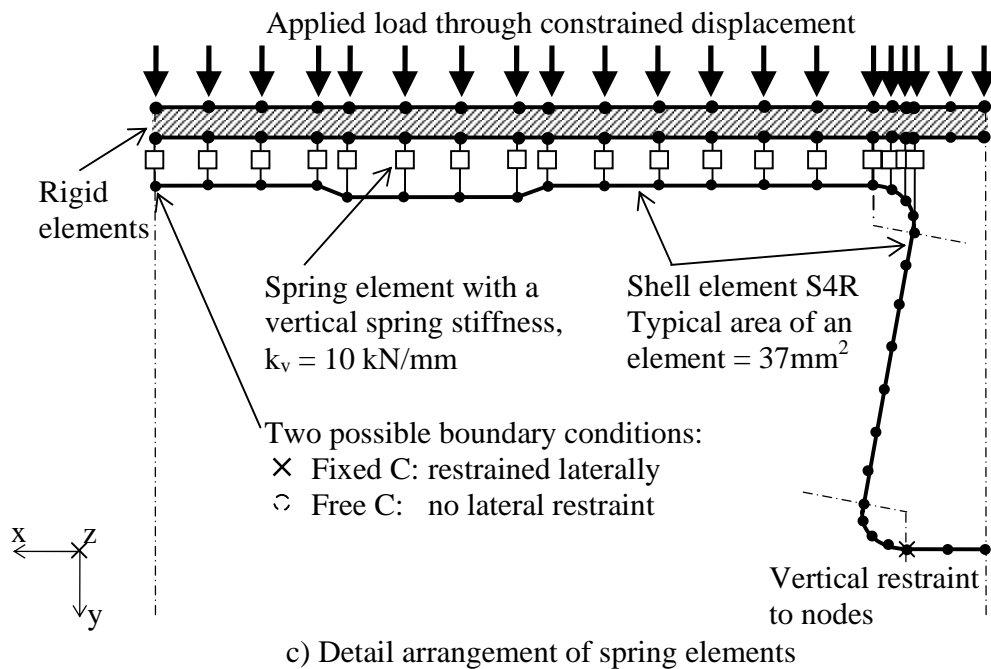
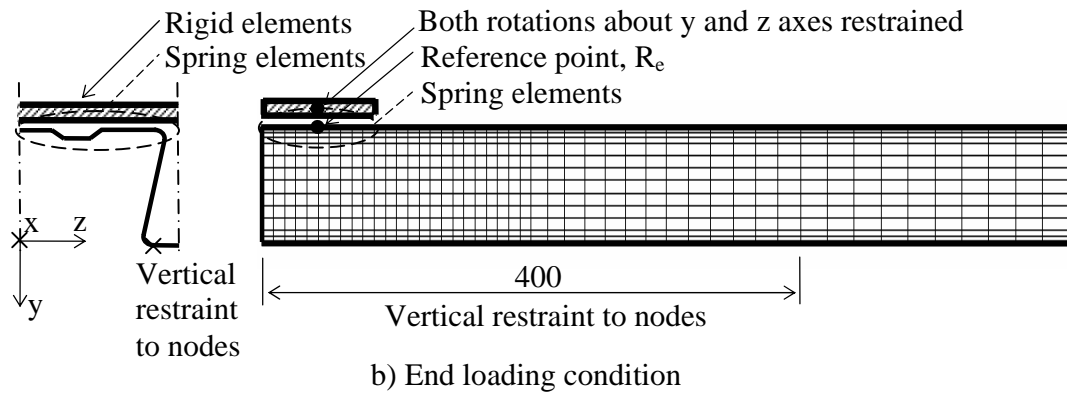
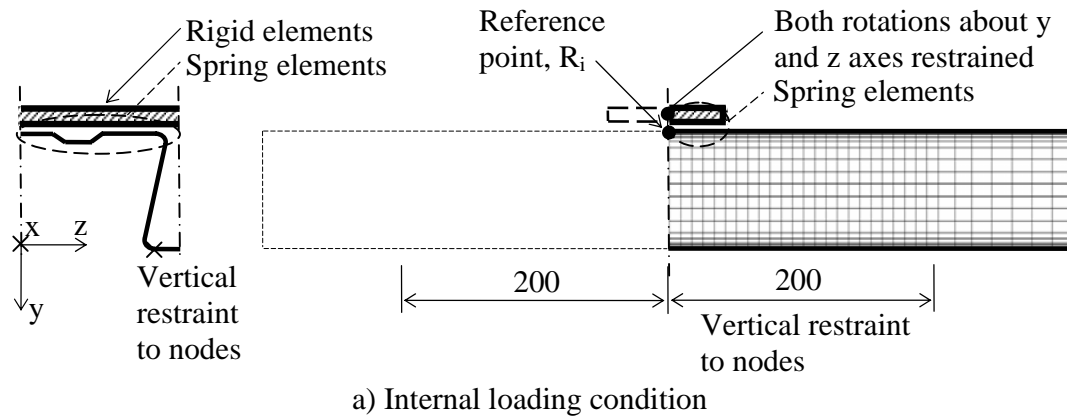


Figure 4.3: Boundary and loading conditions of finite element models.

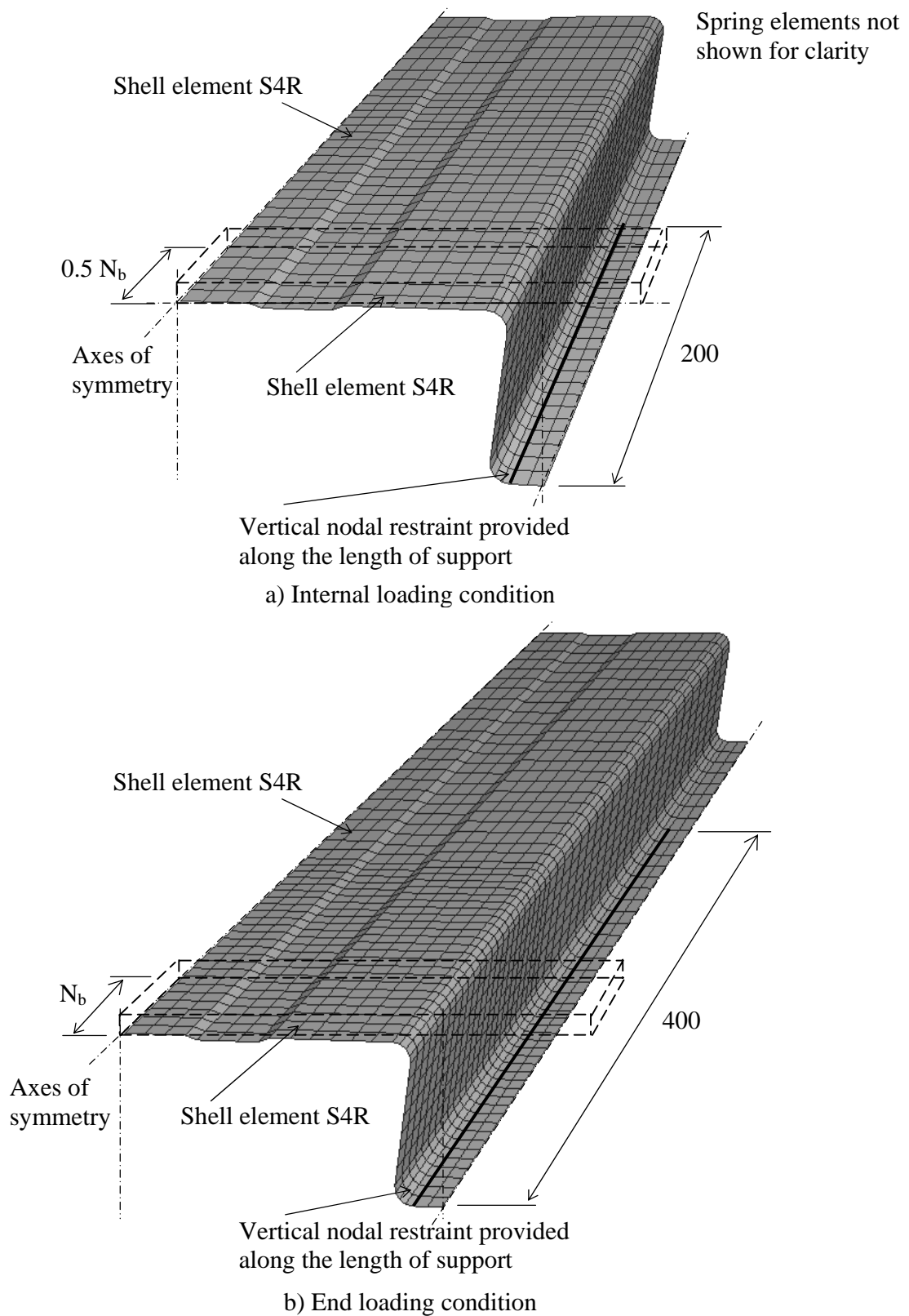


Figure 4.4: Geometry of finite element models.

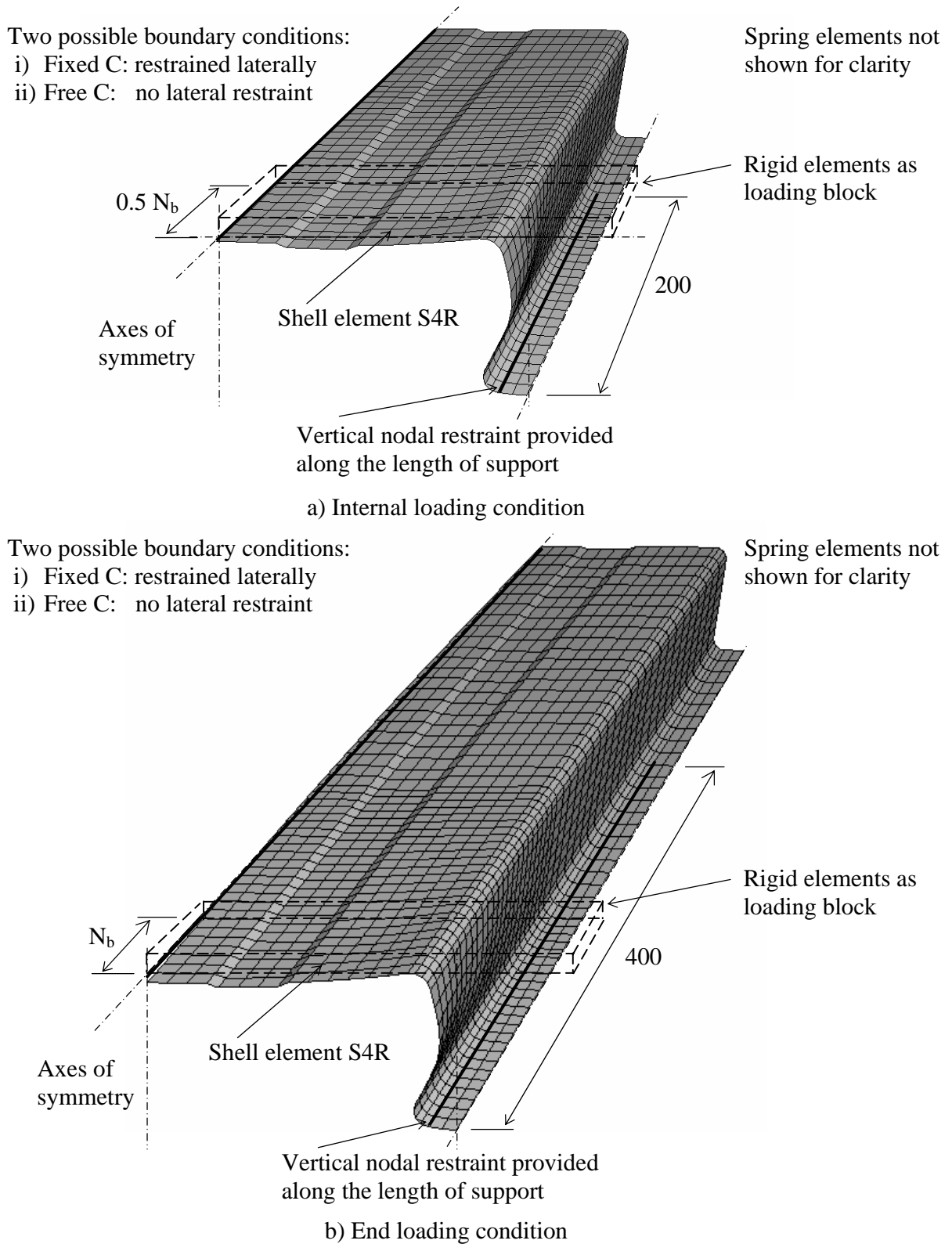
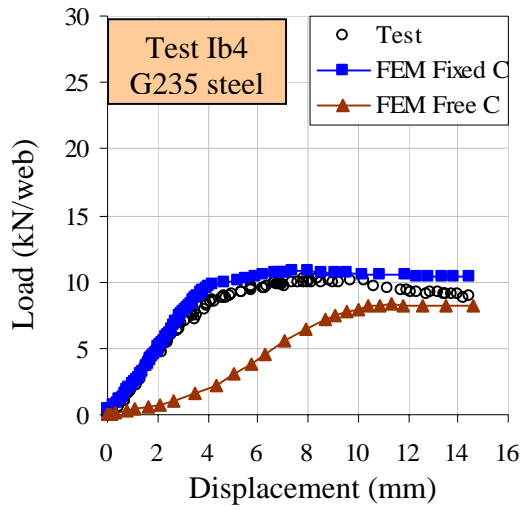
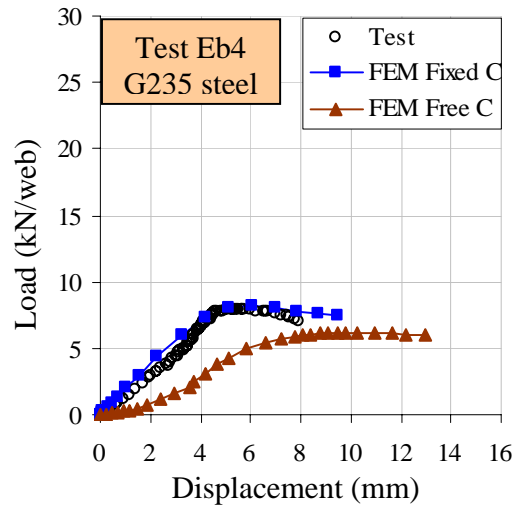


Figure 4.5: Detailed finite element models with initial geometrical imperfection.



a) Internal loading condition,
 $t = 1.00\text{mm}$, $N_b = 200\text{mm}$



b) End loading condition,
 $t = 1.00\text{mm}$, $N_b = 200\text{mm}$

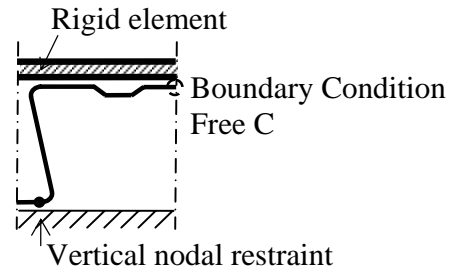
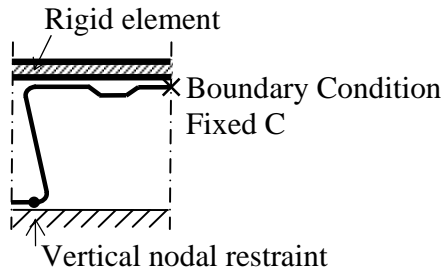
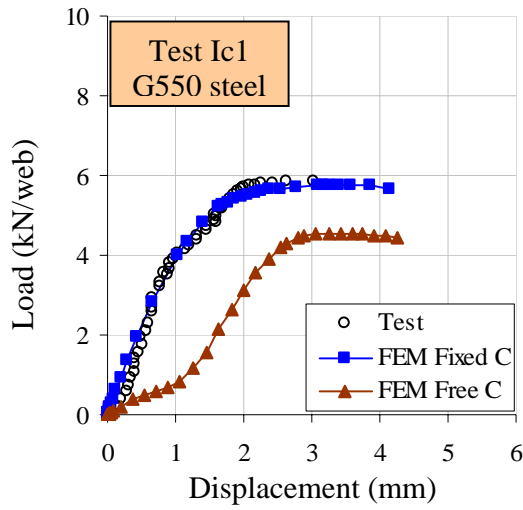
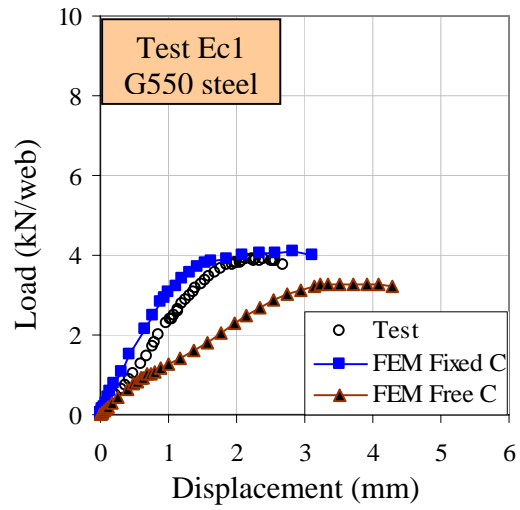


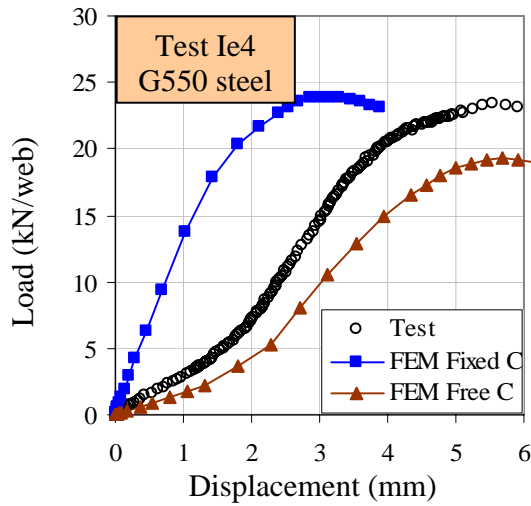
Figure 4.6: Load-displacement curves of Decks R50 with G235 steel.



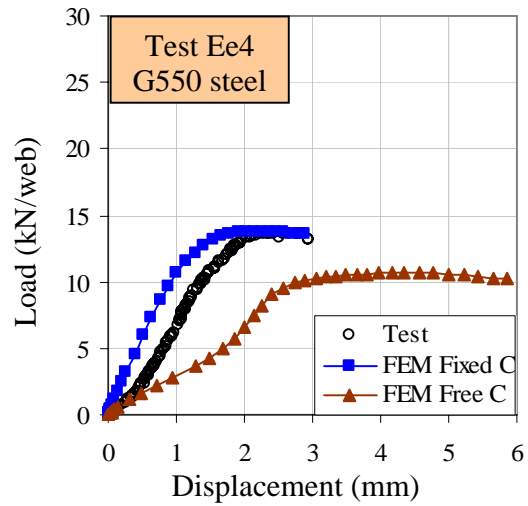
a) Internal loading condition,
 $t = 0.75\text{mm}$, $N_b = 50\text{mm}$



b) End loading condition,
 $t = 0.75\text{mm}$, $N_b = 50\text{mm}$



c) Internal loading condition,
 $t = 1.20\text{mm}$, $N_b = 200\text{mm}$



d) End loading condition,
 $t = 1.20\text{mm}$, $N_b = 200\text{mm}$

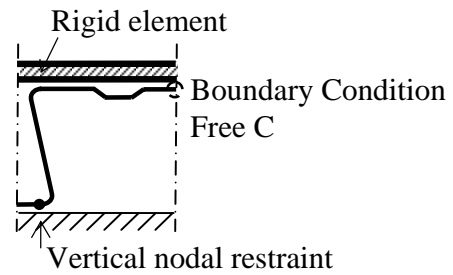
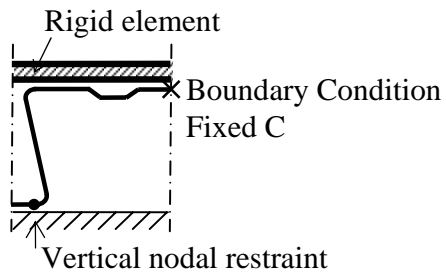


Figure 4.7: Load-displacement curves of Decks R50 with G550 steel.

FEM Ib4

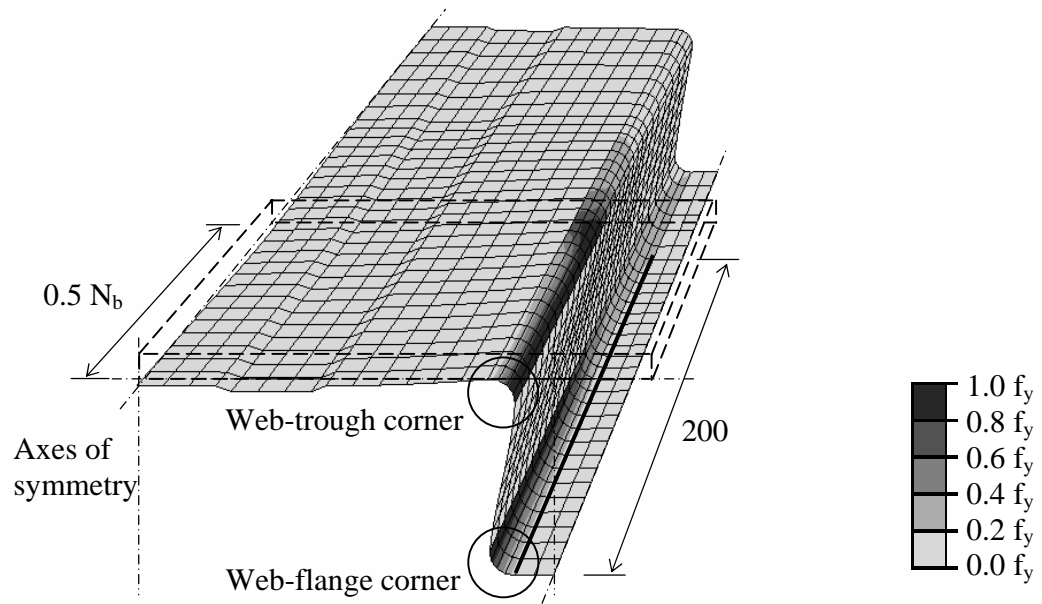


Figure 4.8: Deformed finite element models of G235 steel at failure
– Fixed C, internal loading condition.

FEM Eb4

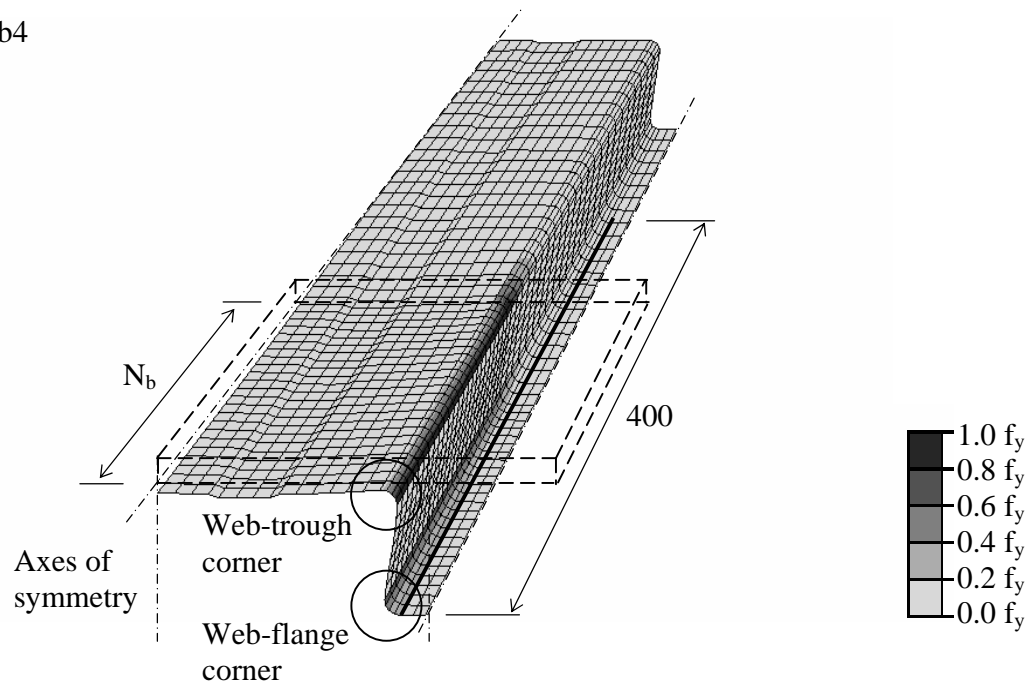
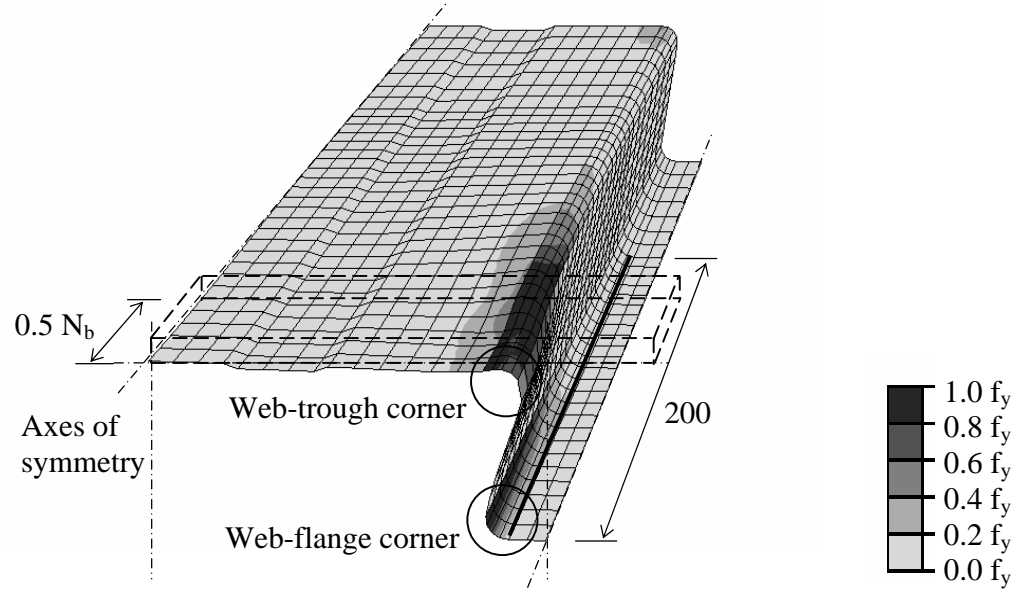


Figure 4.9: Deformed finite element models of G235 steel at failure
– Fixed C, end loading condition.

FEM Ic1

a) Fixed C, $t = 0.75\text{mm}$, $N_b = 50\text{mm}$, $r = 5\text{mm}$

FEM Ic4

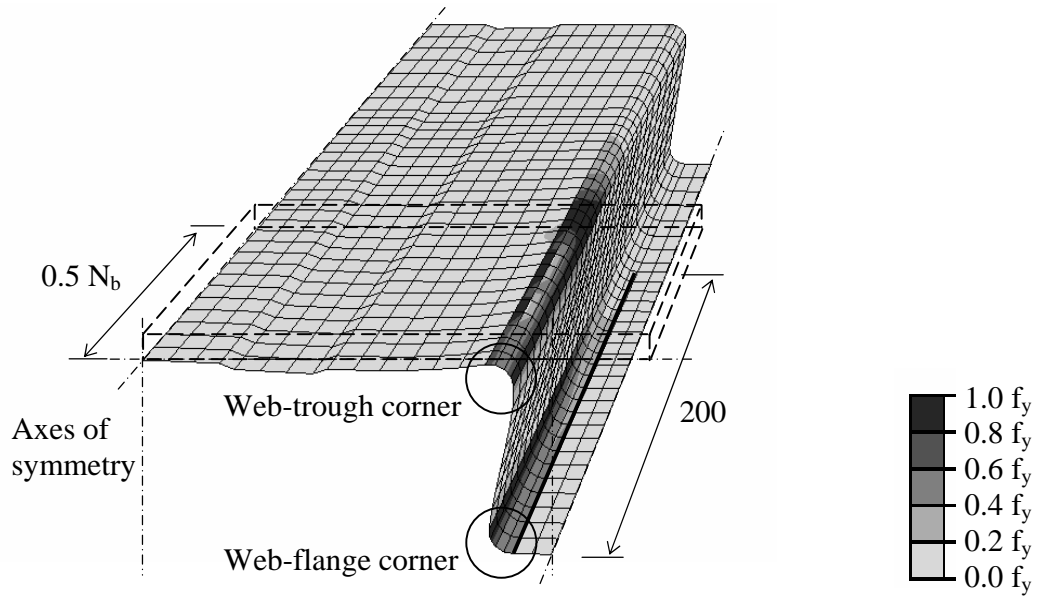
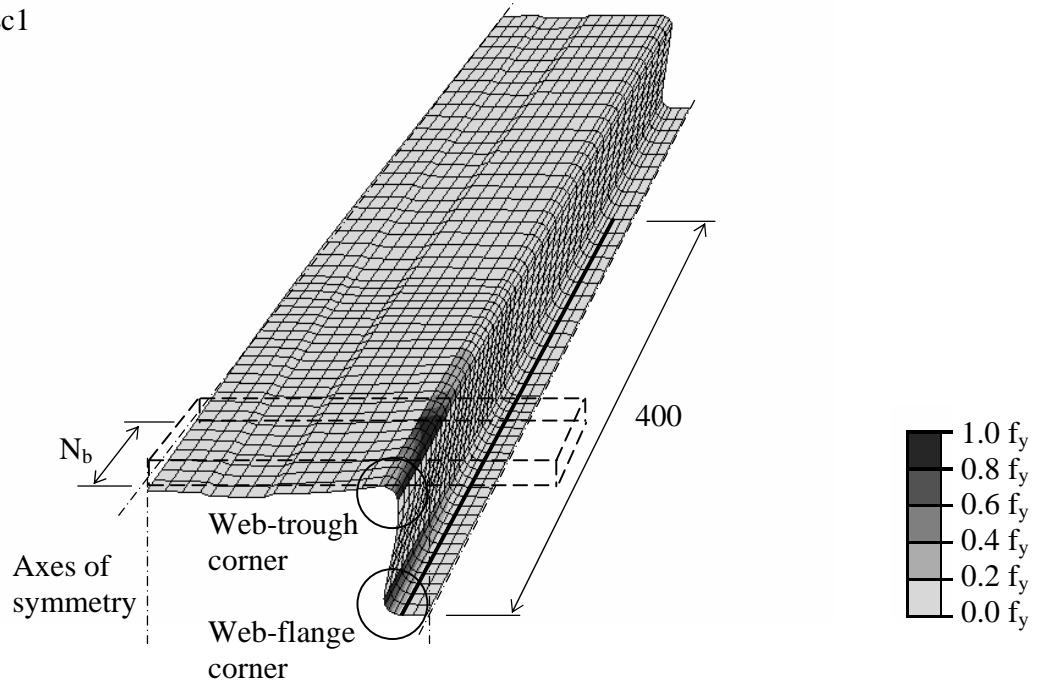
b) Fixed C, $t = 1.20\text{mm}$, $N_b = 200\text{mm}$, $r = 5\text{mm}$

Figure 4.10: Deformed finite element models of G550 steel at failure
 – Fixed C, internal loading condition.

FEM Ec1

a) Fixed C, $t = 0.75\text{mm}$, $N_b = 50\text{mm}$, $r = 5\text{mm}$

FEM Ee4

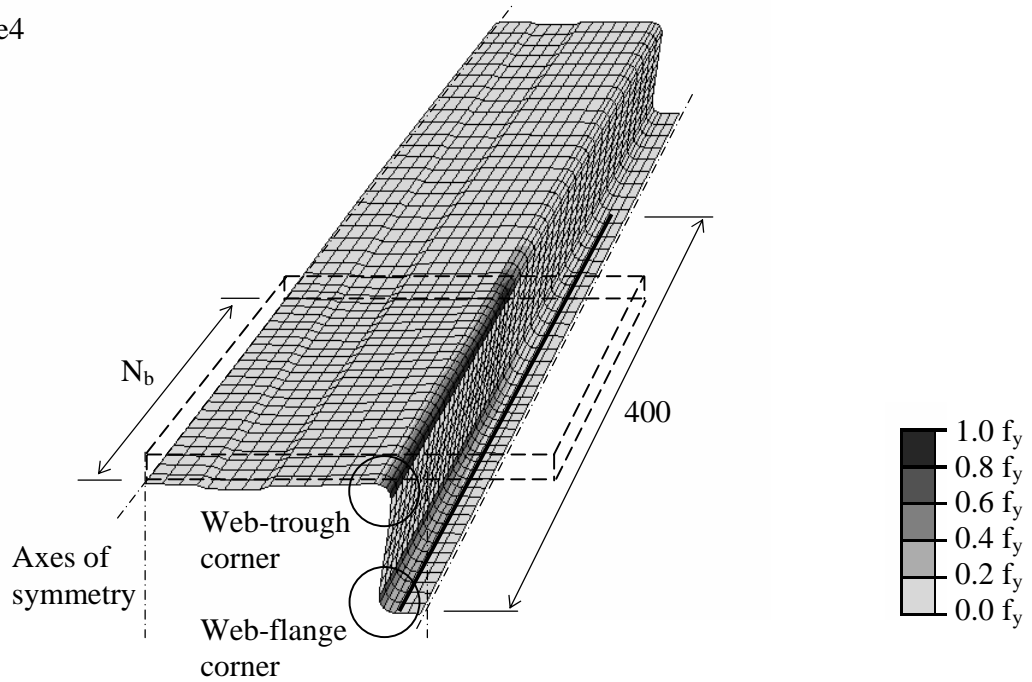
d) Fixed C, $t = 1.20\text{mm}$, $N_b = 200\text{mm}$, $r = 5\text{mm}$

Figure 4.11: Deformed finite element models of G550 steel at failure
– Fixed C, end loading condition.

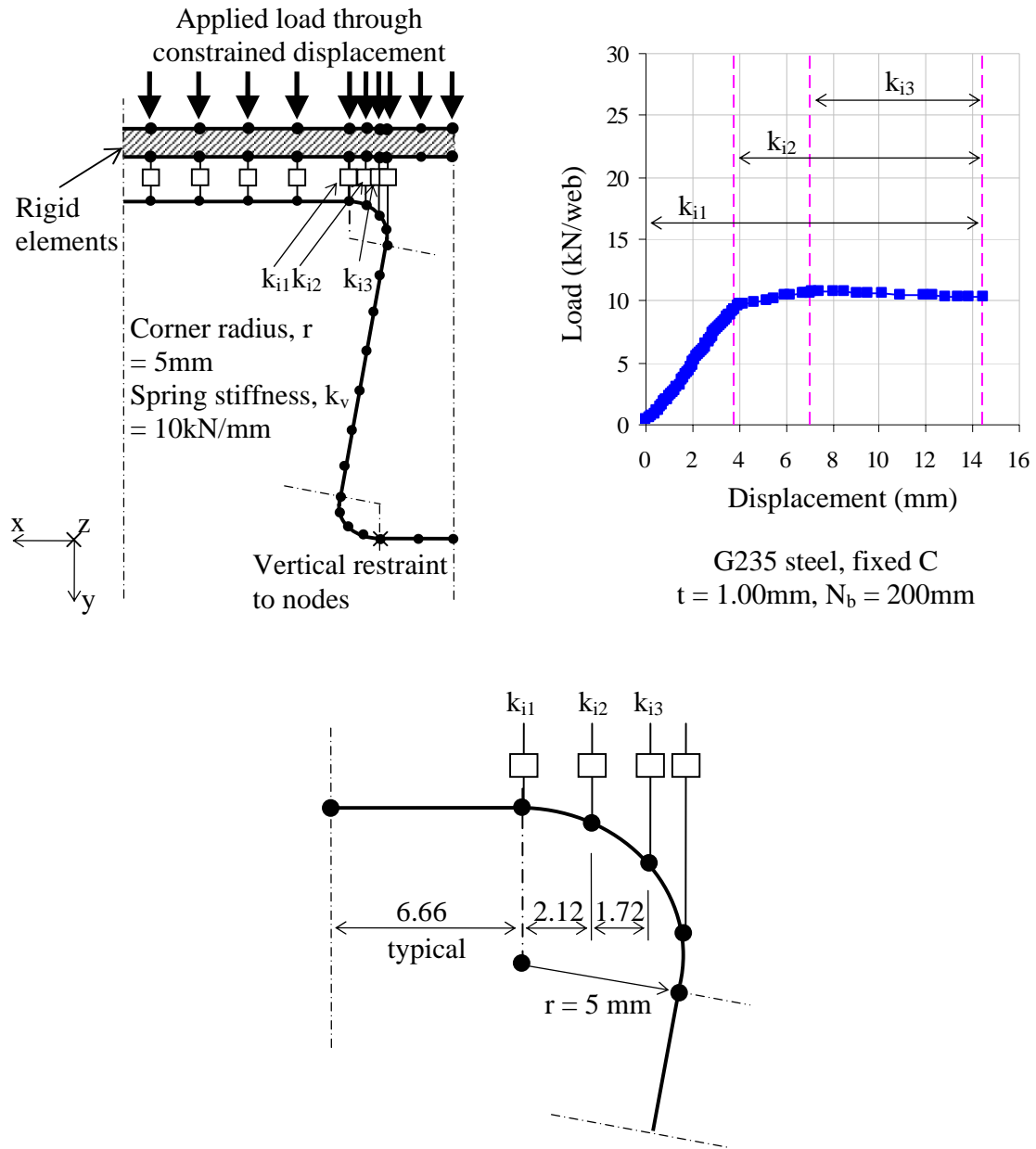


Figure 4.12: Change of contact area near the web-trough corner: internal loading condition
G235, $t = 1.00\text{ mm}$ and $N_b = 200\text{ mm}$.

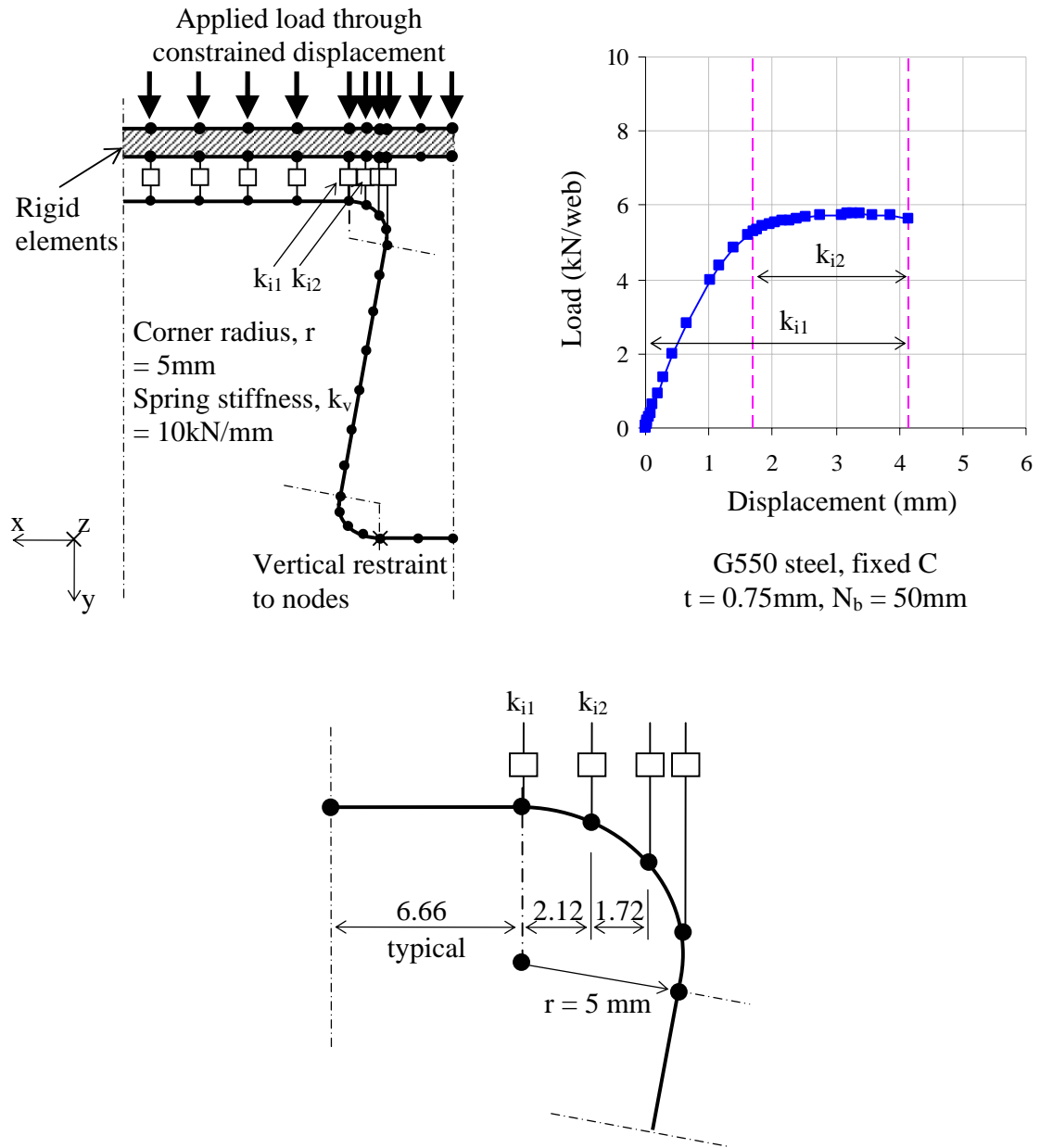


Figure 4.13: Change of contact area near the web-trough corner: internal loading condition G550, $t = 0.75\text{ mm}$ and $N_b = 50\text{ mm}$.

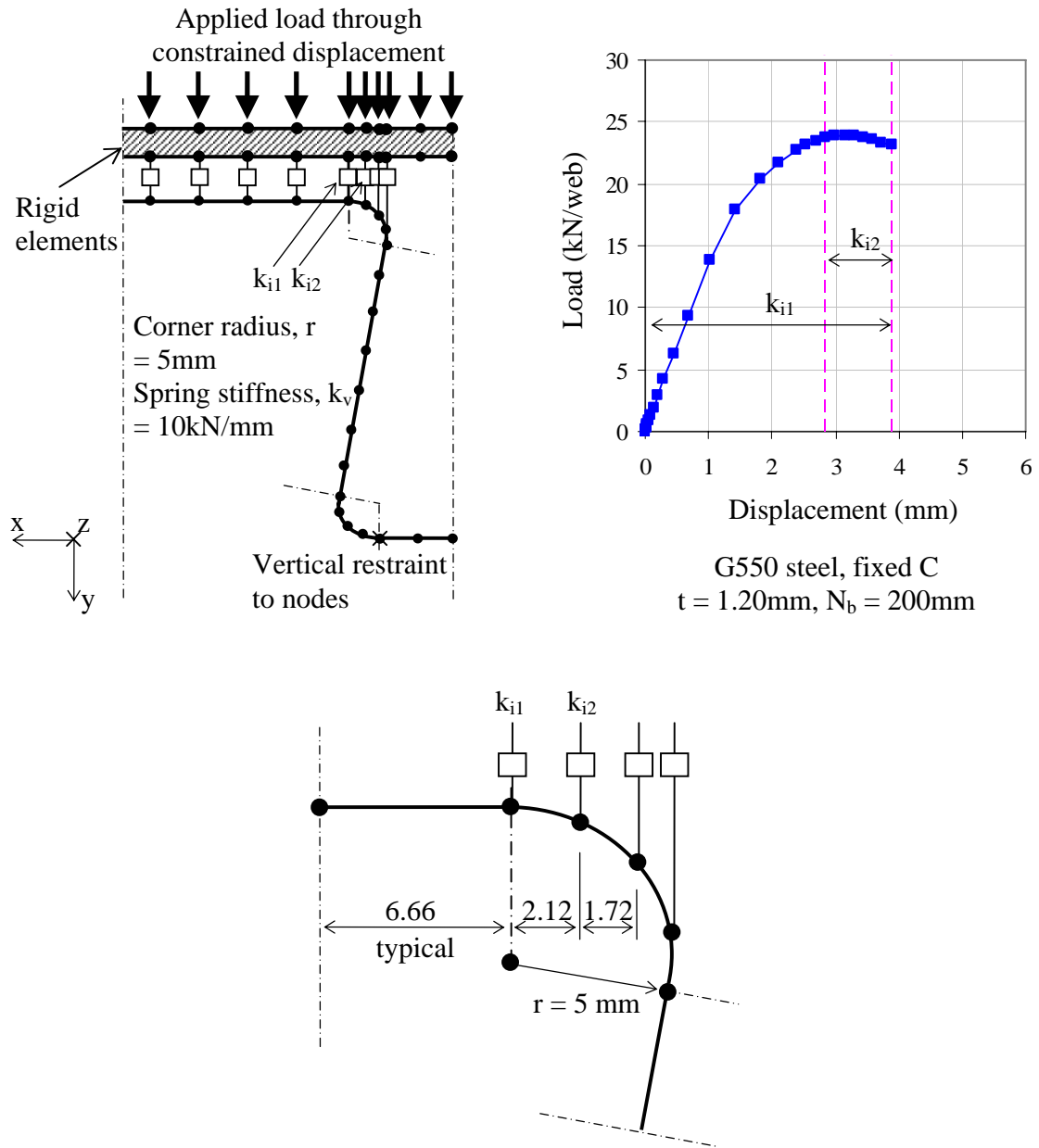
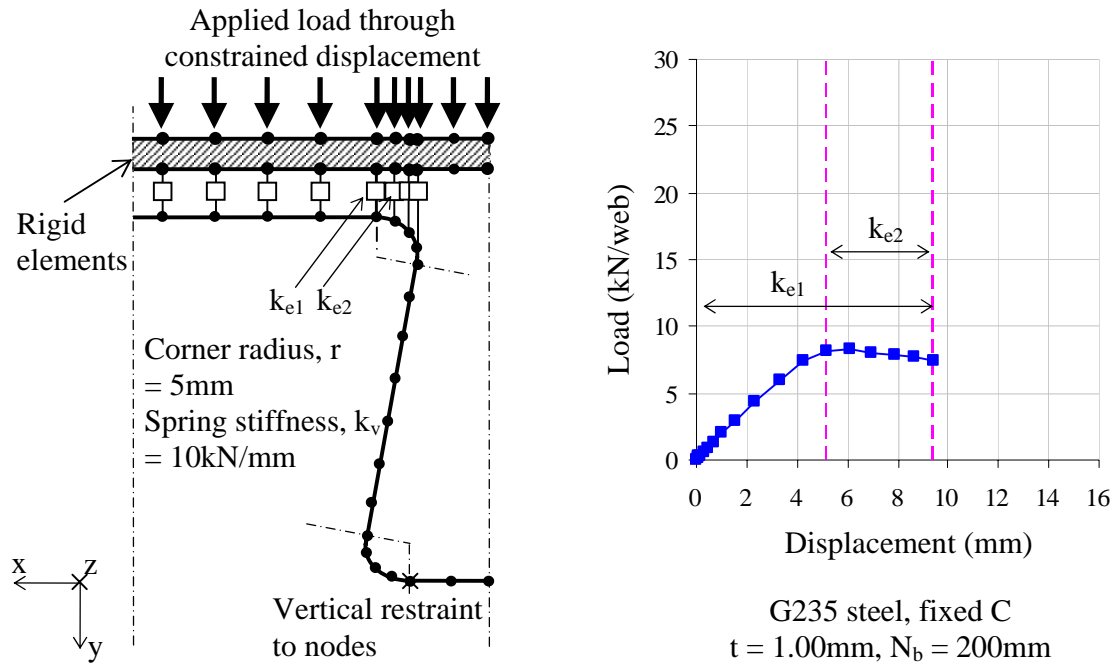
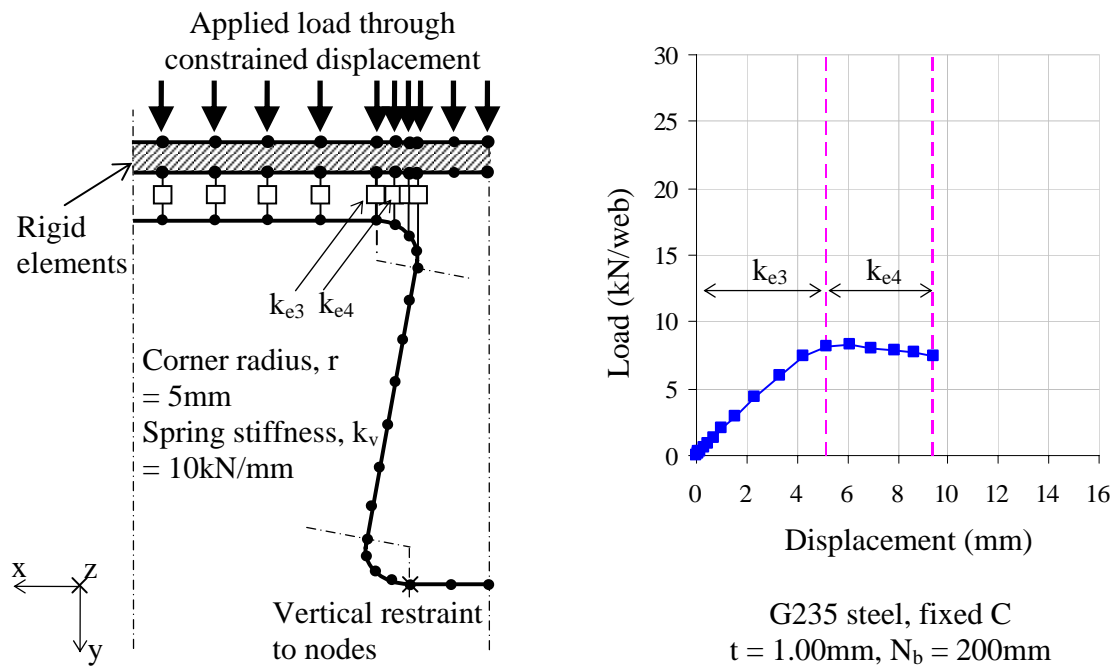


Figure 4.14: Change of contact area near the web-trough corner: internal loading condition G550, $t = 1.20\text{mm}$ and $N_b = 200\text{mm}$.



a) Inner side of load bearing width



b) Outer side of load bearing width

Figure 4.15: Change of contact area near the web-trough corner: end loading condition
G235, $t = 1.00\text{mm}$ and $N_b = 200\text{mm}$.

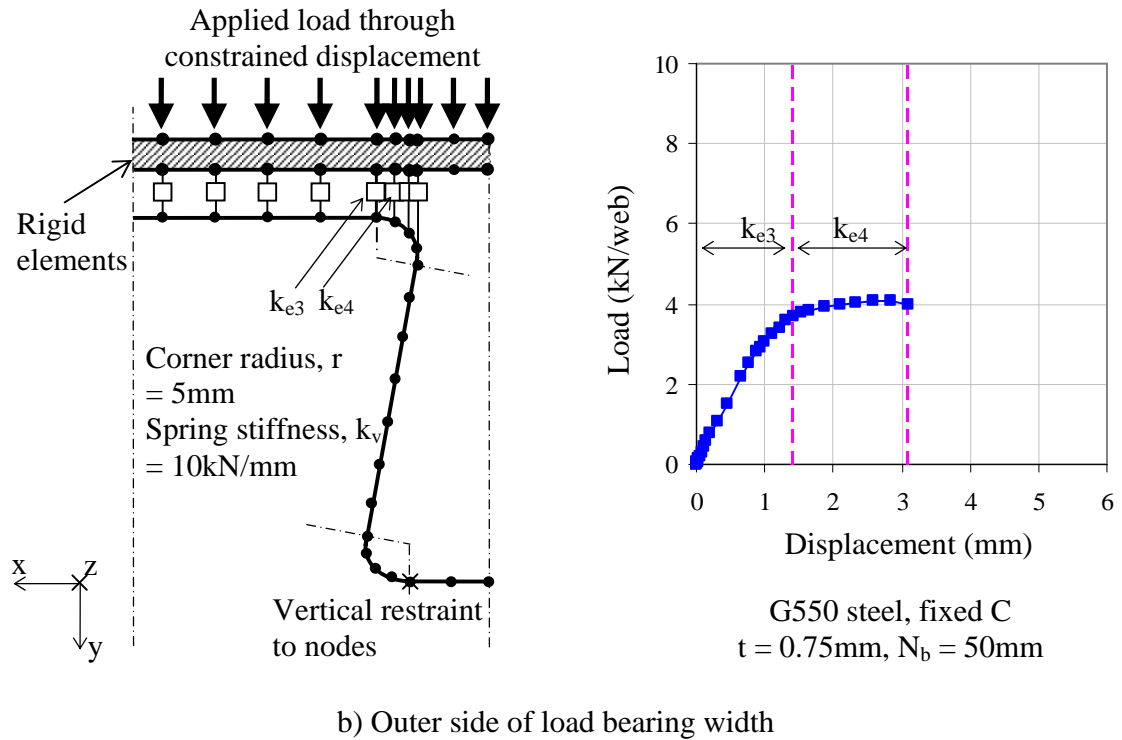
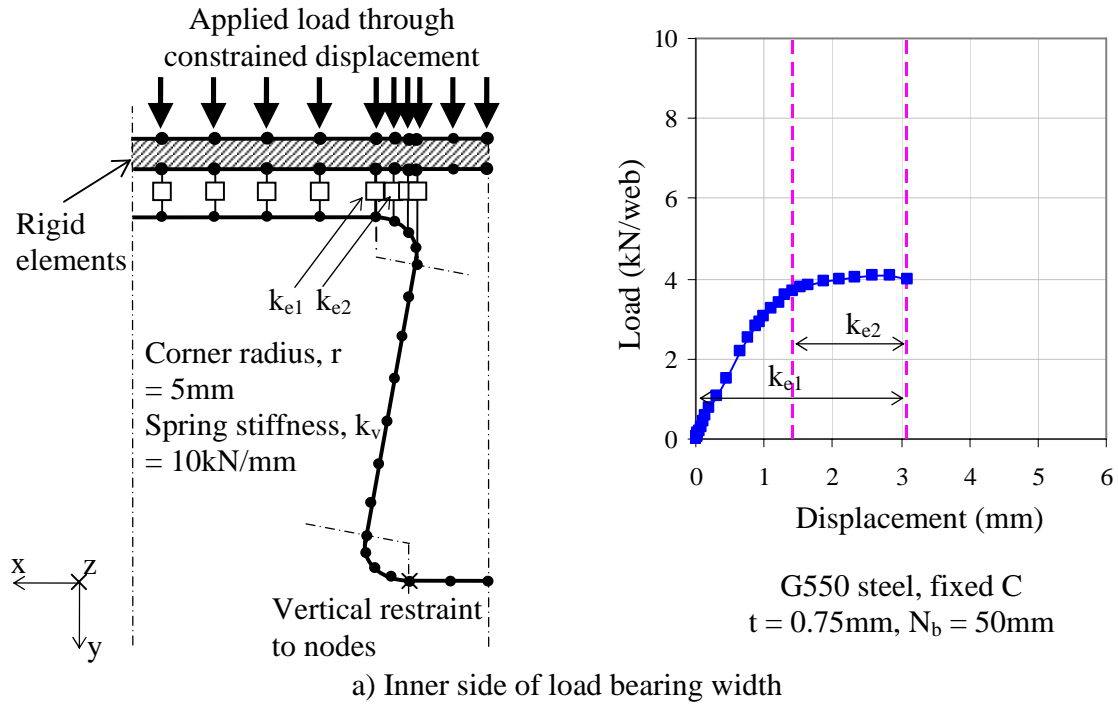


Figure 4.16: Change of contact area near the web-trough corner: end loading condition
G550, $t = 0.75\text{mm}$ and $N_b = 50\text{mm}$.

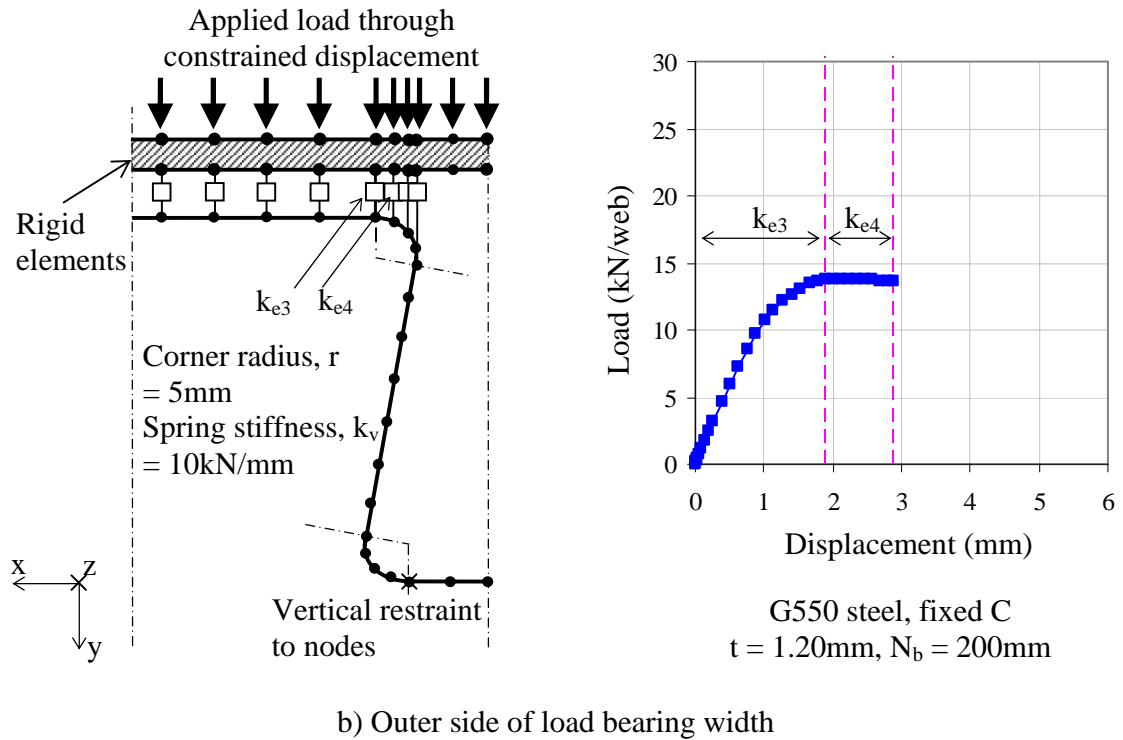
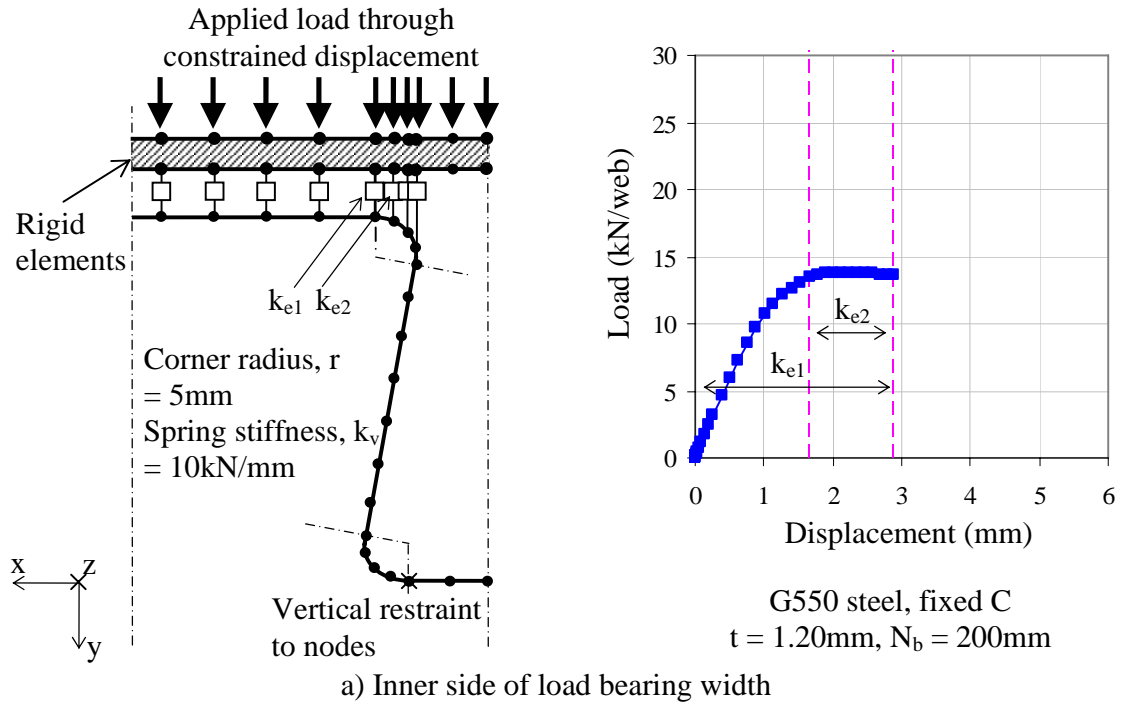


Figure 4.17: Change of contact area near the web-trough corner: end loading condition
G550, $t = 1.20\text{mm}$ and $N_b = 200\text{mm}$.

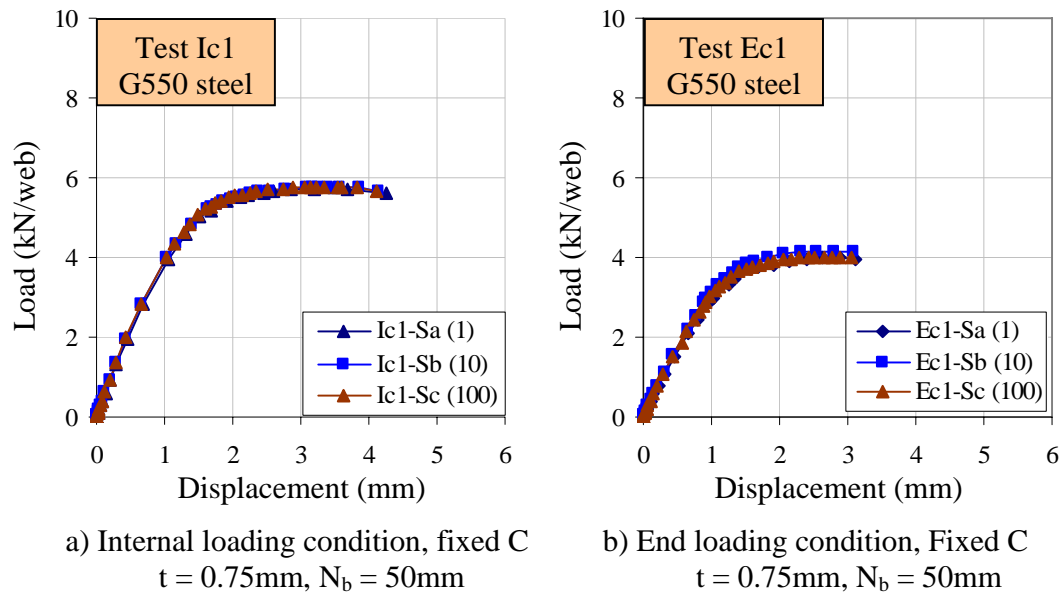


Figure 4.18: Load-displacement curves of finite element models with different values of spring stiffness.

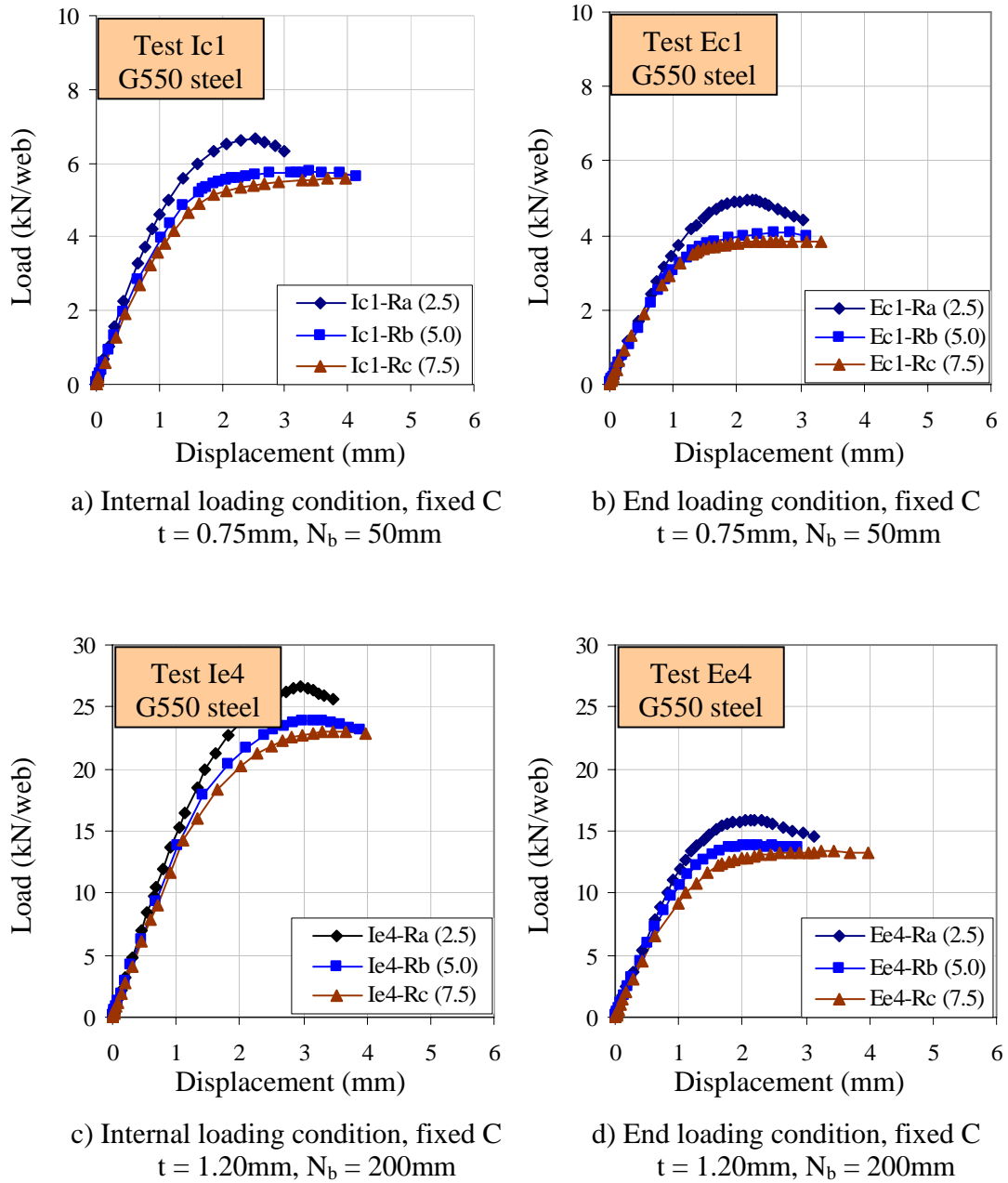


Figure 4.19: Load-displacement curves of numerical models with different corner radii.

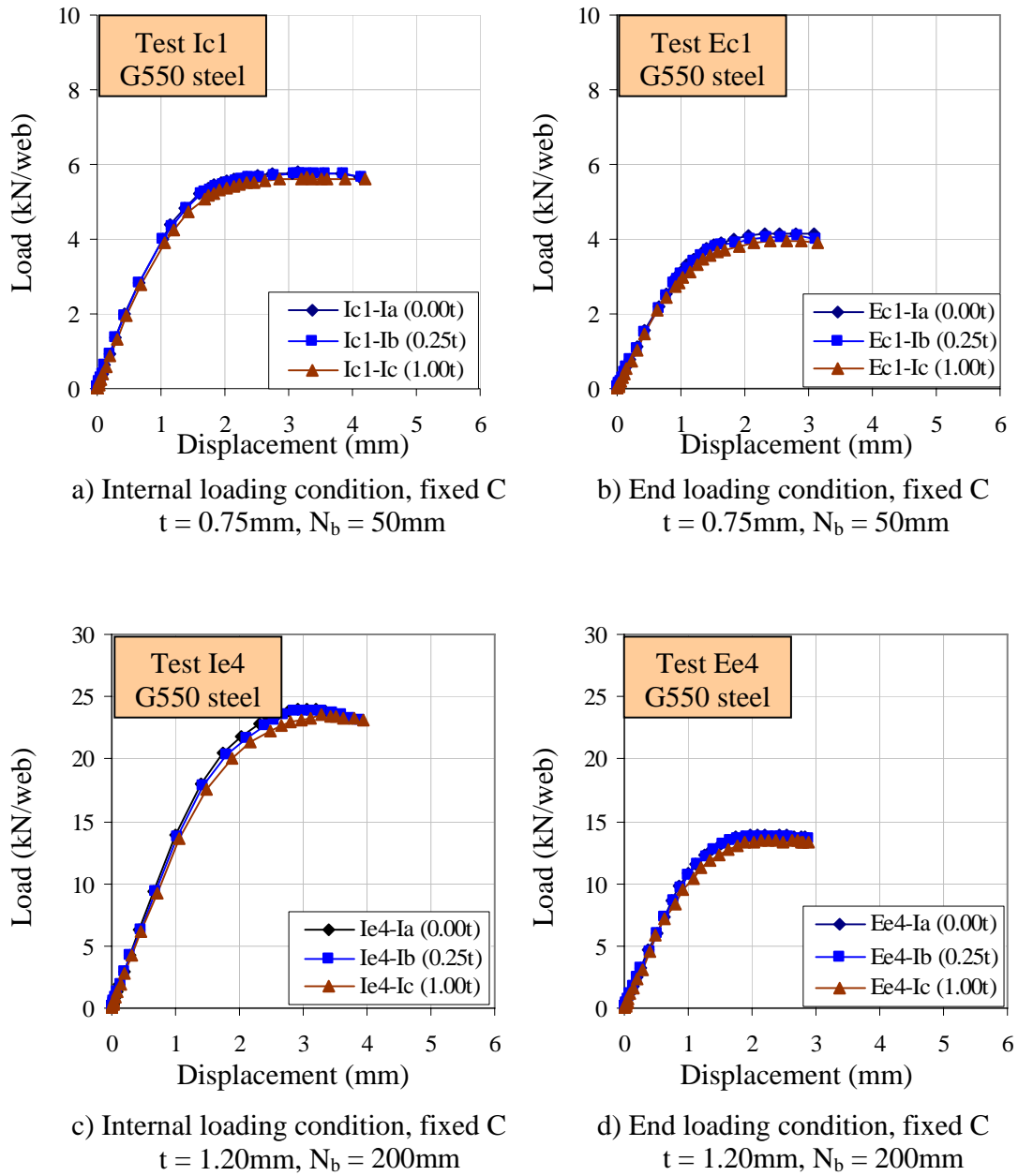
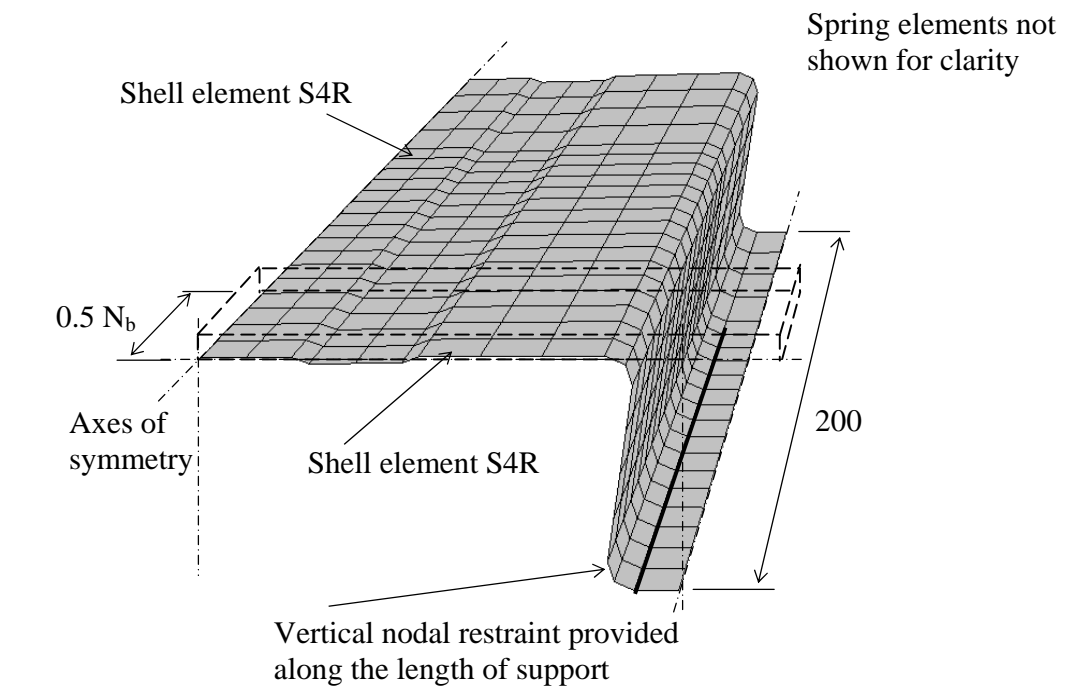
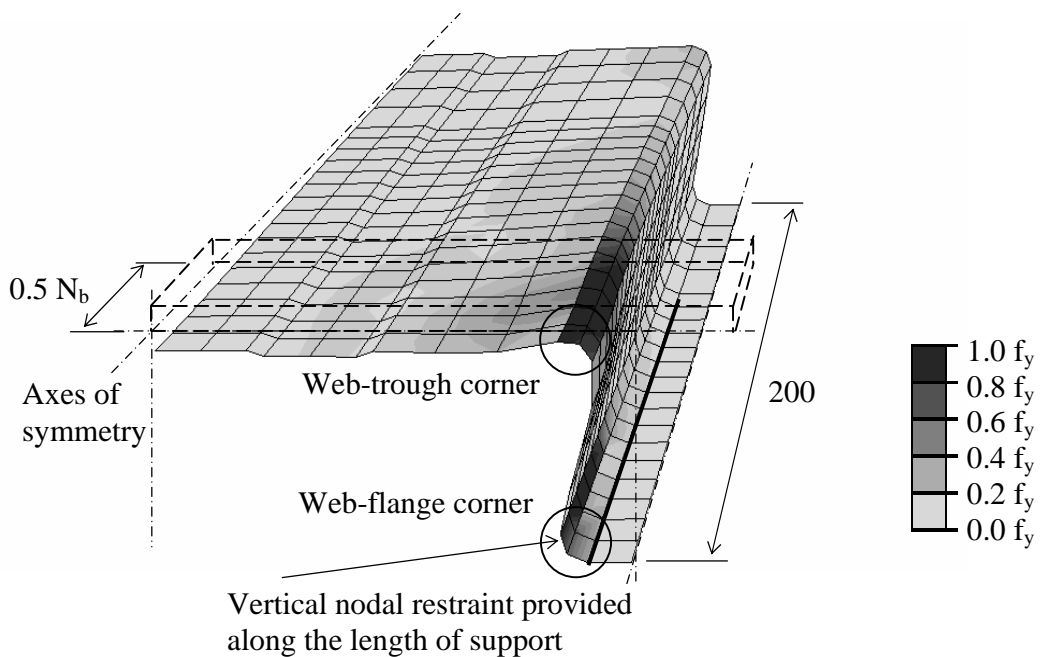


Figure 4.20: Load-displacement curves of numerical models with different values of initial imperfection.

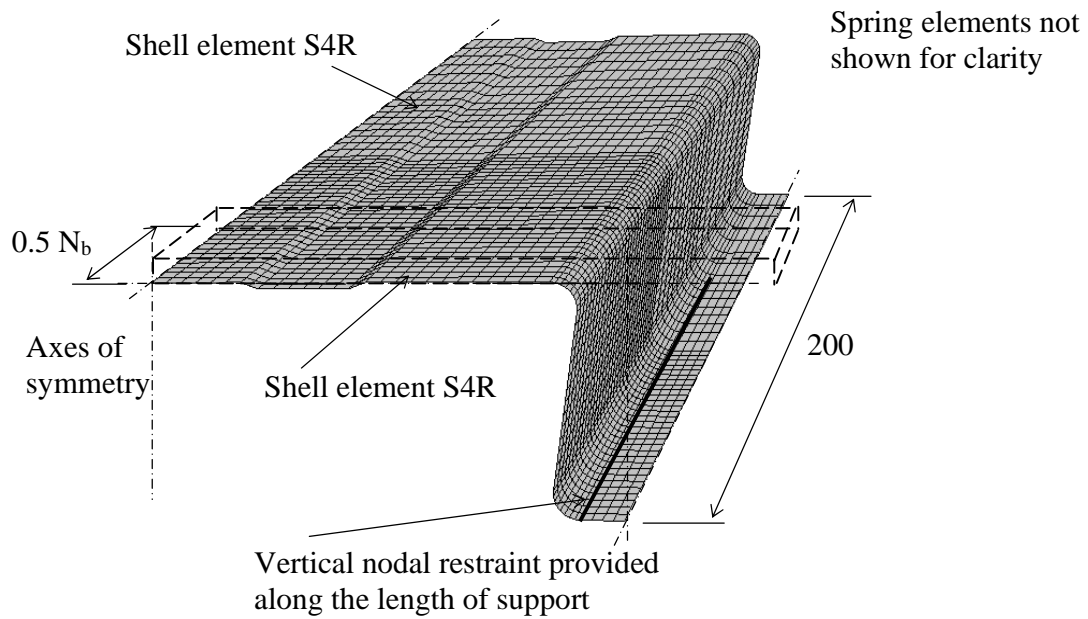


a) Geometry of finite element model

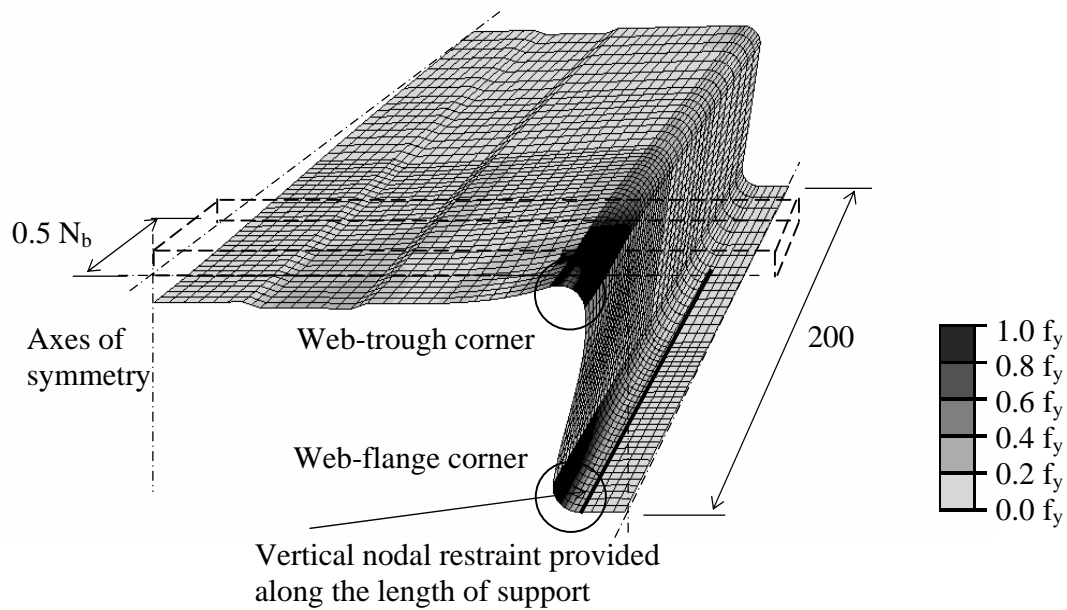


b) Deformed shape

Figure 4.21: Finite element model Ic1-Ma.
 – Fixed C, internal loading condition.



a) Geometry of finite element model



b) Deformed shape

Figure 4.22: Finite element model Ic1-Mc.
– Fixed C, internal loading condition.

Table 4.1: Summary of finite element model series.

FEM	Yield strength, p_y (N/mm ²)	Loading condition	Thickness, t (mm)	Load bearing width, N_b (mm)
Ib4	235	Internal	1.00	200
Eb4		End	1.00	200
Ic1	550	Internal	0.75	50
Ie4			1.20	200
Ec1		End	0.75	50
Ee4			1.20	200

Table 4.2: Summary of finite element models with different corner strength enhancement, boundary and loading conditions.

FEM	Yield strength, p_y (N/mm ²)	Loading condition	Lateral restraint	Load bearing width, N_b (mm)	Thickness, t (mm)	P_{FEM} $p_{y,c} = p_y$ (kN/web)	P_{FEM} $p_{y,c} = 1.25p_y$ (kN/web)	P_{Test} (kN/web)	P_{Test} / P_{FEM} $p_{y,c} = p_y$	P_{Test} / P_{FEM} $p_{y,c} = 1.25p_y$
Ib4-Ba	235	Internal	Fixed	200	1.00	10.17	10.79	10.48	1.03	0.97
Ib4-Bb			Free	200	1.00	7.50	8.28	10.48	1.40	1.27
Eb4-Ba		End	Fixed	200	1.00	7.52	8.24	7.99	1.06	0.97
Eb4-Bb			Free	200	1.00	5.45	6.18	7.99	1.47	1.29
Ic1-Ba	550	Internal	Fixed	50	0.75	5.35	5.77	5.72	1.07	0.99
Ic1-Bb			Free	50	0.75	4.07	4.55	5.72	1.41	1.26
Ie4-Ba			Fixed	200	1.20	22.43	23.90	23.48	1.05	0.98
Ie4-Bb			Free	200	1.20	17.54	19.25	23.48	1.34	1.22
Ec1-Ba		End	Fixed	50	0.75	3.57	4.02	3.94	1.10	0.98
Ec1-Bb			Free	50	0.75	2.80	3.27	3.94	1.41	1.20
Ee4-Ba			Fixed	200	1.20	12.74	13.82	13.80	1.08	1.00
Ee4-Bb			Free	200	1.20	9.61	10.71	13.80	1.44	1.29

Note:

 $p_{y,c}$ = design yield strength of corner radii

Other properties used in the numerical models:

Corner radius, $r = 5.0\text{mm}$ Initial imperfection = $0.25t$ Spring stiffness, $k_v = 10\text{ kN/mm}$

Table 4.3: Summary of finite element models with different spring stiffness.

Model name	Loading condition	Load bearing width, N_b (mm)	Thick-ness, t (mm)	Spring stiffness, k_v (kN/mm)	P_{FEM} (kN/web)	P_{Test} (kN/web)	P_{Test} / P_{FEM}
Ic1-Sa Ic1-Sb Ic1-Sc	Internal	50	0.75	1.0	5.74	5.72	1.00
				10	5.77		0.99
				100	5.78		0.99
Ec1-Sa Ec1-Sb Ec1-Sc	End	50	0.75	1.0	4.00	3.94	0.99
				10	4.02		0.98
				100	4.02		0.98
Other properties used in the numerical models: Yield strength, $p_y = 550 \text{ N/mm}^2$ Initial imperfection = 0.25t Corner radius, r = 5.0mm							

Table 4.4: Summary of finite element models with different corner radii.

Model name	Loading condition	Load bearing width, N_b (mm)	Thick-ness, t (mm)	Corner radius, r (mm)	P_{FEM} (kN/web)	P_{Test} (kN/web)	P_{Test} / P_{FEM}
Ic1-Ra Ic1-Rb Ic1-Rc	Internal	50	0.75	2.5	6.66	5.72	0.86
				5.0	5.79		0.99
				7.5	5.55		1.03
Ie4-Ra Ie4-Rb Ie4-Rc	Internal	200	1.20	2.5	26.62	23.48	0.88
				5.0	23.90		0.98
				7.5	23.07		1.02
Ec1-Ra Ec1-Rb Ec1-Rc	End	50	0.75	2.5	4.95	3.94	0.80
				5.0	4.02		0.98
				7.5	3.86		1.02
Ee4-Ra Ee4-Rb Ee4-Rc	End	200	1.20	2.5	15.90	13.80	0.87
				5.0	13.82		1.00
				7.5	13.34		1.04
Other properties used in the numerical models: Yield strength, $p_y = 550 \text{ N/mm}^2$ Initial imperfection = 0.25t Spring stiffness, $k_v = 10 \text{ kN/mm}$							

Table 4.5: Summary of finite element models with different values of initial imperfection.

Model name	Loading condition	Load bearing width, N_b (mm)	Thick-ness, t (mm)	Initial imperfection	P_{FEM} (kN/web)	P_{Test} (kN/web)	$\frac{P_{Test}}{P_{FEM}}$
Ic1-Ia Ic1-Ib Ic1-Ic	Internal	50	0.75	0.00 t	5.79	5.72	0.99
				0.25 t	5.77		0.99
				1.00 t	5.65		1.01
Ie4-Ia Ie4-Ib Ie4-Ic	Internal	200	1.20	0.00 t	24.03	23.48	0.98
				0.25 t	23.90		0.98
				1.00 t	23.50		1.00
Ec1-Ia Ec1-Ib Ec1-Ic	End	50	0.75	0.00 t	4.17	3.94	0.94
				0.25 t	4.02		0.98
				1.00 t	3.96		0.99
Ee4-Ia Ee4-Ib Ee4-Ic	End	200	1.20	0.00 t	13.90	13.80	0.99
				0.25 t	13.82		1.00
				1.00 t	13.46		1.03
Other properties used in the numerical models: Yield strength, $p_y = 550 \text{ N/mm}^2$ Corner radius, $r = 5.0\text{mm}$ Spring stiffness, $k_v = 10 \text{ kN/mm}$							

Table 4.6: Summary of finite element models with different numbers of elements.

Model name	Yield strength, p_y (N/mm ²)	Thickness, t (mm)	Number of elements	P_{FEM} (kN/web)	P_{Test} (kN/web)	P_{Test} / P_{FEM}
Ia1-Ma Ia1-Mb Ia1-Mc	235	0.75	20 x 18	3.65	3.39	0.93
31 x 31			3.45	0.98		
46 x 62			3.45	0.98		
Ic1-Ma Ic1-Mb Ic1-Mc	550	0.75	20 x 18	6.02	5.72	0.95
31 x 31			5.77	0.99		
46 x 62			5.74	0.99		
Ie1-Ma Ie1-Mb Ie1-Mc		1.20	20 x 18	12.52	11.89	0.95
31 x 31			11.92	1.00		
46 x 62			11.80	1.01		
Other properties used in the numerical models: Internal loading condition Load bearing width = 50mm Initial imperfection = 0.25t Corner radius, r = 5.0mm Spring stiffness, k _v = 10 kN/mm						

Table 4.7: Summary of parameters for finite element modeling.

Finalised parameters for FEM establishment	
Corner radius (mm)	5
Lateral restraint	Fixed C for upper bound solution Free C for lower bound solution
Spring stiffness (kN/mm)	10
Unit area per spring (mm ²)	37 (6.66mm x 5.55mm)
Number of shell elements per corner	4
Value of initial geometrical imperfection	0.25 t for internal loading condition 1.00 t for end loading condition
Effective strength enhancement at corner region	1.25 p_y

Chapter 5

Experimental Investigation into Section Failure

5.1 Introduction

For a multi-span profiled steel decking subjected to a uniformly distributed load, section failure against combined bending, shear and web crippling forces is of principal concern. A study of this section failure under combined actions involves complex interaction among three different actions as well as their interactions. Empirical design equations using linear relationships between the co-existing moments and shear forces as well as the co-existing moments and support reactions forces are adopted in various national codes of cold-formed steel structures, e.g. NAS, AISI, EC3 and BS5950: Part 6 (1995). In general, it is considered that such expressions are very conservative and over-predicts the severity of co-existing forces, in particular when some of these actions are relatively small. For these reasons, it is aimed to examine the structural behaviour of cold-formed steel profiled deckings Deck R50 subjected to this combined action through experimental investigation. A total of 42 one-point load tests are carried out to study the structural behaviour of section failure, and to provide test data for calibration of the finite element models as well as for comparison with design values.

5.2 Experimental Investigation

An extensive experimental investigation on one-point load tests of the profiled decking is carried out to examine the structural behaviour of section failure under combined bending, shear and web crippling forces. Similar to the web crippling tests reported in Chapter 3, all the test specimens are manufactured from the same steel coils as those for the web crippling tests. This will improve the consistency of the test results due to minimized variations in both materials and manufacturing process. Furthermore, the test results between the web crippling tests and the one-point load tests can be directly compared.

5.2.1 Test Program of One-Point Load Tests

For profiled deckings with various steel grades and thicknesses, three different span lengths, i.e. 600, 1000 and 2500mm, are tested in the one-point load tests, and with each span length, a number of load bearing widths, namely, 50, 100, 150 and 200mm are adopted. Table 5.1 summarizes the test program of the one-point load tests. A designation is given to each test specimen according to the thickness, the span length, and the load bearing width. The representation of each designation is explained as follows:

$$“T_{sw}”$$

where T denotes the one point load tests of profiled deckings with different steel grades

= C for one-point load test of profiled deckings with G550 steel

= D for one-point load test of profiled deckings with G235 steel

s denotes the specimen type

= a for profiled deckings with a thickness of 0.75mm and a clear span of 600 mm

= b for profiled deckings with a thickness of 0.75mm and a clear span of 1000 mm

= c for profiled deckings with a thickness of 0.75mm and a clear span of 2500 mm

= d for profiled deckings with a thickness of 1.00mm and a clear span of 600 mm

= e for profiled deckings with a thickness of 1.00mm and a clear span of 1000 mm

= f for profiled deckings with a thickness of 1.00mm and a clear span of 2500 mm

= g for profiled deckings with a thickness of 1.20mm and a clear span of 600 mm

= h for profiled deckings with a thickness of 1.20mm and a clear span of 1000 mm

= i for profiled deckings with a thickness of 1.20mm and a clear span of 2500 mm

w denotes the load bearing width

= 1 for a loading bearing width of 50 mm

= 2 for a loading bearing width of 100 mm

= 3 for a loading bearing width of 150 mm

= 4 for a loading bearing width of 200 mm

A total of 12 and 30 one-point load tests are carried for profiled deckings with G235 and G550 steel, respectively.

5.2.2 Instrumentation

Typical view of the test setup is shown in Figures 5.1 and 5.2. In order to simulate the structural behavior of cold-formed steel profiled deckings over internal supports, one point load tests spanning over the hogging moment regions of the profiled deckings are carried out, and all the test specimens are tested in an inverted position. A concentrated load is applied to the mid-span in order to simulate the reaction force at the internal supports of multi-span profiled decking. At both end supports, wooden blocks are placed beneath the profiled decking to allow direct transfer of reaction forces at the troughs of the profiled decking in addition to those transferred through the web of the profiled decking. The profiled decking is simply supported over three different span lengths, namely 600, 1000 and 2500 mm, while the load bearing lengths are 50, 100, 150 and 200 mm.

Two displacement transducers are placed at the mid-span of the profiled decking to measure their vertical deflections. The transducers are positioned in such a way to measure the vertical deflections of the flanges which are in tension. Such arrangement is adopted in order to eliminate any measurement error caused by possible local buckling in the profiled deckings.

5.2.3 Test Results

The measured load deflection curves of the profiled deckings are presented in Figure 5.4 to 5.6 while the failure loads are summarised in Tables 5.2 and 5.3. The typical failure mode is shown in Figure 5.3. It should be noted that prior to attaining the ultimate loads, local buckling is observed at the compression flange at the mid-span in all test specimens; the typical buckled shape of the profiled deckings is shown in Figure 5.3a. While for profiled deckings under ultimate loads, section failure against bending and web crippling is observed at mid-span, as shown in Figure 5.3b. No obvious sign of shear failure is involved among all the tests performed. The negligible shear effect in comparison with web crippling is proven in Figures 5.11 and 5.12 where the shear force ratios are less than 0.30 in all tests performed. It should be noted that for profiled deckings with G550 steel, the moment ratios are relatively reduced for a span length of 2500 mm when compared against the results with a span length of 1000 mm. In theory, an increase of span length will reduce the effect of shear and web crippling effects, hence larger moment resistance can be achieved. However, in contrast, distortional buckling trends to occur in profiled deckings of medium span which increases the moment capacities by a maximum of 10%. Therefore, the moment capacities for profiled deckings with a span length of 2500 mm are not the largest among all the test results.

Tables 5.4 and 5.5 summarize the normalized resistances which are rearranged from Tables 5.2 and 5.3, respectively. Rearrangement is made to the data so that direct comparison on the moment capacities under different load bearing widths and clear spans can be readily

achieved. Through the use of larger load bearing widths, the resultant moment resistances have significantly increased due to the reduced web crippling effect. This web crippling effect is also presented in a graphical form as shown in Figures 5.11 and 5.12. For example, for Deck R50 of G550 steel with a thickness of 0.75mm and a span length of 1000mm, a 44.6% increase in the moment resistance is found when the load bearing width is increased from 50mm to 200mm.

5.3 Comparison of Design Results against Experimental Results

BS5950: Part 6 (1995) recommends two individual checks for internal supports of cold-formed steel profiled deckings under combined actions, namely i) combined bending and shear, and ii) combined bending and web crippling, as shown in Figure 5.7. Detailed comparison between the measured and the design values according to the two checks are presented in Section 5.3.1 and Section 5.3.2, respectively.

5.3.1 Combined Bending and Shear

For cold-formed steel profiled deckings subjected to combined bending and shear, the following design criteria should be satisfied:

$$F_v \leq P_v \tag{5.1}$$

$$M \leq M_c \quad (5.2)$$

$$\left(\frac{F_v}{P_v} \right)^2 + \left(\frac{M}{M_c} \right)^2 \leq 1 \quad (5.3)$$

where P_v is the design shear capacity; M_c is the design moment capacity; F_v and M are the applied shear force and moment obtained from one-point load tests, respectively. For ease of comparison, non-dimensionalized test-to-design ratios are provided in Tables 5.6 and 5.7 for profiled deckings of G550 and G235 respectively. The bending shear interaction curves for the profiled deckings are plotted in Figures 5.8 and 5.9. It is shown in Table 5.6 that the shear force ratios in all tests are relatively small in comparison with the moment ratio. For instance, for G550 steel Deck R50 with thickness of 0.75mm, load bearing width of 150mm and span length of 1000mm, the shear ratio is 0.14 while the moment ratio is 1.14. Hence, the shear effect does exist but is in general not as critical as to the moment effect in the section failure of profiled deckings under practical loading and support conditions.

5.3.2 Combined Bending and Web Crippling

For cold-formed steel profiled deckings subject to combined bending and concentrated load, the following design criteria shall be satisfied:

$$F_w \leq P_w \quad (5.4)$$

$$M \leq M_c \text{ and} \quad (5.5)$$

$$\frac{F_w}{P_w} + \frac{M}{M_c} \leq 1.25 \quad (5.6)$$

where P_w is the design web crippling resistance, M_c is the design moment capacity; and F_w and M are the applied load and moment at failure obtained from one-point load tests, respectively. The results are summarized in Tables 5.8 and 5.9, as well as Figures 5.8 and 5.9. In comparison with the effect of combined bending and shear where the shear effect is considered to be less of a concern, the web crippling effect plays an important role in the section failure under combined bending and web crippling. For example, for the same decking mentioned in Section 5.3.1, i.e. profiled decking of G550 steel with a thickness of 0.75mm, a span length of 1000mm and a load bearing width of 150mm, the web crippling resistance ratio is found to reach 0.30 while the moment resistance ratio is 1.14. It should be noted that the shear ratio is 0.14. Hence, it is shown from the test results that both bending moment and concentrated load play important roles towards the section failure of cold-formed profiled steel deckings, while the shear effect is of minor importance. Nevertheless, the shear effect should never be ignored.

5.3.3 Structural Efficiency of Design Rules

Model factors, which are defined as the tested load, P_{Test} , divided by the design load, P_{Design} , are calculated for all the tests. As there are two separate checks namely, combined bending and shear, and combined bending and web crippling, the value of P_{Design} is taken to be the minimum value derived from the two checks.

The model factors computed for all the tests are presented in Figure 5.10. In most cases except for three tests found with a 0.75mm thick G550 profiled decking, the model factors are larger than one, indicating that the current design provisions are generally conservative for the profiled deckings. However, the design equations may be too conservative as the maximum value of the model factors is found to be 1.4. Hence, finite element models are established to examine the structural behaviour of profiled decking undergoing section failure, and the numerical results are presented in Chapter 7.

5.4 Summary

An experimental investigation into the cold-formed profiled steel deckings subjected to combined actions is presented, and the one-point load tests are carried out to examine the structural behaviour of section failure under combined actions. It is shown that shear force tends to have minor effect while both bending and web crippling play important roles towards the section failure of the profiled deckings. Based on the experimental

investigation into section failure of profiled deckings over a practical range of steel grades, thicknesses, load bearing widths and span lengths, it is concluded that large web crippling force often induces a significant adverse effect to the load carrying capacity of the profiled deckings under hogging moments.

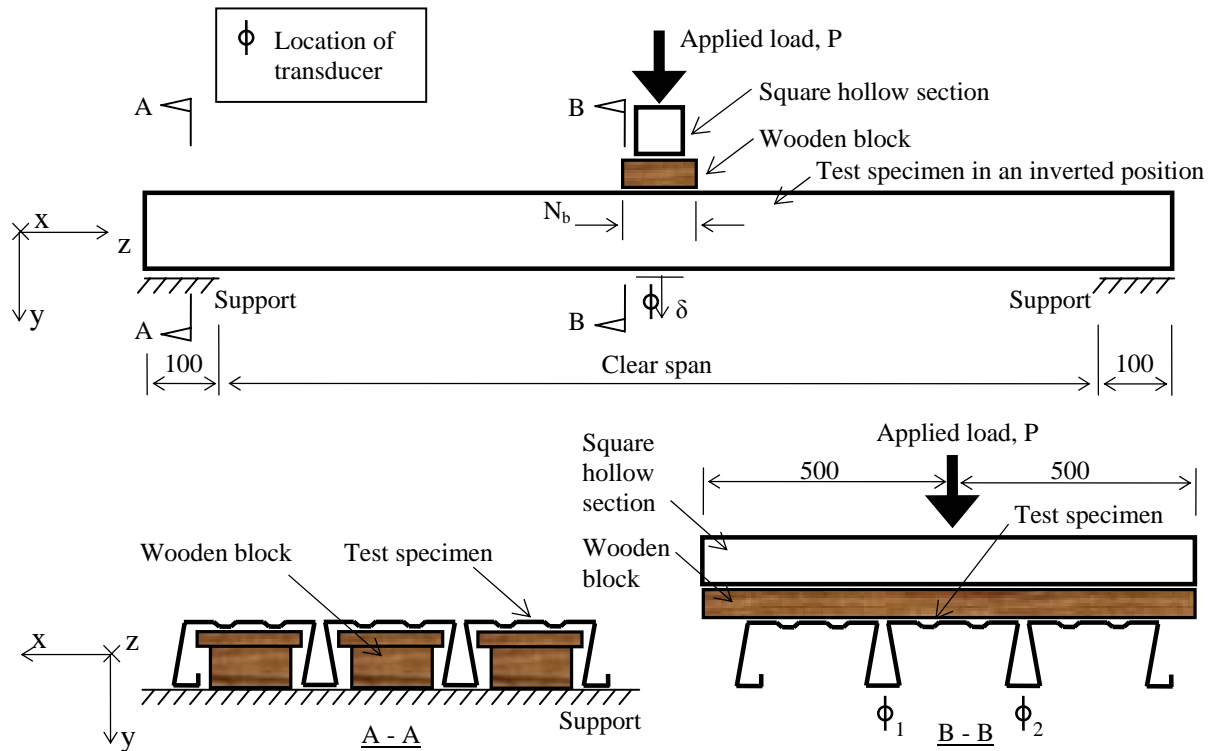


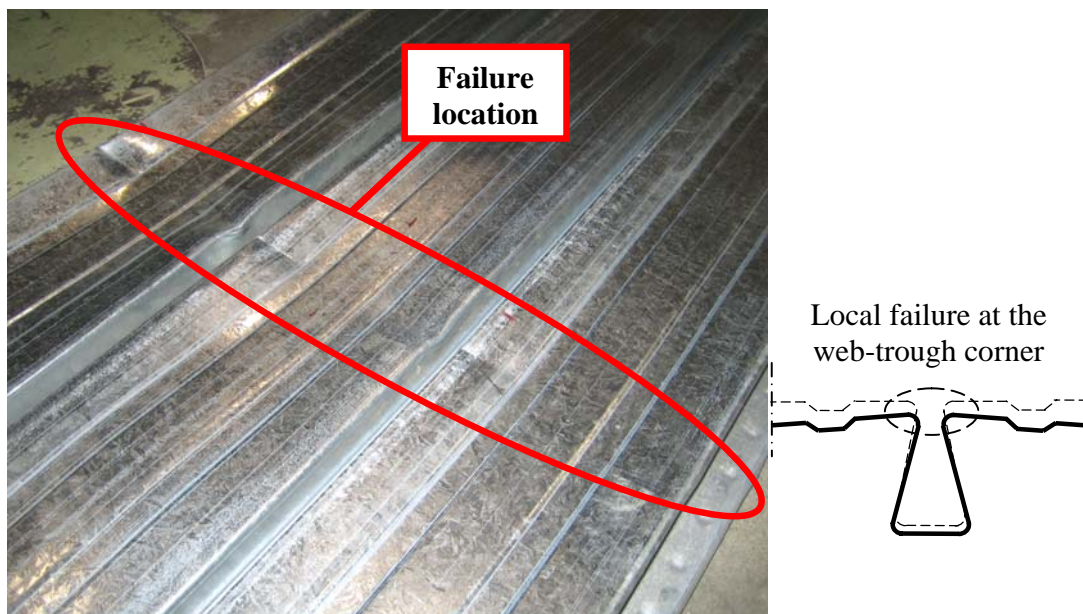
Figure 5.1: Typical set-up of one-point load test.



Figure 5.2: General view of one-point load test.

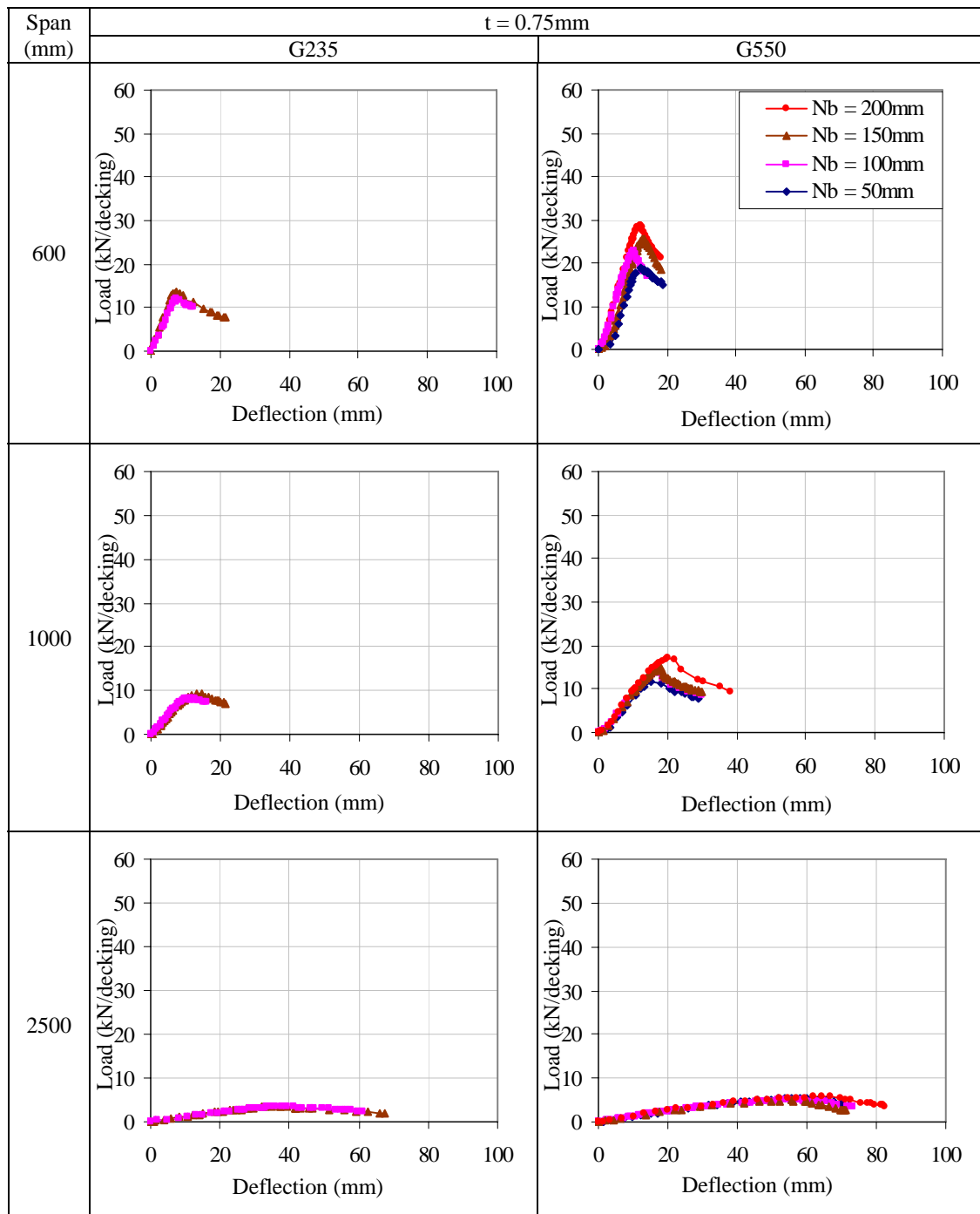


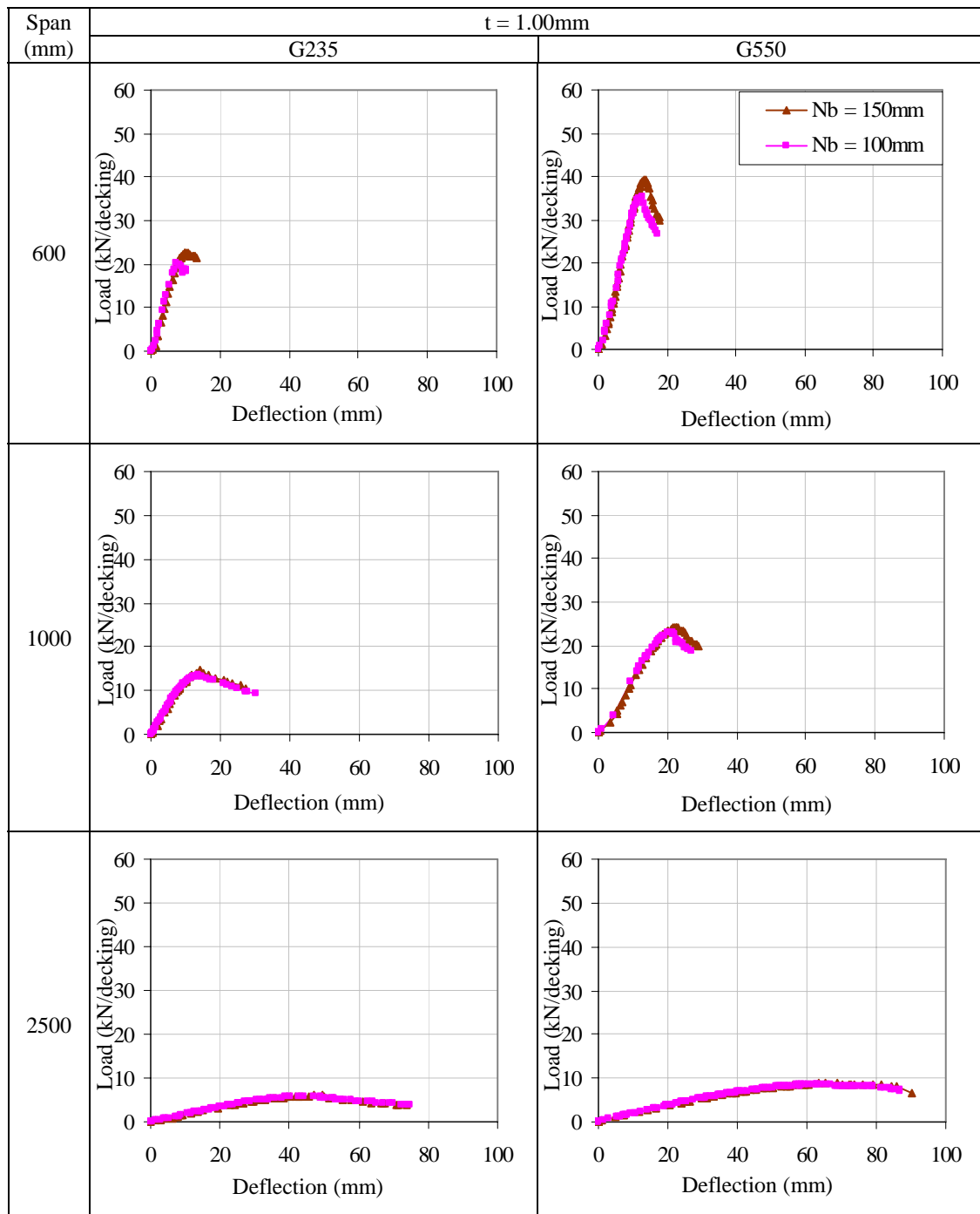
a) Significant local plate buckling in trough



b) Section failure in the profiled decking over the load bearing width

Figure 5.3: Typical failure mode of one point load test.

Figure 5.4: Load-deflection curves of one-point load tests: $t = 0.75\text{mm}$.

Figure 5.5: Load-deflection curves of one-point load tests: $t = 1.00\text{mm}$.

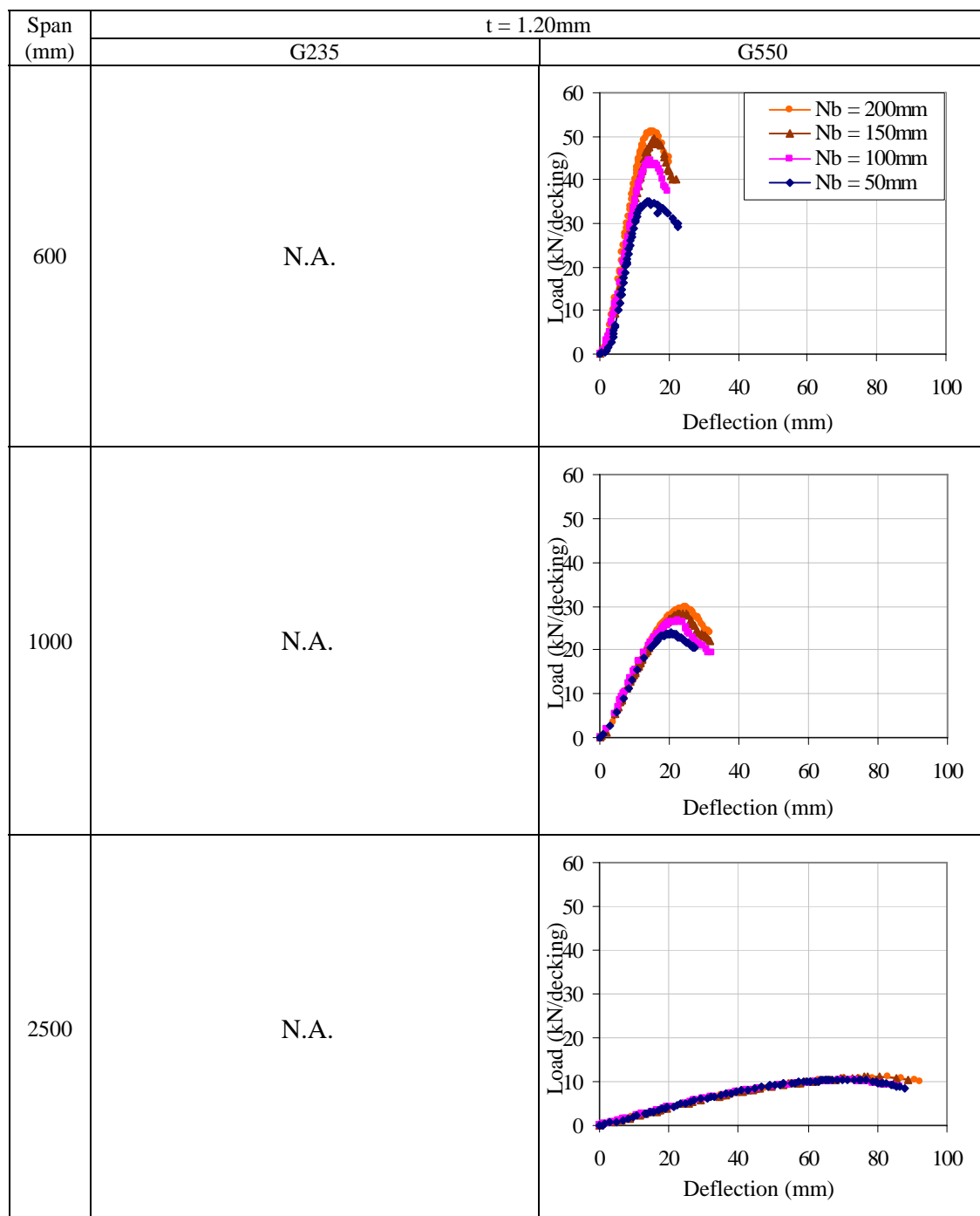


Figure 5.6: Load-deflection curves of one-point load tests: t = 1.20mm.

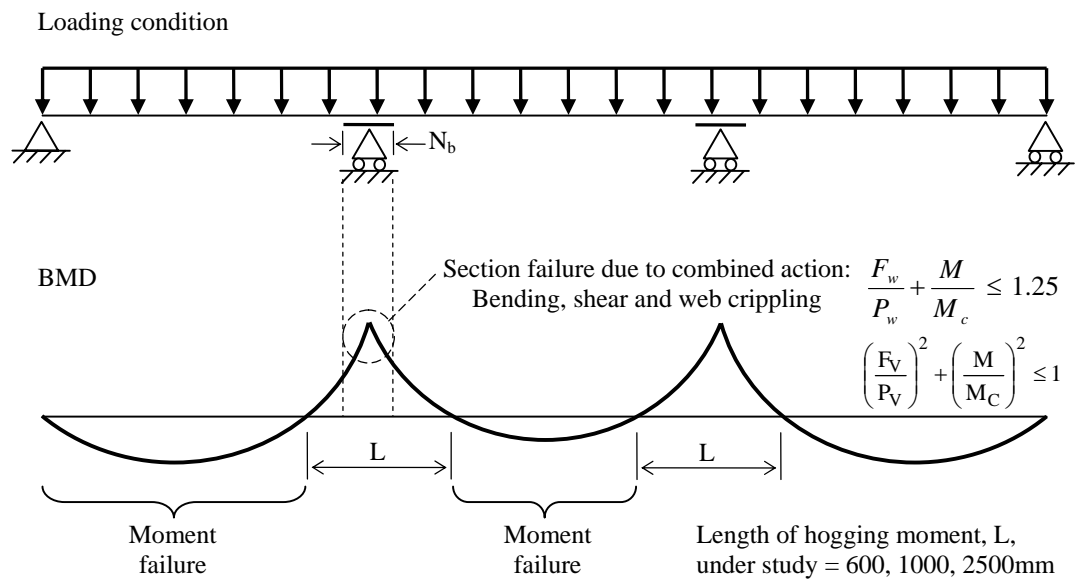


Figure 5.7: Continuous structure under section failure.

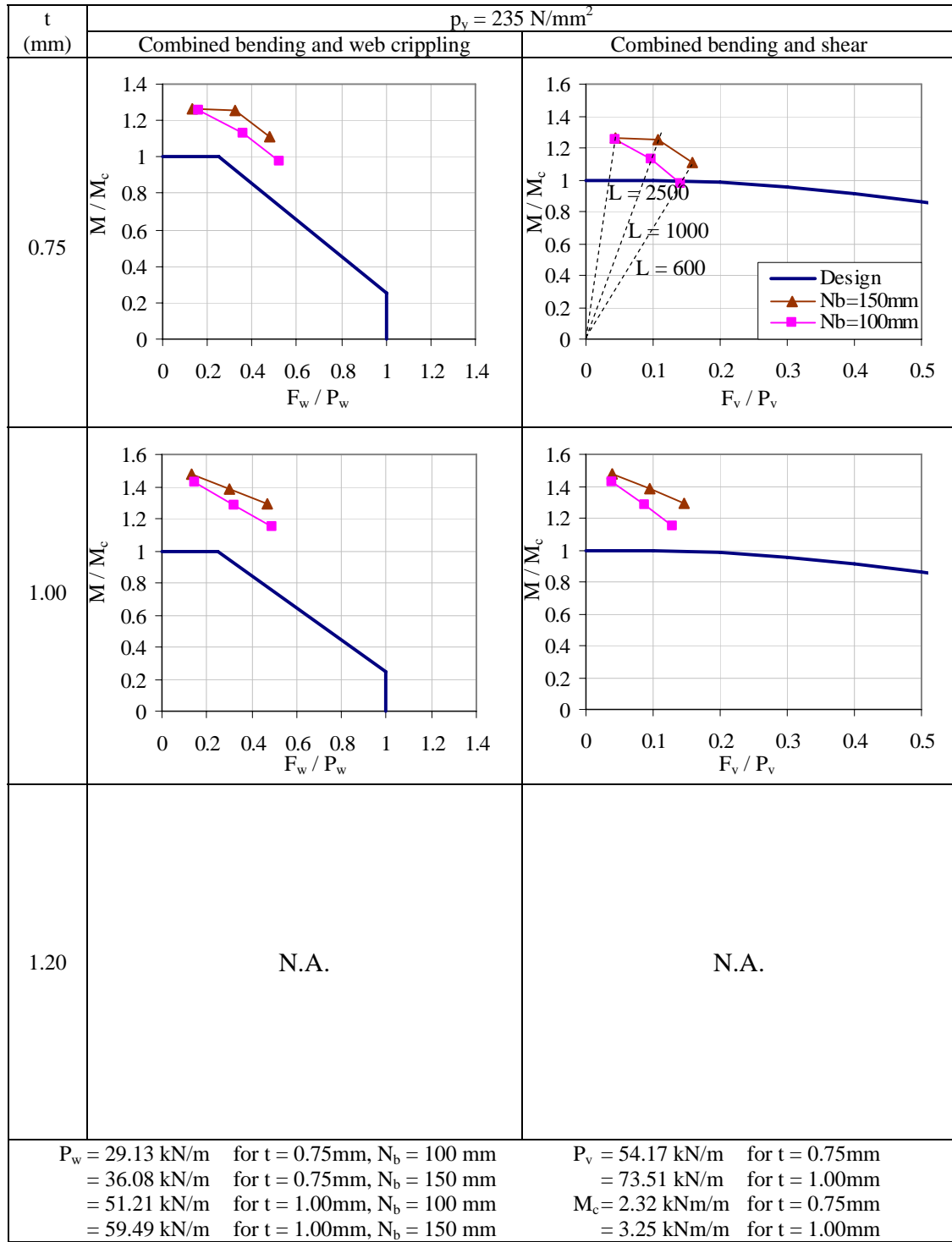


Figure 5.8: Summary of section failure resistances for G235 steel.

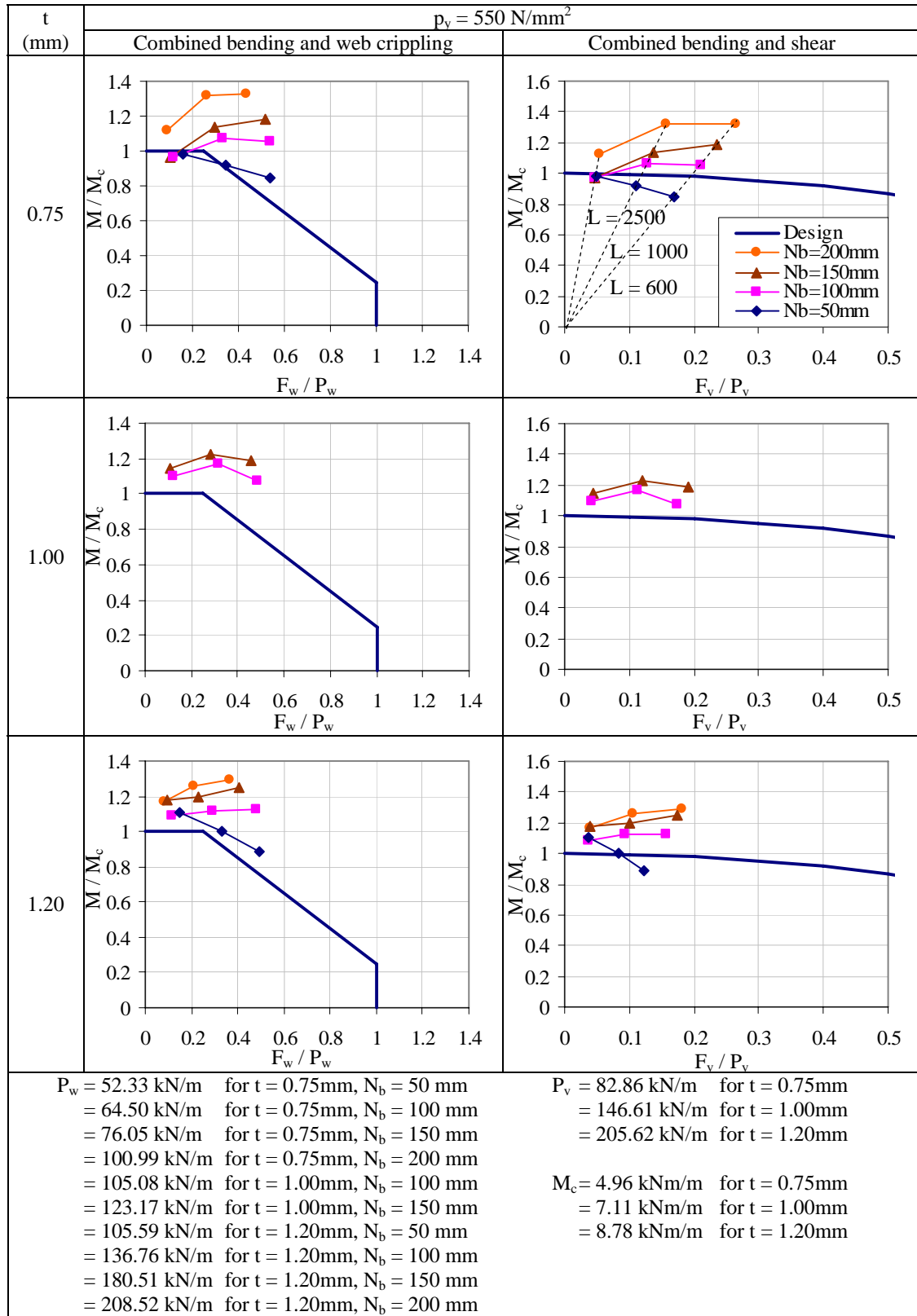


Figure 5.9: Summary of section failure resistances for G550 steel.

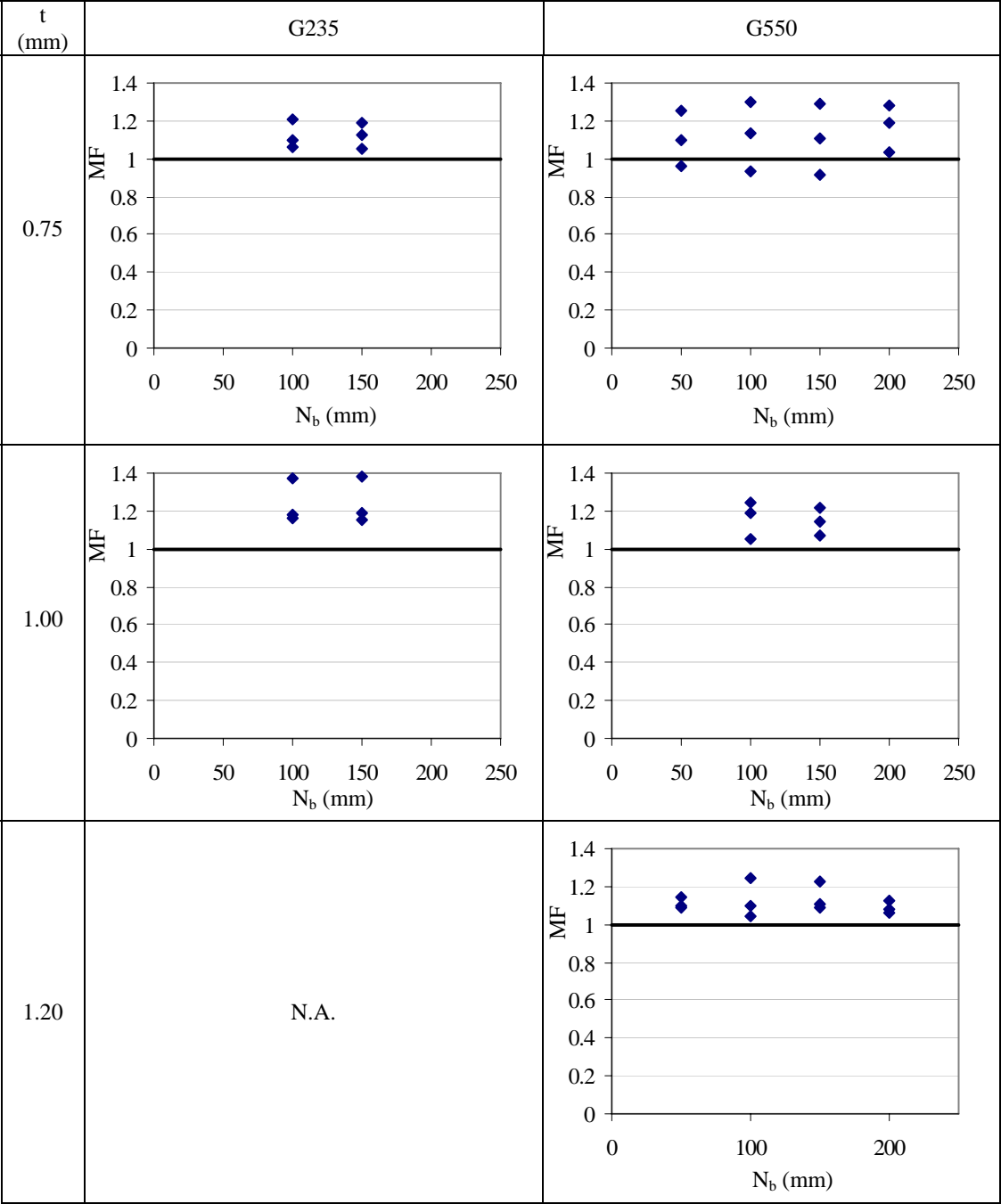


Figure 5.10: Model factors for section failure.

Table 5.1: Summary of test program for one-point load test.

Load bearing width, N_b (mm)	Thick-ness, t (mm)	Span length (mm)	G550		G235	
			No. of tests	Test designation	No. of tests	Test designation
50	0.75	600	1	Ca1	-	-
		1000	1	Cb1	-	-
		2500	1	Cc1	-	-
	1.00	600	-	-	-	-
		1000	-	-	-	-
		2500	-	-	-	-
	1.20	600	1	Cg1	-	-
		1000	1	Ch1	-	-
		2500	1	Ci1	-	-
100	0.75	600	1	Ca2	1	Da2
		1000	1	Cb2	1	Db2
		2500	1	Cc2	1	Dc2
	1.00	600	1	Cd2	1	Dd2
		1000	1	Ce2	1	De2
		2500	1	Cf2	1	Df2
	1.20	600	1	Cg2	-	-
		1000	1	Ch2	-	-
		2500	1	Ci2	-	-
150	0.75	600	1	Ca3	1	Da3
		1000	1	Cb3	1	Db3
		2500	1	Cc3	1	Dc3
	1.00	600	1	Cd3	1	Dd3
		1000	1	Ce3	1	De3
		2500	1	Cf3	1	Df3
	1.20	600	1	Cg3	-	-
		1000	1	Ch3	-	-
		2500	1	Ci3	-	-
200	0.75	600	1	Ca4	-	-
		1000	1	Cb4	-	-
		2500	1	Cc4	-	-
	1.00	600	-	-	-	-
		1000	-	-	-	-
		2500	-	-	-	-
	1.20	600	1	Cg4	-	-
		1000	1	Ch4	-	-
		2500	1	Ci4	-	-

Table 5.2: Summary of one-point load test results for profiled decking with G550 steel.

Load bearing width, N_b (mm)	Thickness, t (mm)	Span length (mm)	Test designation	Applied load at failure P_{test} (kN/decking)	Applied moment at failure M_{test} (kNm/decking)
50	0.75	600	Ca1	18.43	2.76
		1000	Cb1	11.90	2.97
		2500	Cc1	5.11	3.19
	1.00	600	-	-	-
		1000	-	-	-
		2500	-	-	-
	1.20	600	Cg1	35.00	5.25
		1000	Ch1	23.85	5.96
		2500	Ci1	10.52	6.57
100	0.75	600	Ca2	22.77	3.42
		1000	Cb2	13.89	3.47
		2500	Cc2	5.02	3.14
	1.00	600	Cd2	35.48	5.32
		1000	Ce2	23.11	5.78
		2500	Cf2	8.70	5.44
	1.20	600	Cg2	44.44	6.67
		1000	Ch2	26.59	6.65
		2500	Ci2	10.34	6.46
150	0.75	600	Ca3	25.67	3.85
		1000	Cb3	14.80	3.70
		2500	Cc3	5.03	3.14
	1.00	600	Cd3	39.21	5.88
		1000	Ce3	24.31	6.08
		2500	Cf3	9.04	5.65
	1.20	600	Cg3	49.51	7.43
		1000	Ch3	28.45	7.11
		2500	Ci3	11.21	7.01
200	0.75	600	Ca4	28.70	4.30
		1000	Cb4	17.16	4.29
		2500	Cc4	5.83	3.64
	1.00	600	-	-	-
		1000	-	-	-
		2500	-	-	-
	1.20	600	Cg4	51.23	7.68
		1000	Ch4	29.79	7.45
		2500	Ci4	11.10	6.94
Failure mode: Local collapse of compression flange and web at mid-span in all tests					

Table 5.3: Summary of one-point load test results for profiled decking with G235 steel.

Load bearing width, N_b (mm)	Thickness, t (mm)	Span length (mm)	Test designation	Applied load at failure P_{test} (kN/decking)	Applied moment at failure M_{test} (kNm/decking)
50	0.75	600	-	-	-
		1000	-	-	-
		2500	-	-	-
	1.00	600	-	-	-
		1000	-	-	-
		2500	-	-	-
	1.20	600	-	-	-
		1000	-	-	-
		2500	-	-	-
100	0.75	600	Da2	12.20	1.83
		1000	Db2	8.44	2.11
		2500	Dc2	3.74	2.34
	1.00	600	Dd2	20.39	3.06
		1000	De2	13.57	3.39
		2500	Df2	6.07	3.79
	1.20	600	-	-	-
		1000	-	-	-
		2500	-	-	-
150	0.75	600	Da3	13.78	2.07
		1000	Db3	9.39	2.35
		2500	Dc3	3.77	2.36
	1.00	600	Dd3	22.84	3.43
		1000	De3	14.76	3.69
		2500	Df3	6.24	3.90
	1.20	600	-	-	-
		1000	-	-	-
		2500	-	-	-
200	0.75	600	-	-	-
		1000	-	-	-
		2500	-	-	-
	1.00	600	-	-	-
		1000	-	-	-
		2500	-	-	-
	1.20	600	-	-	-
		1000	-	-	-
		2500	-	-	-
Failure mode: Local collapse of compression flange and web at mid-span in all tests					

Table 5.4: Normalized results of one-point load tests for profiled decking with G550 steel.

Thick-ness, t (mm)	Span length (mm)	Applied load at failure P_{test} (kN/m)				Applied moment at failure M_{test} (kNm/m)			
		$N_b = 50\text{mm}$	$N_b = 100\text{mm}$	$N_b = 150\text{mm}$	$N_b = 200\text{mm}$	$N_b = 50\text{mm}$	$N_b = 100\text{mm}$	$N_b = 150\text{mm}$	$N_b = 200\text{mm}$
0.75	600	28.12	34.74	39.17	43.79	4.21	5.22	5.87	6.56
	1000	18.16	21.19	22.58	26.18	4.53	5.29	5.65	6.55
	2500	7.79	7.66	7.67	8.90	4.86	4.79	4.79	5.55
1.00	600	-	50.98	56.34	-	-	7.64	8.45	-
	1000	-	33.21	34.93	-	-	8.31	8.74	-
	2500	-	12.50	12.99	-	-	7.82	8.12	-
1.20	600	51.79	65.76	73.26	75.80	7.77	9.87	10.99	11.36
	1000	35.29	39.34	42.10	44.08	8.82	9.84	10.52	11.02
	2500	15.57	15.30	16.59	16.42	9.72	9.56	10.37	10.27
Notes	Normalized results to yield strength of 550 N/mm ² and thicknesses of 0.75, 1.00 and 1.20 mm through linear interpolation.								

Table 5.5: Normalized results of one-point load tests for profiled decking with G235 steel.

Thick-ness, t (mm)	Span length (mm)	Applied load at failure P_{test} (kN/m)				Applied moment at failure M_{test} (kNm/m)			
		$N_b = 50\text{mm}$	$N_b = 100\text{mm}$	$N_b = 150\text{mm}$	$N_b = 200\text{mm}$	$N_b = 50\text{mm}$	$N_b = 100\text{mm}$	$N_b = 150\text{mm}$	$N_b = 200\text{mm}$
0.75	600	-	15.25	17.22	-	-	2.29	2.58	-
	1000	-	10.55	11.74	-	-	2.64	2.93	-
	2500	-	4.67	4.71	-	-	2.92	2.95	-
1.00	600	-	24.99	27.99	-	-	3.75	4.20	-
	1000	-	16.63	18.09	-	-	4.16	4.52	-
	2500	-	7.44	7.65	-	-	4.65	4.78	-
1.20	600	-	-	-	-	-	-	-	-
	1000	-	-	-	-	-	-	-	-
	2500	-	-	-	-	-	-	-	-
Notes	Normalized results to yield strength of 235 N/mm ² and thicknesses of 0.75, 1.00 and 1.20 mm through linear interpolation.								

Table 5.6: Design against combined bending and shear for profiled decking with G550 steel.

Thick- ness, t (mm)	Span length (mm)	Load bearing width, N_b (mm)	Applied shear force at failure, V_{Test} (kN/m)	Applied moment at failure, M_{Test} (kNm/m)	Shear capacity, V_c (kN/m)	Moment capacity, M_c (kNm/m)	$v =$ V_{Test} / V_c	$m =$ M_{Test} / M_c	$p =$ $P_{w, Test} / P_{w, c}$	$v^2 + m^2$
0.75	600	50	14.06	4.21	82.86	4.96	0.17	0.85	0.54	0.75
		100	17.37	5.22	82.86	4.96	0.21	1.05	0.54	1.15
		150	19.58	5.87	82.86	4.96	0.24	1.19	0.51	1.46
		200	21.89	6.56	82.86	4.96	0.26	1.32	0.43	1.82
	1000	50	9.08	4.53	82.86	4.96	0.11	0.91	0.35	0.85
		100	10.60	5.29	82.86	4.96	0.13	1.07	0.33	1.16
		150	11.29	5.65	82.86	4.96	0.14	1.14	0.30	1.32
		200	13.09	6.55	82.86	4.96	0.16	1.32	0.26	1.77
	2500	50	3.90	4.86	82.86	4.96	0.05	0.98	0.15	0.97
		100	3.83	4.79	82.86	4.96	0.05	0.97	0.12	0.94
		150	3.84	4.79	82.86	4.96	0.05	0.97	0.10	0.94
		200	4.45	5.55	82.86	4.96	0.05	1.12	0.09	1.26
1.00	600	50	-	-	-	-	-	-	-	-
		100	25.49	7.64	146.61	7.11	0.17	1.07	0.49	1.18
		150	28.17	8.45	146.61	7.11	0.19	1.19	0.46	1.45
		200	-	-	-	-	-	-	-	-
	1000	50	-	-	-	-	-	-	-	-
		100	16.60	8.31	146.61	7.11	0.11	1.17	0.32	1.38
		150	17.47	8.74	146.61	7.11	0.12	1.23	0.28	1.52
		200	-	-	-	-	-	-	-	-
	2500	50	-	-	-	-	-	-	-	-
		100	6.25	7.82	146.61	7.11	0.04	1.10	0.12	1.21
		150	6.50	8.12	146.61	7.11	0.04	1.14	0.11	1.30
		200	-	-	-	-	-	-	-	-
1.20	600	50	25.89	7.77	205.62	8.78	0.13	0.88	0.49	0.80
		100	32.88	9.87	205.62	8.78	0.16	1.12	0.48	1.29
		150	36.63	10.99	205.62	8.78	0.18	1.25	0.41	1.60
		200	37.90	11.36	205.62	8.78	0.18	1.29	0.36	1.71
	1000	50	17.64	8.82	205.62	8.78	0.09	1.00	0.33	1.02
		100	19.67	9.84	205.62	8.78	0.10	1.12	0.29	1.27
		150	21.05	10.52	205.62	8.78	0.10	1.20	0.23	1.45
		200	22.04	11.02	205.62	8.78	0.11	1.26	0.21	1.59
	2500	50	7.78	9.72	205.62	8.78	0.04	1.11	0.15	1.23
		100	7.65	9.56	205.62	8.78	0.04	1.09	0.11	1.19
		150	8.29	10.37	205.62	8.78	0.04	1.18	0.09	1.40
		200	8.21	10.27	205.62	8.78	0.04	1.17	0.08	1.37

Table 5.7: Design against combined bending and shear for profiled decking with G235 steel.

Thick- ness, t (mm)	Span length (mm)	Load bearing width, N_b (mm)	Applied shear force at failure, V_{Test} (kN/m)	Applied moment at failure, M_{Test} (kNm/m)	Shear capacity, V_c (kN/m)	Moment capacity, M_c (kNm/m)	$v =$ V_{Test} / V_c	$m =$ M_{Test} / M_c	$p =$ $P_{w, Test} / P_{w, c}$	$v^2 + m^2$
0.75	600	50	-	-	-	-	-	-	-	-
		100	7.62	2.29	54.17	2.32	0.14	0.98	0.52	0.99
		150	8.61	2.58	54.17	2.32	0.16	1.11	0.48	1.26
		200	-	-	-	-	-	-	-	-
	1000	50	-	-	-	-	-	-	-	-
		100	5.27	2.64	54.17	2.32	0.10	1.13	0.36	1.30
		150	5.87	2.93	54.17	2.32	0.11	1.26	0.33	1.61
		200	-	-	-	-	-	-	-	-
	2500	50	-	-	-	-	-	-	-	-
		100	2.33	2.92	54.17	2.32	0.04	1.26	0.16	1.58
		150	2.36	2.95	54.17	2.32	0.04	1.27	0.13	1.61
		200	-	-	-	-	-	-	-	-
1.00	600	50	-	-	-	-	-	-	-	-
		100	12.50	3.75	73.51	3.25	0.17	1.15	0.49	1.36
		150	13.99	4.20	73.51	3.25	0.19	1.29	0.47	1.70
		200	-	-	-	-	-	-	-	-
	1000	50	-	-	-	-	-	-	-	-
		100	8.31	4.16	73.51	3.25	0.11	1.28	0.32	1.65
		150	9.05	4.52	73.51	3.25	0.12	1.39	0.30	1.95
		200	-	-	-	-	-	-	-	-
	2500	50	-	-	-	-	-	-	-	-
		100	3.72	4.65	73.51	3.25	0.05	1.43	0.15	2.05
		150	3.82	4.78	73.51	3.25	0.05	1.47	0.13	2.16
		200	-	-	-	-	-	-	-	-
1.20	600	50	-	-	-	-	-	-	-	-
		100	-	-	-	-	-	-	-	-
		150	-	-	-	-	-	-	-	-
		200	-	-	-	-	-	-	-	-
	1000	50	-	-	-	-	-	-	-	-
		100	-	-	-	-	-	-	-	-
		150	-	-	-	-	-	-	-	-
		200	-	-	-	-	-	-	-	-
	2500	50	-	-	-	-	-	-	-	-
		100	-	-	-	-	-	-	-	-
		150	-	-	-	-	-	-	-	-
		200	-	-	-	-	-	-	-	-

Table 5.8: Design against combined bending and web crippling for profiled decking with G550 steel.

Thick- ness, t (mm)	Span length (mm)	Load bearing width, N_b (mm)	Applied load at failure, $P_{w, Test}$ (kN/m)	Applied moment at failure, M_{Test} (kNm/m)	Web crippling capacity, $P_{w, c}$ (kN/m)	Moment capacity, M_c (kNm/m)	$p =$ $P_{w, Test}$ $/ P_{w, c}$	$m =$ M_{Test} $/ M_c$	$v =$ V_{Test} $/ V_c$	$(p + m)$ $/ 1.25$
0.75	600	50	28.12	4.21	52.33	4.96	0.54	0.85	0.17	1.11
		100	34.74	5.22	64.50	4.96	0.54	1.05	0.21	1.27
		150	39.16	5.87	76.05	4.96	0.51	1.19	0.24	1.36
		200	43.78	6.56	100.99	4.96	0.43	1.32	0.26	1.41
	1000	50	18.16	4.53	52.33	4.96	0.35	0.91	0.11	1.01
		100	21.20	5.29	64.50	4.96	0.33	1.07	0.13	1.12
		150	22.58	5.65	76.05	4.96	0.30	1.14	0.14	1.15
		200	26.18	6.55	100.99	4.96	0.26	1.32	0.16	1.26
	2500	50	7.79	4.87	5.12	4.96	0.15	0.98	0.05	0.91
		100	7.66	4.79	64.50	4.96	0.12	0.97	0.05	0.87
		150	7.68	4.79	76.05	4.96	0.10	0.97	0.05	0.85
		200	8.90	5.55	100.99	4.96	0.09	1.12	0.05	0.97
1.00	600	50	-	-	-	-	-	-	-	-
		100	50.98	7.64	105.08	7.11	0.49	1.07	0.17	1.25
		150	56.34	8.45	123.17	7.11	0.46	1.19	0.19	1.32
		200	-	-	-	-	-	-	-	-
	1000	50	-	-	-	-	-	-	-	-
		100	33.20	8.31	105.08	7.11	0.32	1.17	0.11	1.19
		150	34.94	8.74	123.17	7.11	0.28	1.23	0.12	1.21
		200	-	-	-	-	-	-	-	-
	2500	50	-	-	-	-	-	-	-	-
		100	12.50	7.82	105.08	7.11	0.12	1.10	0.04	0.97
		150	13.00	8.12	123.17	7.11	0.11	1.14	0.04	1.00
		200	-	-	-	-	-	-	-	-
1.20	600	50	51.78	7.77	105.59	8.78	0.49	0.88	0.13	1.10
		100	65.76	9.87	136.76	8.78	0.48	1.12	0.16	1.28
		150	73.26	10.99	180.51	8.78	0.41	1.25	0.18	1.33
		200	75.80	11.36	208.52	8.78	0.36	1.29	0.18	1.33
	1000	50	35.28	8.82	105.59	8.78	0.33	1.00	0.09	1.07
		100	39.34	9.84	136.76	8.78	0.29	1.12	0.10	1.13
		150	42.10	10.52	180.51	8.78	0.23	1.20	0.10	1.15
		200	44.08	11.02	208.52	8.78	0.21	1.26	0.11	1.17
	2500	50	15.56	9.72	105.59	8.78	0.15	1.11	0.04	1.00
		100	15.30	9.56	136.76	8.78	0.11	1.09	0.04	0.96
		150	16.58	10.37	180.51	8.78	0.09	1.18	0.04	1.02
		200	16.42	10.27	208.52	8.78	0.08	1.17	0.04	1.00

Table 5.9: Design against combined bending and web crippling for profiled decking with G235 steel.

Thick- ness, t (mm)	Span length (mm)	Load bearing width, N_b (mm)	Applied load at failure, $P_{w, Test}$ (kN/m)	Applied moment at failure, M_{Test} (kNm/m)	Web crippling capacity, $P_{w, c}$ (kN/m)	Moment capacity, M_c (kNm/m)	$p =$ $P_{w, Test}$ $/ P_{w, c}$	$m =$ M_{Test} $/ M_c$	$v =$ V_{Test} $/ V_c$	$(p + m)$ $/ 1.25$
0.75	600	50	-	-	-	-	-	-	-	-
		100	15.25	2.29	29.13	2.32	0.52	0.98	0.14	1.21
		150	17.22	2.58	36.08	2.32	0.48	1.11	0.16	1.27
		200	-	-	-	-	-	-	-	-
	1000	50	-	-	-	-	-	-	-	-
		100	10.55	2.64	29.13	2.32	0.36	1.13	0.10	1.20
		150	11.74	2.93	36.08	2.32	0.33	1.26	0.11	1.27
		200	-	-	-	-	-	-	-	-
	2500	50	-	-	-	-	-	-	-	-
		100	4.67	2.92	29.13	2.32	0.16	1.26	0.04	1.13
		150	4.72	2.95	36.08	2.32	0.13	1.27	0.04	1.12
		200	-	-	-	-	-	-	-	-
1.00	600	50	-	-	-	-	-	-	-	-
		100	24.99	3.75	51.21	3.252	0.49	1.15	0.17	1.31
		150	27.99	4.20	59.49	3.252	0.47	1.29	0.19	1.41
		200	-	-	-	-	-	-	-	-
	1000	50	-	-	-	-	-	-	-	-
		100	16.63	4.16	51.21	3.252	0.32	1.28	0.11	1.28
		150	18.09	4.52	59.49	3.252	0.30	1.39	0.12	1.36
		200	-	-	-	-	-	-	-	-
	2500	50	-	-	-	-	-	-	-	-
		100	7.44	4.65	51.21	3.252	0.15	1.43	0.05	1.26
		150	7.65	4.78	59.49	3.252	0.13	1.47	0.05	1.28
		200	-	-	-	-	-	-	-	-
1.20	600	50	-	-	-	-	-	-	-	-
		100	-	-	-	-	-	-	-	-
		150	-	-	-	-	-	-	-	-
		200	-	-	-	-	-	-	-	-
	1000	50	-	-	-	-	-	-	-	-
		100	-	-	-	-	-	-	-	-
		150	-	-	-	-	-	-	-	-
		200	-	-	-	-	-	-	-	-
	2500	50	-	-	-	-	-	-	-	-
		100	-	-	-	-	-	-	-	-
		150	-	-	-	-	-	-	-	-
		200	-	-	-	-	-	-	-	-

Chapter 6

Numerical Investigation into Section Failure

6.1 Introduction

The aim of this investigation is to provide structural understanding to section failure in cold-formed steel profiled deckings under combined bending, shear and web crippling forces through numerical analyses. A series of advanced finite element models are established in this chapter using the finite element package ABAQUS (2004) with material and geometrical non-linearity in order to simulate the actual testing conditions in one-point load tests. Furthermore, the load resistances due to the change of steel grades, thicknesses, load bearing widths, span lengths and magnitudes of initial geometrical imperfection are studied, and detailed deformation characteristics of profiled deckings are examined.

6.2 Numerical Models

Numerical models are established in accordance with the one-point load tests reported in Chapter 5. For Decks R50 of G550 steel, three different span lengths of 600, 1000 and

2500mm are studied. Similar to the numerical models for the web crippling tests, upper and lower bound solutions are determined through the use of different thicknesses and load bearing widths, i.e. a thickness of 0.75mm and a load bearing of 50mm for the lower bound solution while a thickness of 1.20mm and a load bearing of 200mm for the upper bound solution. In each model, different magnitudes of initial geometrical imperfection are adopted for a sensitivity study. A summary of the numerical models with different thicknesses, load bearing widths, span lengths and magnitudes of initial geometrical imperfection is presented in Table 6.1.

6.2.1 Material Properties

The material properties of the numerical models are based on the coupon tests performed, which are the non-linear stress-strain relationships identical to the material properties used in Figure 4.1. Furthermore, corner strength enhancement of 1.25 times the yield strength at the flat portions of the profiled decking is also adopted at the corner regions.

6.2.2 Geometry

Due to symmetry, only one web portion over half of the span of the test specimen is modeled with suitably selected boundary conditions, as shown in Figure 6.1. Shell elements S4R with six degrees of freedom at each node are adopted to all numerical

models. As shown in the numerical models on web crippling failure of profiled decking where the load resistance is sensitive to the corner radius as well as the change in the loading area at the corner regions, the same modeling details are adopted in the present models for section failure.

6.2.3 Boundary and Loading Conditions

6.2.3.1 Boundary conditions

Nodal restraints in the y-direction are applied to the nodes of the finite element model at the trough 100mm from the end of the profiled decking, as shown in Figure 6.2. These nodal restraints are provided only at those nodes intersecting the tangent point of the rounded corner and the trough. This follows from the experimental observation that the trough at the support was found to have buckled, and hence a large portion of the trough at the support would have lost contact with the support.

6.2.3.2 Loading Conditions

The loading condition of the finite element model is shown in Figure 6.2. Similar to the finite element models reported in Chapter 4, the loading condition is simulated by applying spring elements to the trough of the profiled deckings, as well as to the stiff loading blocks. Only half of the load bearing width is modeled due to symmetry, and they

are established using rigid elements in order to eliminate any local deformation. Each spring connected to the profiled decking and the stiff loading block consists of a vertical compressive spring stiffness of 10kN/mm, while zero tensile spring stiffness is applied in both the vertical as well as the horizontal directions.

6.2.4 Initial Geometrical Imperfection

By utilizing the eigen-mode obtained from bifurcation analysis on the finite element model, initial geometrical imperfection is implemented to the geometry of the model in a way similar to the approach reported in Chapter 4. Hence, the magnitudes of the initial geometrical imperfection are selected as 0.00, 0.25t and 1.00t where t is the thickness of the profiled decking in order to study its effect to the load resistances for section failure. Table 6.1 summarises the model name under different magnitudes of imperfection.

6.3 Numerical Results

6.3.1 Predicted Deformation at Failure

The geometry of the finite element models is presented in Figure 6.3 while the typical finite element models with initial geometrical imperfection are shown in Figure 6.4. Despite the three different span lengths established in the finite element models, same

deformed shapes are found for analyses of initial geometrical imperfection, which all models involve local deformation at the trough region at mid-span.

By implementing the initial geometrical imperfection into the finite element models, non-linear analyses are carried out and the deformed finite element models of the profiled deckings R50 for span lengths of 600, 1000 and 2500mm at failure are shown in Figure 6.5. In addition to the deformed shapes, the mid-thickness Von Mises stresses are also plotted on the deformed shaped for easy comparison. It is shown in the models that highly localized stresses are concentrated at mid-span while material yielding is developed along the bearing length at the web-flange intersection of the profiled decking. Moreover, cross-section distortion is also apparent which bears close resemblance to the observed deformed shapes at failure. Hence, the models are considered to be sufficiently accurate to simulate section failure of the profiled deckings.

It should be noted that in long profiled decking, material yielding is apparent at the web-trough corner as well as in the tension flange at mid-span owing to large bending moments. Lastly, despite the pressure of the longitudinal stiffeners in the troughs, local buckling is apparent in the troughs. Hence, this phenomenon raises the effectiveness issue of the trough stiffeners.

6.3.2 Predicted Load Resistances

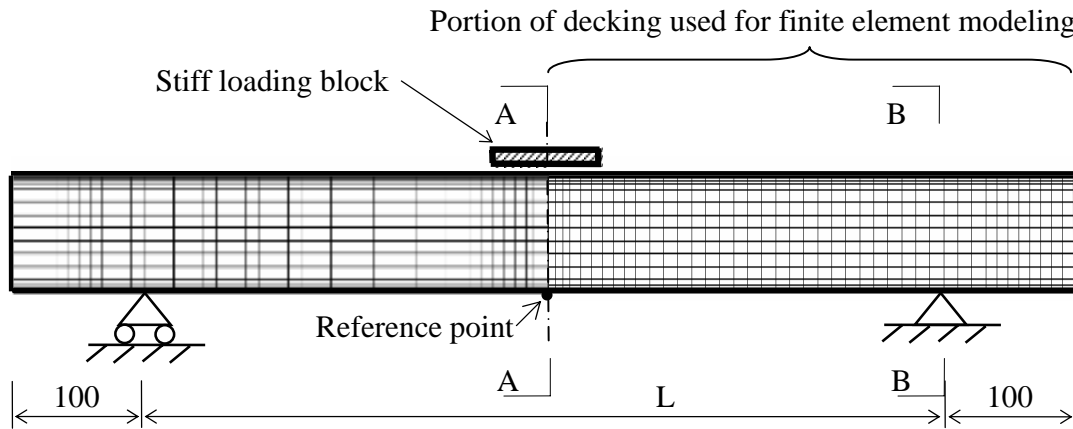
The predicted load resistances are summarised in Table 6.2 while the predicted load deflection curves are plotted in Figures 6.6 and 6.7. It is shown that the discrepancy in the load-deflection curves is very small. While for the comparison of analysed load resistances from different magnitude of initial geometrical imperfection against test results, analyzed load resistances from finite element models of 1.00t initial geometrical imperfection generally give the most accurate results. It should be noted that the magnitude of initial geometrical imperfection is not made consistence with the finite element models established for web crippling failure. Such discrepancy is explained by larger magnitudes of initial geometrical imperfection commonly occur in long profiled deckings. Nevertheless, minor effect to the numerical modeling on the behaviour of decking is resulted by adopting a magnitude of initial geometrical imperfection with either 0.25t or 1.0t. Hence an increase with a factor of 4 on the magnitude of the initial geometrical imperfection only give raise to 2 to 3% difference in the load resistances.

6.4 Summary

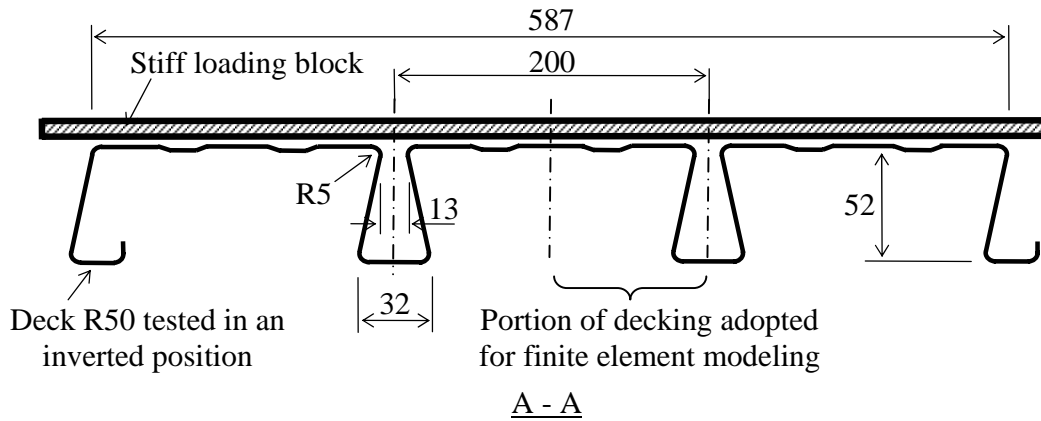
An numerical investigation into the structural behaviour of cold-formed steel profiled deckings in one-point load test is reported, and finite element models on section failure of profiled decking is presented. The numerical models are established in accordance with the one-point load tests. All numerical parameters, such as the value of spring stiffness,

used in the finite element models in this chapter are identical to the values established in Chapter 4 for consistence reasons. Furthermore, different thicknesses, steel grades, span lengths and load bearing widths are considered.

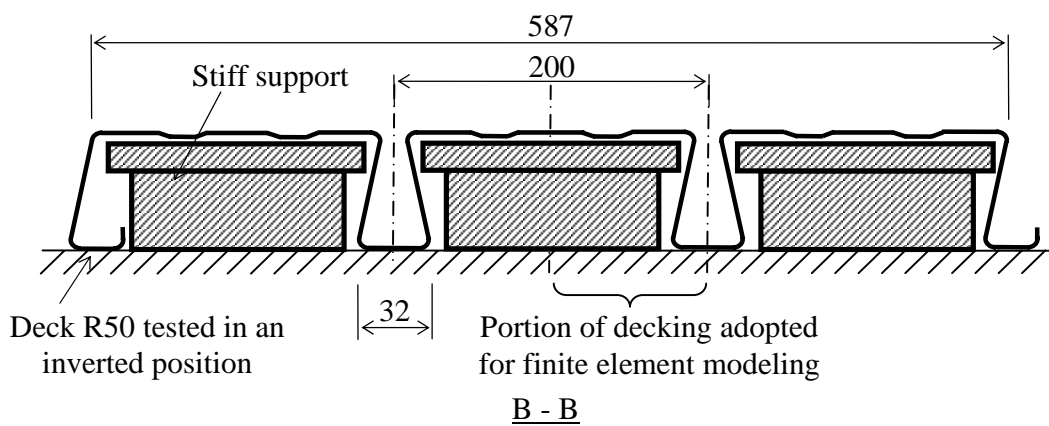
All numerical models are capable to predict both the ultimate load and deflection characteristic with relatively high level of accuracy. Furthermore, based on the stress patterns of the finite element models of increasing span lengths, a change of material yielding is noticed. In general, highly localized stresses are concentrated at mid-span while material yielding is developed along the bearing length at the web-flange intersection of the profiled decking. While for long profiled decking, material yielding is apparent at the web-trough corner as well as in the tension flange at mid-span owing to large bending moments.



a) Overview of one-point load test



b) Cross sectional detail of the test specimen at the loaded position



c) Cross sectional detail of the test specimen at the support

Figure 6.1: Idealization of finite element models.

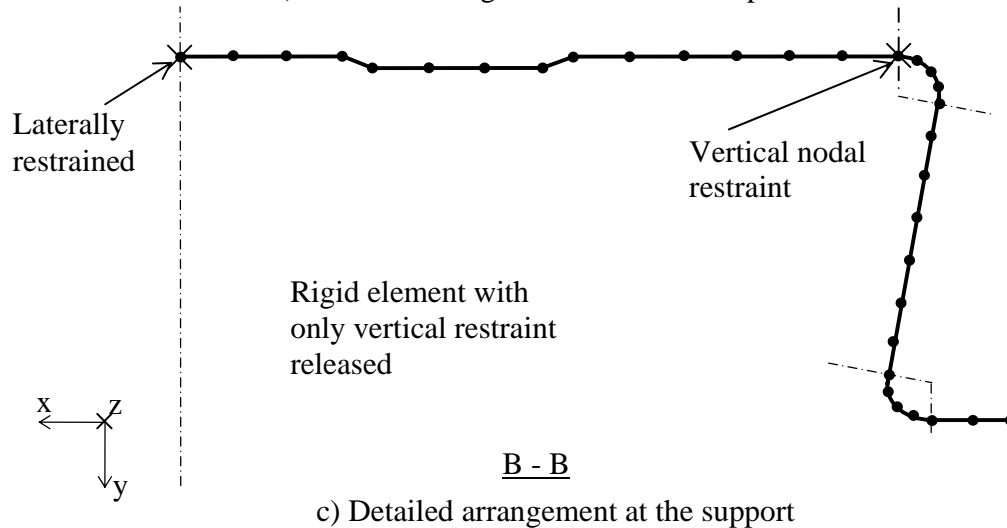
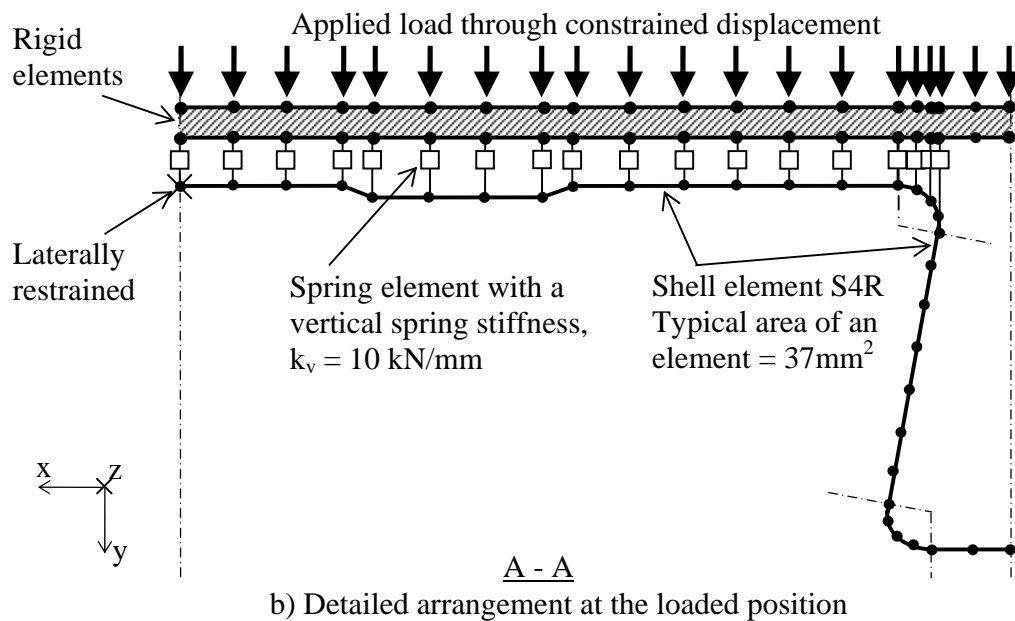
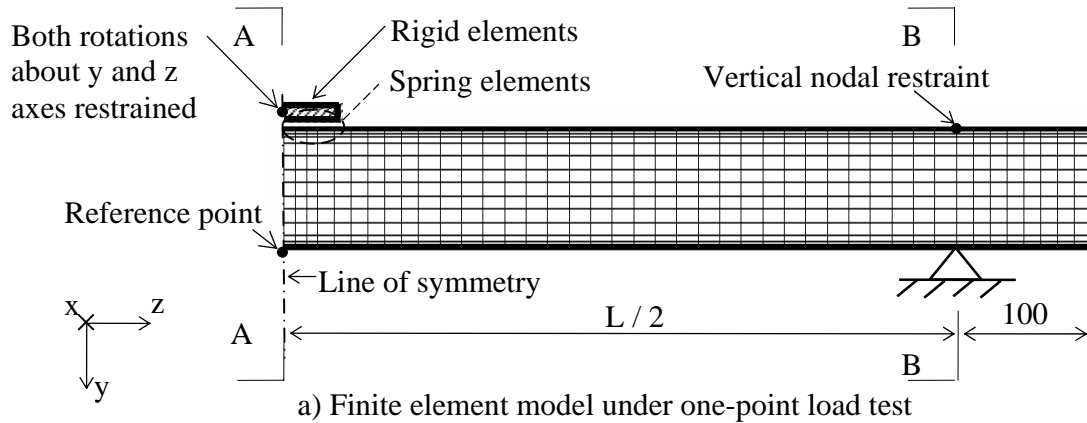


Figure 6.2: Boundary and loading conditions of finite element models.

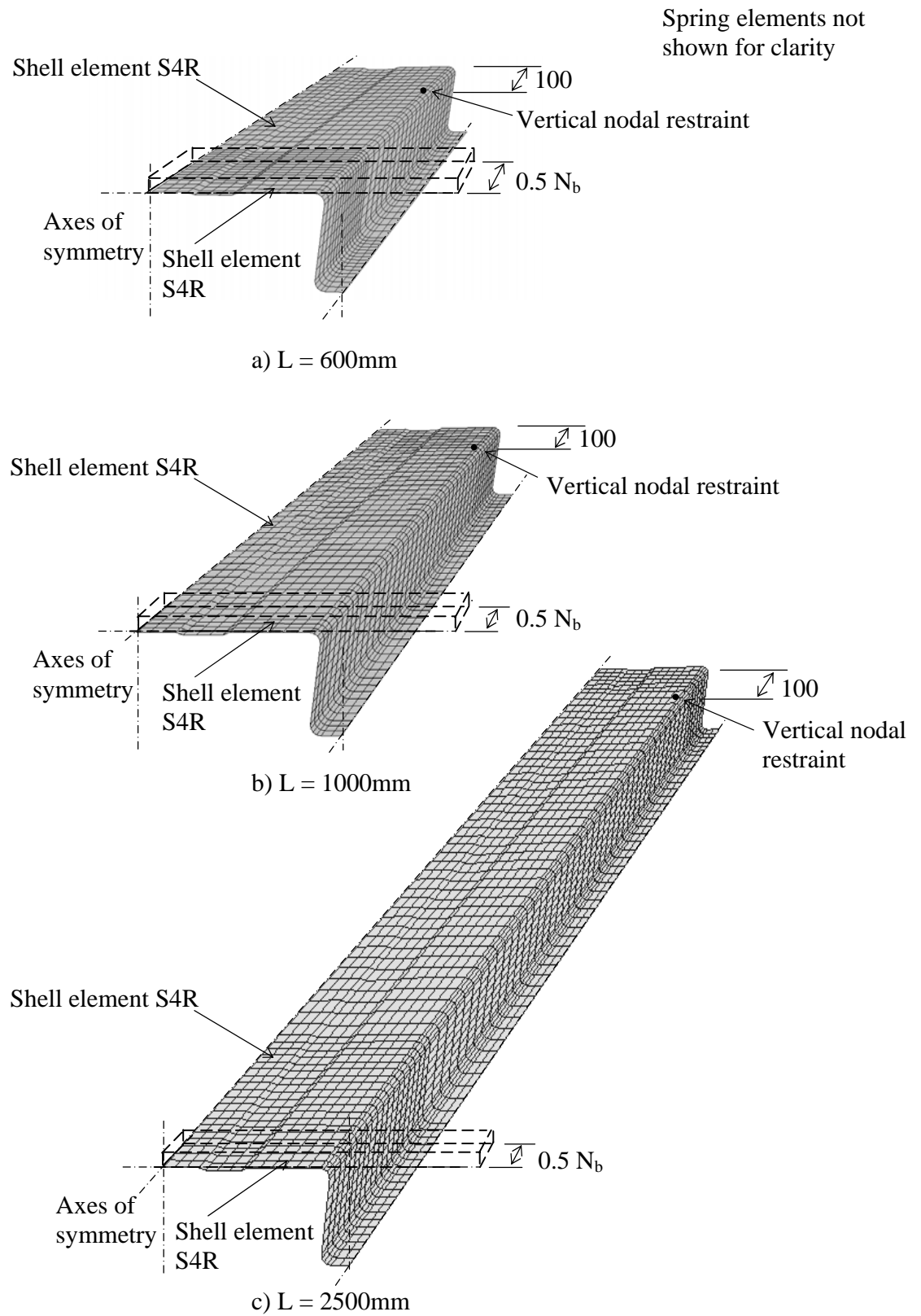


Figure 6.3: Geometry of finite element models.

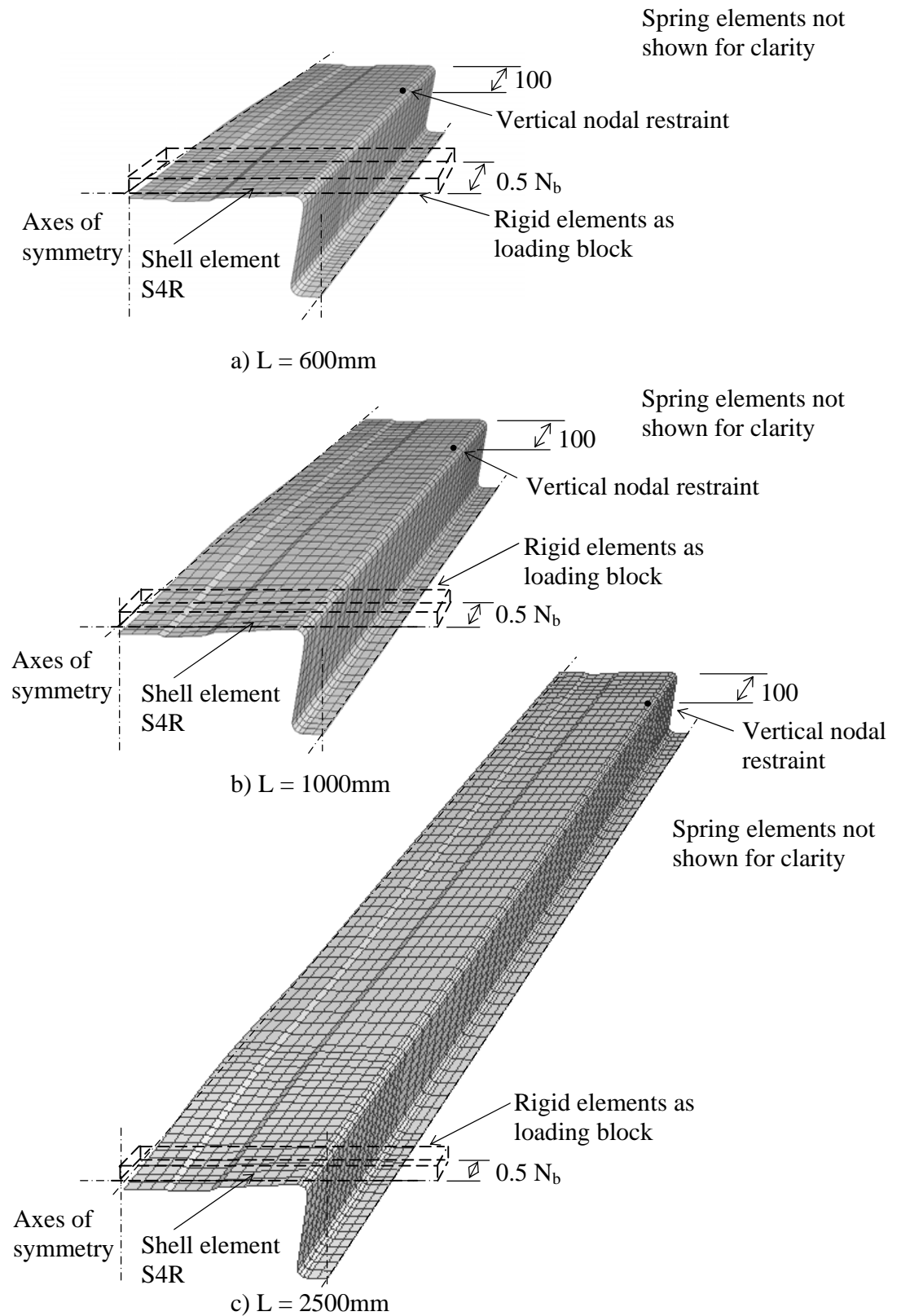
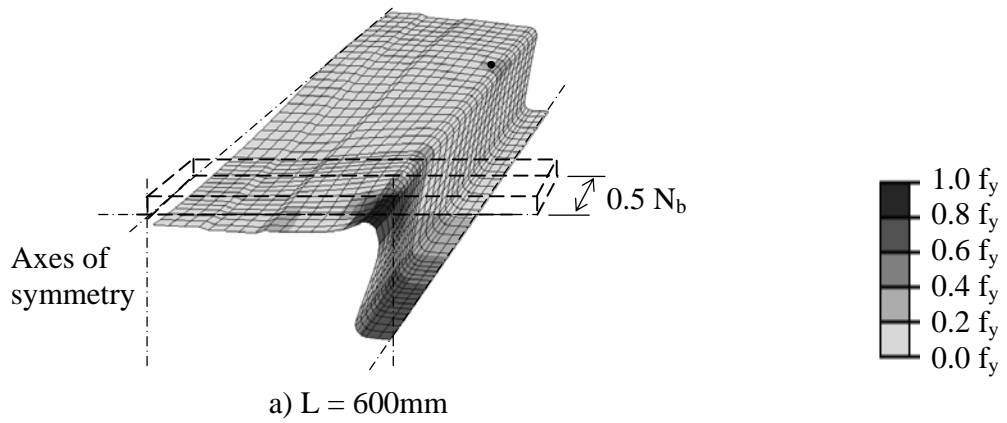
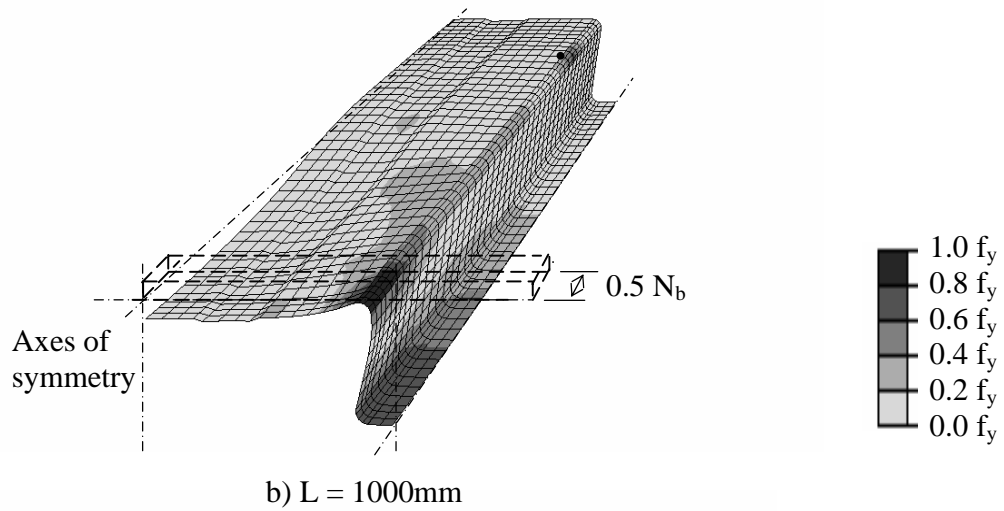


Figure 6.4: Detailed finite element models with initial geometrical imperfection.

FEM Ca1



FEM Cb1



FEM Cc1

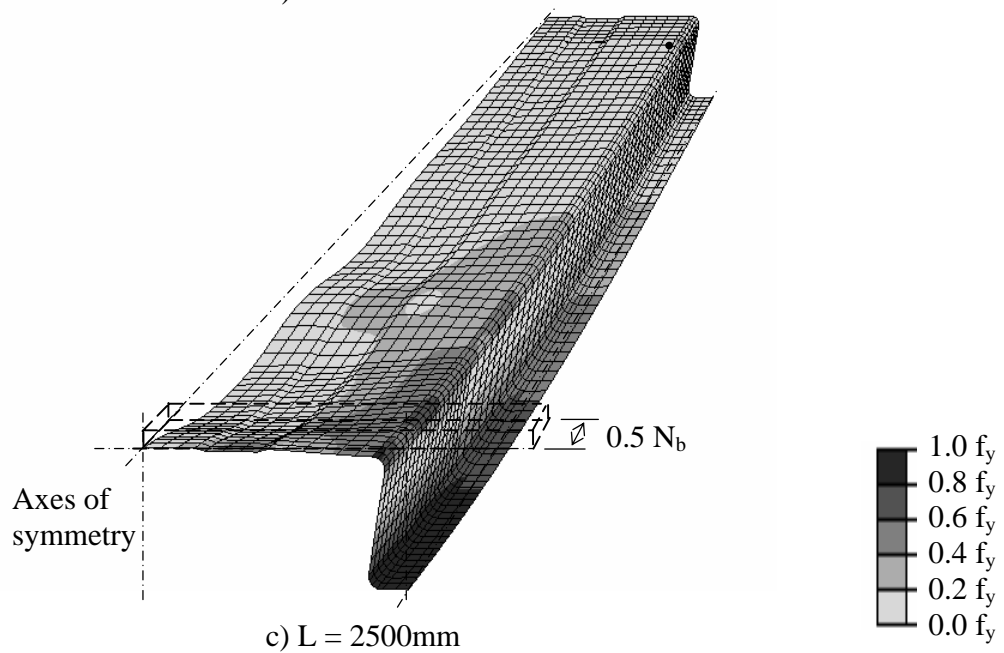


Figure 6.5: Deformed finite element models of G550 steel at failure.

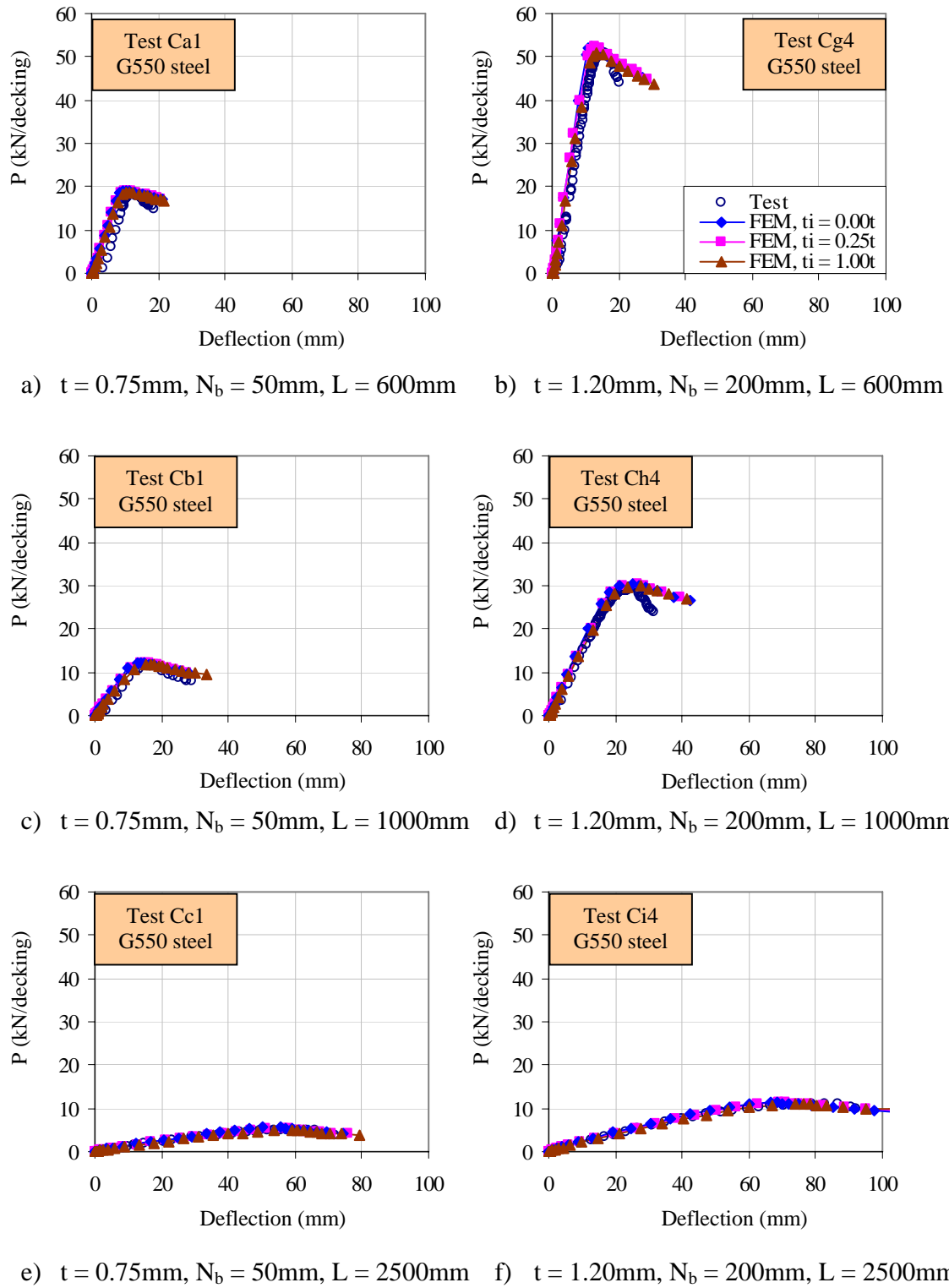


Figure 6.6: Load-deflection curves of Decks R50 with G550 steel.

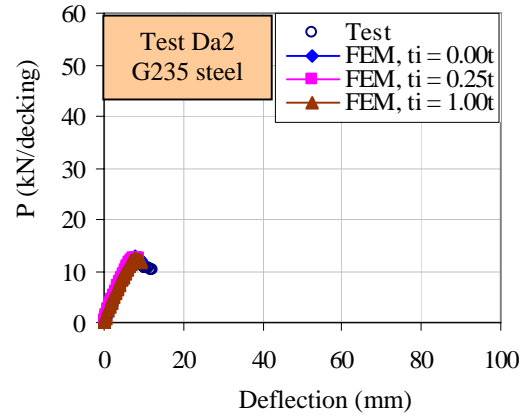
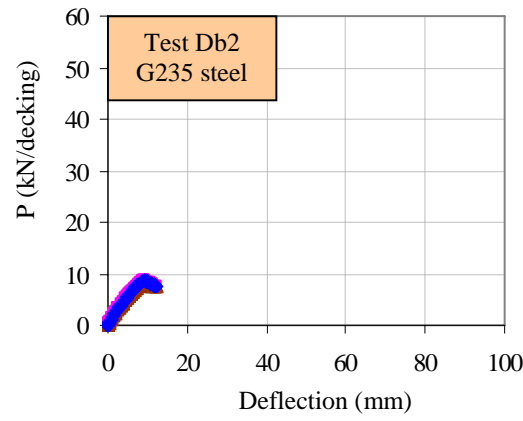
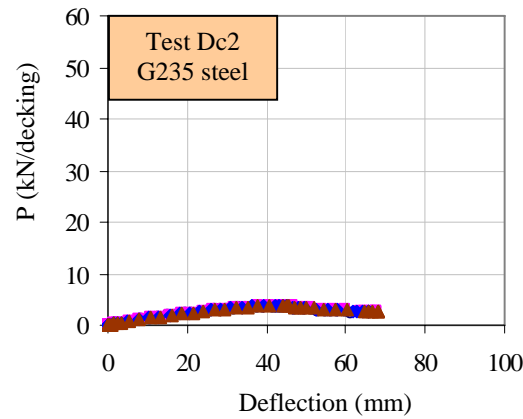
a) $t = 0.75\text{mm}$, $N_b = 100\text{mm}$, $L = 600\text{mm}$ b) $t = 0.75\text{mm}$, $N_b = 100\text{mm}$, $L = 1000\text{mm}$ c) $t = 0.75\text{mm}$, $N_b = 100\text{mm}$, $L = 2500\text{mm}$

Figure 6.7: Load-deflection curves of Decks R50 with G235 steel.

Table 6.1: Summary of numerical models.

Model name	Yield strength, p_y (N/mm ²)	Span length, L (mm)	Load bearing width, N_b (mm)	Thickness, t (mm)	Initial imperfection (mm)		
					0.00t	0.25 t	1.00t
Ca1	550	600	50	0.75	0.00	0.19	0.75
Cg4			200	1.20	0.00	0.30	1.20
Cb1		1000	50	0.75	0.00	0.19	0.75
Ch4			200	1.20	0.00	0.30	1.20
Cc1		2500	50	0.75	0.00	0.19	0.75
Ci4			200	1.20	0.00	0.30	1.20
Da2	235	600	100	0.75	0.00	0.19	0.75
Db2		1000	100	0.75	0.00	0.19	0.75
Dc2		2500	100	0.75	0.00	0.19	0.75
Other properties used in the numerical models: Corner radius, r = 5.0mm Spring stiffness, k _v = 10 kN/mm							

Table 6.2: Summary of load resistance under section failure.

Model name	P_{FEM} (kN/decking)			P_{Test} (kN/decking)	P_{Test} / P_{FEM}		
	Initial imperfection				Initial imperfection		
	0.00t	0.25t	1.00t		0.00t	0.25t	1.00t
Ca1	19.03	19.01	18.87	18.43	0.97	0.97	0.99
Cg4	52.40	52.36	52.04	51.23	0.98	0.98	1.01
Cb1	12.13	12.05	12.01	11.90	0.98	0.99	1.02
Ch4	30.41	30.37	30.24	29.79	0.98	0.98	1.00
Cc1	5.32	5.28	5.04	5.11	0.96	0.97	1.01
Ci4	11.28	11.22	11.16	11.10	0.98	0.99	1.01
Da2	12.72	12.56	12.43	12.20	0.96	0.97	0.98
Db2	8.78	8.66	8.60	8.44	0.96	0.97	0.98
Dc2	3.85	3.80	3.77	3.74	0.97	0.98	0.99

Chapter 7

Proposed Guidance for Web Crippling Failure and Section Failure

7.1 Introduction

The current design provisions for web crippling resistances of profiled decking prescribe non-linear relationships between different parameters such as yield strength, thickness and load bearing width. However, it is proven from experiments that a simple linear relationship between the web crippling resistances and the load bearing width is sufficient. Furthermore, the current design provisions for section failure require checks the combined bending and shear failure, and the combined bending and web crippling failure. However, all the applied bending moment, shear and web crippling forces are found to exist at the a same time as proven through experimental and numerical investigations, hence these two separate checks for section failure should be replaced by a simple design rule which allows the consideration of co-existing bending moment, and shear as well as web crippling forces. In order to provide simple, but yet effective design guidance for the web crippling failure and the section failure of profiled decking, extensive parametric

studies have been carried out to compile design guidance for the web crippling failure and the section failure with accurate predictions.

7.2 Design Guidance for Web Crippling Resistances

In order to generate design data for web crippling resistances in cold-formed steel profiled deckings, an extensive numerical parametric study on the finite element models verified in Chapter 4 is performed with different steel grades and thicknesses under both internal and end loading conditions with a practical range of bearing lengths. Figure 7.2 and Table 7.1 summarize the results of the parametric study, and the numerical data is tabulated under different steel grades, thicknesses, loading conditions and load bearing widths. It should be noted that the use of the proposed design charts in Figure 7.2 is considered to be simple and straightforward, and no attempt is made to generalize the numerical data to avoid unnecessary over-development.

The web crippling resistances analysed using the finite element models are compared against the British cold-formed steel code BS5950: Part 6 (1995) using model factors. Model factors, η_1 calculated as P_{FEM} divided by P_{Design} are as shown in Figures 7.3 to 7.6. It should be noted that there are significant discrepancies in each of the graphs for Decks R50 with specific yield strengths and thicknesses, and such discrepancies are observed under both loading conditions and are found to be more significant with increase thicknesses and steel grades.

7.3 Design Guidance for Section Failure

In order to generate design data for section failure against combined bending, shear and web crippling forces in cold-formed steel profiled deckings, an extensive numerical parametric study on profiled deckings with different steel grades and clear spans is performed over a practical range of bearing lengths as shown in Figure 7.7. Two sets of figures are presented in Figures 7.8 and 7.9, the first set being the moment shear interaction curves while the second set the moment web crippling interaction curves.

It is shown that all the non-linear moment shear interaction curves converge to the basic moment capacities of the profiled deckings with long clear spans under low shear forces, but drop at different rates to give reduced moment resistances under large shear forces and small load bearing widths of the concentrated forces. Hence, the moment shear interaction curves are considered to be highly dependent on the importance of the web crippling behavior in the profiled deckings under local concentrated (reaction) forces. Furthermore, in the check for combined bending and shear, unconservative designs are found mostly for short span length with small load bearing widths. In contrast, the check for combined bending and web crippling indicates the design rule is generally conservative for profiled deckings.

Although the non-linear interaction curves shown in Figures 7.8 and 7.9 are of similar patterns, the moment web crippling interaction curves shown in Figure 7.9 have in fact neglected the relationship of the shear effect in section failure. The values of the design

web crippling resistances, P_w , shown in the x-axes of Figure 7.9 are predefined from finite element analyses and these values vary with the use of different load bearing widths. Therefore, similar web crippling ratios, F_w divided by P_w , between different load bearing widths are resulted; hence, the interaction curves within each chart shown in Figure 7.9 are very similar and illustration of the shear effect cannot be carried out using the moment web crippling interaction curves.

In contrast, the bending and shear effects are presented in Figure 7.8 in the y-axes and x-axes, respectively, while the web crippling effect is presented in the reduced moment ratios in interaction curves with different load bearing widths. Due to the complete presentation of the coexisting bending, shear and web crippling effects, the moment shear interaction curves shown in Figure 7.8 are considered to be most suitable for design of profiled deckings.

7.3.1 Design Procedures

Through the use of design charts provided in Figure 7.8, less effort is required in comparison with the current design code. For the design of multi-span profiled deckings subjected to uniformly distributed load, the layout of the profiled deckings is first determined with predefined span lengths. Strength checks of the profiled deckings are then carried out. In general, provided the span length, the steel grade and thickness of the

profiled deckings are known, the design of profiled decking can be carried out using the following design procedures:

- 1) Determine the load bearing width and the span length. Calculate the length of the hogging moment region, L_s , using the known span length.
- 2) Based on the specific steel grade and thickness of the profiled decking, select the corresponding design chart in Figure 7.8.
- 3) In each design chart, four interaction curves, each represents a load bearing width are shown. Within each interaction curve, five markers are shown which represent the span lengths, L_s of 6000, 2500, 1000, 600 and 400mm. This order of span length begins from left to right in each interaction and they are repeated of every other curve in Figure 7.8. Select the interaction curve corresponds to the design load bearing width, and then select the marker corresponds to the design span length.
- 4) Draw a straight vertical line from the selected marker until it intersects the x-axis, or known as the axis of F_v / P_v ratio.
- 5) Read the F_v / P_v ratio and calculate the design shear resistance, P_v , using BS5950: Part 6.
- 6) Computed the value of F_v and hence the design load can be determined.

In order to establish the structural efficiency of the proposed design method, a model factor, η_2 is defined as P_{FEM} divided by P_{Design} . As shown in Figures 7.10 and 7.11, the model factors are found to range from 1.01 to 1.33 with an average value of 1.19. This

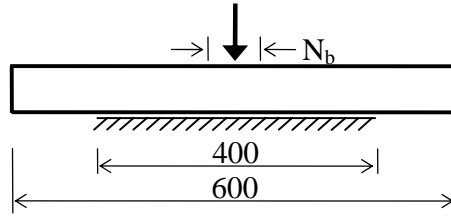
implies that the current design rules in BS5950: Part 6 is conservative by 20% in general. Therefore, while the proposed design charts for design of multi-span profiled deckings subjected to uniformly distributed load requires less computational effort, higher level of accuracy in prediction of load resistance can also be made, hence, a more economical solution is achieved.

7.4 Summary

The numerical results of the parametric studies for web crippling failure and section failure have been presented and the proposed design charts that enable accurate prediction of the load resistances of cold-formed steel profiled deckings are reported. For web crippling failure, a set of design charts with linear interaction relationship is proposed.

For section failure, two sets of design charts are presented. The first being the moment shear interaction curves while the second set is the moment web crippling curves. The two sets of design charts are evaluated and it is concluded that the moment shear interaction curves provide a complete understanding between the coexisting moment, shear and web crippling effects, while the shear effect is neglected in the moment web crippling curves.

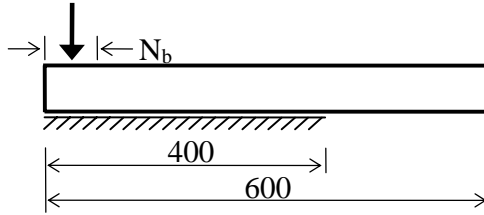
Due to the deficiency of the moment web crippling curves, the non-linear relationships between moment and shear ratios are adopted for design of multi-span profiled deckings. The proposed design procedures are provided and the design methods are considered to be simple and yet, highly efficient to predict the section failure of profiled decking under coexisting bending, shear and web crippling forces.



a) Internal loading condition

Variables covered in the parametric study

$N_b = 50, 100, 150, 200 \text{ mm}$
 $p_y = 235, 350, 450, 550 \text{ N/mm}^2$
 $t = 0.75, 1.00, 1.20 \text{ mm}$



b) End loading condition

Variables covered in the parametric study

$N_b = 50, 100, 150, 200 \text{ mm}$
 $p_y = 235, 350, 450, 550 \text{ N/mm}^2$
 $t = 0.75, 1.00, 1.20 \text{ mm}$

Figure 7.1: Parametric study for web crippling failure.

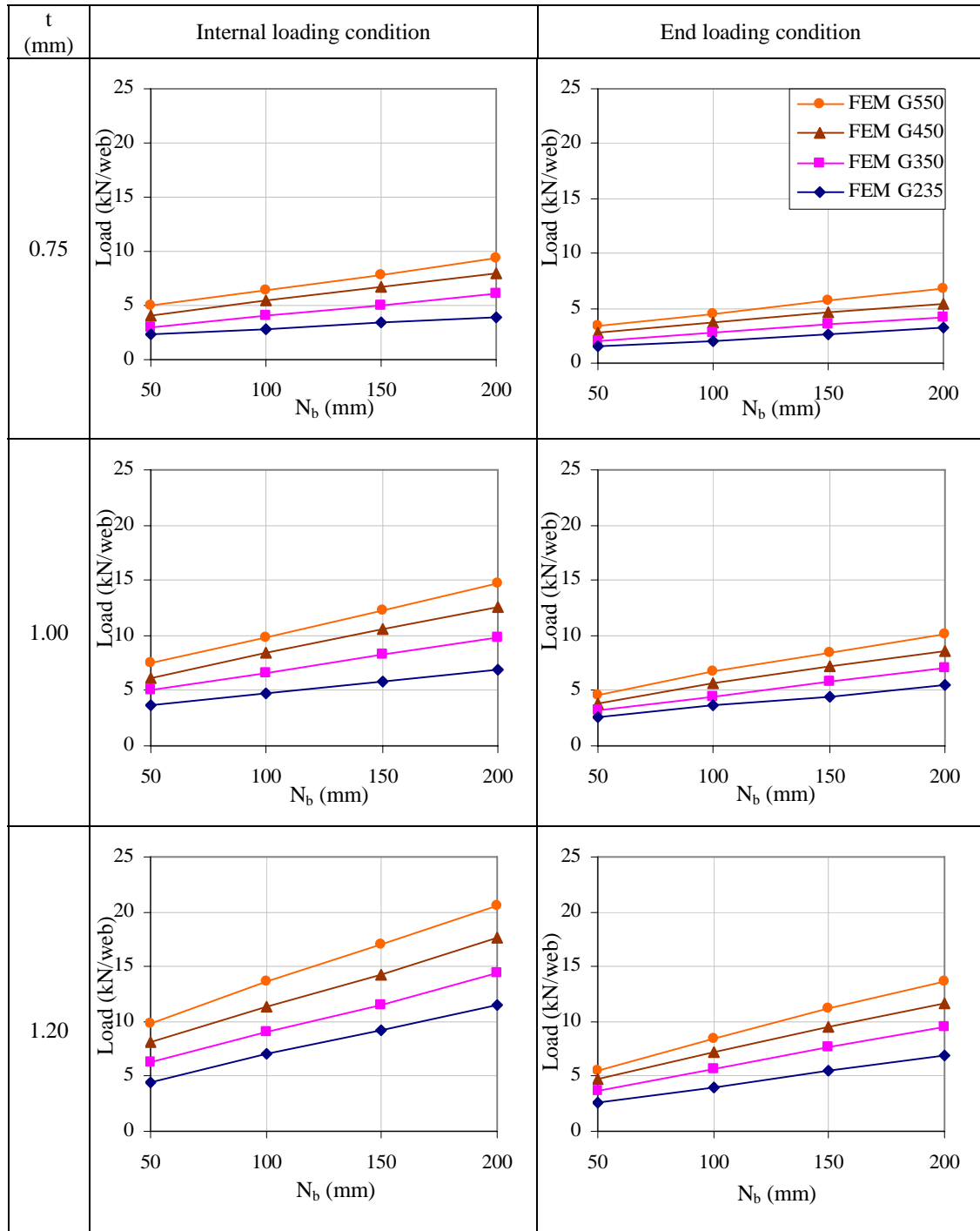


Figure 7.2: Summary of web crippling results.

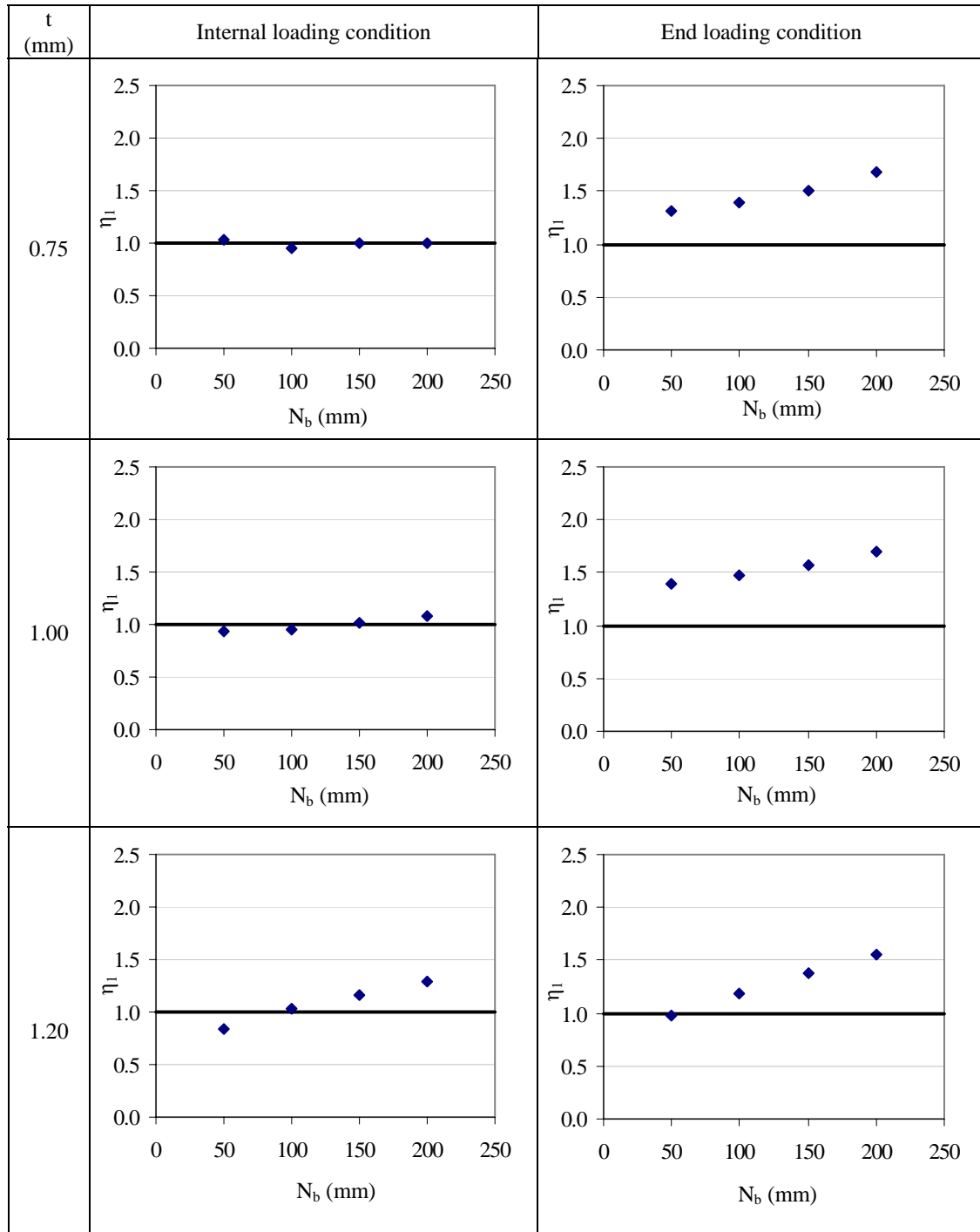


Figure 7.3: Model factors: P_{FEM} / P_{Design} for profiled decking with G235 steel under web crippling failure.

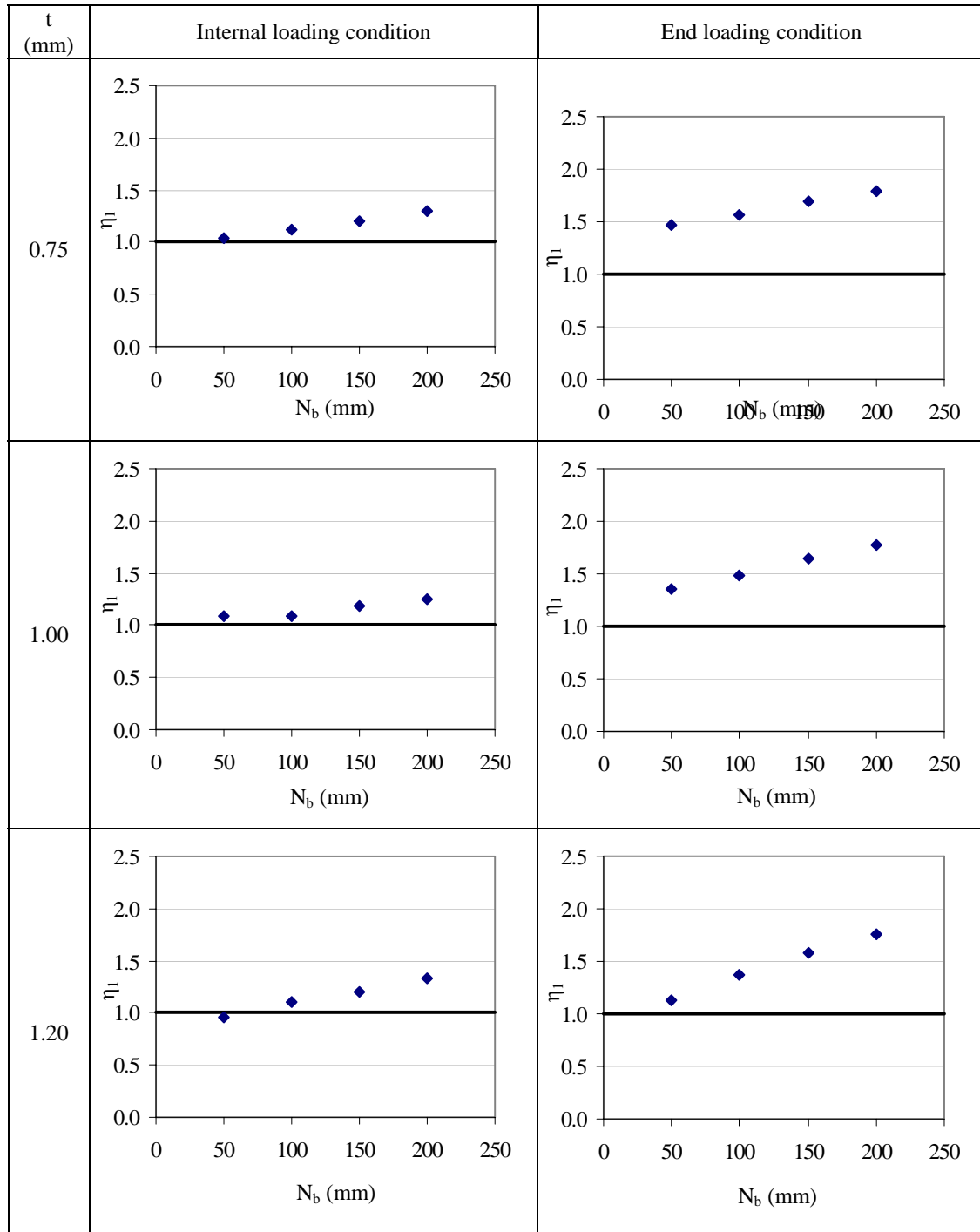


Figure 7.4: Model factors: P_{FEM} / P_{Design} for profiled decking with G350 steel under web crippling failure.

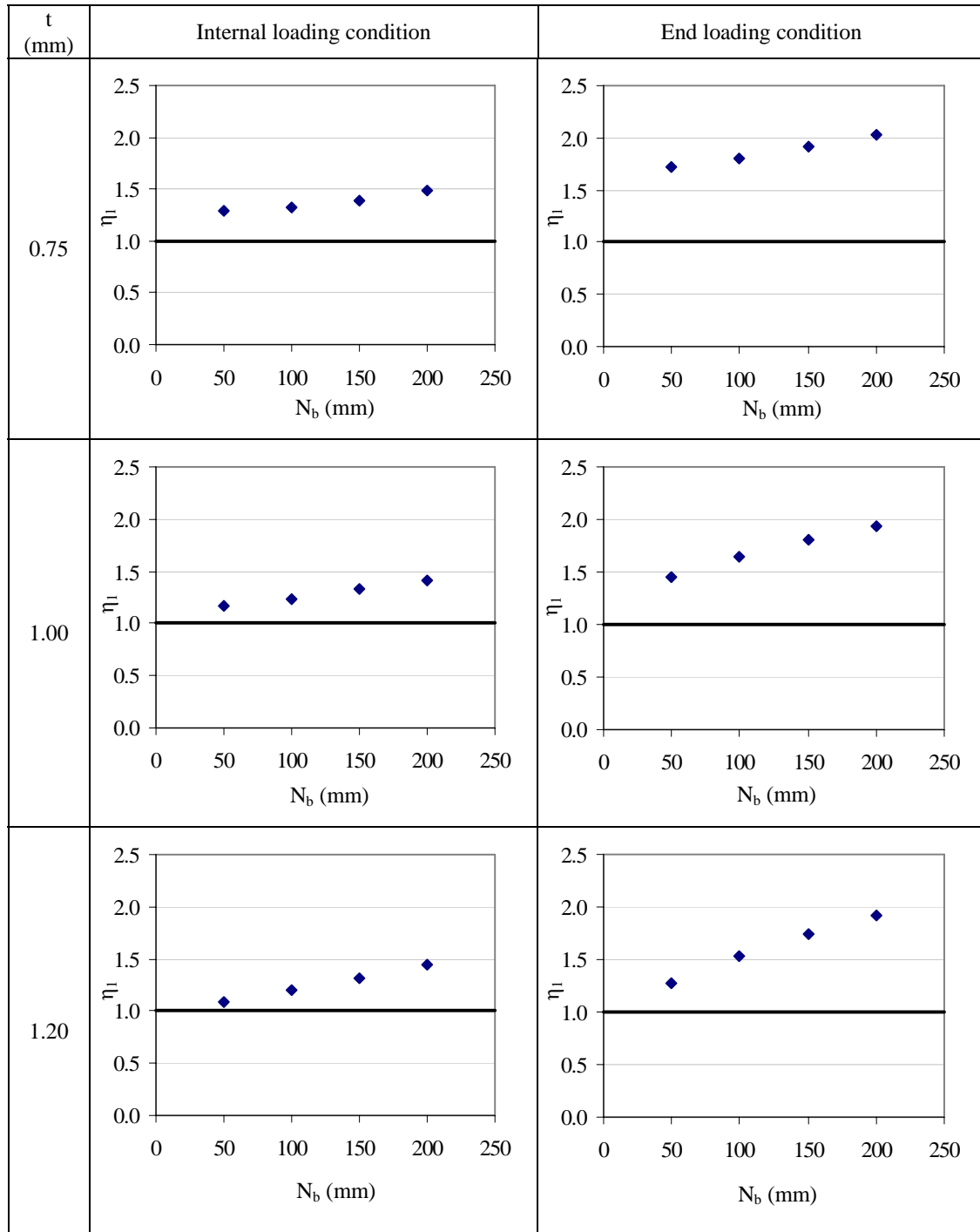


Figure 7.5: Model factors: P_{FEM} / P_{Design} for profiled decking with G450 steel under web crippling failure.

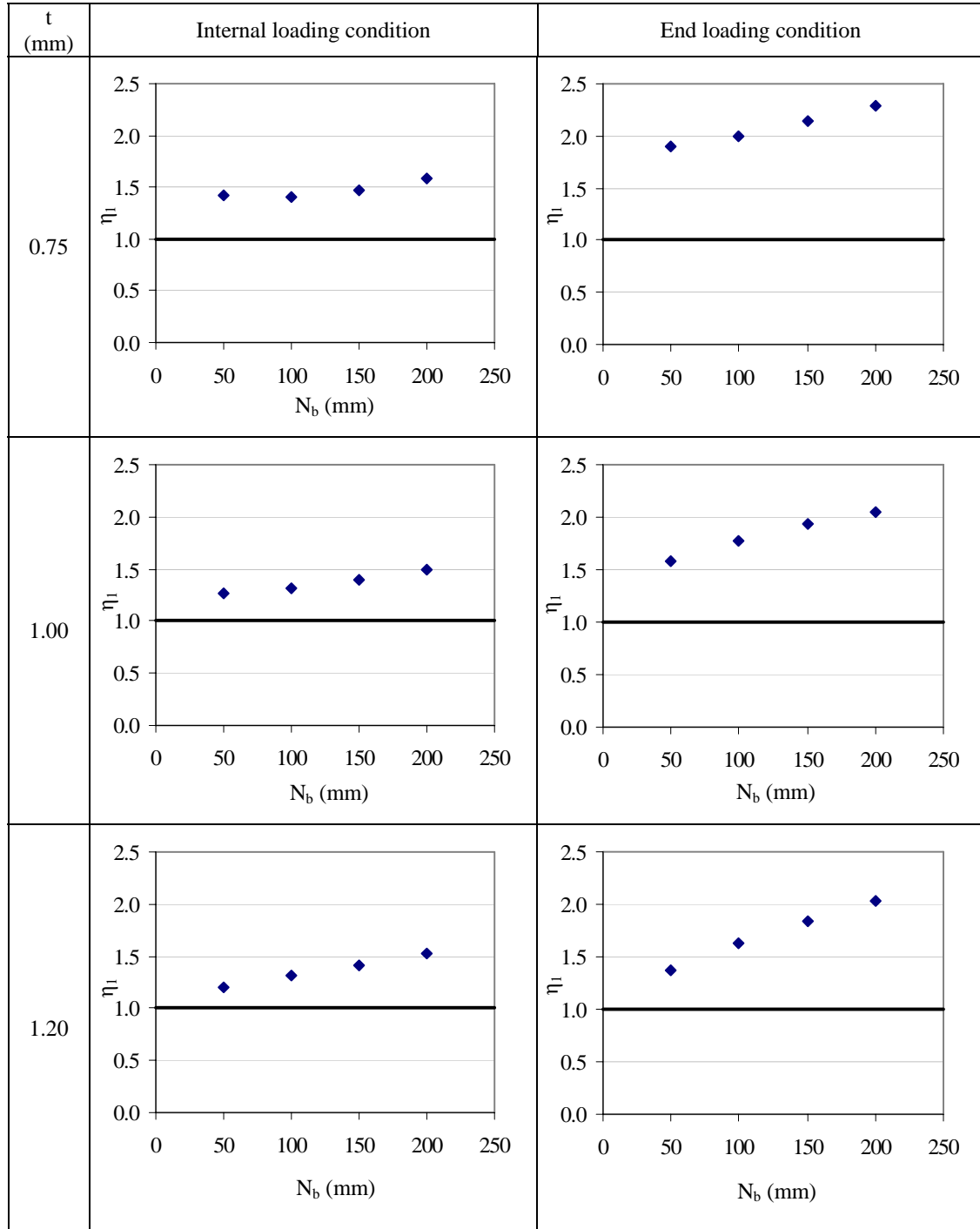


Figure 7.6: Model factors: P_{FEM} / P_{Design} for profiled decking with G550 steel under web crippling failure.

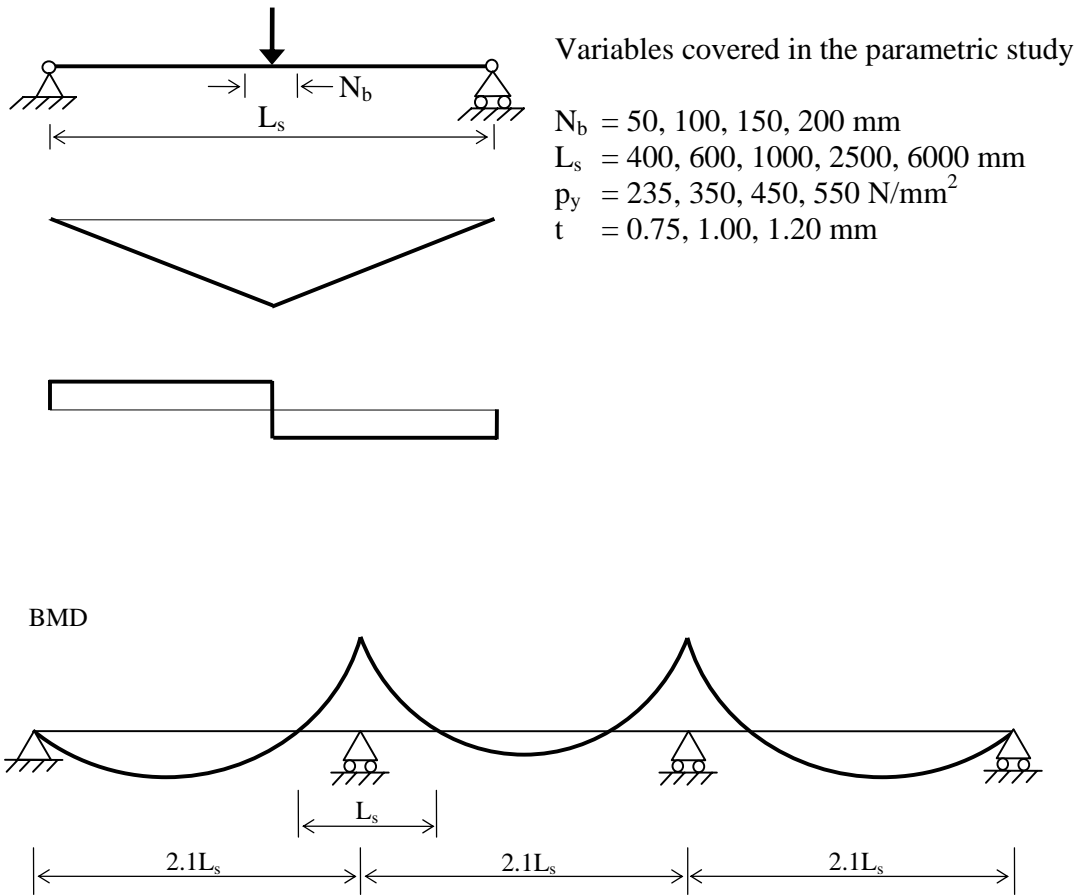


Figure 7.7: Scope of parametric study for section failure.

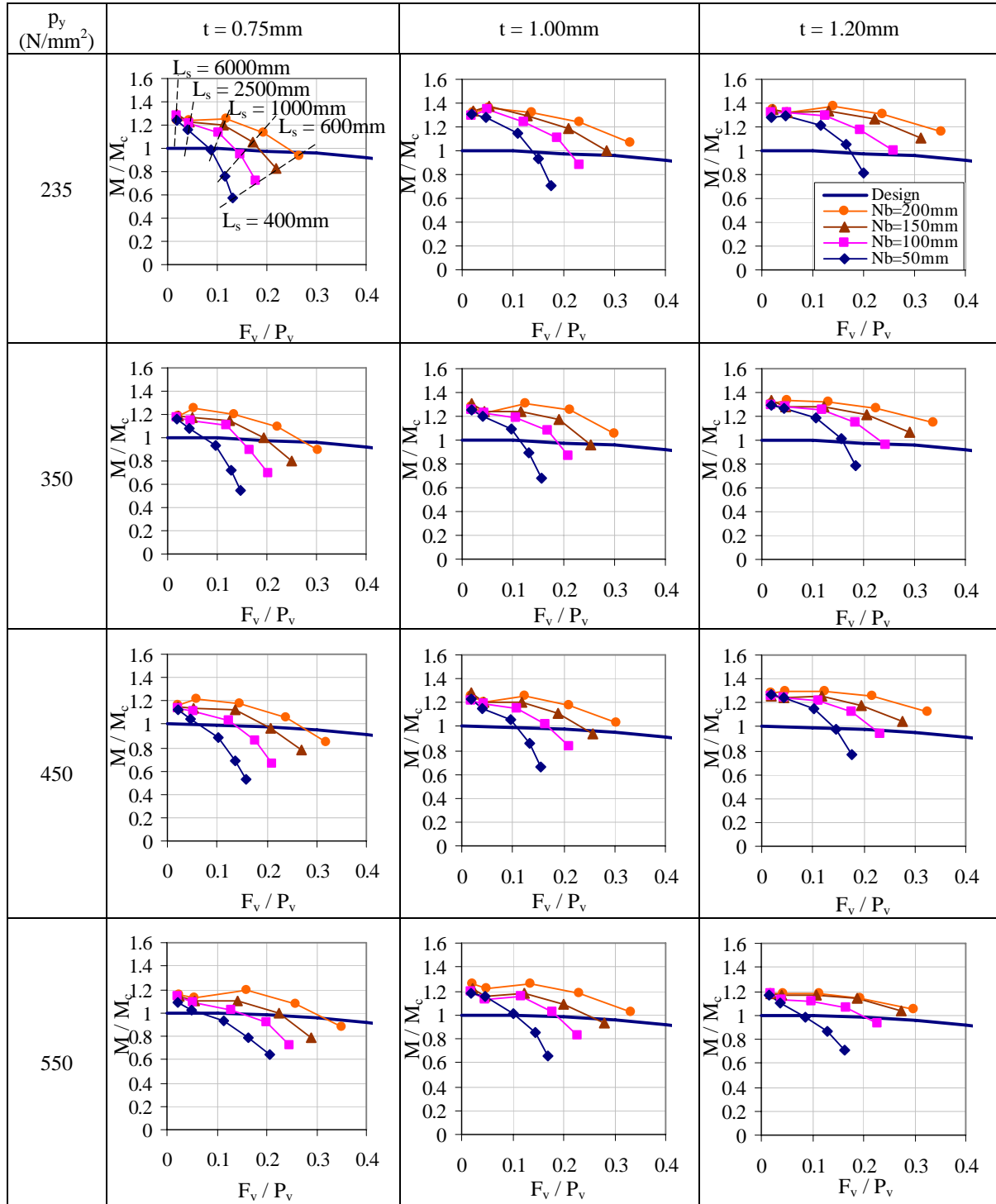


Figure 7.8: Bending and shear interaction curves.

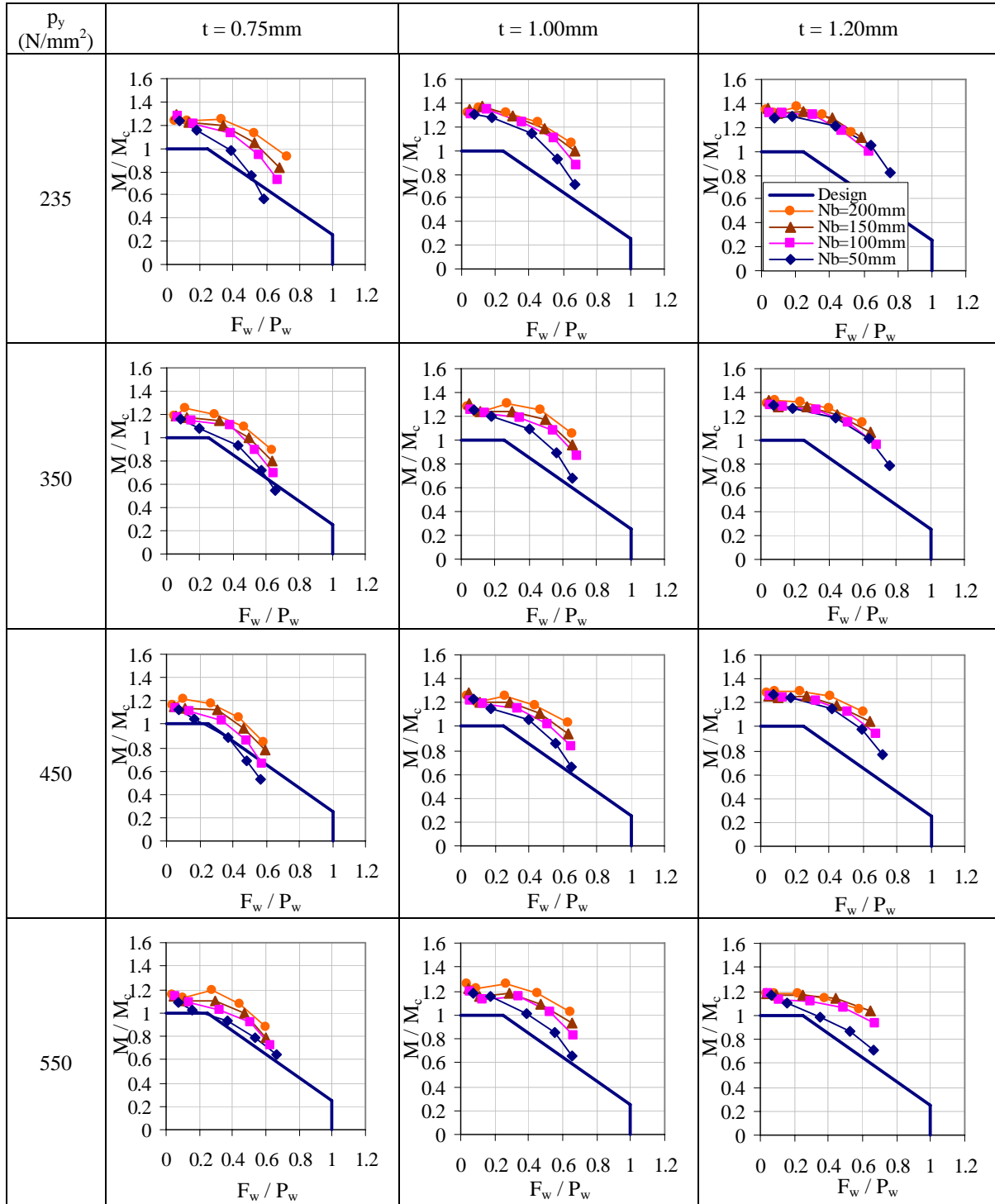


Figure 7.9: Bending and web crippling interaction curves.

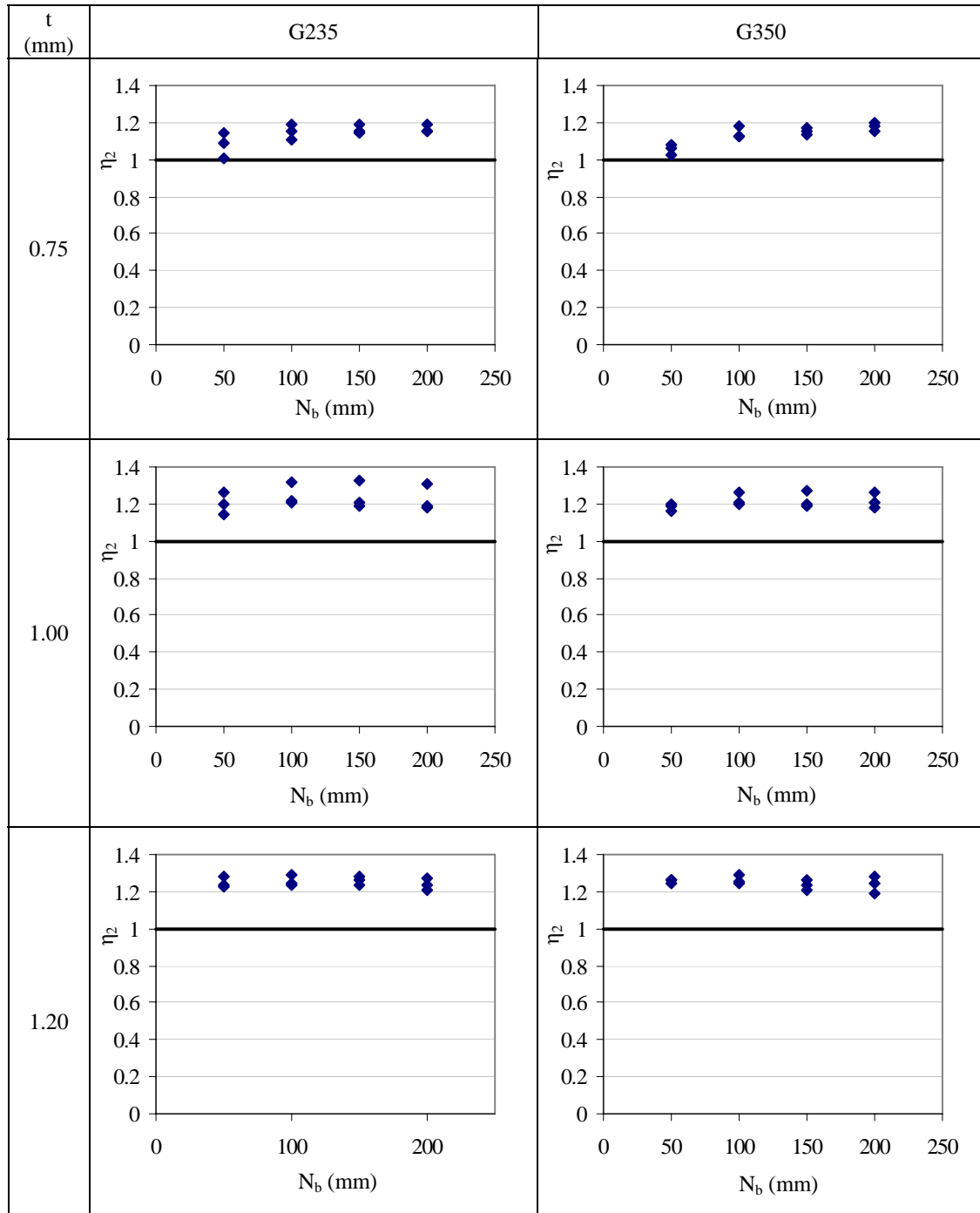


Figure 7.10: Model factors: P_{FEM} / P_{Design} for profiled decking with G235 and G350 steel under section failure.

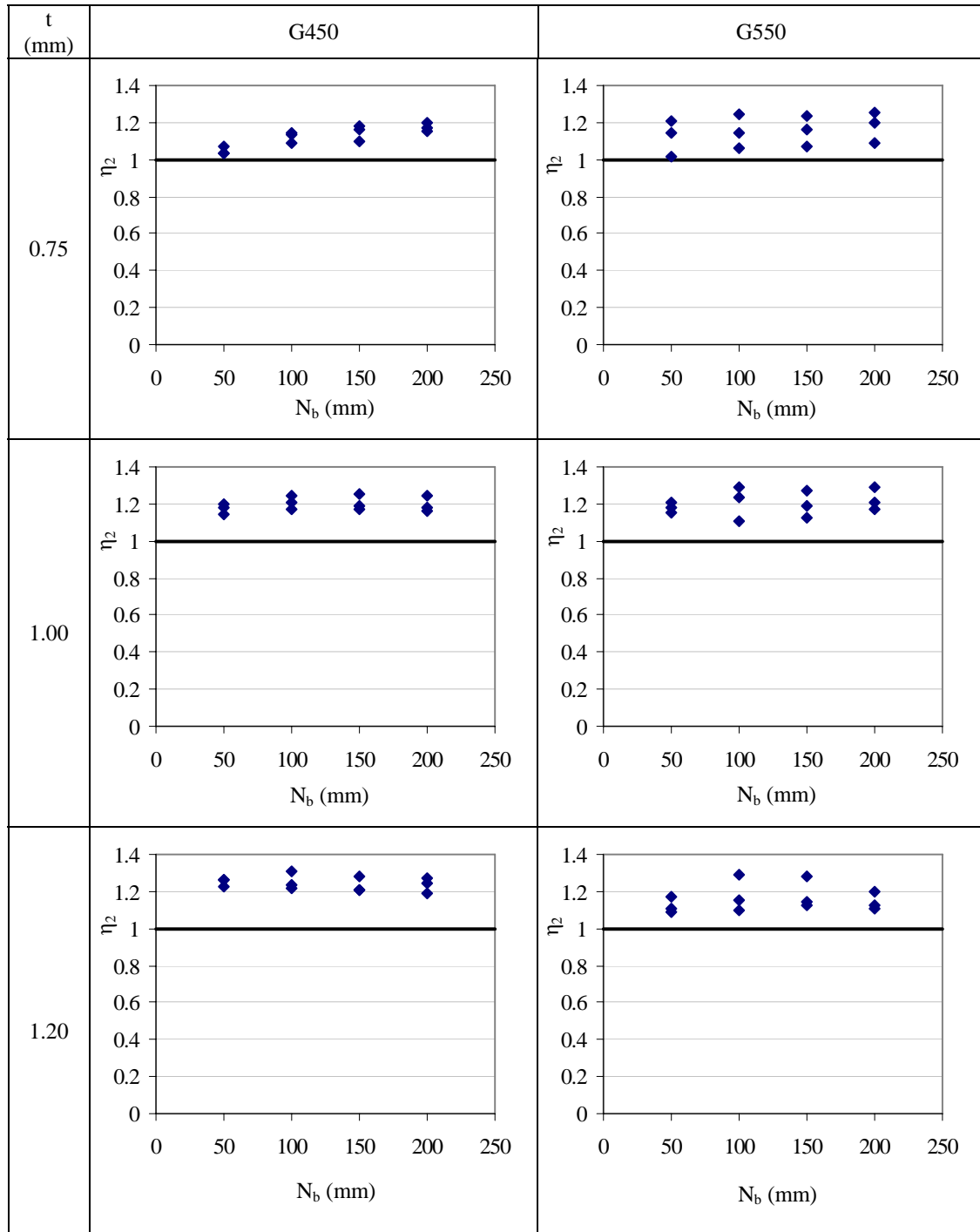


Figure 7.11: Model factors: P_{FEM} / P_{Design} for profiled decking with G450 and G550 steel under section failure.

Table 7.1: Summary of web crippling resistances.

Design yield strength p_y (N/mm ²)	Load bearing width, N_b (mm)	Thick-ness, t (mm)	Analysed load, P_{FEM} (kN/web)	
			Internal loading condition	End loading condition
235	50	0.75	2.38	1.50
		1.00	3.61	2.68
		1.20	4.50	2.61
	100	0.75	2.80	2.06
		1.00	4.69	3.62
		1.20	7.06	4.06
	150	0.75	3.45	2.60
		1.00	5.79	4.52
		1.20	9.21	5.45
	200	0.75	3.89	3.27
		1.00	6.96	5.47
		1.20	11.44	6.84
350	50	0.75	2.91	2.05
		1.00	5.09	3.19
		1.20	6.26	3.68
	100	0.75	4.03	2.82
		1.00	6.55	4.47
		1.20	9.12	5.70
	150	0.75	5.08	3.56
		1.00	8.25	5.75
		1.20	11.55	7.61
	200	0.75	6.13	4.24
		1.00	9.81	6.99
		1.20	14.35	9.47
450	50	0.75	4.10	2.73
		1.00	6.20	3.90
		1.20	8.10	4.71
	100	0.75	5.39	3.67
		1.00	8.43	5.62
		1.20	11.29	7.18
	150	0.75	6.66	4.57
		1.00	10.53	7.17
		1.20	14.32	9.49
	200	0.75	8.01	5.45
		1.00	12.55	8.64
		1.20	17.59	11.71
550	50	0.75	5.00	3.33
		1.00	7.44	4.65
		1.20	9.80	5.60
	100	0.75	6.38	4.52
		1.00	9.85	6.68
		1.20	13.66	8.49
	150	0.75	7.81	5.67
		1.00	12.24	8.47
		1.20	17.09	11.16
	200	0.75	9.38	6.78
		1.00	14.70	10.12
		1.20	20.61	13.69

Table 7.2: Summary of numerical results for section failure.

Load bearing width, N_b (mm)	Thick-ness, t (mm)	Span length (mm)	P_{FEM} (kN/m)			
			G235	G350	G450	G550
50	0.75	400	14.17	19.52	23.78	34.16
		600	12.40	16.94	20.42	27.17
		1000	9.44	12.81	15.45	18.81
		2500	4.36	5.84	7.12	8.18
		6000	1.93	2.61	3.19	3.59
	1.00	400	24.60	34.13	41.50	49.68
		600	21.09	29.08	35.37	42.05
		1000	15.25	21.01	25.52	29.49
		2500	6.71	9.11	10.99	13.33
		6000	2.84	3.94	4.84	5.63
	1.20	400	34.96	48.53	59.37	66.83
		600	29.36	40.80	49.46	52.90
		1000	20.07	28.17	34.45	35.41
		2500	8.42	11.81	14.60	15.66
		6000	3.45	5.03	6.21	6.88
100	0.75	400	19.30	26.70	31.77	40.92
		600	15.96	21.85	26.53	33.26
		1000	11.09	15.69	18.50	21.29
		2500	4.62	6.30	7.67	8.78
		6000	2.01	2.67	3.25	3.82
	1.00	400	32.50	46.11	56.21	67.10
		600	26.08	36.71	43.98	52.63
		1000	17.02	23.51	28.79	34.53
		2500	7.12	9.39	11.51	13.12
		6000	2.84	3.94	4.85	5.71
	1.20	400	45.80	63.88	78.41	93.80
		600	34.32	48.32	59.49	68.24
		1000	22.01	30.72	37.55	41.06
		2500	8.65	12.08	14.82	16.10
		6000	3.57	5.03	6.19	6.97
150	0.75	400	23.84	33.16	40.50	47.77
		600	18.68	25.76	31.36	37.41
		1000	12.07	16.63	20.60	23.68
		2500	4.72	6.48	7.90	9.03
		6000	2.03	2.69	3.29	3.84
	1.00	400	39.78	55.71	68.49	82.04
		600	29.29	42.02	50.08	58.90
		1000	18.11	25.10	30.88	36.20
		2500	7.36	9.55	11.74	13.61
		6000	2.94	4.14	5.12	5.88
	1.20	400	55.01	75.86	93.33	112.46
		600	39.01	53.60	65.63	76.73
		1000	23.28	32.23	39.76	44.19
		2500	8.78	12.20	14.98	16.86
		6000	3.68	5.21	6.21	6.98
200	0.75	400	28.89	39.87	48.08	57.95
		600	21.12	29.32	35.76	42.70
		1000	12.98	17.94	22.03	26.29
		2500	4.82	7.03	8.62	9.34
		6000	1.96	2.72	3.33	3.88
	1.00	400	46.30	65.49	80.86	97.04
		600	32.26	46.83	55.88	67.43
		1000	19.11	27.32	32.84	39.62
		2500	7.38	9.62	11.91	14.53
		6000	2.90	4.06	5.03	6.09
	1.20	400	62.06	88.39	109.28	122.98
		600	41.93	58.97	73.08	80.26
		1000	24.62	34.15	41.92	46.20
		2500	8.87	12.87	15.80	17.22
		6000	3.67	5.13	6.36	6.99

Chapter 8

Conclusions

8.1 General

In this thesis, two failure modes, namely web crippling failure and section failure are studied through experimental and numerical investigations. Design formulae from BS5950: Part 6 (1995) is also evaluated. The purpose of this thesis is to examine detail structural behaviour of multi-span cold-formed profiled steel Decks R50 subjected to gravity uniformly distributed load, which section failure occurs at the internal supports are often critical. Moreover, web crippling effect inherent in the section failure influence greatly on the resultant load resistance. These two failure modes have successfully investigated in accordance with the objectives listed in Section 1.2 and the corresponding conclusions are made as follows.

8.2 Results and Conclusions

8.2.1 Web Crippling Failure

A series of web crippling tests have been carried out with different steel grades and

thicknesses under a practical range of load bearing widths and loading conditions. For the case of internal loading condition, typical web crippling failure was observed at the web-trough corners at the point of load application. While for the end loading condition, similar mode of failure is resulted as to the internal loading condition but additional web buckling at the web-flange corners at the outer side of the profiled decking was noticed. Such deformed shape is caused by the discontinuity of specimen. From the experimental results, linear interaction lines between the web crippling resistances and the load bearing widths are developed. This linear relationship applies to profiled steel Decks R50 with steel grades range from G235 to G550, thicknesses from 0.75 to 1.20mm and load bearing widths from 50 to 200mm.

For further investigation into the web crippling failure, finite element models are established in accordance with the test program. Two different lateral restraints are adopted in the finite element models, one being having lateral restraint fixed at the symmetric axis, which simulates the shear studs are being applied at every trough. In contrast, the use of shear stud at every second trough is simulated by releasing the lateral restraint at the symmetric axis of the models. Numerical results of such models indicate approximate 25% and 35% reduction in web crippling resistances for internal and end loading conditions, respectively. Furthermore, different numerical variables, i.e. initial geometrical imperfection, spring stiffness are investigation but minor effect on the web crippling resistance is resulted. Finally, a set of parameters including the value of initial geometrical imperfection, spring stiffness, corner radius and number of elements are defined for reference of future numerical study.

Comparisons of test results against design value computed using BS5950: Part 6 (1995) are made and the design loads under-estimate the test values for the profiled Decks R50 under both internal and end loading conditions. Among all the comparison of the profiled Decks R50 of different thicknesses, steel grades and under different widths of bearing and loading conditions, the minimum and maximum design-to-test ratio of 1.13 and 2.68 are computed, respectively. Due to such a great discrepancy, the current design equation is not recommended to apply to profiled Decks R50 especially with high steel grades.

Due to the under-estimation of the web crippling resistances, design charts are proposed which enable accurate prediction of web crippling resistances for profiled Decks R50 of different thicknesses and steel grades under both internal and end loading conditions and are applicable to different load bearing widths. However, due to the scope of study, these charts are limited to profiled Decks R50 and therefore risk a potential inapplicability to decks other than profiled Deck R50.

8.2.2 Section Failure

Section failure of the profiled Decks R50 is studied experimentally with various thicknesses and steel grades under different span lengths and load bearing widths. Finite element models are established using the predefined parameters as to values used in the web crippling investigation, e.g. value of spring stiffness. Precise prediction of both load resistance and deflection characteristic are obtained.

Through the extensive experimental and numerical investigation into the section failure of the profiled Decks R50, two sets of interaction curves are developed. The first set being the non-linear moment shear interaction curves while the second set is the moment web crippling interaction curves.

The proposed coexisting moment, shear and web crippling effects is illustrated graphically using the moment shear interaction curves. The web crippling effect is demonstrated using different load bearing width and results have shown that by reducing the load bearing width, significant reduction in moment resistance is resulted. In contrast, the contribution of shear effect has verified to have effect to the load resistance but it is relatively minor compared with the web crippling effect. In general, combined bending, shear and web crippling failure should be considered as a whole for profiled deckings subjected to concentrated reaction force.

In comparison with the moment shear interaction curves, the moment web crippling interaction curves provide similar non-linear patterns. However, the moment web crippling curves present solely the moment and web crippling effects. Based on the neglected shear effect in the moment web crippling interaction curves, it is considered that the moment shear interaction curves provide better understanding of the section failure.

The design provision given in BS5950: Part 6 (1995) comprises of two separate checks, one being the combined bending and shear as well as the combined bending and web crippling. The design equations for these checks are evaluated against numerical results

and model factors are computed. In general, model factors of 1.20 are resulted, indicating that the design equations are over-conservative by 20%. Due to the over-conservative design load predicted as well as the complication in the current design procedures, proposed design charts are developed.

In order to overcome the complexity of the current design procedures as well as to improve the accuracy of the design resistance, proposed design charts are developed from a series of moment shear interaction curves. The proposed design charts allow reduction in computational effort while enable accurate load resistances to be predicted. Furthermore, the proposed design charts inherent the coexisting moment, shear and web crippling effects, which allows a complete understanding in the relationship between the load resistances to different steel grades, thickness of profiled deckings, as well as to different span lengths and load bearing widths. However, the proposed design charts should only be adopted for profiled Decks R50 with thicknesses range from 0.75 to 1.20mm, steel grades from 235 to 550 and under load bearing widths from 50 to 200mm.

8.3 Recommendations for Future Research

Studies into the web crippling failure and the section failure on cold-formed steel deckings of different configurations are recommended, and results are encouraged to be incorporated into the proposed design charts. Some commonly used profiled deckings including trapezoidal deckings should be covered. The effect of shear studs used to transfer shear forces between the concrete slab and the steel section is also suggested to

be included in any experimental investigation. Furthermore, in order to further increase the effectiveness of load transfer between the concrete slab and the steel section, embossments are often made at the webs of the profiled deckings. The existence of embossments will not only enhance the effectiveness of load transfer but increase the web crippling resistance due to increase in the cross-sectional area. Therefore, a study into the effect of the embossment to the web crippling behaviour of profiled decking is recommended.

References

AISI, Specification for the design of cold-formed steel structural members, American Iron and Steel Institute , Washington, DC, 1996.

Akhand A.M., Badaruzzaman W.H.W. and Wright H.D., 2004, Combined flexure and web crippling strength of a low-ductility high strength steel decking: experiment and a finite element model, *Thin-Walled Structures* 42, p1067-1082.

AQABUS version 6.4. Hibbitt, Karlsson & Sorensen, Inc.

Australian Standard, AS/NZS 4600 Cold-formed steel structures, 2005.

Bakker M.C.M., 1994, Theoretical and experimental research on web crippling of cold-formed flexural steel members, *Thin-Walled Structures* 18, p261-290.

British Standards Institution, BS5950 Structural use of steelwork in building. Part 1: Code of practice for design – rolled and welded sections, 2000.

British Standards Institution, BS5950 Structural use of steelwork in building. Part 5: Code of practice for design of cold formed thin gauge sections, 1998.

British Standards Institution, BS5950 Structural use of steelwork in building. Part 6: Code of practice for design of light gauge profiled steel sheeting, 1995.

British Standards Institution, BS EN 10002-1: 2001 Metallic Materials - Tensile Testing. Part 1: Method of Test at Ambient Temperature.

British Standards Institution, BS EN 1993-1-3: 2005 Eurocode 3: Design of steel structures. Part 1.3: General rules and supplementary rules for cold-formed steel structures.

Beshara B. and Schuster R.M., 2000, Web crippling of cold-formed steel C- and Z-sections, Fifteenth International Specialty Conference on Cold-Formed Steel Structures, p23-42.

Davies J.M. and Jiang C., 1997, Design procedures for profiled metal sheeting and decking, Thin-Walled Structures 27 (1), p43-53.

European Prestandard Eurocode 3, ENV 1993-1-3, Design of Steel Structures, Part 1-3: General rules – Supplementary rules for cold formed thin gauge members and sheeting.

Fox. S.R. and Brodland G.W., 2003, Design expressions based on a finite element model of a stiffened cold-formed steel C-section, Journal of Structural Engineering 130 (5), p708-714.

Hetrakul, N., and Yu W. W., 1978, Structural behavior of beam webs subjected to web crippling and a combination of web crippling and bending, Final Report, Civil Engineering Study 78-4, University of Missouri-Rolla.

Hofmeyer H., Kerstens J.G.M., Snijder H.H. and Bakker M.C.M., 2001, New prediction model for failure of steel sheeting subjected to concentrated load (web crippling) and bending, *Thin-Walled Structures* 39, p773-796.

Hofmeyer H., Kerstens J.G.M., Snijder H.H. and Bakker M.C.M., 2002, Combined web crippling and bending moment failure of first-generation trapezoidal steel sheeting, *Journal of Constructional Steel Research* 58, p1509-1529.

Holesapple M.W. and LaBoube R.A., 2003, Web crippling of cold-formed steel beams at end supports, *Engineering Structures* 25, p1211-1216.

Korvink S.A., Van Den Berg G.J. and Van De Merwe P., 1995, Web crippling of stainless steel cold-formed beams, *Journal of Construction Steel Research* 34, p225-248.

LaBoube R.A., Yu W.W., Deshmukh S.U. and Uphoff C.A., 1999, Crippling capacity of web elements with openings, *Journal of Structural Engineering* 125 (2), p137-141.

North American Specification for the Design of Cold-Formed Steel Structural Members, American Iron and Steel Institute , Washington, DC, 2002.

Rhodes J. and Nash D., 1998, An investigation of web crushing behaviour in thin-walled beams, *Thin-Walled Structures* 32, p207-230.

Roberts T.M. and Newark A.C.B., 1997, Strength of web subjected to compressive edge

loading, Journal of Structural Engineering 123 (2), p176-183.

Shan M.Y., LaBoube R.A. and Yu W.W., 1996, Bending and shear behaviour of web elements with openings, Journal of Structural Engineering 122 (8), p854-859.

Sivakumaran K.S., 1989, Analysis for web crippling behaviour of cold-formed steel members, Computers & Structures 32 (3/4), p707-719.

Sutton F.S. and LaBoube R.A., 2003, Web crippling and combined bending and web crippling of cold-formed steel beam headers, Thin-Walled Structures 41, p1073-1087.

Winter, G., and Pian R. H. J., 1946, Crushing Strength of Thin Steel Webs, Cornell Bulletin 35, pt. 1.

Winter, G., 1940, Stress distribution in and equivalent width of flanges of wide, thin-walled steel beams. NACA Technical Note 784.

Xiao R.Y., Chin G.P.W. and Chung K.F., 2002, Testing and numerical analysis of cold-formed C-sections subjected to patch load, Advances in Steel Structures 1, p351-356.

Young B. and Hancock G.J., 2001, Design of cold-formed channels subjected to web crippling, Journal of Structural Engineering 127 (10), p1137-1144.

Young B. and Hancock G.J., 2002, Tests of channels subjected to combined bending and

web crippling, *Journal of Structural Engineering* 128 (3), p300-308.

Young B. and Hancock G.J., 2003, Cold-formed steel channels subjected to concentrated bearing load, *Journal of Structural Engineering* 129 (8), p1003-1010.

Young B. and Hancock G.J., 2004, Web crippling of cold-formed unlipped channels with flanges restrained, *Thin-Walled Structures* 42, p911-930.

Yu W.W., 2000, *Cold-formed steel design*, John Wiley & Sons, Inc., Canada.

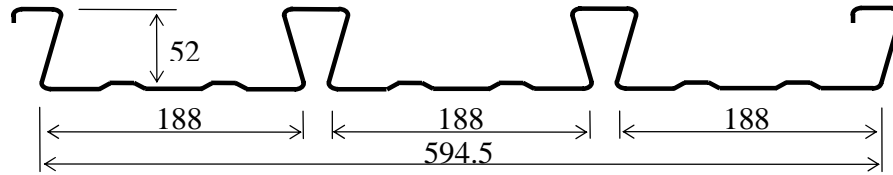
Zetlin, L., 1955, Elastic instability of flat plates subjected to partial edge loads, *Journal of the Structural Division, ASCE Proceedings* 81.

Zhao X.L. and Hancock G.J., 1995, Square and rectangular hollow sections under transverse end-bearing force, *Journal of Structural Engineering* 121 (9), p1323-1329.

Zhao X. L., Wilkinson T. and Hancock G., 2005, *Cold-formed tubular members and connections, structural behaviour and design*, Elsevier Ltd., UK.

Zhou F. and Young B., 2006, Cold-formed stainless steel sections subjected to web crippling, *Journal of Structural Engineering* 132 (1), p134-144.

Appendix A: Tensile Tests



Specimen A1 } Nominal G235, $t = 0.75\text{mm}$
 Specimen A2 }

Specimen B1 } Nominal G235, $t = 1.00\text{mm}$
 Specimen B2 }

Specimen C1 } Nominal G550, $t = 0.75\text{mm}$
 Specimen C2 }

Specimen D1 } Nominal G550, $t = 1.00\text{mm}$
 Specimen D2 }

Specimen E1 } Nominal G550, $t = 1.20\text{mm}$
 Specimen E2 }

Figure A.1: Decking profile.

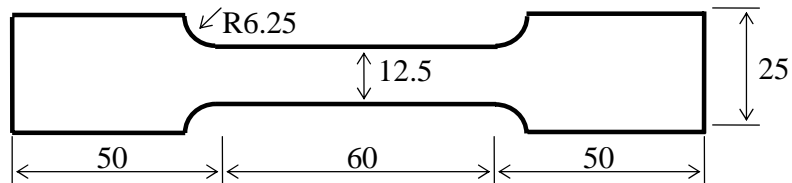


Figure A.2: Typical dimensions of coupon tensile specimen.



Figure A.3: Typical setup of tensile test.

Table A.1: Result summary of specimens A1/2 and B1/2.

	Specimen		Averaged value	Specimen		Averaged value
	A1	A2		B1	B2	
Thickness (mm)	0.77	0.78	0.78	0.99	0.99	0.99
Yield stress $f_{0.2\%}$ (N/mm ²)	315	300	308	330	340	335
Ultimate stress (N/mm ²)	359	347	353	365	354	359
Young's modulus (kN/mm ²)	191.0	176.9	183.9	183.8	192.0	187.9
Elongation (%)	40.0	40.0	40.0	25.0	42.5	33.8

Table A.2: Result summary of specimens C1/2, D1/2 and E1/2.

	Specimen		Averaged value	Specimen		Averaged value	Specimen		Averaged value
	C1	C2		D1	D2		E1	E2	
Thickness (mm)	0.79	0.78	0.79	1.05	1.06	1.05	1.20	1.21	1.21
Yield stress $f_{0.1\%}$ (N/mm ²)	576	590	583	623	619	621	630	626	628
Ultimate stress (N/mm ²)	587	599	593	636	639	637	635	633	634
Young's modulus (N/mm ²)	200	181	190	206	189	197	192	198	195
Elongation (%)	10.0	10.0	10.0	15.0	10.0	12.5	10.0	15.0	12.5

Tensile tests of specimens A1 and A2

Table A.3: Summary of specimens A1 and A2.

	Specimen		Averaged value
	A1	A2	
Thickness (mm)	0.77	0.78	0.78
Yield stress $f_{0.2\%}$ (N/mm ²)	315	300	308
Ultimate stress (N/mm ²)	359	347	353
Young's modulus (kN/mm ²)	191.0	176.9	183.9
Elongation (%)	40.0	40.0	40.0

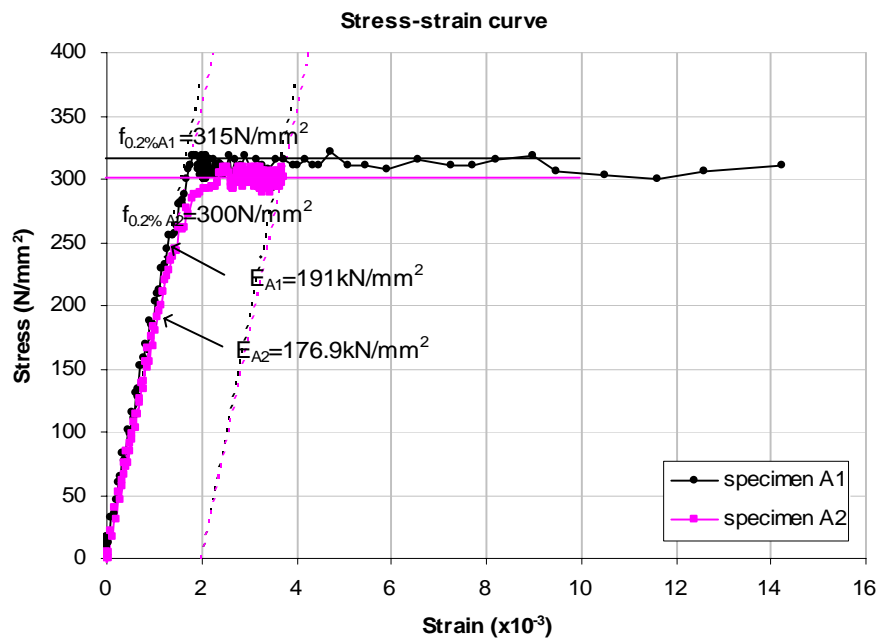
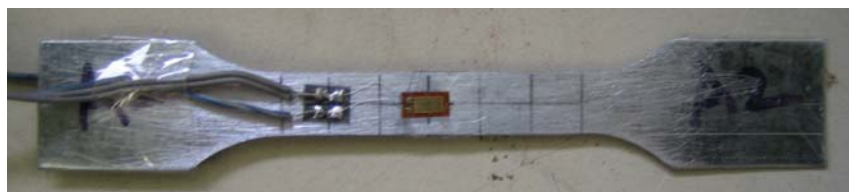
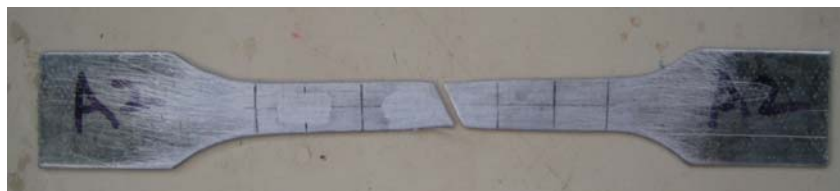


Figure A.4: Stress-strain curves of specimens A1 and A2.



a) Position of the strain gauge of the specimen



b) Failure mode of the specimen

Figure A.5: Series A specimens.

Tensile tests of specimens B1 and B2

Table A.4: Summary of specimens B1 and B2.

	Specimen		Averaged value
	B1	B2	
Thickness (mm)	0.99	0.99	0.99
Yield stress $f_{0.2\%}$ (N/mm ²)	330	340	335
Ultimate stress (N/mm ²)	365	354	359
Young's modulus (kN/mm ²)	183.8	192.0	187.9
Elongation (%)	25.0	42.5	33.8

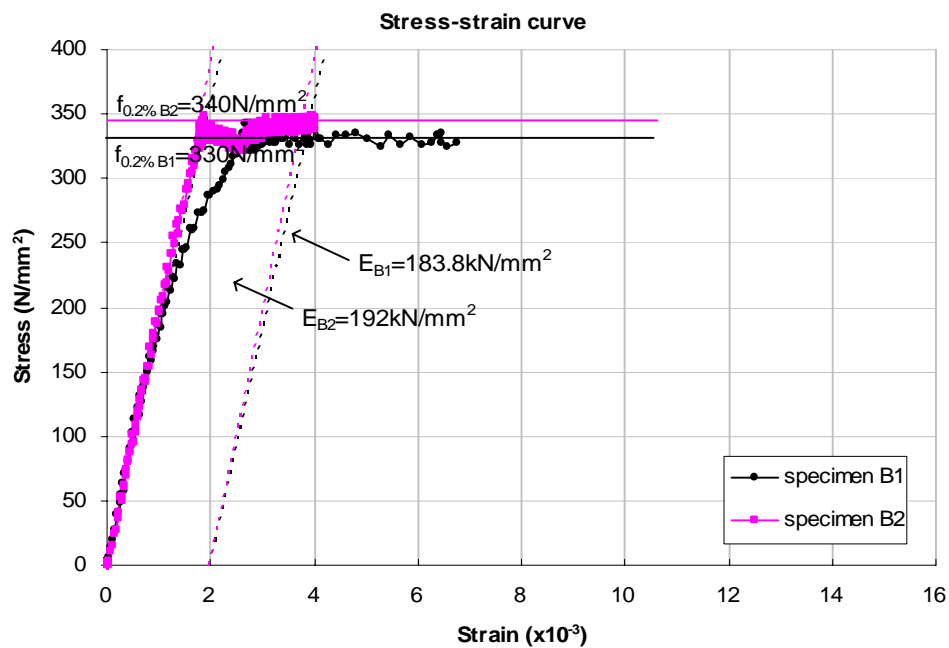


Figure A.6: Stress-strain curves of specimens B1 and B2.



a) Position of the strain gauge of the specimen



b) Failure mode of the specimen

Figure A.7: Series B specimens.

Tensile tests of specimens C1 and C2

Table A.5: Summary of specimens C1 and C2.

	Specimen		Averaged value
	C1	C2	
Thickness (mm)	0.79	0.78	0.79
Yield stress $f_{0.1\%}$ (N/mm ²)	576	590	583
Ultimate stress (N/mm ²)	587	599	593
Young's modulus (N/mm ²)	200	181	190
Elongation (%)	10.0	10.0	10.0

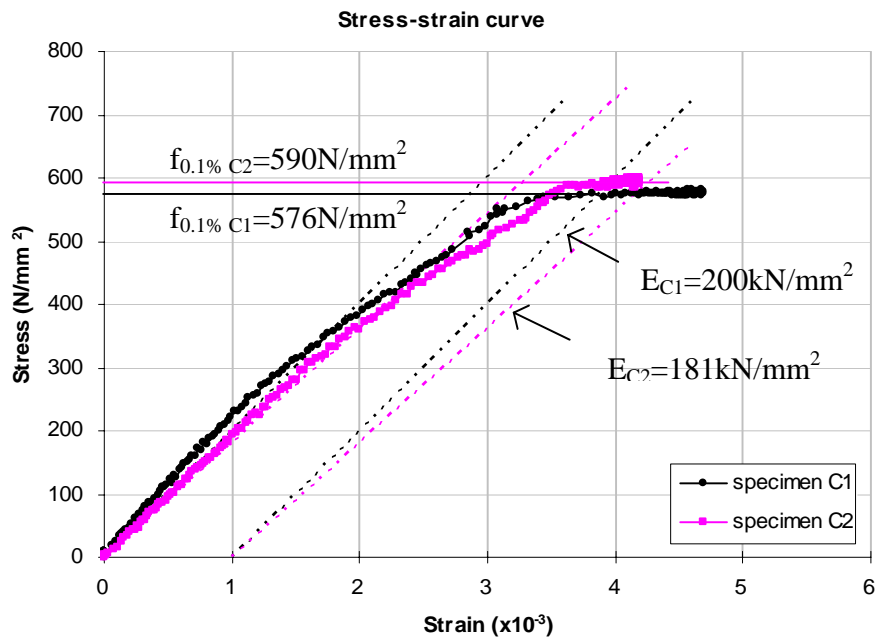
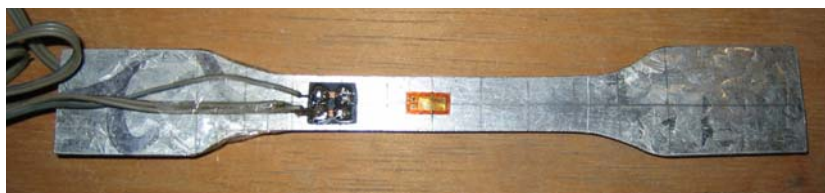


Figure A.8: Stress-strain curves of specimens C1 and C2.



a) Position of the strain gauge of the specimen



b) Failure mode of the specimen

Figure A.9: Series C specimens.

Tensile tests of specimens D1 and D2

Table A.6: Summary of specimens D1 and D2.

	Specimen		Averaged value
	D1	D2	
Thickness (mm)	1.05	1.06	1.05
Yield stress $f_{0.1\%}$ (N/mm ²)	623	619	621
Ultimate stress (N/mm ²)	636	639	637
Young's modulus (N/mm ²)	206	189	197
Elongation (%)	15.0	10.0	12.5

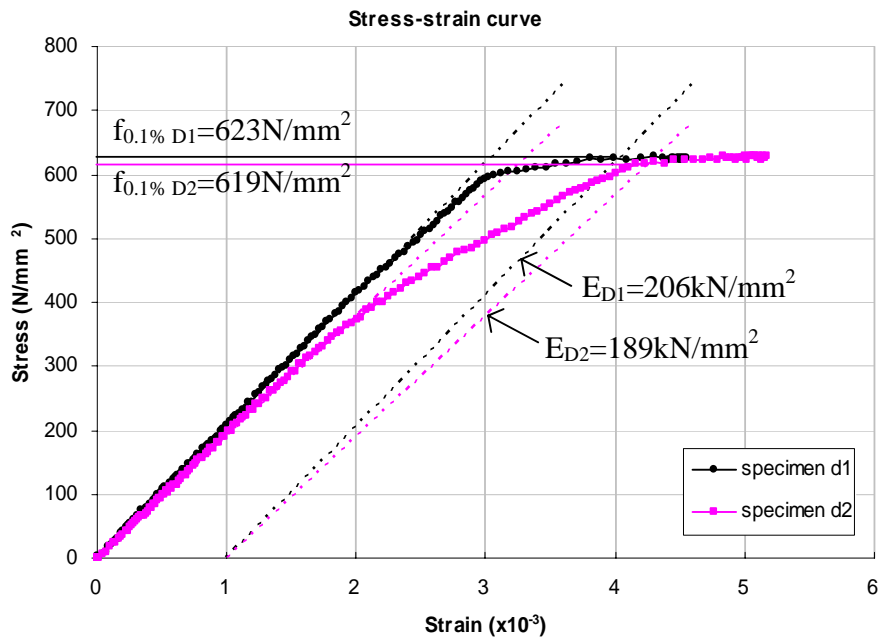
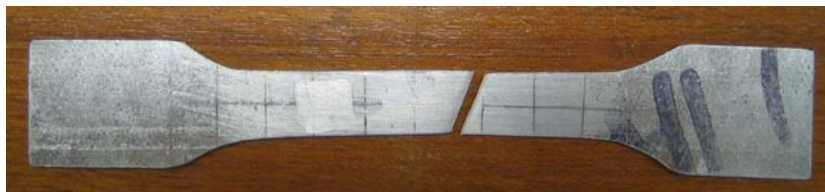


Figure A.10: Stress-strain curves of specimens D1 and D2.



a) Position of the strain gauge of the specimen



b) Failure mode of the specimen

Figure A.11: Series D specimens.

Tensile tests of specimens E1 and E2

Table A.7: Summary of specimens E1 and E2.

	Specimen		Averaged value
	E1	E2	
Thickness (mm)	1.20	1.21	1.21
Yield stress $f_{0.1\%}$ (N/mm ²)	630	626	628
Ultimate stress (N/mm ²)	635	633	634
Young's modulus (N/mm ²)	192	198	195
Elongation (%)	10.0	15.0	12.5

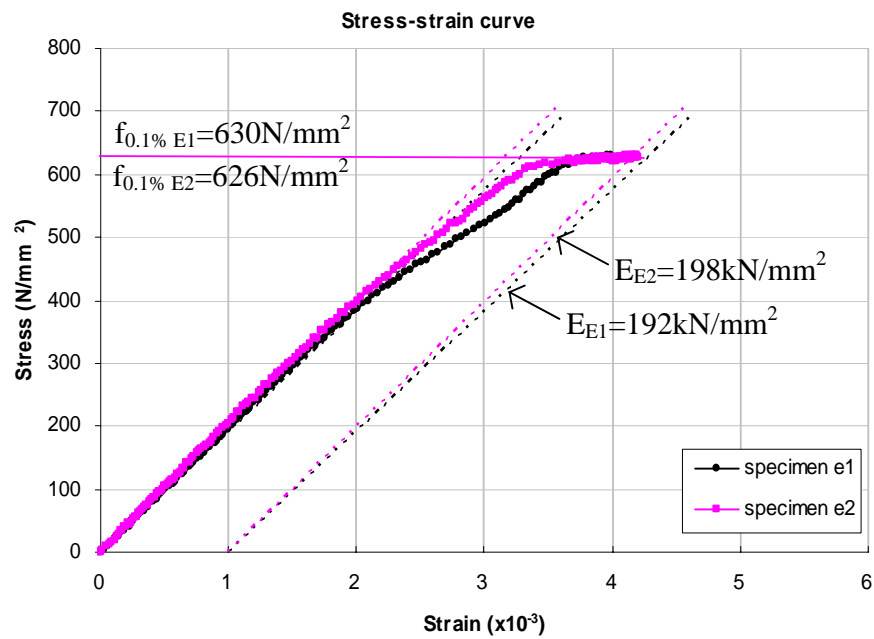
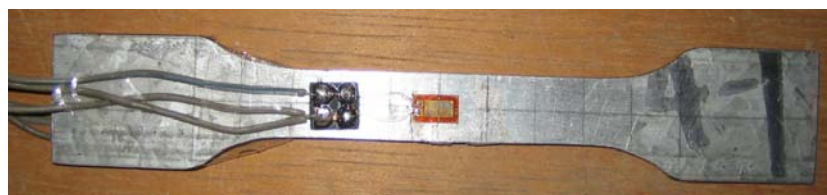


Figure A.12: Stress-strain curves of specimens E1 and E2.



a) Position of the strain gauge of the specimen



b) Failure mode of the specimen

Figure A.13: Series E specimens.